Novel approaches to improving the monitoring and mechanistic understanding of intrahepatic cholestasis of pregnancy

Vasavan, Tharni

Awarding institution:
King's College London

Novel approaches to improving the monitoring and mechanistic understanding of intrahepatic cholestasis of pregnancy

Tharni Vasavan

0719894

Thesis submitted to King's College London for the degree of Doctor of Philosophy

Supervisors

Professor Catherine Williamson

Professor Martyn Boutelle

Department of Women and Children's Health, School of Life Course Sciences, Faculty of Life Sciences and Medicine

Contents

List of figures

List of tables

Acknowledgements

First and foremost, I would like to thank my supervisors Professor Catherine Williamson and Professor Martyn Boutelle. I am incredibly lucky to have been under the tutelage of people who are not only world-renowned experts in their respective fields, but who have also ensured their door was held open to answer every question I had.

Thank you to all the women, with or without ICP, who donated their time and energy to participate in this research.

Thank you to current members of our research group (in no particular order): Jenny Chambers, Peter Dixon, Caroline Ovadia, Cyrus Fan, Aliya Amin, Alice Mitchell, Sian Chivers and Ge (Haggie) Han. You have been an absolute joy to work with and I wouldn't have completed this PhD without your support. Thank you to all the past members of the group who I have been fortunate enough to work with including Victoria Geenes, Leslie McMurtry, Dominic Lawrance and, our collaborators at Imperial College, Sung Hye Kim and Franka Schultz. Special thanks to lab alumni Saraid McIlvride, Vanya Nikolova, Elena Bellafante and Vanessa Formigo Pataia for all the laughs and post-work nights out. A massive thank you to the research midwives and technicians who recruited patients for the fetal ECG studies: Alice Lewin, Julie Wade, Jessamine Hunt, Charlotte Mungeam, Laura McCabe, Hayley Tarft, Zoe Vowles, Declan Symington, Holly Lovell, Rachel Woodcock, Maria Slaney, Jess Keane, Hilary Thompson, Hannah Wilson, Mavis Matchiori, Ruth Holmes, Emma Meadows, Vivian Cannons, Marta Vazquez Lopez, Rachel Crone, Louise Briggs and Hiten Mistry. Thank you also to Cally Gill for brightening up every visit to St. Thomas' Hospital.

Thank you to all my lovely friends outside of work who have supported me in more ways than I can describe. The biggest thank you to Emily Drew for being my number one champion. Thank you to the other amazing embryologists who I met during my first foray into women's health and have continued to support me – particularly Susannah Wood, Suzanne Cawood, Holly Exeter and Rabi Odia. Thank you to my undergraduate friends Dawn Lau and Anne Krishna Wolfes for all their sage advice and wisdom – I am so grateful to have had you both in my life for so long. Thank you to the people I met during my MSc who I now regard as friends for life: Angeliki Bolou, Giannis Karapanos, Pablo Hurtado-Gonzalez, Netta Nyrhinen, Natalie Getreu and Helen O'Neill. Thank you to Sahil and Shani Deepak for all the National Trust adventures and to Nikita Dattani for her 20-year strong support. Thank you to my extended family and numerous cousins, aunties and uncles who have cheered me on throughout.

Thank you to Tom Janes for giving me all your love, warmth and patience for the past few years, and also to the rest of the Janes clan for all your support. Thank you to my niece, who was born the month after starting this PhD and has been my endless source of joy and sunshine throughout.

I dedicate this thesis to my sister, my mum and my dad - thank you for being there every step of the way.

Statement of originality

Chapter 2: All experiments, analyses and write up were performed by myself.

Chapter 3: Initial ethical approval applications for setting up participant recruitment for this study were written by Phillip Bennet (Imperial College London). Biopsies of myometrium were taken by Vasso Terzidou (Imperial College London). Primary cell isolation was performed by Sung Hye Kim (Imperial College London). Subsequent cell culture and optical recording experiments was conducted in collaboration with Francisca Schultz (Imperial College London). All analysis and write up was performed by myself.

Chapter 4: Initial ethical approval applications for setting up the observational study were written by Jenny Chambers, Victoria Geenes and Catherine Williamson (King's College London). All subsequent ethical approval applications and maintenance of the study was conducted by myself with help and advice from Jenny Chambers and Catherine Williamson (King's College London). Ethical approval applications for the collection of mechanistic samples via the PITCHES study were written by Catherine Williamson, Peter Dixon, Lucy Chappell (King's College London) and Jim Thornton (Nottingham University). Recruitment of participants and fitting of the ECG monitor at Nottingham City Hospital was performed by Indu Asanka Jayawardane (Nottingham University). Recruitment of participants and fitting of the ECG monitor at St. Thomas', Queen Charlotte's and St. Richard's Hospital was conducted by the NIHR Clinical Research Network team at each site. Some participants at St. Thomas' Hospital and Queen Charlotte's hospital also had the ECG monitor fitted by Sahil Deepak (King's College London) or myself.

Umbilical venous blood was collected by the clinical team who were at each site at the time of delivery and processed/frozen by the research laboratory staff on site. Individual bile acid measurement of these samples via UPLC-MS was conducted by Anita Lövgren-Sandblom and Hanns-Ulrich Marschall (Karolinska Institute). NT-proBNP measurement via ELISA was conducted by myself. MATLAB scripts used to analyse heart rate variability were written by Maristella Lucchini, Joel Yang and William Fifer (Columbia University). Measurement of heart rate variability parameters was performed by myself and measurement of cardiac time interval parameters was performed by myself with Sahil Deepak as a second independent

observer. Statistical analysis was conducted by myself with advice from Paul Seed (King's College London). All other analyses and write up of data was performed by myself, however, some sections of this chapter have been taken from a draft manuscript for publication that has been read, edited and approved by (in institutional order): Sahil Deepak, Catherine Martin, Victoria Geenes, Paul Seed, Peter Dixon, Lucy Chappell, Catherine Williamson (King's College London), Jenny Chambers, Julia Gorelik (Imperial College London), Indu Asanka Jayawardane, Jim Thornton, Pam Loughna, Fiona Broughton Pipkin, Barrie Hayes-Gill (Nottingham University), Maristella Lucchini, William Fifer (Columbia University) and Hanns-Ulrich Marschall (Karolinksa Insititute).

Abstract

Introduction: Intrahepatic cholestasis of pregnancy (ICP) is characterised by elevated total serum bile acid (TSBA) concentrations and adverse fetal outcomes such as preterm labour (PTL) and intrauterine death (IUD); the risk of which is directly associated with the degree of maternal TSBA derangement. Assays for measurement of TSBA concentration are not readily available at every clinical laboratory nor are results provided immediately. The exact mechanisms of ICP-associated PTL and IUD are unknown, however the current hypotheses are that elevated bile acids increase sensitivity to oxytocin in the myometrium and induce a sudden cardiac arrythmia in the fetus, resulting in the increased rate of PTL and IUD respectively. ICP is currently commonly treated using ursodeoxycholic acid (UDCA) pharmacotherapy. Although there is some experimental and observational evidence that UDCA is cardioprotective, data from randomised controlled trial data suggests that it does not improve a composite of adverse fetal outcomes. We aimed to improve the monitoring of ICP via the development of a novel electrochemical bile acid biosensor that can function in a point-of-care setting. We also aimed to improve the mechanistic understanding of ICP-associated PTL and IUD via exposure of bile acids to a myometrial cell model and an observational study of the fetal cardiac phenotype affected by ICP.

Materials and Methods: An electrochemical biosensor was developed using commercially available carbon screen-printed electrodes (CSPEs) that had been manually modified with the electron mediators meldola's blue (MDB) or methylene blue (MEB). Pooled human serum was spiked with 0-100 µmol/L of the bile acid taurocholic acid (TCA) along with the bile acid-specific enzyme 3α-hydroxysteroid dehydrogenase (3α-HSD) and oxidised coenzyme nicotinamide adenine dinucleotide (NAD^+). The redox current generated from reduction of NAD^+ (NADH) was measured via chronoamperometry.

Myometrial biopsies were taken from women undergoing elective caesarean sections and the primary cells were subsequently isolated and cultured until passage 5 or 6. Cells were incubated with the intracellular calcium ($[Ca^{2+}]_i$) dye Fluo4-AM prior to administration of 10 nmol/L oxytocin (OT) (n=3), 100 µmol/L taurocholic acid

(TCA) (n=3), a combination of OT and TCA (n=3), 10 nmol/L prostaglandin E_2 (PGE_2) (n=4) or $F_{2\alpha}$ ($PGF_{2\alpha}$) (n=7) with or without concomitant administration of 100 µmol/L UDCA using HBSS as the vehicle. Optical recording of $[Ca^{2+}]_i$ transients was performed via time-lapse imaging and the amplitude, time to peak, duration and time to decay of the $[Ca^{2+}]_i$ transients was measured.

Pregnant women who were ≥20 weeks of gestation who had either uncomplicated pregnancies (controls, n=43), untreated ICP (n=26) or UDCA-treated ICP were recruited for fetal ECG recordings (n=22). A separate cohort of controls (n=15), untreated ICP (n=36) and UDCA-treated ICP (n=40) cases provided umbilical venous blood samples at delivery. Overnight fetal ECG recording was conducted in the first cohort. A 2-hour period from this recording was taken and the cardiac time intervals (PR and QT interval length) was measured. Time-domain measures of fetal heart rate variability (RMSSD and SDNN) were analysed in the context of fetal behavioural state 1F (quiet sleep) or 2F (active sleep). Assays to measure the concentration of NT-proBNP and individual bile acids, and the hydrophobicity index were performed on the umbilical venous serum.

Results: MEB was found to be a more effective electron mediator than MDB. The current generated from the reduction of NAD^+ to NADH did not have a linear relationship with TCA concentration. Measurements had a relative standard deviation between 20.4 and 47.9%; sensitivity of the biosensor was found to be 1.053 µA per µmol/L of TCA.

Oxytocin administration resulted in a significant increase in the amplitude of $[Ca^{2+}]_i$ transients when compared to the control ($p=0.003$). Co-administration with TCA also resulted in an increase in amplitude compared to the control ($p<0.0005$). Subsequent concomitant UDCA administration resulted in a significant reduction of amplitude ($p=0.002$). Co-administration of UDCA with PGE_2 resulted in a decrease in the PGE2-induced increase in the time to decay of $[Ca^{2+}]_i$ transients ($p = 0.043$).

A positive correlation was found between fetal NT-proBNP concentrations and maternal TSBA concentrations ($p = 0.026$) fetal TSBA concentrations ($p = 0.019$), their hydrophobicity index ($p = 0.039$), glycocholic acid ($p = 0.007$) and taurocholic acid ($p = 0.039$). No significant correlations between bile acid concentrations and

NT-proBNP were observed in the UDCA-treated cohort. Fetal PR interval length positively correlated with maternal TSBA in untreated ($p = 0.027$) and UDCA-treated ICP ($p = 0.026$). Fetal RMSSD values in active sleep ($p = 0.028$) and SDNN values in quiet sleep ($p = 0.013$) and active sleep ($p = 0.003$) were significantly higher in untreated ICP cases than controls. UDCA treatment was associated with a significant reduction in RMSSD values in active sleep ($p = 0.030$).

Discussion: Substantial preliminary work has been done towards development of a bile acid biosensor, however further advancement is required with the aim of increasing sensitivity at the pertinent TCA concentration of 100 µmol/L. MEB has been established as a suitable electron mediator.

TCA acts via OT to increase the amplitude of $[Ca^{2+}]_i$ transients in human myometrial cells, which supports previous data suggesting that ICP increases sensitivity to OT via upregulation of the OT receptor. UDCA has shown some protective attributes against contractile agonists in this model, suggesting further investigations are required to assess whether it is beneficial for ICP-associated PTL.

Untreated ICP is associated with an abnormal fetal cardiac phenotype which is closely associated with maternal and fetal TSBA concentrations and fetal bile acid hydrophobicity; this data supports the hypothesis that ICP-associated IUD is due to a fetal arrythmia. This phenotype was partially ameliorated in UDCA-treated cases, implying that UDCA treatment may be cardioprotective in a certain subset of ICP cases. However, further investigations are required to elucidate the clinical impact of this work.

Abbreviations

3α-HSD – 3α-hydroxysteroid dehydrogenase

11β-HSD2 – 11β-hydroxysteroid dehydrogenase type 2

20α-HSD – 20α-hydroxysteroid dehydrogenase

ABCB4 / MDR2 – *ATP-binding cassette, sub-family B member 4* / Multidrug resistance-associated protein 3

ABCB11 / BSEP – *ATP-binding cassette, sub-family B member 11* / Bile salt export pump

ABCG5/G8 – ATP-binding cassette, sub-family G member 5 / member 8 heterodimer

ABCC2 / MDR2 – *ATP-binding cassette, sub-family C member 2* / Multidrug resistance-associated protein 2

ADAMTS-12 – A Disintegrin-like Metalloproteinase with ThromboSpondin motif 12

ALP – alkaline phosphatase

ALT – alanine aminotransferase

ANS – autonomic nervous system

AP – action potential

AST – aspartate aminotransferase

ASBT – apical sodium-dependent bile acid transporter

ATP8B1 / FIC1 – *ATPase phospholipid transporting 8B1* / familial intrahepatic cholestasis type 1 protein

AV - atrioventricular

BAAT – bile acid CoA: amino acid N-acyltransferase

BACS – bile acid-CoA synthase

BCRP – breast cancer related protein

BKCa – The large-conductance calcium- and voltage-sensitive potassium channel

BMI – body mass index

Ca^{2+} – calcium ions

$[Ca^{2+}]_i$ – intracellular calcium ions

CA – cholic acid

CACC – calcium-activated chloride channel

CaM – calmodulin

CAP – contraction-associated proteins

CCL2 – chemokine ligand 2

CD – cluster of differentiation

CDCA – chenodeoxycholic acid

CHD – coronary heart disease

CHI3L1 – chinitase-3-like protein 1

Cl^- – chloride ions

CRH – corticotropin-releasing hormone

CSPE – carbon screen-printed electrode

CTG – cardiotocograph

CTI – cardiac time interval

cTnI – cardiac troponin I

Cx43 – connexin43

CYP7A1 – cytochrome p450 family 7 subfamily A member 1, encodes cholesterol 7-α hydroxylase

CYP8B1 – cytochrome p450 family 8 subfamily B member 1, encodes sterol 12-α hydroxylase

CYP27A1 - cytochrome p450 family 27 subfamily A member 1, encodes sterol 27 hydroxylase

DAG – 1,2-diacylglycerol

DCA – deoxycholic acid

ECG - electrocardiogram

ER – endoplasmic reticulum

ET-1 – Endothelin-1

fECG – fetal electrocardiogram

FHR – fetal heart rate

fHRV – fetal heart rate variability

FXR – Farnesoid-X receptor

GDM – gestational diabetes mellitus

GGST – gamma glutamyl transferase

GPBAR1 / TGR5 – G protein-coupled bile acid receptor 1 / Takeda G protein-coupled receptor 5

GPCR – G protein-coupled receptor

GPx – glutathionine peroxidase

hERG – human ether-a-go-go-related gene

HIF-1α – hypoxia-induced factor 1-α

HPLC – high performance liquid chromatography

HRV – heart rate variability

hTERT – human telomerase reverse transcriptase

IBABP – intestinal bile acid binding protein

ICAM-1 – inflammation cell adhesion molecule-1

ICP – Intrahepatic cholestasis of pregnancy

IL – interleukin

IP_3 – inositol triphosphate

IUD – intrauterine death

K^+ – potassium ions

K_{ATP} – ATP-sensitive potassium channel

K_v – voltage-gated potassium channel

LCA – lithocholic acid

LDH – lactate dehydrogenase

LMPI – left ventricular myocardial performance index

MDB – Meldola's blue

MEB – Methylene blue

MLCK – myosin light chain kinase

MLCP – myosin light chain phosphatase

MMP – matrix metalloproteinase

MPI – myocardial performance index

mPTP – mitochondrial permeability transition pore

MPV – mean platelet volume

Na^+ – sodium ion

NAD^+ / NADH – nicotinamide adenine dinucleotide (oxidised) / nicotinamide adenine dinucleotide (reduced)

NAFLD – non-alcoholic fatty liver disease

NALCN – sodium-activated leak channel non-selective

NCX – sodium-calcium exchanger

NF-ƙB – Nuclear Factor kappa-light-chain-enhancer of activated B cells

NK – natural killer

NICE – National Institute for Health and Care Excellence

NO – nitric oxide

NPY – neuropeptide Y

NTCP – sodium-taurocholate co-transporting polypeptide

NT-proBNP – N terminal pro-B-type Natiuretic Peptide

OATP – organic anion transporting polypeptide

OLETF – Otsuka Long-Evans Tokushima Fatty

OST α/β – organic solute transport α/β

OT – oxytocin

OTR – oxytocin receptor

P4 – progesterone

PAC – premature atrial contraction

PGE_2 – prostaglandin E_2

$PGF_{2\alpha}$ – prostaglandin $F_{2\alpha}$

PGl_2 – prostacyclin

PHM – Pregnant Human Myometrium

PKC – protein kinase C

PLB – phospholamban

PLC-β – phospholipase C β

POC – point of care

PPROM – preterm premature rupture of membranes

PRA / PRB – progesterone receptor A / B

PSC – primary sclerosing cholangitis

PTB – preterm birth

PTGS2 / COX-2 – *prostaglandin-endoperoxidase synthase 2* / cyclooxygenase 2

PTHrP – parathyroid hormone-related peptide

PTL – preterm labour

PVS – portal vein stnosis

PXR – Pregnane-X receptor

RhoA – ras homolog family member A

RMSSD – root mean squared of successive differences

ROC – receiver-operating characteristic

ROCE – receptor-operated calcium entry

ROCK – Rho-associated protein kinase

RSD – relative standard deviation

SAMe – S-adenosyl-L-methionine

SDNN – standard deviation of N-N intervals

SERCA – sarco/endoplasmic reticulum Ca^{2+}-ATPase

SHP – small heterodimer protein

SK – small conductance calcium-sensitive potassium channels

SOCE – store-operated calcium entry

SPE – screen-printed electrode

SR – sarcoplasmic reticulum

SUR – sulphonylurea receptor

SVT – supraventricular tachycardia

TCA – taurocholic acid

TCDCA – taurochenodeoxycholic acid

TNF-α – tumour necrosis factor-α

TIMP – tissue inhibitor of matrix metalloproteinase

TRPC – transient receptor potential cation channel subfamily C

TSBA – total serum bile acid

TUDCA – tauroursodeoxycholic acid

UDCA – ursodeoxycholic acid

VCAM-1 – vascular adhesion molecule-1

VDCC – voltage-dependent calcium channel

VDNC – voltage-dependent sodium channels

VEGF – vascular endothelial growth factor

ZEB1/2 – zinc finger E-box-binding homeobox 1

Chapter 1:

Introduction

1. Introduction

1.1 Intrahepatic cholestasis of pregnancy

1.1.1 Aetiology and epidemiology

Intrahepatic cholestasis of pregnancy (ICP) is the most common pregnancy-specific liver disease. It was first described in literature in 1883 as "recurrent jaundice in pregnancy", however, nowadays it is described as "obstetric cholestasis" in most current reports. Typically, women with ICP present with maternal pruritus without a rash and elevated maternal total serum bile acid (TSBA) concentrations that are often concurrent with deranged serum liver enzyme concentrations; all of which tend to spontaneously resolve within 48 hours of delivery of the fetus (Williamson and Geenes, 2014).

The global incidence of ICP is known to vary with geographic location and ethnic origin of the mother, however it is estimated to affect approximately 0.2-2.0% of pregnancies worldwide (Geenes and Williamson, 2009). Historically, inhabitants of Chile were found to have the highest rates of the disease, particularly women of the indigenous Araucanian Mapuche Native American population who were reported to have a 27.6% prevalence of ICP (Reyes et al., 1978). These rates have now fallen according to more recent studies; the reason for this decrease over time is unclear as diagnostic criteria for the disease has become more inclusive (Reyes, 2008). In the United Kingdom, the incidence of ICP is estimated to be 0.7% of the pregnant population, however women of South Asian descent having rates of up to 1.5% (Abedin et al., 1999). Apart from ethnicity, other risk factors for the disease include Hepatitis C seropositivity and women who >35 years old at the time of pregnancy (Paternoster et al., 2002, Koivurova et al., 2002).

The disease has a complex aetiology, however in general it is thought that women with certain genotypes are predisposed to developing ICP due to environmental impact and pregnancy-induced hormonal changes (Dixon and Williamson, 2016). The latter is evidenced by exogenous estrogen treatment, multifetal pregnancies, hormonal contraception and assisted conception using *in vitro* fertilisation being

associated with higher rates of ICP (Kreek et al., 1967, Gonzalez et al., 1989, Batsry et al., 2019, Alemdaroğlu et al., 2020). Studies have shown that the disease has familial clustering, with significant concurrence between first degree relatives (Eloranta et al., 2001). With regard to genomic studies, there has been a particular research emphasis on evaluation of potential mutations of biliary transport encoding genes ATP binding cassette *(ABC) B4* (MDR3), *B11* (BSEP) and *C2* (MDR2), ATPase phospholipid transporting 8B1 (*ATP8B1)* (FIC1) and the genes encoding bile acid receptors Pregnane-X receptor (PXR) and Farnesoid-X receptor (FXR) (Dixon and Williamson, 2016). Additionally, there appears to be a seasonal susceptibility to the disease in some European countries during winter months, which is thought to be due to selenium and/or Vitamin D deficiency (THORLING, 1955, Fisk et al., 1988, Johnston and Baskett, 1979, Williamson and Geenes, 2014, Gençosmanoğlu Türkmen et al., 2018).

In normal pregnancy, the fetal serum concentrations of bile acids are higher than in the maternal circulation, consistent with the fetus having relative hypercholanaemia compared to its mother. There is also a progressive increase of fetal serum bile acid concentrations with gestation which is thought to be due to the limited ability of the immature fetal liver and kidneys to excrete these compounds (Lunzer et al., 1986, Marin et al., 2008). Bile acids are therefore mainly transferred from the fetus to the maternal compartment via the placental barrier, however, pathological cholestasis has not been reported in either compartment due to their small amounts. In pregnancies complicated by ICP, the feto-maternal gradient for bile acid transfer is reversed and a high concentration of circulating bile acids in the mother leads to the accumulation of a high level of bile acids in the fetal compartment (Figure 1.1) (Laatikainen, 1975, Monte et al., 1995).

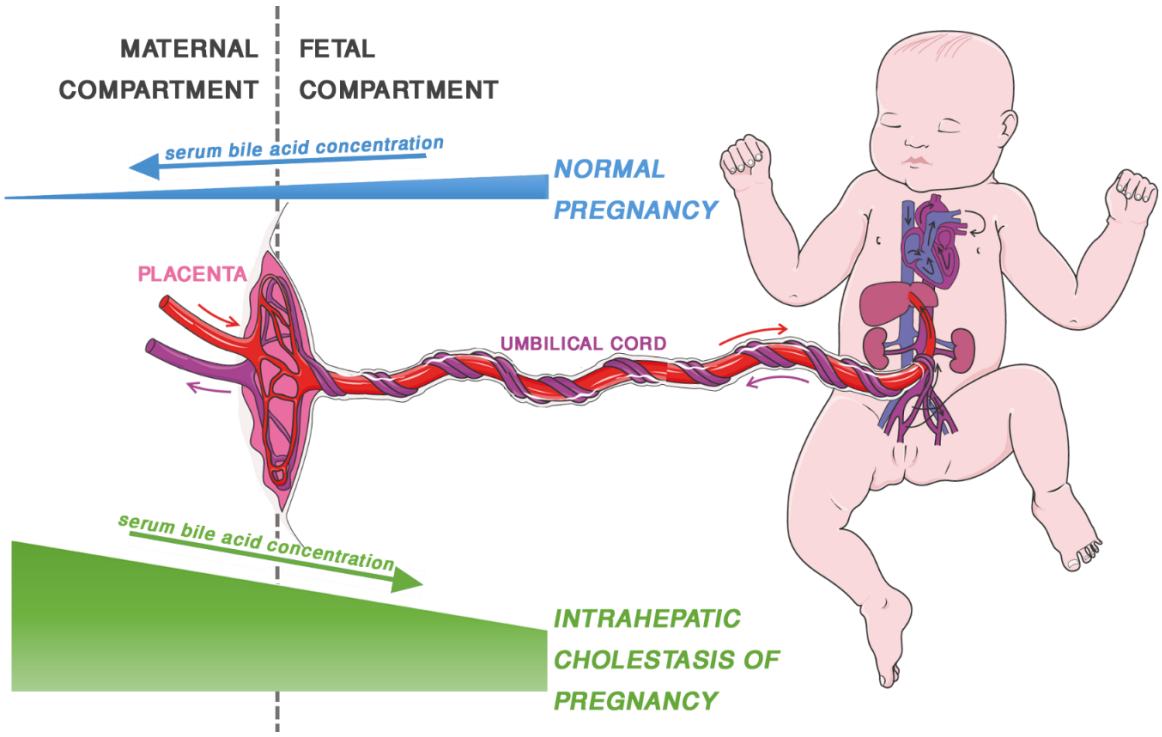

Figure 1.1: Schematic representation of the feto-maternal serum bile acid concentration gradient in normal pregnancies and pregnancies complicated by ICP.

1.1.2 Bile acid structure, synthesis, transport and the role of bile acids in ICP

Bile acids are detergent compounds which are the end products of cholesterol catabolism and have the essential function of emulsifying lipids into micelles after consumption of food. They can also act as signalling molecules to upregulate genes encoding their own synthesis and transportation (Chiang, 2013). Bile acids are steroid structures made of three 6-carbon rings and one 5-carbon ring with a carbon side chain terminating in a carboxyl group with differing attached hydroxyl groups depending on the specific bile acids. The hydroxyl groups can either be positioned above (described as β) or below (described as α) the steroid nucleus. All human bile acids are formed by 24 carbon atoms and have hydroxyl groups at the 3α, 7α and/or 12α positions. The orientation of these groups contribute to the amphipathic nature of bile acids as the α side of the molecule is hydrophilic and the β side is hydrophobic (Monte et al., 2009).

Synthesis of bile acids can occur via one of two pathways: the classical (or neutral) pathway and the alternative (or acidic) pathway (Chiang, 1998). The classical pathway accounts for 90% of synthesised bile acids. It occurs in the hepatocytes of the liver via the hydroxylation of cholesterol by the cytochrome p450 enzymes cholesterol 7-α hydroxylase (*CYP7A1*), the rate-limiting enzyme, along with sterol 12-α hydroxylase (*CYP8B1*) and which make the primary bile acid cholic acid (CA) (Chiang, 2013). Without the latter enzyme, the other primary bile acid chenodeoxycholic acid (CDCA) is formed (Chiang, 2013). The remaining 10% of bile acids are synthesised via the alternative pathway which is initiated in by sterol 27 hydroxylase (*CYP27A1*), an enzyme which is widely distributed in the mitochondria of macrophages and other tissues and also leads to the formation of the primary bile acid CDCA (Chiang, 2013).

To prevent the cytotoxic accumulation of bile acids in hepatocytes, they are transported into the bile canaliculi or hepatic vein. Canalicular transport occurs via the bile salt export pump (BSEP), encoded by *ABCB11*, which acts as the rate limiting step for bile acid removal from the blood (Kullak-Ublick et al., 2000). Prior to primary bile acids being transported into the canalicular lumen, they are conjugated at their carboxyl group to the amino acids glycine and taurine at a ratio of 3:1 with the aid of the enzymes bile acid-CoA synthase (BACS) and bile acid CoA: amino acid N-acyltransferase (BAAT). Conjugation of bile acids further increases their amphipathic nature. Bile itself is made from bile salts, phospholipids and cholesterol. The phospholipid phosphatidyl choline is exported into the canaliculi via the multidrug resistance 3 protein (MDR3), which is encoded by *ABCB4*, and cholesterol is exported via the *ABCG5/G8* heterodimer, thereby allowing the formation of bile micelles in the canaliculi (Graf et al., 2003, Oude Elferink and Paulusma, 2007).

The micelles are then transported into the gallbladder and released into the duodenum of the intestine after food consumption. In the intestine, conjugated CA and CDCA are deconjugated then converted to the secondary bile acids deoxycholic acid (DCA) and lithocholic acid (LCA) respectively via 7α-dehydroxylation by the

intestinal flora. Approximately 95% of bile acids are re-absorbed from the distal ileum and transported back into the liver via the portal vein with the aid of the apical sodium-dependent bile acid transporter (ASBT), intestinal bile acid binding protein (IBABP) and organic solute transporters (OST) α and β, in a process known as enterohepatic circulation (Stieger and Meier, 2011). They are then taken back up into the hepatocytes by sodium (Na^+)-taurocholate co-transporting polypeptides (NTCP) or organic anion transporting polypeptides (OATP) (Meier and Stieger, 2002) (Figure 1.2).

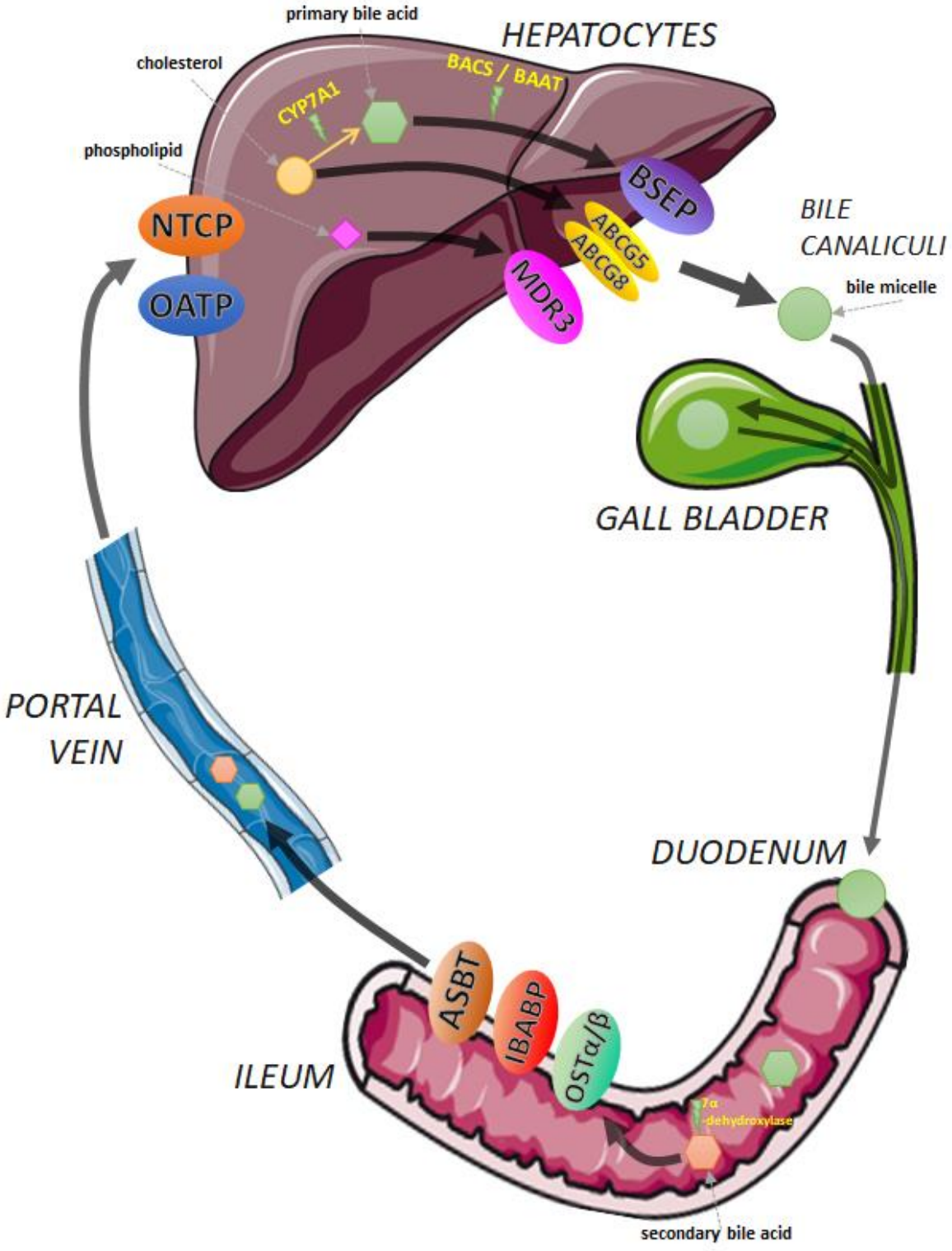

Figure 1.2: : Schematic representation of bile acid synthesis and enterohepatic circulation.

1.1.3 Risk of ICP-associated adverse outcomes and the importance of disease severity

ICP has traditionally been stratified as either mild or severe depending on maternal TSBA concentration, mild ICP is diagnosed in women who have elevated TSBA concentrations whilst severe ICP is determined by further elevated TSBA concentrations of ≥40 μmol/L.

Although ICP generally resolves spontaneously after delivery and was initially thought to be benign for the mother, it has since been shown to be associated with other comorbidities such as gestational diabetes mellitus (GDM), maternal dyslipidaemia, and preeclampsia during the gestational period (Wikström Shemer et al., 2013, Dann et al., 2006, Martineau et al., 2014b, Rezai et al., 2015). In addition to this, long-term follow up studies have shown that ICP is associated with the development of postpartum metabolic disease in the mother, including an increased risk of type 2 diabetes and hypothyroidism (Wikström Shemer et al., 2015, Hämäläinen et al., 2019). A higher incidence of gallstones, chronic liver disease and liver cancer after an ICP-complicated pregnancy has also been reported (Marschall et al., 2013, Erlinger, 2016). Evidence from human studies and mice also suggests that ICP programmes the fetus to be predisposed to metabolic disease later on in life; 16 year-old children whose mothers had ICP during their pregnancy had an increased BMI, waist girth and fasting insulin compared to a control cohort from uncomplicated pregnancies (Papacleovoulou et al., 2013). This corresponds with data that neonates born from ICP-complicated pregnancies have a higher birthweight and ponderal index, however there is also conflicting evidence that ICP increases the rate of small for gestational age infants and cholestasis induces intrauterine growth restriction in mice (Martineau et al., 2014b, Li et al., 2020, Madazli et al., 2015, Chen et al., 2019b).

The focus of research and clinical management has been on improving fetal and neonatal outcomes since it was first reported that the prognosis of the fetus from an ICP pregnancy can be poor; this was later confirmed by data from a small Finnish cohort which showed increased rates of intrauterine death (IUD), fetal distress and

meconium stained amniotic fluid (Friedlaender and Osler, 1967, Laatikainen and Ikonen, 1977). The increased rates of these adverse outcomes in pregnancies complicated by ICP were further confirmed in Australian, North and South American cohorts (Fisk and Storey, 1988, Alsulyman et al., 1996, Rioseco et al., 1994). Later studies of larger Swedish and UK cohorts by Glantz et al. (2004) and Geenes et al. (2014) confirmed that ICP is associated with the increased risk of intrauterine death (IUD), iatrogenic and spontaneous preterm labour (PTL), meconium staining of amniotic fluid, fetal hypoxia and neonatal unit admission (Geenes et al., 2014a, Glantz et al., 2004). Importantly, the latter investigations highlighted that fetal complications did not arise until maternal TSBA concentrations reached the severe threshold of 40 μmol/L and regression analysis showed that the risk increased with every increasing unit of TSBA concentration (Glantz et al., 2004, Geenes et al., 2014a). The association of risk of adverse outcomes increasing with severity of ICP has also been confirmed in smaller cohorts as well as the more recent findings of an increased risk of fetal respiratory distress syndrome (Estiú et al., 2017, Günaydin et al., 2017, Cui et al., 2017, Wikström Shemer et al., 2013, Lee et al., 2008, Zecca et al., 2006) .

A recent study by Ovadia et al. (2019) found that peak maternal TSBA concentrations are the most effective biomarker and predictor for IUD; the equivalent was not found when investigating other markers of liver dysfunction such as serum alanine aminotransferase (ALT), aspartate aminotransferase (AST) or bilirubin concentrations (ROC area under the curve 0.94 vs. 0.56, 0.58 and 0.79 respectively) (Ovadia et al., 2019). Furthermore, when comparing the individual patient data of 5269 ICP participants and 165,123 control participants, it was found that the patients most at risk of ICP-associated IUD and/or spontaneous PTL can be further stratified as maternal TSBA concentrations of ≥100 μmol/L causing the highest risk (Ovadia et al., 2019) (Figure 1.3). The threshold of ≥100 μmol/L for identifying the women at highest risk of IUD has also been supported by other studies of smaller cohorts (Di Mascio et al., 2019, Herrera et al., 2018, Kawakita et al., 2015, Brouwers et al., 2015).

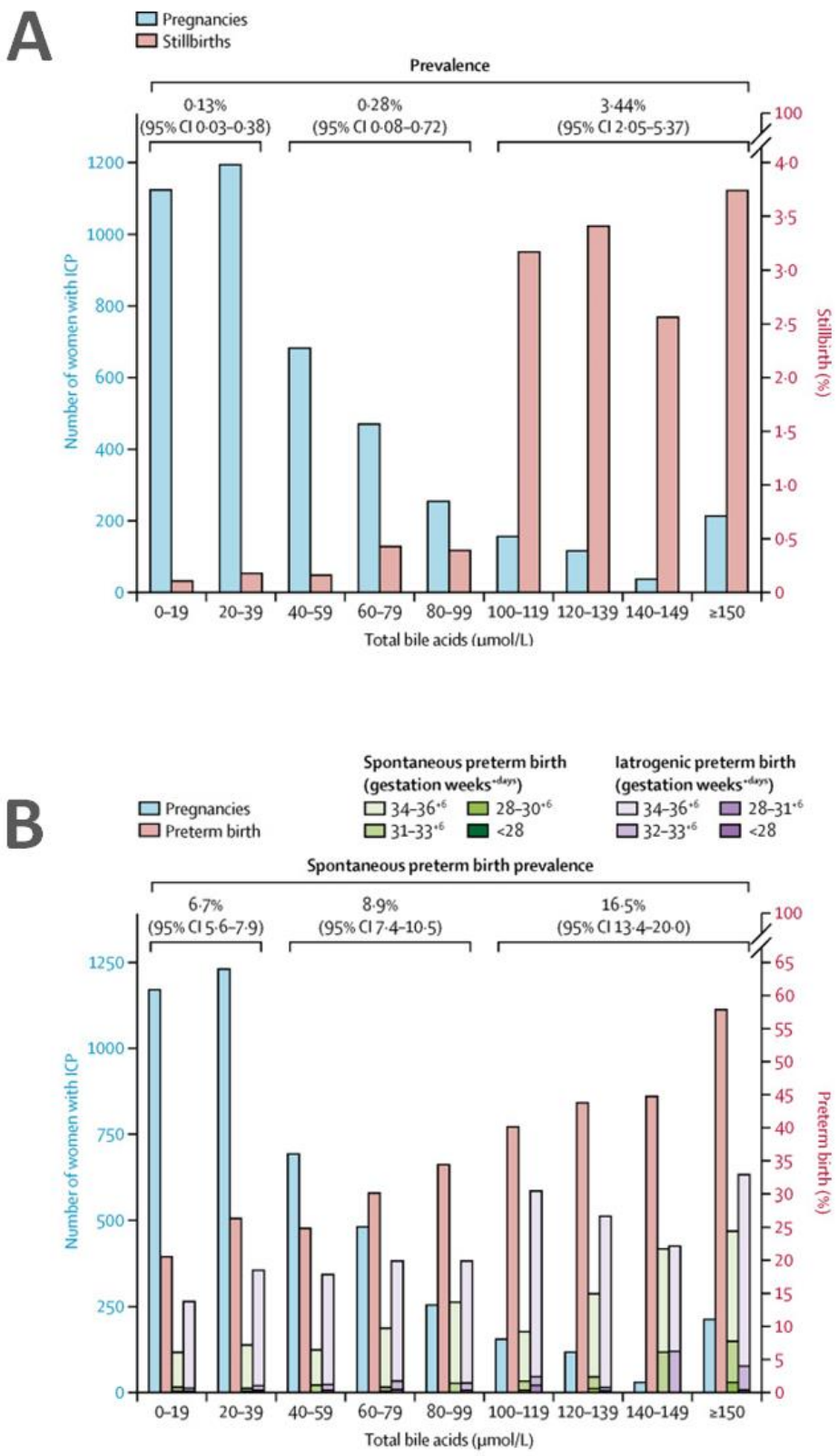

Figure 1.3: Graphs taken from the Ovadia et al. publication depicting the relationship between maternal TSBA concentrations and the perinatal outcomes of (A) intrauterine death and (B) spontaneous preterm labour (adapted from (Ovadia et al., 2019))

These data were reported from singleton pregnancies. However, data from twin pregnancies (the incidence of which is strongly associated with assisted conception and relatively elevated hormone levels) have shown that these pregnancies generally have earlier an onset of ICP, higher TSBA concentrations during pregnancy, higher rates of spontaneous preterm birth (PTB) and earlier IUD events compared to singleton pregnancies (Batsry et al., 2019). Composite adverse perinatal outcomes in twin pregnancies complicated by ICP compared to control twin pregnancies in Chinese cohorts also correlated with severity of disease; a stratified subgroup of participants with TSBA concentrations ≥100 μmol/L were not studied (Mei et al., 2018, Mei et al., 2019, Shan et al., 2016). In addition, twin pregnancies conceived via assisted conception had worse perinatal outcomes than twin pregnancies conceived spontaneously (Feng et al., 2018).

The duration of ICP also affects the prognosis of the fetus in singleton pregnancies; recent data has shown that ICP which had a gestational onset of ≤30 weeks, i.e. an early-onset diagnosis is associated with an increased rate of PTL, meconium-stained amniotic fluid and fetal distress compared to later-onset diagnosis (Lin et al., 2019, Jin et al., 2015, Estiú et al., 2017).

1.1.4 Diagnostic criteria for ICP

Given the above data, the focus of ICP diagnosis should be on accurate testing of maternal TSBA concentrations and subsequent targeted management of women with TSBA concentrations ≥100 μmol/L in order to decrease the likelihood of ICP-associated adverse perinatal outcomes. The diagnostic criteria of ICP, however, can vary between centres. Measurement of maternal serum TSBA is not a routine test in clinical sites that manage ICP patients nor is it always available, and hence it is not always used for diagnosis and management (Bacq and Sentilhes, 2014). The majority of women who are eventually diagnosed with ICP initially present with pruritus and are then found to have deranged tests of liver function which can include a combination of TSBA, ALT, AST, alkaline phosphatase (ALP), gamma glutamyl transferase (GGST) and/or bilirubin (Williamson and Geenes, 2014). ICP

is diagnosed when other causes of these two symptoms have been excluded, however recent evidence suggests that differential diagnosis does not result in a significant number of women being diagnosed with an alternative disorder (Williamson and Geenes, 2014, Donet et al., 2020). Most women are diagnosed after thirty weeks of gestation, however the disease can present as early as eight weeks into pregnancy (Berg et al., 1986).

Bile acids circulate around the body whilst bound to the albumin in serum. Due to the nature of their synthesis and function, TSBA concentrations are raised post-prandially and have displayed a diurnal rhythm (Gälman et al., 2005). The typical bile acid concentration threshold for diagnosis of ICP, if maternal TSBA results are used for diagnosis, is 10-14 μmol/L in a non-fasted patient or 6-10 μmol/L if the patient has fasted (Williamson and Geenes, 2014). If the TSBA concentration initially presents at, or eventually surpasses a threshold of 40 μmol/L, then women are typically classed as having severe ICP. Whether the patient is fasted prior to their TSBA test is dependent on the centre they present at, however postprandial TSBA concentrations have been shown to be more sensitive for diagnosing liver disease and predicting perinatal outcomes (Kaplowitz et al., 1973, Laatikainen, 1978, Sargın Oruç et al., 2014). Furthermore, unpublished data from our group suggests that postprandial tests are more accurate for identifying women with severe ICP, suggesting that centres that use fasted tests may be underdiagnosing this subgroup of cases (Mitchell and Ovadia et al., unpublished). It has been suggested that ratio of CA:CDCA could act as a useful diagnostic test for women with ICP, however its efficacy is not yet confirmed (Jurate et al., 2017). In normal pregnancies, the 3:1 glycine to taurine conjugation ratio results in glycine-conjugated bile acids being more concentrated in serum, however ICP pregnancies result in a switch in the ratio and a higher concentration of taurine-conjugated bile acids; particularly the concentration of taurocholic acid (TCA) is significantly increased although neither the ratio of CA:CDCA nor TCA alone have been proven as efficient markers of the disease (Tribe et al., 2010).

1.2 Measuring bile acids

1.2.1 Current methods of measuring bile acids

In addition to being used for diagnosis and management of ICP, measurement of TSBA concentrations is also used for managing patients with a other liver diseases including hepatobiliary disease, liver sclerosis and bile acid malabsorption (Ferraris et al., 1983, Luo et al., 2018). Although it is clear that TSBA concentrations, particularly those exceeding 100 µmol/L, provide the best predictive biomarker for ICP-associated IUD and PTL, the specificity and sensitivity of the use of TSBA concentrations for diagnosis of ICP has been debated due to the relatively low concentrations of bile acids in the blood and the lack of capacity of the most clinically available versions of this assay to determine individual bile acid concentrations (Jurate et al., 2017, Manzotti et al., 2019).

There are currently many different assays capable of measuring TSBA or the serum bile acid profile in the clinical laboratory including chromatographic methods coupled with mass spectrometry, immunoassays, enzymatic assays, fluorometry, ultraviolet detection and proton nuclear magnetic resonance spectroscopy (Manzotti et al., 2019). The former more complex chromatography and spectrometry separation methods in this list are the ideal technique for measuring bile acid concentrations due to their high accuracy and ability to detect specific individual bile acids, however they have long turnaround times, equipment is costly and rarely available in clinical laboratories (Danese et al., 2017). Enzymatic assays are more commercially available and cheaper, and therefore are more commonly used in clinical laboratories. The most current and advanced versions of these assays measure the TSBA concentration through the use of the enzyme 3α-hydroxysteroid dehydrogenase (3α-HSD) to oxidise the 3α-hydroxyl group on bile acids to a 3-keto/oxo group in the presence of coenzymes nicotinamide adenine dinucleotide (reduced) (NADH) and thio-NAD^+ (which are simultaneously oxidised and reduced into NAD^+ and thio-NADH respectively) (Figure 1.4). The concentration of accumulated thio-NADH is then measured using spectrophotometry at a wavelength of 405/660nm (Zhang et al., 2005). The detection limit using this method is 180 µmol/L and the precision of this method to measure TSBA concentrations in serum

has been reported to be 97%, however not all centres have the equipment to measure TSBA concentrations in their clinical laboratories despite it being relatively inexpensive and more available than other methods (Danese et al., 2017). In addition, clinical laboratories may conduct TSBA assays infrequently and therefore a delay in obtaining serum TSBA results may result in an inaccurate reflection of the current TSBA concentration of the patient. This is particularly concerning when considering the time-sensitive nature of the result: TSBA concentrations can rise to ≥100 µmol/L rapidly, ICP is mostly diagnosed late in pregnancy and the risk of IUD increases with gestational age (Ovadia et al., 2019).

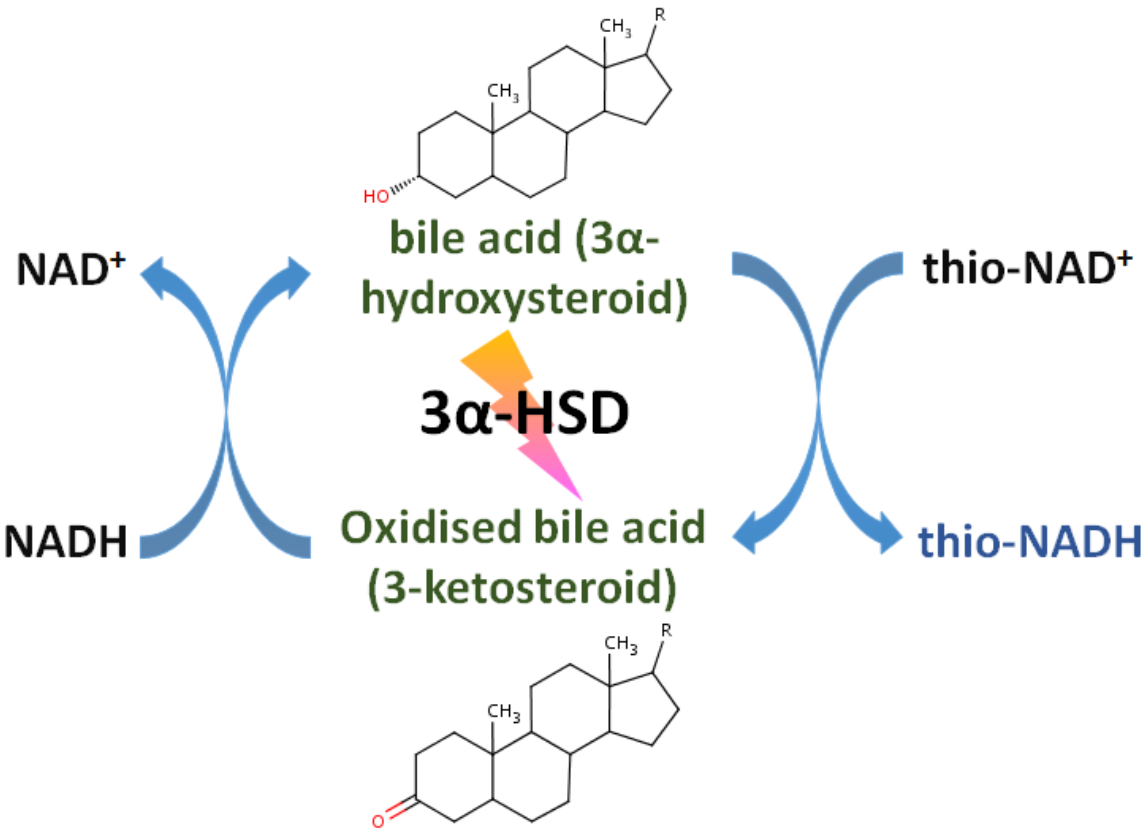

Figure 1.4: Schematic representation of the compounds of the enzymatic reaction used to detect total bile acid concentrations in serum.

1.2.2 Novel methods of ICP diagnosis

Research has therefore moved towards investigating alternative methods to utilise the enzymatic reaction that can provide the same specificity but can also be

inexpensive, widely distributed and provide a quick turnaround to allow the feasibility of frequent testing and provision of rapid results. The development of an effective biosensor would be the logical solution for this problem. Biosensors are analytical devices that rely on a biological component, such as an enzyme, to generate a signal that is transduced and quantified in proportion to the concentration of the chosen analyte present (Bhalla et al., 2016). They can be classed as optical, electrochemical, thermometric, piezoelectric (referring to the electrical charge generated from mechanical stress) or magnetic (Damborský et al., 2016). Since the successful development of the first glucose oxidase biosensor by Clark and Lyons in 1962, there has been an exponential investment into the research, development and implementation of biosensors, particularly in the fields of public health and environmental monitoring as they are cost-effective, provide fast results and require minimal operational time (Clark and Lyons, 1962, Eggins, 2002). There is a particular demand for biosensors that detect biomarkers for highly researched diseases such as cancer, cardiovascular disease and neurodegeneration (Janegitz et al., 2014). Electrochemical biosensors are the most common type that are used for monitoring and diagnosing diseases in clinic due to their inherent sensitivity, however they are often hindered by complications relating to selectivity and stability due to poor coupling between the biological component and transducer (Chaubey and Malhotra, 2002).

1.2.3 Components of an electrochemical biosensor

In the simplest terms, the architecture of an electrochemical biosensor firstly requires a biological recognition element, or receptor, that can specifically bind to the target analyte, or substrate. The biological event triggered by either the binding of the analyte to its recognition element (such as an antibody), or a highly specific reaction of the analyte with the biological element (such as an enzyme) generates a biochemical signal which is picked up by an electrical interface; this is usually made up of electrodes. The biochemical signal is therefore transduced into an electrical signal which is measured, amplified and finally processed to give a comprehensible readout (Figure 1.5). In addition to the recognition element being highly specific to the target analyte, the biosensor must show little variation between assays, be

reproducible within the target analyte's physiological concentration range, provide a rapid or real-time readout if it is to be used in a point-of-care (POC) setting and be free from any electrical or physical interference such as pH and/or temperature. Furthermore, in order for the biosensor to be a viable device for use in clinical settings, it must be cheap, small, portable and require minimal training for the operator to use (Grieshaber et al., 2008).

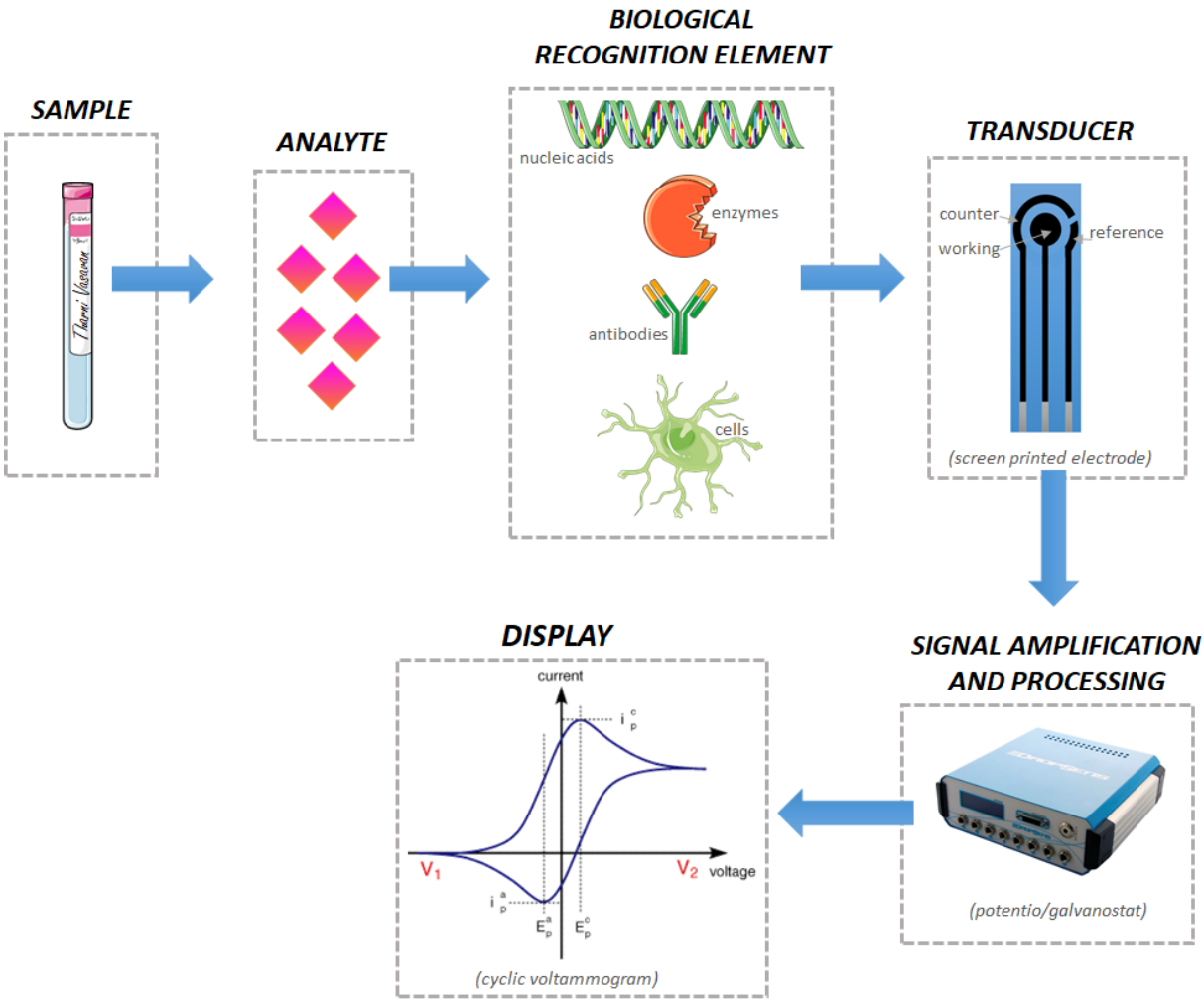

Figure 1.5: Schematic representation of the general elements of an electrochemical biosensor from sample to final result readout.

Electrochemical biosensors require a two- or three-electrode setup; the electrodes themselves are of great importance as they can determine how successful a biosensor is. A two-electrode setup consists of a working (or sensing) and a combined counter/reference (or auxillary) electrode. However, a three-electrode setup that has

an additional separate reference electrode is often preferred due to its increased stability (Liu, 2012). A three-electrode setup is often controlled by an instrument known as a potentiostat, which has the role of regulating the difference in potential (the amount of energy required to move one unit of charge) between the working and reference electrode and measuring the flow of current between the working and counter electrodes. It is connected to a computer interface that can process this signal and display a readout of the measured current. Potentiostats can have varying operating voltages, accuracies, current ranges, sizes and signal processing methods, and therefore need to be chosen carefully depending on the reaction occurring at the biosensor and what its commercial use will be (Doelling, March 2000).

The reference electrode is commonly made from silver that has been coated with a layer of silver/silver chloride (Ag/AgCl). It is kept at a distance from the reaction site and has the important function of maintaining a well-known electrochemical potential (Grieshaber et al., 2008). As it passes a very minimal amount of current during the reaction, there is little lowering of potential due to electrolyte resistance or "iR drop", resulting in a stable potential at this electrode and compensation for iR drop across the whole solution. The working electrode is where the redox reaction takes place and is therefore often referred to as the cathode or anode depending on whether electron donation or acceptance occurs. The biological recognition element used in the reaction, particularly if it is an enzyme, is often immobilised onto the working electrode in order to increase storage stability, sensitivity, selectivity and reproducibility as well as reduce the reaction time (Sassolas et al., 2012). Methods for electrode modification to enable enzyme immobilisation include physical adsorption onto the surface of the electrode, covalent bonding, entrapment using a gel or polymer matrix, crosslinking the element to the electrode or use of a membrane to encapsulate it (Moehlenbrock and Minteer, 2011). The counter electrode does not participate in the redox reaction and instead serves as a source or sink of electrons which allows flow of current between itself and the working electrode. Both the working and counter electrodes are required to be highly conductive but also chemically stable to prevent electrode fouling; materials often used to make these electrodes are platinum, gold, carbon and silicon (Chaubey and Malhotra, 2002).

Biosensors are undergoing an era of miniaturisation to develop the already available microscale components into nanoscale. Nanostructural electrodes, particularly made of nanotubes, nanoparticles and nanorods, are thought to make more effective biosensors. This is due to a combination of the high surface area and provision of particularly active sites for electrochemistry on the recognition element, therefore allowing higher sensitivity and capture efficiency (Patolsky et al., 2006). Fabrication of electrodes using carbon nanotubes is common as they are less likely to be subject to electrode fouling due to their complex structures and are a highly conductive and strong material, although they have been reported to disintegrate with long-term use (Pasinszki et al., 2017). Another disadvantage of nanostructures is that the electrode fabrication technique is likely to have inconsistencies in uniformity even when standardised, which will cause slight variation in analyte measurements between assays (Liu, 2012).

1.2.4 Electrochemical detection techniques

The main types of electrical biosensors measure current generated from redox reactions, changes in electrical potential or changes in the conduction properties of the reaction solution: these biosensors are referred to as amperometric, potentiometric or conductometric respectively (Eggins, 2002). Each of these types of biosensor has its own advantages and disadvantages. Conductometric sensors are inexpensive and reproducible but require a large change in conductance for detection which gives rise to a larger window for inaccuracy. Potentiometric biosensors are governed by the Nernst equation and can continuously measure activity of a wide range of ions, however, are sensitive to interference from changes in pH and temperature.

1.2.5 Amperometric biosensors

Amperometric biosensors are the most commonly used type and importantly function linearly, i.e. the value of the current is directly proportional to the

concentration of the target analyte. Additionally, amperometric biosensors are relatively advantageous compared to the other two types as they possess the highest sensitivity and are more rapid and inexpensive (Mehrvar and Abdi, 2004).

The current generated from these sensors can be measured by a range of techniques which are widely described as voltammetry and amperometry. In amperometry, the electrode is held at a constant potential however in voltammetry, the current is measured as response of a varied applied potential (Eggins, 2002). In chronoamperometry, the potential is stepped up once in a square-wave fashion then kept constant until the end of measurement. There are different techniques within voltammetry, such as cyclic voltammetry where the applied potential is scanned back and forth between two fixed voltages at a specific scan rate, resulting in the measurement of the oxidation and then reduction of the electroactive species. Linear sweep voltammetry is simply the first half of a cyclic voltammogram with the applied potential only scanned in one direction. Differential pulse voltammetry can also be used for measurements, whereby a specific potential is applied as a pulse on top of the gradual linear sweep from one voltage to another (Eggins, 2002) (Figure 1.6).

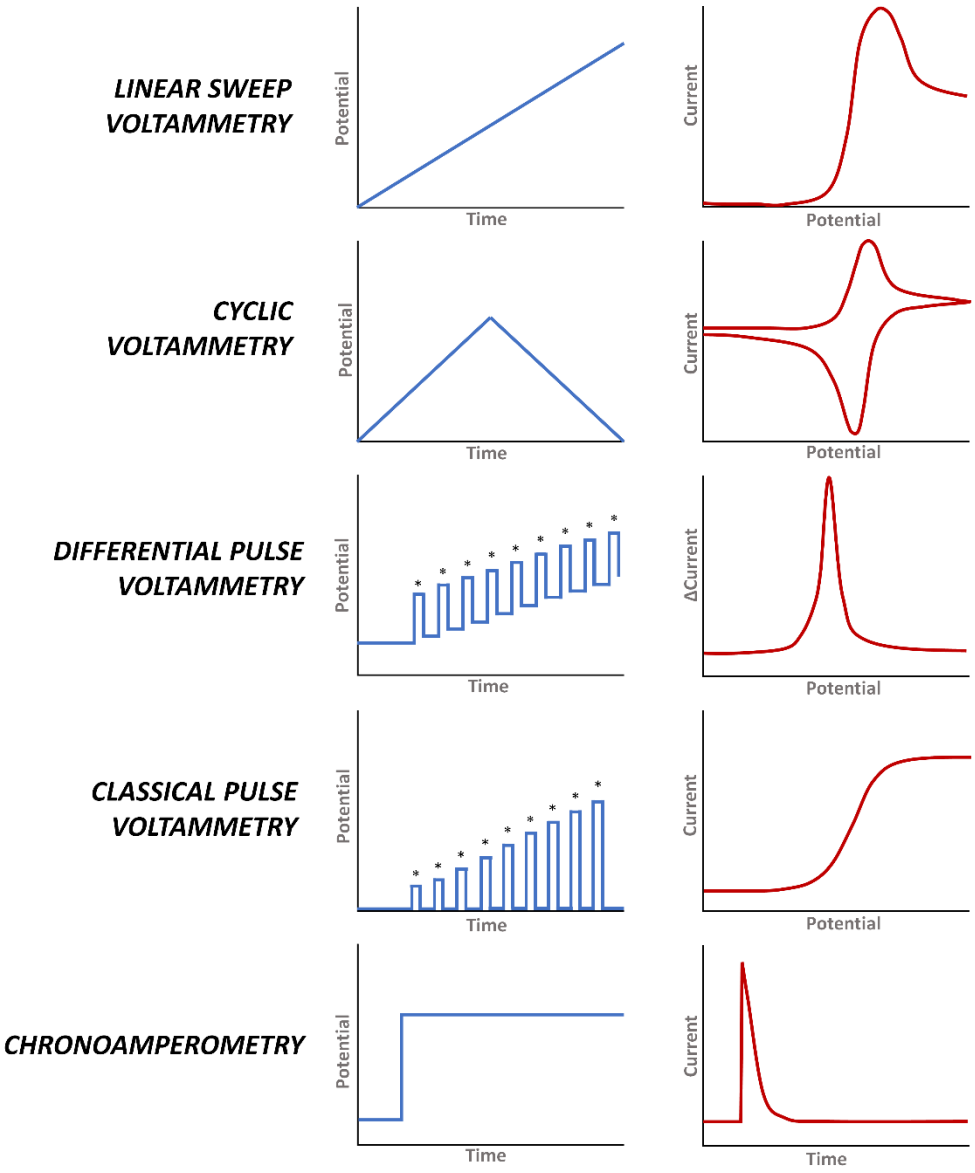

Figure 1.6: Panel of example graphs depicting different types of electrochemical measurement techniques. Methods of changing the applied potential are shown in blue and the resulting currents are shown side by side in red. Asterisks on the pulse voltammetry graphs display when current measurements are taken.

Amperometric sensors are well known for their amenability to miniaturisation and the utilisation of disposable electrodes, which make them ideal for measurements in a POC setting. To take advantage of their disposability, the electrodes used for amperometric biosensors are being increasingly screen-printed, both in commercial and experimental settings. This allows for mass production, improving cost-efficiency and standardisation between assays. However, they do allow interference

from other non-target analytes in the medium and depend on a consistently high concentration of oxygen in the medium throughout the reaction for the enzyme or coenzyme to act as an electron donor or acceptor. Therefore the current flow can be difficult to detect, and sensitivity and specificity may be low. In order to combat this problem, electrodes are often modified with artificial electron transferring agents known as electron mediators.

1.2.6 Electron mediators

Electron mediators act as a "shuttle" and move electrons from the redox reaction directly to the electrode surface to aid electrical communication (Figure 1.7). Electron mediators therefore allow the reaction to take place at a lower working potential, which reduces the likelihood of non-target analytes participating in the redox reaction and electrode fouling taking place (Chaubey and Malhotra, 2002). Some of the main mediators that have been extensively studied include quinones, methylene blue, ruthenium and ferrocene derivatives (Kim et al., 2013). Additionally, dyes such as methylene green, meldola's blue, azure A and B and toluidine blue O have been used for NADH-based sensors (Kumar and Chen, 2008, Zhu et al., 2007, Prieto-Simón and Fàbregas, 2004). The mediators themselves are specifically chosen so their redox potential is lower than the other electrochemically active species in the medium (Mehrvar and Abdi, 2004). Mediators are particularly useful if the redox reaction at the electrode requires a coenzyme such as NADH (the same coenzyme used in the enzymatic method of TSBA testing) that cannot be regenerated at the electrode surface without dramatically increasing the potential and therefore allowing the redox of other electroactive species that are normally present in human serum, such as catecholamines, uric acid and ascorbic acid (Kumar and Chen, 2008). Additionally, the regeneration of NADH at the surface of the electrode can also give way to electrode fouling due to the formation of NAD dimers on the electrode surface (Turner et al., 1987, Yuan et al., 2019). Mediators therefore allow NADH to be used as a coenzyme in the sensor without negatively impacting the sensor's efficiency.

The use of mediators in chemically modified electrodes has allowed the development of what is now termed 2nd generation sensors, however the most recent and advanced 3rd generation biosensors for diagnostic use are working towards going back to a direct electron transfer mechanism, although these are currently still under development and not available for commercial use (Das et al., 2016).

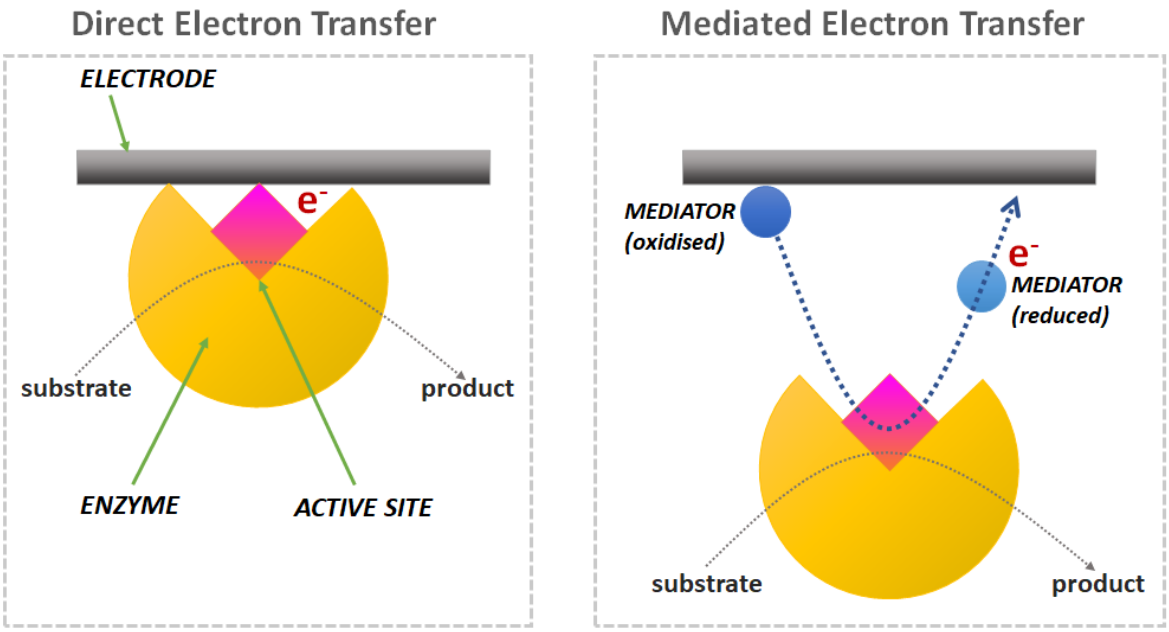

Figure 1.7: Schematic representation of direct electron transfer in the absence of a mediator and mediated electron transfer (mediator is depicted in blue).

1.2.7 Recent developments in creating an electrochemical bile acid biosensor

Possibly the first electrochemical method of bile acid sensing was by Ferri et al. in 1984, who used differential pulse voltammetry to determine the concentrations of conjugated and unconjugated CA in human bile (Ferri et al., 1984). Shortly after, amperometric techniques were used on human serum and plasma with glassy carbon electrodes that had been modified with immobilised 3α-HSD; the detection limit for the sensor used in plasma was 1µM however the full working range was not stated (Teodorczyk and Purdyt, 1990, Albery et al., 1987). In 1990, a microelectrode sensor was developed to detect dynamic bile acid activity for *in vitro* liver cell culture experiments; the sensor appeared to have adequate sensitivity the bile acids DCA, TCA and CA (Yu et al., 1990). Pulse amperometric detection of conjugated and

unconjugated bile acids in combination with reversed-phase high performance liquid chromatography (HPLC) has been successfully conducted with detection limits of ≤10 µmol/L in gallbladder bile and ileal fluid (Chaplin, 1995, Dekker et al., 1991). Determination of ursodeoxycholic acid (UDCA) purity has also been experimentally conducted using this method (Scalia et al., 1995). Flow injection analysis within HPLC using a potentiometric detector of CA concentrations has also been performed (Arias De Fuentes et al., 2000).

Concentrations of CA in bovine and ovine gallbladder bile has also been measured with detection limits of ≤3.3 µmol/L using hanging mercury drop electrodes and square wave stripping voltammetry (Yilmaz et al., 2015). A sensor designed for human urine had a total bile acid detection range of 2-100 µmol/L and utilised the enzymes bile acid sulfate sulfatase and β-hydroxysteroid dehydrogenase with measurement via cyclic voltammetry, however samples required dilution before testing and direct assays of urine were not successful (Koide et al., 2007). Yeast has been used in a biosensor to investigate the toxicity i.e. hydrophobicity of known concentrations of various bile acids by their oxygen metabolism behaviour using chronoamperometry (Campanella et al., 1996). A bare electrode sensor for detection of primary bile acids after they have been subjected to dehydration, which increases their redox reactivity and enables anodic oxidation, has also been reported (Klouda et al., 2018). Anodic electrochemical oxidation of CA with lead dioxide and platinum foil has also been demonstrated, however the process for this is significantly slower than those which utilise mediators (Medici et al., 2001).

The use of screen-printed electrodes (SPEs) has been introduced into bile acid sensing research. Bartling et al. (2009) used the components of the enzymatic method currently commonly used for clinical diagnosis to measure CA, TCA and TCDCA in bovine serum at concentration ranges of 0-200 µmol/L with iridium-modified carbon thick-film SPEs and cyclic voltammetry techniques (Bartling et al., 2009). Lawrance et al. (2015) spiked human serum with up to 150 µmol/L of TCA and used chronoamperometry on carbon SPEs were chemically modified using meldola's blue (MDB) by the manufacturer (Lawrance et al., 2015). The group who

developed the enzymatic technique, Zhang et al., have also further developed the reaction for use in a biosensor made from carbon SPEs modified with MDB and detection with differential pulse voltammetry (Zhang et al., 2016a). This device was able to sense human serum TCA concentrations ranging between 5 and 400 µmol/L and provided similar results to the commercially available enzymatic assay commonly used in clinical laboratories (Zhang et al., 2016a). Most recently, this group have further developed this sensor to have further increased sensitivity to TCA concentrations with detection within a working range of 5-150 pmol/L in human serum that has been diluted 106-fold (Tian et al., 2018). This sensor used ruthenium as an electron mediator which was prepared in a solution with 3α-HSD and NADH, added to the diluted serum and subsequently measured via chronoamperometry on a bare SPE (Figure 1.8) (Tian et al., 2018).

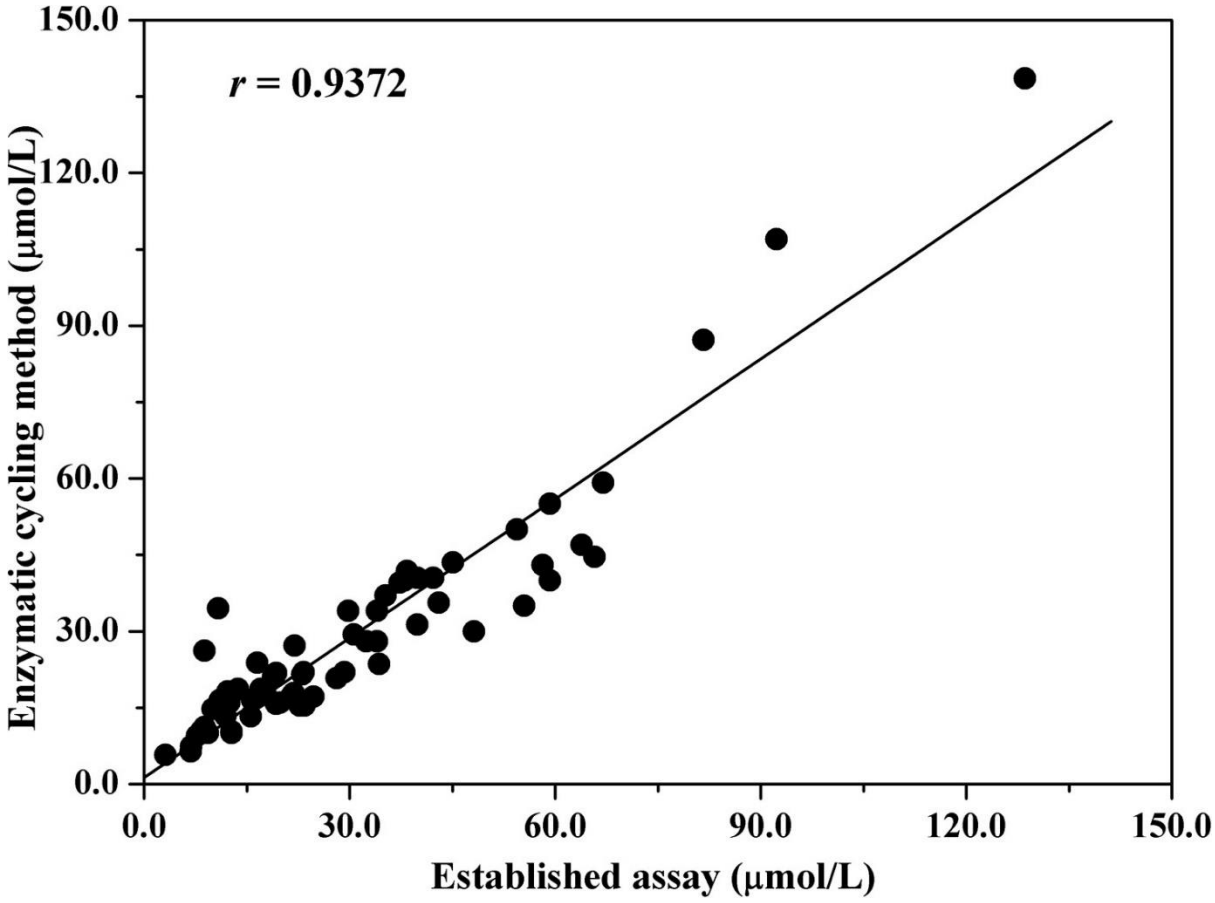

Figure 1.8: Graph from Tian et al.'s publication reporting an indirect electrochemical biosensor for bile acids. Results taken from sera using their biosensor ("established assay") are compared to the results of the enzymatic method conducted in a clinical laboratory (Tian et al., 2018)

Although there has been research and development towards a biosensor that successfully detects TSBA concentrations with large working ranges, there has been very little progress towards finding optimal methods for chemical modification of electrodes to enable commercialisation and implementation of such a biosensor in the clinic. Given the pertinence of the most recent findings regarding thresholds of TSBA concentrations for indicating the risk of IUD and the necessity to manage patients with TSBA concentrations of ≥100 μmol/L to prevent an IUD occurring, a bile acid-detecting biosensor that can sensitively detect bile acids around this range and yield rapid results in a POC setting would dramatically improve clinical management of these patients.

1.3 Treatment of ICP

The most common pharmacotherapy currently used to treat ICP is UDCA, a hydrophilic bile acid which is present in trace amounts in humans and has been identified in large amounts in bear bile in its taurine-conjugated form. There is a large amount of evidence that UDCA therapy significantly improves maternal outcomes in cases of ICP. In observational studies investigating UDCA treatment for ICP, pruritus and deranged liver function markers improved upon initiation of the drug (Diaferia et al., 1996, Davies et al., 1995, Parízek et al., 2016, Zapata et al., 2005, Berkane et al., 2000, Ambros-Rudolph et al., 2007, Palma et al., 1997, Deveer et al., 2011). There is evidence that the maternal serum bile acid profile of women with ICP is significantly altered by UDCA therapy: CA and CDCA concentrations are significantly decreased and the glycine:taurine conjugation ratio that is reversed in women with ICP compared to uncomplicated pregnancies is normalised (Brites et al., 1998, Mazzella et al., 2001). Recent retrospective data has showed that women with severe ICP who had been treated with UDCA had similar outcomes to a matched cohort with mild ICP, although the median peak TSBA concentration of the former group was 56.21 μmol/L and therefore below the 100 μmol/L threshold for substantially increased risk of adverse fetal outcomes (Yang et al., 2019). There is evidence that UDCA therapy is more successful for some women with ICP than others i.e. many women are unresponsive to the drug; the reasons for this are

unknown but genetic factors, dosage and gestation at diagnosis have been postulated as possible causes (Williamson and Geenes, 2014). However, measurements of individual bile acids in serum have demonstrated that UDCA becomes the principal bile acid in all UDCA-treated patients, forming 60% of the TSBA and significantly decreasing the proportion of CA and CDCA (Manna et al., 2019).

In contrast, there is relatively little published data determining whether UDCA is beneficial for the ICP-affected fetus. ICP is known to create a transplacental primary bile acid gradient from the mother to the fetus, leading to accumulation of bile acids of a pathological concentration in the fetal compartment (Monte et al., 1995). Several studies have demonstrated that UDCA lowers deranged TSBA concentrations in the fetus as well as the mother, reducing the impaired transplacental gradient and facilitating placental transfer of bile acids from the fetal to the maternal compartment (Geenes et al., 2014b, Estiú et al., 2015, Brites, 2002).

The first phase of a large randomised controlled trial of UDCA vs. placebo in 2012 by Chappell et al. showed a significant reduction in pruritus and a decrease in meconium-stained amniotic fluid with UDCA treatment, however the number of participants in each cohort were too low to confirm its efficacy at reducing the rate of other adverse perinatal outcomes (Chappell et al., 2012). Since then, the same group have recently published the results of a larger randomised controlled trial of UDCA vs. placebo on 322 and 318 women respectively (Chappell et al., 2019). This study measured the primary composite perinatal outcome of IUD, preterm delivery (i.e. iatrogenic and spontaneous preterm delivery) and neonatal unit admission, as well as the secondary maternal outcomes of liver function marker concentrations, pruritus and delivery details. Although there was a reduction of meconium-stained amniotic fluid as in the previous phase of the study, it was found that UDCA did not change the composite primary outcome in this cohort, therefore suggesting that it has a minimal reduction effect on ICP-associated adverse perinatal outcomes (Table 1.1). UDCA treatment did, however, significantly reduce pruritus and ALT concentrations as well as the estimated blood loss at delivery (Chappell et al., 2019). It is noteworthy that only 73 of the participants who received UDCA therapy had severe

ICP, and 23 of this subgroup had TSBA concentrations of ≥100 µmol/L, suggesting the group most at risk of adverse outcomes was small in number and further investigations with larger numbers severe ICP cases are required to assess the efficacy of UDCA on perinatal outcomes in severe disease (Chappell et al., 2019).

	Ursodeoxycholic acid (n=322)	Placebo (n=318)	Adjusted effect estimate (95% CI)	p value
Perinatal death, preterm delivery,* or neonatal unit admission	74 (23%)	85 (27%)	RR 0·85 (0·62 to 1·15)	0·28
In-utero fetal death	1 (<1%)	2 (1%)	RR 0·51 (0·04 to 6·25)	0·60
Preterm delivery*	54 (17%)	65 (20%)	RR 0·79 (0·57 to 1·10)	0·17
Known neonatal death up to 7 days after birth	0	0	..	..
Neonatal unit admission for ≥4 h	45 (14%)	54 (17%)	RR 0·81 (0·58 to 1·13)	0·21
Livebirth	321 (>99%)	316 (99%)	..	..
Gestational age at delivery, weeks	37·6 (37·1–38·1)	37·4 (37·0–38·1)	Median difference 0·1 (0·0 to 0·3)	0·065
Birthweight, g	3105 (2775–3390)	3040 (2660–3320)	Median difference 94·0 (18·7 to 169·3)	0·014
Birthweight percentile†	59·3 (28·4)	56·3 (27·8)	..	..
<10th percentile	16 (5%)	18 (6%)	RR 0·89 (0·47 to 1·69)	0·73
<3rd percentile	7 (2%)	7 (2%)	RR 1·09 (0·38 to 3·12)	0·88
Mode of delivery				
Spontaneous vaginal (cephalic)	193 (60%)	182 (57%)	RR 1·04 (0·91 to 1·20)	0·56
Vaginal (breech)	1 (<1%)	3 (1%)	..	..
Assisted vaginal (cephalic)	21 (7%)	35 (11%)	..	..
Pre-labour caesarean	71 (22%)	62 (19%)	..	..
Caesarean	36 (11%)	36 (11%)	RR 1·00 (0·68 to 1·46)	1·0
Presence of meconium-stained amniotic fluid	34 (11%)	52 (16%)	RR 0·65 (0·43 to 0·98)	0·040
Apgar score at 5 min after birth‡	9·0 (9·0–10·0)	9·0 (9·0–10·0)	Median difference 0 (–0·4 to 0·4)	1·0
Apgar score of <7 at 5 min after birth‡, n/N (%)	8/321 (2%)	7/316 (2%)	..	..
Umbilical cord blood sampling, N	112	102	..	..
Umbilical arterial pH	7·2 (0·1)	7·2 (0·1)	Mean difference –0·02 (–0·04 to 0·01)	0·18
Nights in the neonatal unit§	5·5 (3·0–13·0)	6·0 (2·0–16·0)	Median difference 0 (–3·2 to 3·2)	1·0
Main diagnosis for first neonatal unit admission				
Prematurity, n/N (%)	14/45 (31%)	17/54 (31%)	..	..
Respiratory disease, n/N (%)	16/45 (36%)	15/54 (28%)	..	..
Infection suspected or confirmed, n/N (%)	5/45 (11%)	7/54 (13%)	..	..
Other¶, n/N (%)	10/45 (22%)	15/54 (28%)	..	..

Data are n (%), median (IQR), or mean (SD), unless otherwise indicated; N is equal to the total number of infants in the group, unless otherwise indicated; <1% of observations are missing, unless otherwise indicated. Adjusted effect estimates and p values are shown for primary outcomes, and for secondary outcomes that were prespecified for testing in the published protocol.[11] RR=risk ratio. *Delivery at <37 weeks' gestation. †Calculated using the INTERGROWTH-21st tool.[19] ‡Data are for livebirths only. §Data are for infants with at least one night in a neonatal unit only. ¶A full list of diagnoses is given in the appendix (p 29).

Table 2: **Perinatal outcomes**

Figure 1.9: Figure taken from the Chappell et al. publication reporting the primary and secondary outcomes of a randomised controlled trial of ursodeoxycholic acid vs. placebo. RR = relative risk (Chappell et al., 2019).

Another common drug that has been used to treat ICP is S-adenosyl-L-methionine (SAMe), an amino acid metabolite which has been shown to regulate hepatocyte growth and apoptosis (Mato and Lu, 2007). Trials where small numbers of

participants have been randomised to either SAMe or UDCA have shown that UDCA had a greater normalising effect on deranged serum biochemistry and there was only a small significant improvement when both therapies were used in combination compared to administering UDCA alone (Roncaglia et al., 2004, Binder et al., 2006, Floreani et al., 1996, Nicastri et al., 1998). Rifampicin, an antibiotic that promotes biliary secretion but has also been suggested to be hepatotoxic with long-term use, has been shown to improve serum TSBA concentrations and transaminitis when used as an adjuvant therapy with UDCA when women were not responding to UDCA monotherapy (Geenes et al., 2015, Liu et al., 2018). UDCA is more beneficial than cholestyramine, a bile acid sequestrant, as well as dexamethasone, a corticosteroid, both of which have also been used for ICP treatment (Kondrackiene et al., 2005, Glantz et al., 2005).

UDCA treatment has therefore been shown to improve maternal outcomes in pregnancies complicated by ICP and is demonstrably more effective than other available pharmacotherapies, but its effect on perinatal outcomes for women affected by severe ICP requires further investigation (Gurung et al., 2013).

The early induction of labour is another form of treatment for ICP. IUD was thought to mainly occur between 37 and 39 weeks of gestation and therefore induction of labour to avoid an IUD event is currently conducted around 38 weeks if ICP cases are actively managed (Geenes and Williamson, 2009). Although this inevitably means the fetus will be at risk of complications that arise from the induction of labour, active management in most published studies have reported minimal adverse outcomes, even in severe ICP (Sharma et al., 2016, Wikström Shemer et al., 2013, Jain et al., 2013, Lee et al., 2008). More recent studies have suggested that the optimum gestational age for induction of labour is 36 weeks for patients who have extremely elevated TSBA concentrations of 100 μmol/L, which could lower IUD rates but simultaneously increase complications associated with preterm birth (Ovadia et al., 2019, Puljic et al., 2015, Lo et al., 2015).

1.4 ICP-associated spontaneous preterm labour

1.4.1 Risk of ICP-associated preterm labour

Although ICP-associated preterm labour (PTL) can be iatrogenic as a result of active management, the risk of spontaneous PTL is also known to increase with ICP. In a Swedish cohort of 96 women with severe ICP, 409 women with mild ICP and 185 controls, women with severe ICP were found to have an increased risk of spontaneous preterm birth (PTB) compared to the other two cohorts (OR 1.02, 95% CI 1.01-1.03) (Glantz et al., 2004). A prospective population-based cohort study using the United Kingdom Obstetric Surveillance System investigated 669 singleton pregnancies complicated with severe ICP and also found a significantly increased risk of PTB when compared to 2,205 control patients (adjusted OR 2.25, 95% CI 1.54-3.27) (Geenes et al., 2014a). A more recent systematic review of a larger cohort of 1936 patients with severe ICP from multiple global sites by Ovadia et al. (2009) showed that risk in these patients can be further stratified in 20 μmol/L increments of maternal TSBA concentrations (Ovadia et al., 2019). There was a higher risk of PTB in singleton pregnancies with maternal TSBA concentrations of ≥100 μmol/L than those with TSBA concentrations of 40-99 μmol/L, showing that this subset of severe participants are most at risk of a PTB (HR 2.77, 95% CI 2.13-3.61 vs. HR 1.31, 95% CI 1.06-1.69) (Ovadia et al., 2019).

1.4.2 Excitation-contraction coupling in the myometrium

To understand how PTB arises, the mechanisms underlying the process of birth at term in uncomplicated pregnancies must be understood. The central mechanical organ involved in birth or parturition is the uterus, which possesses a middle layer of smooth muscle known as the myometrium (Figure 1.10). The myometrium has both tonic and phasic properties, the former is necessary to accommodate fetal growth during gestation whilst the latter allows for the process of uterine contraction during labour (Young, 2007, Csapo et al., 1965). In order for the mechanical event of uterine contraction to take place, or indeed the contraction of any smooth muscle, a rise in the concentration of intracellular calcium ($[Ca^{2+}]_i$) and an increase (depolarisation) in the resting membrane potential must occur, a phenomenon which

is known as excitation-contraction coupling (Parkington et al., 1999b, Sanborn, 2000). During contraction, basal concentrations of $[Ca^{2+}]_i$ in the myocyte have been reported to increase from 150nm to 500nm due to the influx of exogenous Ca^{2+} and release of $[Ca^{2+}]_i$ from intracellular stores which results in the generation of an action potential (AP) (Word et al., 1991). Myocytes in the myometrium are known to have spontaneous activity in the absence of uterotonins i.e. endogenous or exogenous agonists of uterine contraction, this is thought to be due to a specialised non-contractile cell known as interstitial Cajal-like cells or uterine telocytes that act as a 'pacemaker' (Duquette et al., 2005).

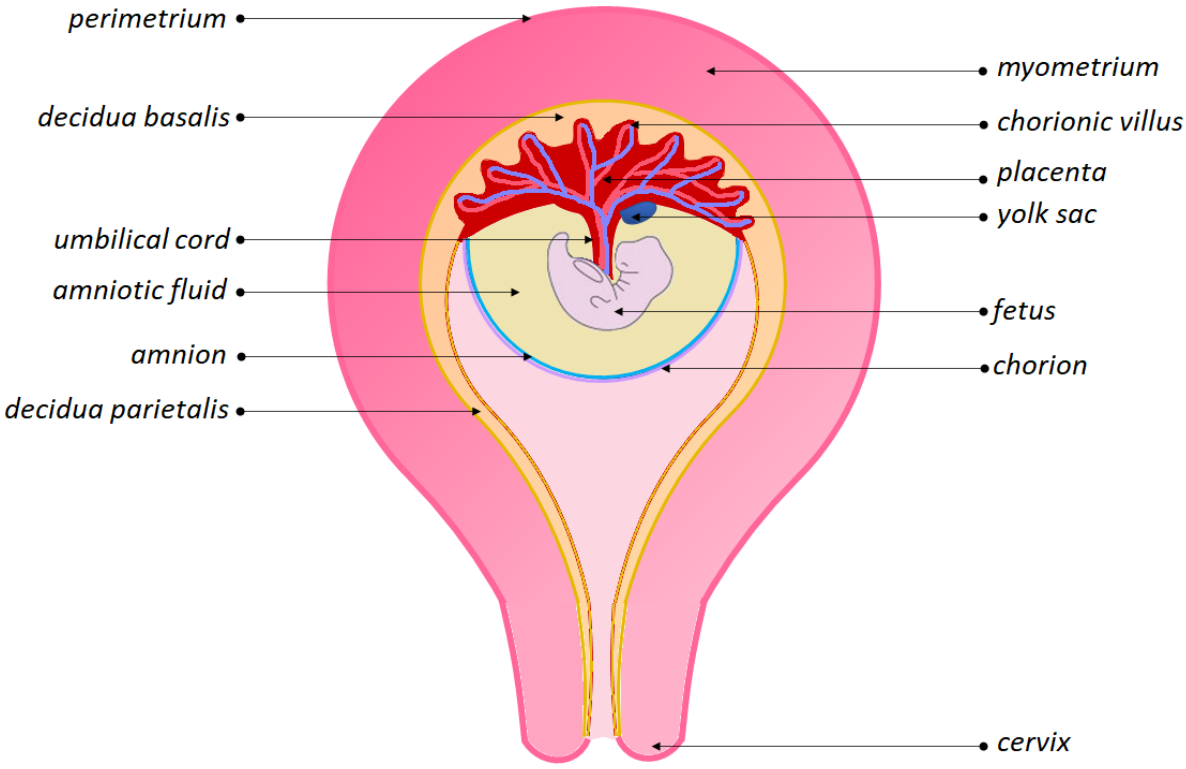

Figure 1.10: Diagram depicting the anatomy of the human uterus during pregnancy

According to microelectrode recordings of APs in non-labouring myometrium, AP waveforms can be one of two types: plateau or spike (Nakao et al., 1997). During plateau APs, which occur in most *in vitro* preparations of human myometrium, there is an initial time to peak is rapid and is followed by a plateaued decay (Parkington et al., 1999a). In contrast, spike APs often occur relatively quickly and in close proximity to each other, resulting in bursts of multiple spikes (Parkington et al.,

1999a). Spike APs are known to cause the myometrium to undergo progressive recruitment, meaning the area of excitation becomes larger within the burst. However, a dual model has recently been proposed in which the contraction of the whole uterus is aided by local APs globally increasing uterine wall tension which results in the mechanical induction of further APs in the tension-induced area (Young, 2016).

Both spike- and plateau-types of AP propagate from cell to cell of the myometrium via gap junction proteins; these are clusters of transmembrane channels which allow a phenomenon known as cell-to-cell coupling/communication whereby ions, small molecules and electrical signals can pass from one neighbouring myocyte to another (Bruzzone et al., 1996). The predominant type of gap junction protein expressed in myometrium is known as connexin43 (*GJA1* or Cx43) and has been established to be expressed at a low density at the time of quiescence and dramatically upregulated at the time of parturition (Balducci et al., 1993). Connexin40 and 45 have also been identified in the myometrium and have displayed differential properties of voltage-dependent conductance in models of other organs (Kilarski et al., 1998, Beblo et al., 1995, Veenstra et al., 1994). The increased connectivity between myocytes that result from gap junction upregulation is essential for transition of the uterus from a quiescent to an active state and allows for a synchronised uterine contraction and peristalsis to occur (Garfield et al., 1977). Gap junctions in myometrial tissue are known to develop spontaneously *in vitro* and the ability to from gap junctions is dependent the stage of myometrial maturation which are governed by cyclooxygenase and lipoxygenase pathways (Garfield et al., 1987).

In the resting myometrial cell, high concentrations of Na^+ and Ca^{2+} ions are found extracellularly whilst a high intracellular concentration of chloride (Cl^-) ions and potassium (K^+) ions is maintained (Sanborn, 2000). Ca^{2+} entry into the cell serves as the excitatory initiation of an AP which eventually leads to contraction. The majority of Ca^{2+} influx into the myocyte is due to voltage-dependent Ca^{2+} channels (VDCCs). In the uterus, L-type (where L stands for long-lasting) VDCCs form the functional majority of these channels, and this has been demonstrated via the

inhibition of the $[Ca^{2+}]_i$ increase and myometrial contraction by L-type VDCC blocking drugs such as nifedipine, magnesium (Mg^{2+}) and nitrendipine (Longo et al., 2003, Maigaard et al., 1986, Tasaka et al., 1991). L-type VDCCs are activated by depolarisation of the membrane potential and have a slow voltage-dependent inactivation (Jmari et al., 1986). More recently, T-type (where T stands for transient) VDCCs have also been shown to play a role in myometrial contraction. These channels are expressed in half of myocytes and their functional importance was demonstrated by the T-type blocker Mibefradil attenuating a $[Ca^{2+}]_i$ increase *in vitro* (Young and Zhang, 2005).

Although voltage-dependent channels have been shown to be the main source of extracellular Ca^{2+} entry, more recently store- or receptor-operated Ca^{2+} entry (SOCE or ROCE) has also been demonstrated as a source of $[Ca^{2+}]_i$ increase (Sanborn, 2007). The sarcoplasmic reticulum (SR), a membrane-bound Ca^{2+} store, encompasses a regulatory complex of Ca^{2+}-ATPases (SERCA), which sequesters $[Ca^{2+}]_i$ by moving it from the cytosol of the cell across the SR membrane to the lumen; inhibition of SERCA it is known to be inhibited by phospholamban (PLB). Transient receptor potential cation channel subfamily C (TRPC) channel homologue expression has been detected in the myometrium and are thought to contribute to SOCE and ROCE; attenuation of TRPC4 and TRPC6 function resulted in a decrease of G protein-coupled receptor (GCPR) -induced $[Ca^{2+}]_i$ increase and, in addition, TRPC3 expression is upregulated in response to myometrial stretch (Dalrymple et al., 2007, Chung et al., 2010, Ulloa et al., 2009). More recently, the STIM and Orai families of proteins are thought to mediate SOCE and ROCE; both families have been reported to be expressed in the labouring myometrium and Orai-1 expression was upregulated in response to cytokine administration (Chin-Smith et al., 2014).

In the majority of smooth muscle cells, there is an intracellular accumulation of Cl^-, the efflux of which results in membrane depolarisation (Leblanc et al., 2005). This occurs via Ca^{2+}-activated Cl^- channels (CACCs) which are expressed in one third of myocytes and cause Cl^- efflux in response to increased $[Ca^{2+}]_i$ and also allow excitability of the myometrium by enabling other VDCCs (Jones et al., 2004).

After the AP, efflux of K^+ ions results in membrane repolarisation and therefore K^+ channels play a major role in maintenance of the resting membrane potential of the myocyte (Brainard et al., 2007). The large-conductance Ca^{2+}- and voltage-sensitive potassium (BKCa) or Maxi-K channel is predominantly responsible for K^+ efflux and is known to reduce membrane excitability and inactivate VDCCs, therefore promoting uterine relaxation during pregnancy (Wang et al., 1998). Towards the end of gestation and during labour, this channel becomes insensitive to Ca^{2+} and therefore promotes a contractile state (Khan et al., 1997). ATP-sensitive potassium channels (K_{ATP}) also contribute to efflux and make up the K^+ channel component of the inward rectifier potassium (Kir6) channel family which is mediated by sulphonylurea receptors (SUR) (Inagaki et al., 1996). Downregulation of this channel occurs at later gestation to facilitate parturition and K_{ATP} agonists have been shown to inhibit oxytocin (OT)-induced contractions in the myometrium (Longo et al., 2003, Curley et al., 2002). Voltage-gated potassium channels (K_v) which are responsive to L-type VDCC activity, are known to be widely expressed in the myometrium, maintain membrane resting potential and K_{v4} channels in particular have been shown to be down-regulated by circulating oestrogen but not progesterone (P4) (Knock et al., 2001). Furthermore, blocking K_{v7} channels increases the frequency of contractions in the myometrium (McCallum et al., 2011). More recently, human ether-a-go-go-related gene (*hERG* or K_{v11}) channels, which play a prominent role in cardiac AP conduction, have been shown to attenuate contraction amplitude and duration in the myometrium before labour; increased hERG inhibition occurs during labour (Parkington et al., 2014). Small conductance Ca^{2+}-sensitive K^+ channels (SK) are a type of channel that is formed by a complex of α pore-forming subunits and constitutively bound calmodulin (CaM) at a CaM binding domain (Xia et al., 1998). Ca^{2+} binding to the SK channel results in a change in the channel conformation and results in mediation of gating (Xia et al., 1998, Lee et al., 2003).

In order to maintain the resting potential, a Na^+/K^+ ATPase pump acts to move Na^+ out of the cell and K^+ into the cell. During active labour, this channel is known to be downregulated in the myometrium to facilitate a contractile state (Esplin et al.,

2003). Voltage-dependent Na^+ channels (VDNCs) are thought to produce fast Na^+ currents which contribute to the inward Na^+ current during myometrial APs, however in general this channel is not well studied and its role in contraction is unclear (Ohya and Sperelakis, 1989). More recently, Na^+-activated leak channel non-selective (NALCN) has revealed to be upregulated during labour and contributes to membrane excitability (Reinl et al., 2015).

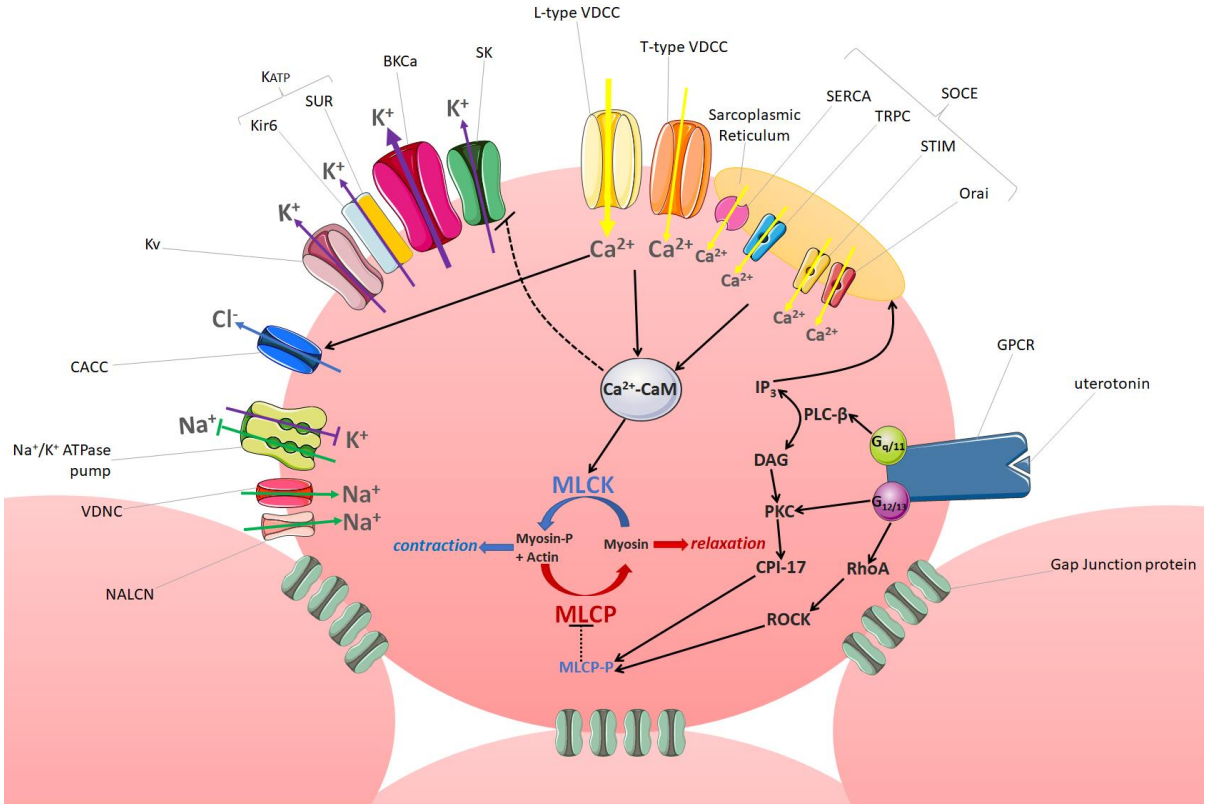

Figure 1.11: Schematic representation of the ion channels and pathways in the myometrial cell that lead to uterine contraction.

1.4.3 Mechanical myocyte contraction

The mechanical contraction of the myometrium occurs due to the sliding of actin and myosin filaments which results from an AP-induced cascade of events within the myocyte, therefore causing the generation of force. In order for actomyosin cross-bridge cycling to occur, actin needs to be converted into a filament form and attach to the cell membrane of the myocyte; therefore causing tension (Yu and López Bernal, 1998). In order for actomyosin cross-bridges to form, myosin is

phosphorylated by the Ca^{2+}-sensitive enzyme myosin light chain kinase (MLCK) which is activated by CaM bound in a complex with $[Ca^{2+}]_i$ (Word et al., 1994). Phosphorylated myosin and actin form complexes which convert ATP in order to induce the mechanical sliding of both types of filament. This process causes a further increase of $[Ca^{2+}]_i$ via the SR and the influx of extracellular Ca^{2+} via VDCCs which therefore acting as a positive feedback loop and further promoting the cross-bridge cycling between actin and myosin.

Release of $[Ca^{2+}]_i$ from the SR is caused by the binding of a uterotonin to a GPCR, resulting in binding of Gαq/11 to phospholipase C Beta (PLC-β) which increases free inositol triphosphate (IP_3) and 1,2-diacylglycerol (DAG) (Walsh, 1991) (Figure 1.11). Binding of IP_3 to its receptor on the SR results in the release of $[Ca^{2+}]_i$ (Luckas et al., 1999). The mechanism of DAG-stimulated $[Ca^{2+}]_i$ increase in the myometrium is less clear, however it is known that DAG is known to activate protein kinase C (PKC) (López Bernal et al., 1995). PKC has 12 known isoforms to date and has been shown to have conversely excitatory or inhibitory effects. Inhibiting PKC has been shown to decrease OT and endothelin-1 (ET-1) induced myometrium contractility however has also been shown to inhibit the PLC-β pathway and therefore decrease IP_3 production (Morrison et al., 1996, Breuiller-Fouché et al., 1998, Phillippe, 1994, Sanborn et al., 2005). Specifically, PKC is known to activate the smooth muscle-specific phosphorylation dependant inhibitor CPI-17, which in turn inhibits myosin phosphatase and leads to increased MLC phosphorylation and therefore enhanced contraction (Kitazawa et al., 2000) (Figure 1.11).

Myometrial contraction by uterotonins can also be Ca^{2+}-independent. Ras homolog family member A (RhoA), a G-protein from the Rho family of GTPases, activates RhoA-GDP to form RhoA-GTP which in turn acts through Rho-associated protein kinases (ROCKs) to inhibit myosin light chain phosphatase (MLCP). This leads to the prolonged phosphorylation of myosin by MLCK and enhanced tension (Moore et al., 2000, Moran et al., 2002) (Figure 1.11). This phenomenon has been described as calcium sensitisation (Amano et al., 1996). Interestingly, arachidonic acid, a

precursor of prostaglandin synthesis and also generated from DAG, has also previously been thought to activate ROCKs (Araki et al., 2001).

Relaxation of the muscle occurs via the dephosphorylation of myosin through myosin phosphatase and the uptake of $[Ca^{2+}]_i$ back into the SR and extrusion through the plasma membrane. The disassociation of the actomyosin complex results in the decrease of force (Walsh, 1991).

1.4.4 Phases of parturition: the role of progesterone

It has been stipulated that parturition occurs in four distinct phases. In phase 0 the uterus is quiescent, phase 1 refers to the activation uterine function, phase 2 refers to the stimulation of the uterus by uterotonins and phase 3 refers to the final uterine involution and expulsion of the fetus and placenta (Figure 1.12) (Lye et al., 1998). During phase 0, uterine quiescence is maintained by high circulating concentrations of the hormone P4 which is initially secreted by the ovarian corpus luteum and later on, the placenta, and mediated by the P4 receptors PRA and to a higher extent PRB (Pieber et al., 2001, Csapo and Pinto-Dantas, 1965). This is contributed to, minorly, by parathyroid hormone-related peptide (PTHrP) which is stimulated by P4 (Ferguson et al., 1992). The beta-adrenergic agonist prostacyclin (PGI_2) and endogenous synthesis nitric oxide (NO) (an agonist of BKCa channels) have also been shown to inhibit myometrial activity (Lye and Challis, 1982, Chwalisz and Garfield, 1997). The combination of these agents, mainly led by P4, results in the inhibition of $[Ca2^{+}]_I$ release via increased cAMP or cGMP (Vannuccini et al., 2016).

The transition from quiescence to the initiation of parturition (phase 1) is a complex process which has been shown to be due to a switch from anti-inflammatory to pro-inflammatory pathways due to a functional withdrawal of P4, whereby high circulating concentrations of P4 are sustained although its bioactivity decreases (Csapo and Pinto-Dantas, 1965). High bioactivity of P4 during quiescence causes the antagonism of transcription factors Nuclear Factor kappa-light-chain-enhancer of activated B cells (NF-ƙB) and activator protein 1 (AP-1) which are known to aid transcript of proinflammatory cytokines and chemokines such as interleukin 1, 6 and

8 (IL-1, IL-6, IL-8), prostaglandin-endoperoxide synthase 2 or cyclooxygenase 2 (*PTGS2* or COX-2) and chemokine ligand 2 (CCl2) (Hardy et al., 2006, Loudon et al., 2003, Dong et al., 2009, Shynlova et al., 2008). P4 also maintains uterine quiescence via the increase in expression of zinc finger E-box-binding homeobox 1 transcription factor (ZEB1) and ZEB2 (Renthal et al., 2010). During phase 1 there is also a decrease in ligand binding to PR, primarily PRA, with P4 in a nuclear P4/PRA complex in association with an increase in the P4 metabolising enzyme 20α-HSD which results in the activation of Cx43 transcription (Nadeem et al., 2016, Nadeem et al., 2017).

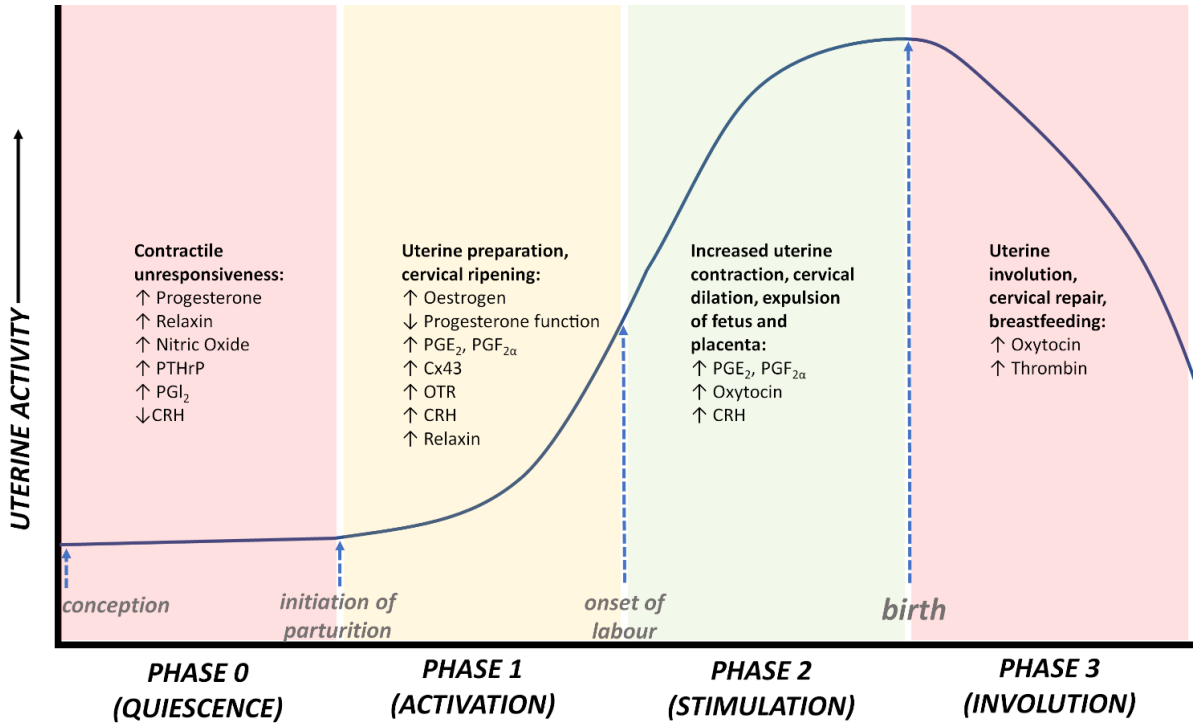

Figure 1.12: Schematic representation of uterine activity during the four phases of parturition and the change in signalling molecules during each phase.

1.4.5 Contraction-associated proteins

Cx43, oxytocin receptor (OTR), prostaglandins and their receptors are part of a group described as "contraction-associated proteins" (CAPs) which have an increased production during phase 1 of parturition and promote the contraction of the myometrium (Chow and Lye, 1994). Myometrial stretch during phase 2 upregulates

the expression of CAP genes, which is thought to explain the high incidence of PTL in multifetal pregnancies (Lye et al., 1998, Turton et al., 2013, Lye et al., 2001).

The hormone OT in an extensively studied stimulant of uterine contraction (Arrowsmith and Wray, 2014). Plasma concentrations of OT are known to rise during parturition, likely via a pulsatile manner of secretion from the pituitary gland and local secretion from the amnion, chorion and decidua (Blanks and Thornton, 2003, Chibbar et al., 1993) (Figure 1.10). OT receptor (OTR), a GPCR which leads to $[Ca^{2+}]_i$ mobilisation when activated, is known to be exponentially upregulated during gestation which allows the myometrium to be extremely sensitive to OT at the time of parturition (Kimura et al., 1992). Expression of OTRs is known to be increased in PTL as well as full-term labour (Fuchs et al., 1984). OTRs are also differentially expressed throughout the uterus to aid peristalsis, with the highest expression observed in the fundus and a relatively low expression in the lower segment (Mitchell and Schmid, 2001). Regulation of OTR expression is thought to be contributed by circulating steroids; with oestrogen and cholesterol causing an upregulation whilst P4 causes a downregulation (Gimpl and Fahrenholz, 2000, Fang et al., 1996). Recently, activation of the OTR pathway has also been shown to modulate myometrial contractions by inhibiting Na^+-sensitive K_{ATP} channels and therefore preventing K^+ efflux (Ferreira et al., 2019).

Some prostaglandins, particularly prostaglandin $F_{2\alpha}$ and E_2 ($PGF_{2\alpha}$ and PGE_2 respectively), are potent uterotonins that are known to increase in concentration prior to and during spontaneous labour in humans (Romero et al., 1996). $PGF_{2\alpha}$ and PGE_2 in the myometrium are mediated by the GPCRs FP and EP respectively which are known to have contractile effects via mobilisation of $[Ca^{2+}]_i$ (Abramovitz et al., 1994, Asbóth et al., 1996, Senior et al., 1993). Similar to OTR, prostaglandin EP receptors are heterogeneously expressed throughout the myometrium in order to aid peristalsis and have differential effects when activated. EP1 receptors are more predominant in the fundus of the uterus and their relaxation-inducing counterparts EP2 and EP4 are found in the lower segment of the uterus, therefore allowing uterine peristalsis (Challis et al., 2002, Astle et al., 2005). Prostaglandin receptors increase

$[Ca^{2+}]_i$ in the myometrium by activating PKC. There is also evidence that prostaglandins change membrane fluidity, thereby affecting membrane-bound ion exchangers and therefore $[Ca^{2+}]_i$ (Deliconstantinos and Fotiou, 1986). In addition to enhancing contractility, these prostaglandins are also thought to contribute to cervical ripening prior to delivery by activating enzymes that promote cervical remodelling (Kelly, 2002).

There is evidence that OT also stimulates contraction via mechanisms other than stimulating Ca^{2+} release. PGE_2 and $PGF_{2\alpha}$ synthesis is increased upon OT administration and OTR expression is downregulated after prostaglandin inhibition, suggesting that both families of uterotonins positively interact together in the myometrium to enhance uterine contractions (Jenkin, 1992, Wu et al., 1998). Similar to OT, oestrogen upregulates prostaglandin synthesis whilst P4 downregulates it (Challis et al., 2002). In addition, corticotropin-releasing hormone (CRH) is known to induce prostaglandin synthesis and vice versa, via decreasing levels of 11β-hydroxysteroid dehydrogenase type 2 (11β-HSD2), an oxygen-dependent enzyme that activates the stress-induced hormone cortisol which in turn stimulates further placental CRH production through positive feedback (Gao et al., 2008). Placental CRH is released throughout gestation and acts as a "clock" to signal when the initiation of parturition will take place (McLean et al., 1995).

During the quiescent stages of pregnancy, the cervix is tightly closed due to the strength derived from the collagen fibrils and extracellular matrix. During parturition, cervical ripening or softening takes place. This refers to the process of remodelling the cervix via degradation of the extracellular matrix and collagen by matrix metalloproteinases (MMPs) and collagenases respectively (Uldbjerg et al., 1983, Iwahashi et al., 2003, Nagase and Woessner, 1999). Relaxin is thought to increase the transcription of MMPs and inhibit tissue inhibitors of metalloproteinases (TIMPs), thereby increasing the degradation of cervical extracellular matrices (Palejwala et al., 2001).

1.4.6 Mechanisms of preterm labour

Preterm labour refers to the onset of labour at 20-37 weeks of gestation and affects approximately 7.3% of pregnancies in the UK with the highest global rates of PTB observed to be in India and China (Stock and Ismail, 2016, Blencowe et al., 2012). In 2 out of 3 cases, PTB is caused by spontaneous PTL due to an infection or idiopathic causes, with the remainder due to iatrogenic reasons (Goldenberg et al., 2008). PTB has been shown to be the global leading cause of infant mortality during the first four weeks of life (Blencowe et al., 2012). In addition to this, the implications of PTB for surviving infants can be carried through to adulthood; infants are often born with neurodevelopmental disorders and organ immaturity and PTB has been shown to be the most significant cause of "years of life lost" from a disability (Murray et al., 2012, Mwaniki et al., 2012). The attempt to delay or prevent PTL using pharmacotherapy is known as tocolysis. Although tocolytics have been extensively studied, an efficient tocolytic which works for all cases of PTL has not been discovered and they are often primarily used to delay labour for 48 hours in order to transport the mother to a tertiary centre with adequate neonatal intensive care facilities and administer antenatal corticosteroids to aid fetal lung maturation (van Vliet et al., 2014). Current methods of tocolysis have not demonstrably reduced adverse perinatal outcomes such as neonatal respiratory distress syndrome or neonatal demise (Haas et al., 2009). Tocolytics generally fall into the pharmacological categories of β-sympathomimetics or β2-adrenoreceptor agonists, Ca^{2+} channel blockers, NO donors, OTR antagonists and prostaglandin inhibitors (Younger et al., 2017).

Although a large proportion of spontaneous PTB occurs due to an unknown cause, some mechanisms have been elucidated. Chorioamnionitis is a common cause of PTB in earlier gestations, resulting in an inflammatory cascade leading to the production of cytokines and chemokines within the decidua and amnion. These in turn stimulate prostaglandin production which results in uterine contraction as well as cervical ripening and preterm premature rupture of membranes (PPROM) due to the action of MMPs and overriding the P4 "block" (Romero et al., 1998). The inflammatory response also results in activation of the stress response and therefore

CRH is released from the pituitary gland and placenta which further increases prostaglandin production due to the increase in cortisol (Yoon et al., 1998).

The onset of PTL later on in gestation is more likely to be due to myometrial stretch, placental senescence or oxidative stress (Keelan, 2018). It is thought that premature remodelling of the cervix also contributes to the mechanism of PTL that occurs later on in gestation (Vink and Feltovich, 2016). Relaxin gene expression is dramatically upregulated in patients with PPROM (Bryant-Greenwood, 1991, Petersen et al., 1992). Relaxin is an insulin-like hormone that is mainly secreted by the corpus luteum; women who have ovarian stimulation (and therefore have multiple corpora lutea) as part of assisted reproduction treatments have been shown to have an increased risk of PTB in association with serum relaxin concentrations (Weiss et al., 1993, Weiss et al., 1976). As discussed previously, relaxin plays a key role in cervical ripening. There is also evidence that relaxin increases inflammatory compounds such as natural killer (NK) cells, leukocytes and macrophages in the rhesus monkey endometrium as well as arteriole number (Goldsmith et al., 2004). In humans, it has been shown to stimulate separation of the pubis symphysis in preparation for parturition (MacLennan et al., 1991). Relaxin was previously shown to inhibit myometrial contractile activity in animal models *in vitro*, and was therefore thought to be beneficial as a tocolytic, however it has since been shown there is limited evidence of its efficacy and is species specific in its ability to halt contractions (Bain et al., 2013, MacLennan and Grant, 1991, Petersen et al., 1991).

1.4.7 Bile acid-specific characteristics of preterm infants

As the fetus is developing its hepatobiliary excretion system during pregnancy, there is impaired hepatic clearance and enterohepatic circulation (Macias et al., 2009, de Belle et al., 1979). Consequently, the fetus has a mildly hypercholanaemic phenotype as discussed in section 1.1.1. Due to the lack of intestinal flora in the fetus whilst *in utero*, only primary bile acids are able to be synthesised, although secondary bile acids synthesised by the mother are transferred across the placenta (Setchell et al., 1988). Additionally, there is an increased hydroxylation of bile acids

in order to increase hydrophilicity and aid clearance (Setchell et al., 1988). Preterm infants have a more cholestatic phenotype compared to full-term infants which is thought to be due to their more immature bile acid metabolism and excretion, and this results in the upregulation of alternative pathways of bile acid excretion to compensate for their accumulation in the fetal compartment. This is evidenced by data showing increased concentrations of primary bile acids in urine in early preterm infants and lower concentrations of ketonic bile acids in their urine whilst the reverse has been found in healthy neonates born at full-term (Yamato et al., 2001, Maeda et al., 2003). Bile acid profiling of infants who were born preterm showed higher median bile acid concentrations than that of full-term neonates (Zöhrer et al., 2016). Large concentrations of CDCA and hydroxylated bile acids such as 1β-hydroxylated bile acids and hyocholic acid have been found in preterm infant urine and meconium respectively, with the former persisting even 7 months postnatally (Nishiura et al., 2010, Kumagai et al., 2007). In addition, metabolomics analysis of amniotic fluid from women who had PTL has demonstrated that there were significant increases in concentrations of conjugated primary bile acids compared to women who underwent labour at full term (Menon et al., 2014).

Therefore, preterm infants often have a phenotype of hepatic decompensation (Beath, 2003). It is unclear, however, how elevated bile acid concentration and upregulation of alternative metabolism pathways in the fetal compartment contributes to preterm birth in these infants.

1.4.8 Mechanisms of ICP-associated preterm labour

Liver dysfunction outside of ICP has also been associated with PTL; diseases such as non-alcoholic fatty liver disease (NAFLD) and hepatitis B virus result in higher rates of PTL which is thought to be due to dysfunctional retinoid metabolism (Zhuang et al., 2017, Mawson, 2016). Additionally, gestational diabetes mellitus and preeclampsia, diseases which have an increased incidence in ICP-complicated pregnancies, are also known to cause higher rates of PTB (Deryabina et al., 2016, Morgan, 2016).

There is a large paucity of data regarding how and why ICP induces spontaneous PTL, although some studies have shown elevated bile acids increase contractility of the myometrium. Early experiments by Campos et al. (1986) demonstrated that prolonged intravenous infusion of CA to pregnant sheep, resulting in their serum bile acid concentration being elevated to 829 ± 305 μmol/L compared to the concentration of 24.4 ± 5.7 μmol/L observed in control sheep and caused all lambs to be delivered preterm (Campos et al., 1986). The same group also showed that rat myometrium has an increased contractility in response to *in vitro* administration of CA (Campos et al., 1988). Germain et al. (2003) elucidated a potential mechanism of how elevated bile acids could cause spontaneous preterm labour. In their study, patients diagnosed with ICP required a lower concentration of intravenous OT infusion to increase uterine contractions compared to controls (Germain et al., 2003). Although the patients in this study were not diagnosed using TSBA concentrations, *in vitro* exposure of myometrial strips and cells to CA also resulted in increased sensitivity to OT and OTR upregulation respectively, indicating that elevated bile acids activate the OTR pathway to increase contractility (Figure 1.13) (Germain et al., 2003). The observations of OT-induced increase contractile activity in myometrial strips from ICP cases was also confirmed in experiments by Isreal et al. (1986) (Israel et al., 1986). Interestingly, amniotic fluid taken from patients with ICP showed that $PGF_{2\alpha}$ and PGE_2 increases prior to spontaneous labour suggesting that increased prostaglandin production may also have involvement in ICP-associated PTL (Romero et al., 1996).

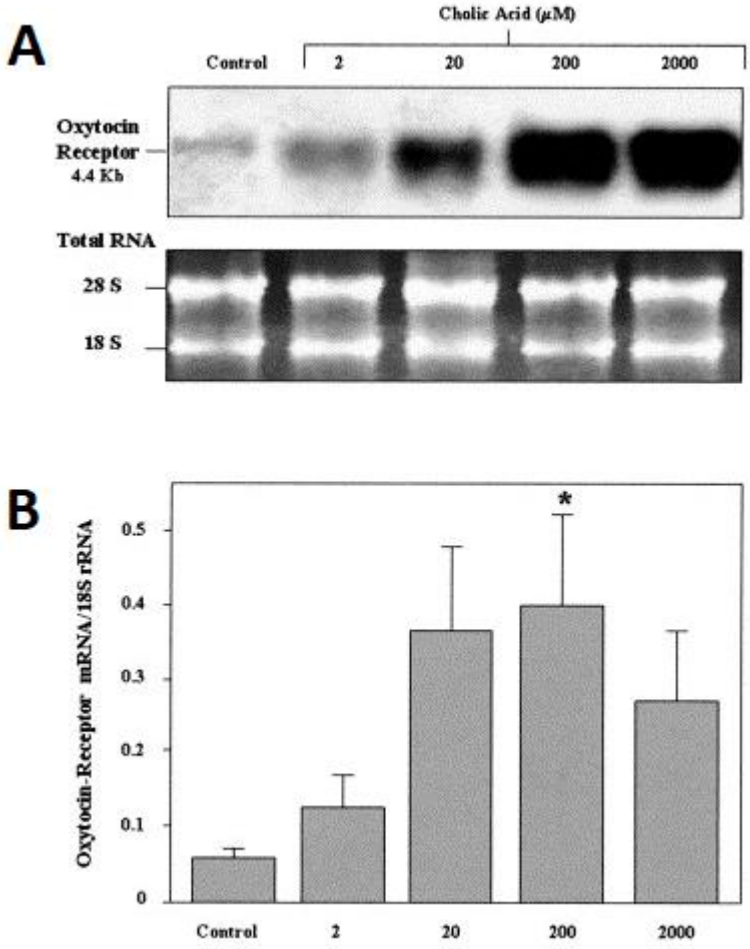

Figure 1.13: Figure taken from the Germain et al. publication depicting (A) a northern blot image for oxytocin receptor mRNA of cultured myometrial cells that were incubated with increasing concentrations of cholic acid and (B) graph showing mean concentrations of cholic acid and (B) graph showing mean concentrations of mRNA/18S rRNA from these experiments (n=5). Asterisk shows where p<0.05 (Germain et al., 2003)

1.4.9 Adverse outcomes due to placental pathologies

There is also evidence that the increase in ICP-associated PTL is triggered by placental oxidative stress due to the elevated bile acid concentration. There are distinct differences in the placental phenotype of pregnancies complicated by ICP. Placental tissue from ICP cases have increased morphological abnormalities such as smaller chorionic villi and blood vessels, decreased villous cavity volume, dense fibrotic stroma, thickened amniotic basement membranes and an increased number

of syncytial knots; the latter morphological characteristic was also observed in placental explant cultures exposed to TCA and TCDCA (Figure 1.12) (Geenes et al., 2011, Costoya et al., 1980, Du et al., 2014b, Wikström Shemer et al., 2012, Herrera et al., 2018) (Figure 1.14). Exposure of CA, TCA and DCA also causes dose-dependent vasoconstriction in isolated chorionic veins (Sepúlveda et al., 1991, Lofthouse et al., 2019). This has been supported by evidence of altered gene-expression profiles for blood vessel formation pathways and placental proteome alterations (Du et al., 2014a, He et al., 2014, Qin et al., 2017a). The hypoxia-inducible transcription factor HIF-1α, which is upregulated in preeclampsia, has also been shown to be upregulated by ICP with subsequent effects on glycometabolic gene regulation (Wei and Hu, 2014).

Placentas from rodent models of ICP have shown markers of apoptosis and increased oxidative stress; human placenta and serum samples have also shown DNA damage from oxidative stress and a higher oxidative stress index which has thought to result in modified mitochondrial gene expression in the placenta (Mella et al., 2016, Perez et al., 2006, Ozler et al., 2014, Wu et al., 2016). ICP severity has also been associated with serum and umbilical vein concentrations of irisin, a hormone which is increased in response to exercise and oxidative stress (Chen et al., 2019a). Irisin concentrations were also found to successfully predict the incidence of severe ICP in this study and thought to be responsible for the reduced placental oxidative stress between mild and severe ICP groups due to irisin's ability to induce metabolic protective pathways (Chen et al., 2019a). An upregulation of placental and serum neuropeptide Y (NPY), which is thought though to act as a vasoconstrictor in response to stress, was observed in women with ICP as was decreased vasodilator enzyme inducible NO synthase (Yue et al., 2018). Increased plasma ET-1, a vasoconstricting peptide, is also known to be markedly increased in women with ICP and associated with neonatal asphyxia and the incidence of PTB (Kebapcilar et al., 2010a). Vascular endothelial growth factor (VEGF) was also highly expressed as a response to *in vitro* hypoxic conditions of ICP placental tissue compared to controls (Zhang et al., 2015). A recent study showed lithocholic acid (LCA) administration induces endoplasmic reticulum (ER) stress in ICP placentas via activation of the P13K/Akt pathway; this was not observed during administration of relatively less

hydrophobic bile acids TCA or UDCA (Chao et al., 2019). In addition, the long non-coding RNA Linc02527was found to be expressed in fetal placenta and serum in association with TSBA concentration; Linc 02527 was shown to promote autophagy in an immortalised placental cell line (Hu et al., 2018).

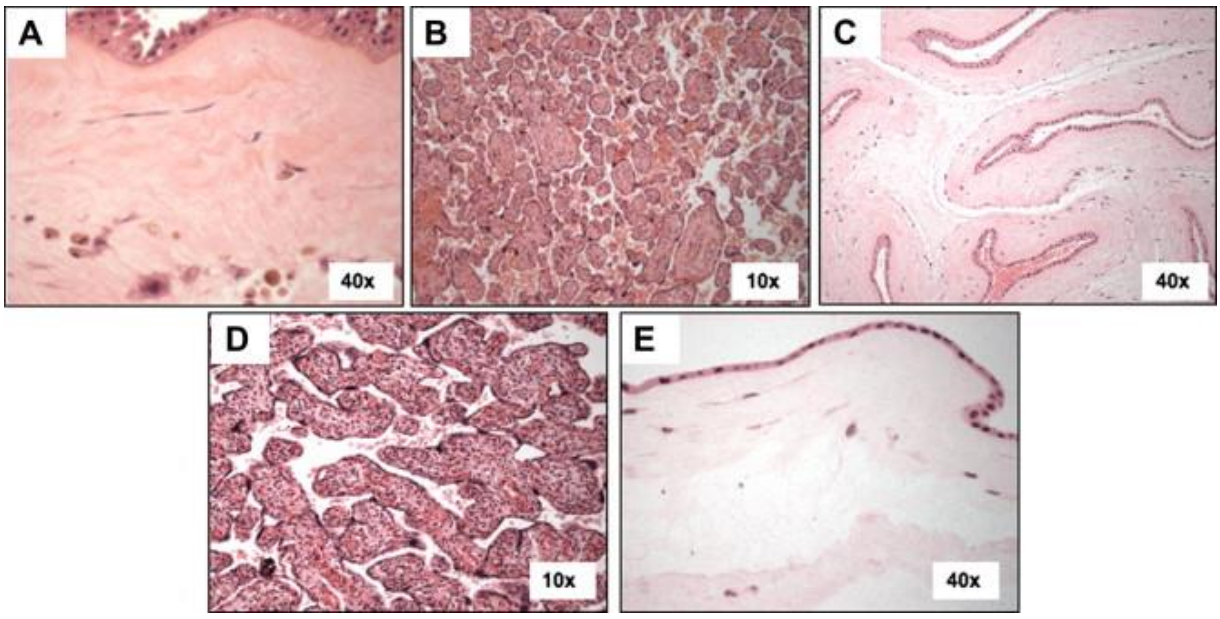

Figure 1.14: Figure taken from Geenes et al. publication of representative light micrographs of H&E stained villous trophoblast sections prepared from women with intrahepatic cholestasis of pregnancy (ICP; n = 28) and normal pregnancies (n = 12). Morphological abnormalities identified in the ICP samples included amnion cell columnarisation, thick glassy amnionic basement membrane and meconium histiocytes (A), small terminal villi (B) and focally thickened dense amniotic membranes (C). Terminal villi (D) and amnionic basement membrane (E) from normal placenta (Geenes et al., 2011).

An ICP-induced increase in markers of oxidative stress has also been observed in other tissues; serum levels of thiol and disulphide, oxidised and reduced forms of compounds that play a role in oxidative balance, were shown to be significantly lower and higher respectively in both mild and severe ICP, therefore indicating oxidative stress in these patients (Sanhal et al., 2018). The serum ischaemia modified albumin/albumin ratio (IMAR), used to measure oxidative status, was found to be significantly higher in women with mild ICP in comparison to controls (Tayyar et al., 2019). Plasma levels of the lipid peroxidation and oxidative stress

biomarkers 8-epimer of $PGF_{2\alpha}$ (8-iso-$PGF_{2\alpha}$) and glutathione peroxidase (Gpx) were found to be negatively associated with ICP severity, which was thought to demonstrate dysfunctional lipid peroxidation and therefore failure of antioxidant pathways (Hu et al., 2015).

These data together therefore suggest that exposure of elevated bile acid concentrations to the placenta causes morphological changes which may result in spontaneous PTL and/or IUD due to fetal asphyxia and intrauterine distress due to insufficient blood flow and placental ischaemia. In support of this hypothesis, placental expression of 11β-HSD2 is reduced in severe ICP specifically by elevated CDCA, therefore reducing levels of active cortisol (Martineau et al., 2014a). Placental levels of CRH, urocortin and wolfram syndrome 1 protein (which has a role in Ca^{2+} homeostasis) were higher in women who had early-onset ICP compared to late-onset ICP and controls (Xu et al., 2019). In contrast to this, one study found fetal serum cortisol to be higher in mild ICP and lower in severe ICP in comparison to controls; the authors postulated that this was due to suppression of the fetal stress response caused by elevated circulating bile acids (Wang et al., 2011).

There is evidence that ICP induces placental inflammation. Increased expression of interleukin (IL)-17, cluster of differentiation (CD)83+ dendritic cells and heat shock proteins have been reported in placentas from ICP cases, as well as lower expression of IL-35 and CD1a+ dendritic cells (Kong et al., 2018, He et al., 2014). Bile acids have also shown to activate the NF-ƙB pathway, resulting in placental inflammation due to the upregulation of vascular cell adhesion molecule-1 (VCAM-1), tumour necrosis factor-α (TNF-α) and IL-4 (Zhang et al., 2016b). A Disintegrin-like Metalloproteinase with ThromboSpondin motif 12 (ADAMTS-12), an enzyme with a role in remodelling vasculature and inflammation, was also found to be higher in ICP placentas (Oztas et al., 2016).

Inflammatory markers in other reproductive tissues are increased in ICP. Bile acids also cause the upregulation of VCAM-1 and inflammation (I)CAM-1 in human

umbilical vein endothelial cells *in vitro* (Qin et al., 2006). An increase in NK cells, NK T cells and interferon gamma has been reported in the decidua of ICP cases (Ling et al., 2007). Serum levels of high sensitivity C-reactive protein (hs-CRP), IL-4, IL-6, IL-12, IL-17, IL-31 and TNF-α are also higher in ICP patients; some of these cytokines have been associated with lower Apgar scores (Wang et al., 2019a, Basile et al., 2017, Kirbas et al., 2016, Zhang et al., 2018, Biberoglu et al., 2016). Levels of neopterin and the soluble receptor for IL-2 have been reported as increased in patients with ICP as well as reduced levels of immunoglobulins (Wang et al., 2004). Serum concentrations of Chinitase-3-like protein 1 (CHI3L1), a growth factor produced by activated macrophages and neutrophils, have been reported as significantly higher in patients with ICP, with an association between concentration of transaminases but not bile acids (Temel Yüksel et al., 2019). Other serum diagnostic tests of inflammation have been associated with PTB and disease severity in ICP such as mean platelet volume (MPV) (OR=2.68, 95% CI 1.13-6.32), circulating D-dimer (a product of fibrinolysis) and neutrophil-to-lymphocyte ratio (Yayla Abide et al., 2017, Oztas et al., 2015, Kebapcilar et al., 2010b, Kirbas et al., 2014).

Bile acid-induced activation of the OTR pathway resulting in $[Ca^{2+}]_i$ mobilisation and myometrial contraction, increased placental vasoconstriction and oxidative stress as well as activation of inflammation pathways induced by ICP are therefore likely to play a part in the increased incidence of spontaneous PTL observed in this disease.

1.4.10 UDCA treatment for ICP-associated preterm labour

As of yet, there have been no clinical trials of UDCA treatment of ICP with a reported reduction in the incidence of spontaneous PTL. A retrospective observational study of untreated vs. UDCA-treated women with ICP showed an increase in PTL in the UDCA-treated group which was attributed to the higher TSBA concentrations observed in this cohort (Joutsiniemi et al., 2015). A larger prospective randomised controlled trial of UDCA vs. placebo showed no beneficial effects of UDCA treatment on PTL, however the majority of women recruited onto

this study had mild ICP (Chappell et al., 2019). The results from this trial have been supported by previous findings from smaller cohorts (Palma et al., 1992, Palma et al., 1997, Glantz et al., 2005).

UDCA treatment has been shown to reduce the number of syncytial knots, collagen levels and villitis observed in placentas from ICP, suggesting it could have a protective effect in the placenta (Geenes et al., 2011, Wikström Shemer et al., 2012, Patel et al., 2014, Gruszczynska-Losy et al., 2019). UDCA perfusion also attenuated TCA-induced vasoconstriction and inhibited TCA uptake by OATP4A1 in the placental villi (Lofthouse et al., 2019). It also inhibited activation of the NF-ƙB pathway and subsequent placental inflammation by competing for bile acid receptor TGR5 (*Gpbar1*) binding (Zhang et al., 2016b). High doses of UDCA treatment in women with ICP resulted in a high expression of bile acid transporter breast cancer related protein (BCRP) in synctiotrophoblast cells of the placental villi, suggesting it aids in bile acid export from the fetus (Azzaroli et al., 2013). UDCA, unlike CDCA, did not repress 11β-HSD2 expression, suggesting another potential benefit of this drug (Martineau et al., 2014a). Placental oxidative stress in a mouse model of ICP was attenuated by an FXR agonist, showing that this bile acid receptor could also have a protective role through its activation (Wu et al., 2015).

UDCA has therefore shown some *in vitro* benefits against pathologies associated with PTL and therefore could provide protection from PTL induced by ICP, however further investigation is required to fully elucidate whether it is appropriate to use UDCA treatment to manage ICP-associated PTL and also to establish its mechanism of action *in vivo*.

1.5 ICP-associated intrauterine death

1.5.1 Hypotheses for the cause of IUD and measurement of cardiac parameters to assess fetal health

The exact cause of ICP-associated IUD is unknown; post-mortem examinations have observed that fetuses are appropriately grown and in the majority of cases there are

no cardiotocograph (CTG) abnormalities in the hours preceding the IUD event (Fisk and Storey, 1988). In addition to the placental phenotype in ICP causing PTL, it has been speculated that fetal hypoxia due to placental chorionic vessel vasoconstriction is a potential mechanism for ICP-associated IUD. Indeed, low Apgar scores as a measure of fetal asphyxia and fetal acidosis as determined by umbilical cord blood testing have both been associated with ICP and TSBA concentrations, the latter of which was a case report of IUD with a TSBA concentration of 220 µmol/L (Oztekin et al., 2009, Sterrenburg et al., 2014).

Acute hypoxia in the fetus can also be determined by alterations in the fetal heart rate (FHR). The FHR can be highly indicative of fetal well-being, with episodic accelerations and decelerations of FHR and reduced fetal heart rate variability (fHRV) being indicative of fetal distress due to chronic hypoxia and fetal acidosis (DiPietro et al., 2015). fHRV is known to increase with gestational age due to the maturation of the autonomic nervous system (ANS) and its increasing influence on FHR (Schneider et al., 2009). Gestational age and fetal behavioural or activity state are the main factors that impact fHRV. However due to its complexity, investigation into other influencing factors are still ongoing. There are no conclusive data about the effect of ICP on fHRV.

Another hypothesis for the cause of ICP-associated IUD is the incidence of a sudden fetal cardiac arrythmia. Fetal cardiac arrythmias are considered fairly common and are detected in 2% of all pregnancies during routine ultrasound (Bravo-Valenzuela et al., 2018). The majority of arrythmias are caused by ectopic beats that result from premature atrial contractions (PACs), a subset of arrythmias which are classed as non-sustained or transient and are generally considered to be benign (Donofrio et al., 2014). In contrast, sustained arrythmias, such as supraventricular tachycardia (SVT) and atrial fibrillation, are known causes of fetal hydrops and IUD (Batra and Balaji, 2019). Typically, echocardiography is used to detect fetal arrythmias. However using ECG as a diagnostic tool is the current gold standard to investigate electrical anomalies in cardiac rhythm via the investigation of cardiac time intervals (CTI) such as PR, QRS and QT interval lengths and fHRV (Strasburger et al., 2007).

Measuring the ECG in the fetus, however, has proven difficult and until the recent advancement of signal processing technology was not possible to do whilst *in utero* (Simpson, 2006).

Investigation of the CTIs mentioned above is useful for diagnosis of various disorders. An prolongated QTc interval length, a QT interval that has been corrected for heart rate, is a symptom observed in Long QT Syndrome and Torsades De Pointes and associated with arrythmia-induced sudden death in adults (Moss et al., 1985, Myerburg et al., 1997). An prolongated PR interval length is a clinical indicator for atrioventricular (AV) block, which has been shown to lead to the development of atrial fibrillation and a higher risk of mortality (Cheng et al., 2009).

1.5.2 Cardiac time interval lengths in ICP-complicated pregnancies

It is now well known that liver disease in adults can lead to cardiac dysfunction (Ludvigsson et al., 2014, Czul et al., 2013, Kempler et al., 1994) . Approximately 50% patients with liver cirrhosis develop a multifactorial syndrome known as cirrhotic cardiomyopathy, which can involve QTc interval prolongation, contractile dysfunction, cardiac hypertrophy, and dysfunctional cardiac hemodynamics (Zardi et al., 2010). Women with ICP have been reported to also have an prolongated QT interval length and an increased QT dispersion as measured by ECG, and these findings were associated with the severity of ICP (Kirbas et al., 2015). However, the same findings were not observed in fetuses of ICP pregnancies. A recent study showed no difference in QT interval length or ST segment depression between case and control fetuses upon examination of intrapartum ECGs (Joutsiniemi et al., 2019). However, the mean TSBA concentration in the case cohort was 15.9 µmol/L and most participants were UDCA-treated (Joutsiniemi et al., 2019).

Several studies have demonstrated ICP-associated changes the physiology of the fetal heart, with one of the most interesting findings being the change in PR interval length. In a cohort of patients with UDCA-treated mild ICP who had a mean TSBA concentration of 28.3 µmol/L, the fetal mechanical PR interval as measured by

echocardiography was significantly longer when compared to the control cohort (Figure 1.15) (Strehlow et al., 2010). Although a significant correlation between TSBA concentration and fetal PR interval length was not present, there was an association between the presence of ICP and the prolongation of fetal PR interval length when confounding factors were removed (Strehlow et al., 2010). A study with an untreated cohort of women diagnosed with ICP also found an prolonged fetal mechanical PR interval length (Rodríguez et al., 2016). TSBA concentrations were not measured in this cohort and ICP was diagnosed by persistent palm and sole pruritus, although all ICP women were stated to have significantly deranged serum concentrations of total bilirubin and transaminases (Rodríguez et al., 2016). Multiple linear regression showed that the prolongation in PR interval length persisted even after controlling for the liver dysfunction markers that had been measured (Rodríguez et al., 2016). An investigation that included women with both mild and severe ICP showed a significant association between disease severity and mechanical PR interval length (Kadriye et al., 2019). *In vitro* experiments on whole neonatal rat hearts showed a prolongation of PR interval length upon perfusion of TCA at a concentration of 400 µmol/L, an effect that was prevented by co-treatment with UDCA (Adeyemi et al., 2017).

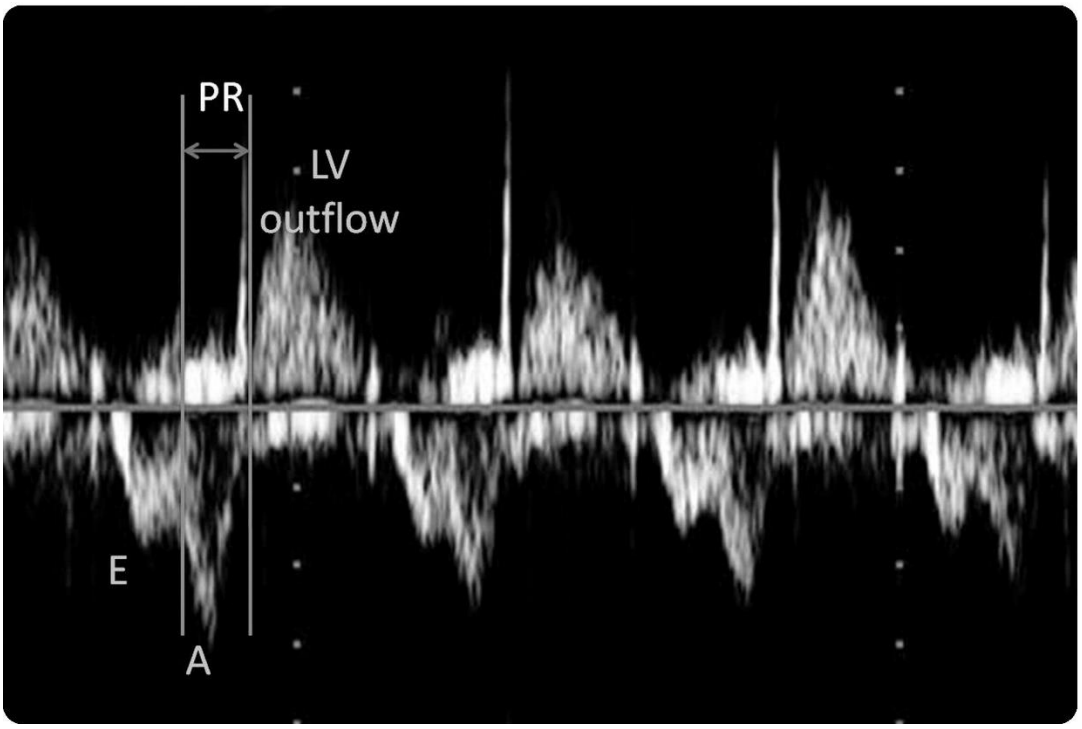

Figure 1.15: Figure taken from Stehlow et al. depicting a pulsed doppler tracing of combined mitral inflow and aortic outflow waveforms used to detect PR interval length in their study. The mechanical PR interval, which is shown between the 2 vertical lines, begins at the start of the A wave and ends at the initiation of systole. (Strehlow et al., 2010)

1.5.3 Fetal left ventricular dysfunction in ICP

Echocardiography analysis of severe ICP cases have shown evidence of left ventricular dysfunction in fetal hearts of mothers with ICP. Investigation into the fetal modified myocardial performance index (MPI) showed increased isovolumetric contraction and relaxation times (Henry and Welsh, 2015). The differences in left ventricular MPI (LMPI) in particular were found to be exacerbated in patients with severe ICP as opposed to mild; the majority of women in this study had not commenced UDCA treatment at the time of measurement (Henry and Welsh, 2015). In addition to the increase in LMPI values in ICP, a non-significant decrease in E/A ratio has been reported, suggesting further abnormalities in ventricular diastolic function (Sanhal et al., 2017). Contrary to previous data, the LMPI in this study was not affected by severity of ICP, however investigating the predictive ability of these

LMPI values on adverse perinatal outcomes yielded a statistically significant ROC curve (Sanhal et al., 2017). There was no difference between untreated and UDCA-treated disease cohorts (Sanhal et al., 2017). The aforementioned data are further supported by a more recent study which found an increased LMPI, isovolumetric contraction and relaxation times in a larger cohort with a mean TSBA concentration of 39.4 μmol/L and also found a significant correlation between adverse perinatal outcomes and LMPI; all participants in this study had been treated with UDCA (Ozel et al., 2018).

Patients with severe ICP have demonstrated increased fetal diastolic myocardial tissue velocities of the mitral and tricuspid annuli when compared to matched control and mild ICP cohorts, particularly the mean systolic and early and late diastolic motion velocities (Ataalla et al., 2016). The use of UDCA treatment in the ICP cases was not clarified (Ataalla et al., 2016). Left ventricular global longitudinal strain, diastolic and systolic strain rates were found to be significantly decreased in patients with ICP, this impairment was associated with severity of ICP (Fan et al., 2014). Again, it was not clear whether this cohort has been treated with UDCA (Fan et al., 2014). In addition to dysfunctional myocardial deformation, concentrations of N terminal pro-B-type Natiuretic Peptide (NT-proBNP), a marker of cardiac failure, in umbilical cord blood were found to be increased in ICP participants, a result that was again associated with severity of ICP (Fan et al., 2014). An increase in another marker of cardiac failure, cardiac troponin I (cTnI), has also been found to be significantly higher in a cohort of fetuses from ICP-complicated pregnancies; the mean maternal TSBA concentration in this cohort was 36 μmol/L (Zhang et al., 2009a). Concentrations of fetal cTnI and LMPI values were found to positively correlate with maternal TSBA concentration (Zhang et al., 2009a).

1.5.4 Cardiotocograph abnormalities and case reports in ICP

There have been numerous investigations that have found ICP-associated abnormalities in CTG tracings during parturition, some of which have preceded fetal demise. According to National Institute for Health and Care Excellence (NICE)

guidelines, a non-reassuring or abnormal CTG is defined by the observation of irregularities in baseline heart rate, baseline heart rate variability and/or heart rate decelerations and accelerations (NICE, 2017). Laatikainen et al. first reported the association between the increased occurrence of CTG abnormalities and severe ICP (Laatikainen and Tulenheimo, 1984). This finding has since been confirmed in multiple studies which have reported a higher incidence of fetal distress, abnormal FHR and non-reassuring events in intrapartum CTGs in women with ICP (Al Shobaili et al., 2011, Wong et al., 2008, Heinonen and Kirkinen, 1999).

Some ICP case reports have highlighted fetal arrhythmic activity detected via CTG monitoring and/or echocardiography. One report presented a patient with ICP that had tachydysrhythmia leading to atrial flutter confirmed by ultrasound; the severity of ICP and usage of UDCA treatment in this patient was not stated (Al Inizi et al., 2006). SVT with secondary hydrops fetalis was reported antenatally via echocardiogram in a patient at 28 weeks of gestation, this patient was later diagnosed with mild ICP and the SVT resolved with antiarrhythmic therapy; UDCA treatment was administered to treat the ICP (Shand et al., 2008). A similar case was also reported whereby the SVT only resolved after the fetus was delivered, demonstrating that fetuses from pregnancies complicated by ICP can be resistant to antiarrhythmic therapy (Altug et al., 2015). Lee et al. have described sudden fetal bradycardia in two cases diagnosed with TSBA concentrations of 79 μmol/L and 36 μmol/L respectively (Lee et al., 2009). The former case had a sudden prolonged deceleration after the onset of labor which resulted in fetal demise (Figure 1.16). The latter case resulted in a live birth however prolonged decelerations were observed during labor; UDCA treatment normalised this patient's TSBA concentration prior to labor (Lee et al., 2009). Fetal bradycardia has also been reported in a case of a pregnancy complicated by primary sclerosing cholangitis (PSC) which resulted in an extreme elevation of circulating TSBA concentrations (Nolan et al., 1994). One case of a woman diagnosed with severe ICP who had her TSBA concentrations lowered by UDCA treatment reported sudden fetal demise with CTG parameters shown as normal one day prior (Sentilhes et al., 2006). However, IUD in ICP is not always preceded by CTG abnormalities, as reported by one case where there was careful antenatal monitoring prior to the IUD event (Laatikainen and Tulenheimo, 1984).

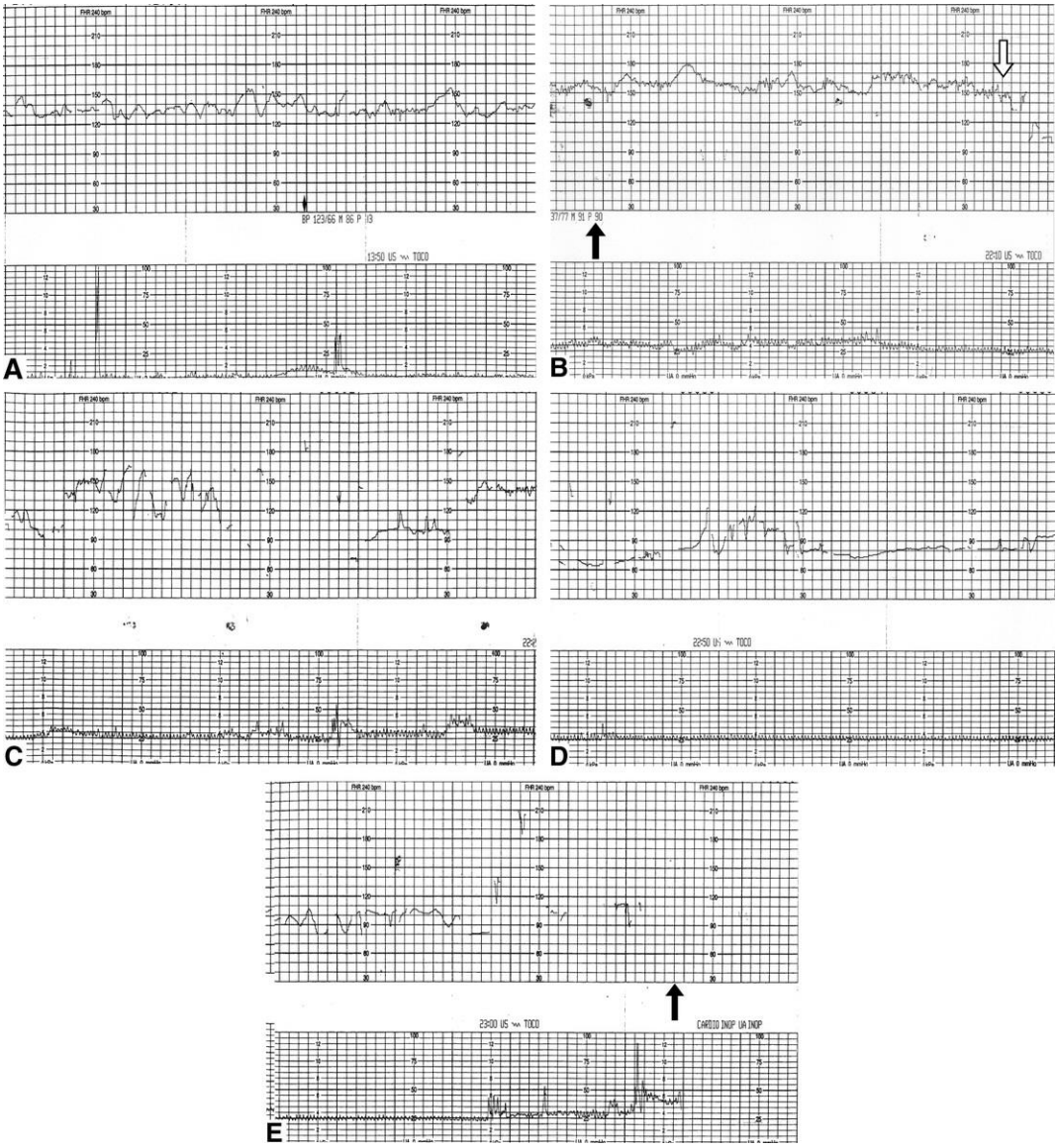

Figure 1.16: Images of a CTG trace taken from the Lee et al. publication depicting the onset of a prolonged deceleration (B) which eventually resulted in cessation of heart rate and fetal demise (E) (Lee et al., 2009).

1.5.5 Experimental evidence of bile acid-induced cardiac dysfunction

In addition to the above data that has been recorded in humans, there is also substantial *in vitro* evidence of elevated bile acid concentrations causing contractile dysfunction in the heart. Early experiments on rats demonstrated that injection of CA resulted in dose-dependent bradycardia (Joubert, 1978). Negative ionotropic effects were also observed upon administration of conjugated and deconjugated

primary and secondary bile acids on rat ventricular muscle resulted in a decrease in active tension (Binah et al., 1987). The transmembrane action potential in the ventricular myocytes was also found to be reduced which resulted from a disruption in the movement of inwards Ca^{2+} and outwards K^{+} currents (Binah et al., 1987). Administration of CA on mice ventricular muscle strips has also been demonstrated to cause a decrease in contractile tension (Zavecz and Battarbee, 2010). Perfusion of TCA in whole neonatal rat hearts results in slowing conduction velocity at the atrioventricular node, an effect which was attributed to abnormal modulation of T-type VDCCs (Adeyemi et al., 2017). Investigations on human atrial trabeculae have also shown that conjugated primary bile acids cause a dose-dependent increase in arrhythmic contractions; TCA in particular was the most effective in doing this (Rainer et al., 2013). Incubation of rat cardiac mitochondria with bile acids caused an induction in mitochondrial permeability transition pore (mPTP) opening, an effect that was more significant for the most hydrophobic bile acids tested (Ferreira et al., 2005).

Knocking out bile acid receptor genes *Fxr* and small heterodimer (*Shp)* in mice results in cardiac hypertrophy, bradycardia and prolongated PR and QT interval lengths, an effect that is mimicked upon injection of bile acids into wild type mice (Desai et al., 2017). Moreover, administration of the bile acid sequestering drug cholestyramine resulted in restoration of normal cardiac function in the double knockout mice (Desai et al., 2017). Inducing cholestasis in mice also resulted in bradycardia, hypertrophy and an increase in ejection fraction and cardiac stress markers (Desai et al., 2015). The same group also found “cholecardia” in these models, a term used to describe metabolic dysfunction in hearts subjected to a cholestatic state. A metabolic switch from fatty acid to glucose oxidation was observed based on gene expression studies, suggesting the presence of cardiac stress; this was again reversed by the normalisation of circulating bile acid concentrations (Desai et al., 2017).

Administration of TCA to early versions of a neonatal rat model consisting of a synchronously beating neonatal rat cardiomyocyte monolayer resulted in a dose-

dependent reduction in the rate and amplitude of contractions (Williamson et al., 2001). It is thought the alteration in Ca^{2+} dynamics caused by TCA, and other conjugated bile acids, is mediated via the acetylcholine muscarinic M2 receptor (Sheikh Abdul Kadir et al., 2010, Ibrahim et al., 2018). Further evidence from neonatal mouse ventricular cardiomyocytes has shown conjugated bile acids act partially through the Gi pathway, however unconjugated bile acids are potent agonists for Tgr5 (Ibrahim et al., 2018). A further developed version of the above model, consisting of co-culture of rat neonatal cardiomyocytes and myofibroblasts, has been established to reflect the transient expression of myofibroblasts observed in the fetal heart during the later trimesters of gestation (Figure 1.17) (Miragoli et al., 2011). Importantly, the TCA-induced dysfunction is not observed in a corresponding cardiomyocyte-only maternal model, which supports the majority of evidence pointing to a fetus-specific cardiac dysfunction in observed in ICP (Miragoli et al., 2011, Schultz et al., 2016).

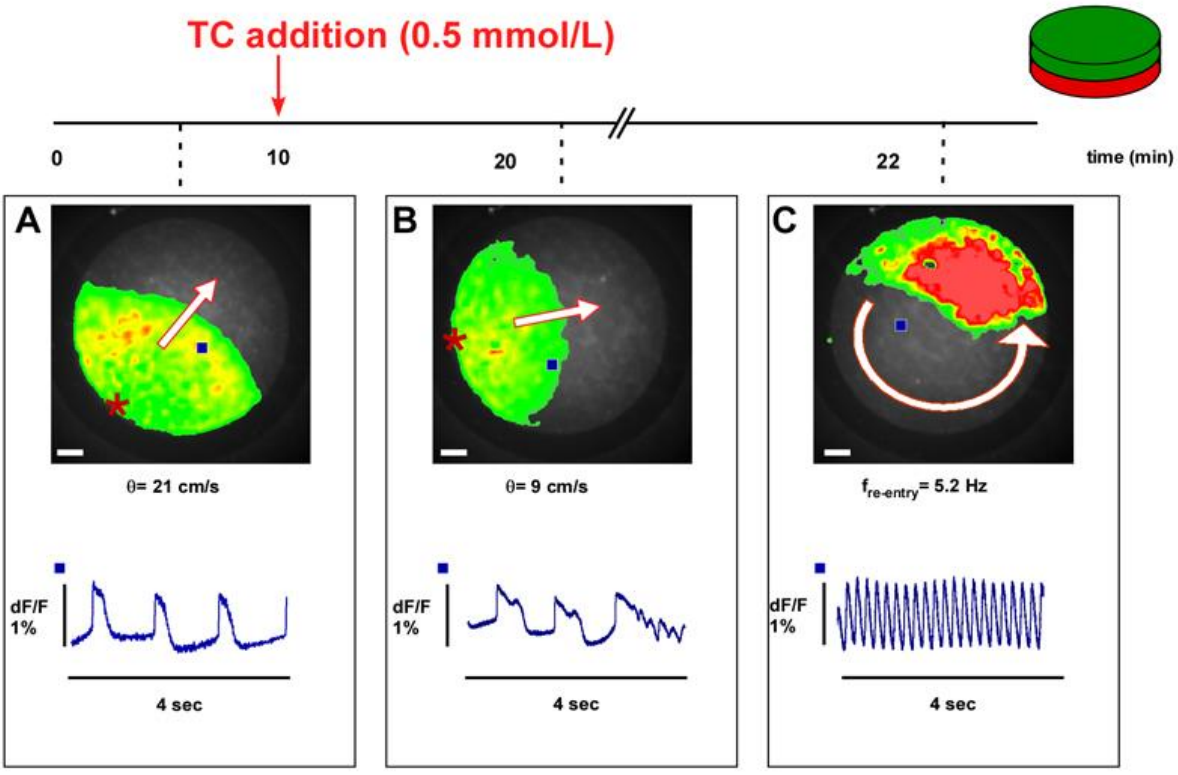

Figure 1.17: Figure of optical recording taken from the Miragoli et al. publication depicting (A) normal spontaneous electrical activity observed in a monolayer of cardiomyocytes coated with a monolayer of myofibroblasts (B) reduction of

conduction velocity upon administration of taurocholic acid (C) self-sustained re-entrant excitation arrhythmic activity (Miragoli et al., 2011)

1.5.6 UDCA treatment in ICP-induced fetal heart dysfunction

As demonstrated by data from echocardiography studies investigating LMPI and PR interval length, UDCA treatment does not appear to have a protective effect against ICP-induced increase in these parameters. Case reports have also not conclusively shown that UDCA improves ICP-induced CTG abnormalities, although this has not been addressed in a prospective study. The largest clinical trial thus far investigating the efficacy of UDCA on ICP-associated perinatal outcomes, demonstrated that UDCA treatment in ICP does not have a significant effect in preventing a composite outcome that included all preterm birth (iatrogenic and spontaneous), IUD and neonatal unit admission (Chappell et al., 2019). Although 76% of women enrolled onto this trial had mild ICP, a sub-group analysis of only women with serum bile acid concentrations ≥40 μmol/L did not demonstrate a difference in the composite outcome between UDCA and placebo treated women (Chappell et al., 2019). However, the number of women in this trial who had peak TSBA concentrations of >100 μmol/L prior to treatment was low (9 vs. 7 women in each group), which suggests further studies on UDCA treatment are required to form conclusions about this subset of women who are most at risk of an IUD (Chappell et al., 2019, Ovadia et al., 2019).

Although *in vivo* data has not demonstrated a beneficial effect of UDCA in fetal hearts of pregnancies complicated by ICP, very few studies have addressed this question in severe cases, and *in vitro* models suggest it has a protective effect against TCA-induced dysfunction. Incubation of neonatal rat cardiomyocytes with UDCA resulted in the attenuation of TCA-induced contractile dysfunction and changes in Ca^{2+} dynamics (Miragoli et al., 2011). This was also seen in preparations of human atrial trabeculae exposed to TCA (Rainer et al., 2013). A protective effect was also observed in TCA-induced slowing of ventricular conduction in perfusions of neonatal rat hearts, an effect that was thought to occur through targeting of

developmentally regulated T-type VDCCs (Figure 1.18) (Adeyemi et al., 2017). It has been shown that UDCA attenuates TCA-induced depolarisation of the resting membrane potential of neonatal myofibroblasts but not cardiomyocytes in a fetal heart model consisting of both cell types, an effect thought to be mediated by the SUR subunits of the K_{ATP} channel (Schultz et al., 2016, Miragoli et al., 2011). Evidence from a neonatal mouse ventricular cardiomyocyte model has shown UDCA to be a potent agonist for Tgr5 expressed in this cell type, although it did not decrease the contraction rate as seen in the above studies (Ibrahim et al., 2018). Other studies suggest UDCA acts by displacing more hydrophobic bile acids rather than having a direct action on the heart, as demonstrated by UDCA attenuating portal vein stenosis (PVS)-induced Ca^{2+} influx dysfunction in rat ventricular muscle strips but having no effect on acute exposure of CA to rat papillary muscle (Zavecz and Battarbee, 2010).

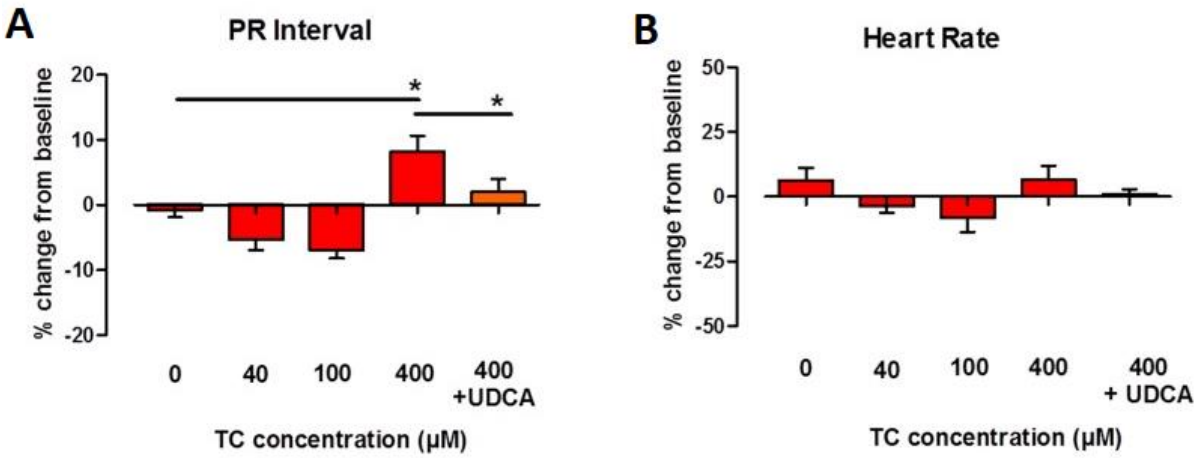

Figure 1.18: Graphs taken from the Adeyemi et al. publication depicting (A) percentage change of PR interval length from baseline (B) percentage change of fetal heart rate from baseline in neonatal rat hearts perfused with increasing concentrations of taurocholic acid and ursodeoxycholic acid (amended from (Adeyemi et al., 2017))

.

1.5.7 UDCA treatment of the heart in the absence of ICP

In the absence of ICP or elevated hydrophobic bile acids, treatment with UDCA has been shown to be protective against cardiac dysfunction in various animal models of

disease. Historic experiments by Ro *et al.* demonstrated the ability of UDCA to cease spontaneous and pharmacologically induced arrythmias in rabbit atria *in vitro* (Ro et al., 1986). UDCA treatment prior to induction of global ischemia and reperfusion injury in isolated rat hearts improved the recovery of myocardial contractility and decrease lactate dehydrogenase (LDH) concentrations (Lee et al., 1999). Taurine-conjugated UDCA (TUDCA) prevented apoptosis in rats that have had induced myocardial infarction (Rivard et al., 2007). In mice that had transverse aortic constriction, administration of TUDCA reduced ER stress markers, myocardial fibrosis and cardiac hypertrophy (Rani et al., 2017). TUDCA administration in mice with abdominal aortic aneurysm resulted in a reduction in the amount of apoptosis markers and ER stress chaperones (Qin et al., 2017b). In a rat model of $CoCl_2$-induced hypoxia, UDCA inhibited the activation of p53 and HIF-1α; transcription factors which have been implicated in dysregulation of cardiac function in hypoxia (Mohamed et al., 2017). It has also been shown to increase cell viability and reduce the effects of $CoCl_2$-induced hypoxia via upregulation of ERK and PI3K-Akt signalling pathways and inhibition of sphingomyelinases (SMases) in neonatal rat cardiomyocytes (Hanafi et al., 2016). The cytoprotective effects via the PI3k-Akt pathway has also been found in rats with left coronary artery occlusion due to inhibition of mPTP; UDCA was also found to improve post-ischemic recovery of myocardial ATP content in these rats (Rajesh et al., 2005). Mice with induced myocardial fibrosis had significantly decreased fibrosis, collagen I and III and TGFβ-1 expression upon administration of UDCA (Li et al., 2017). In mouse models of obesity, TUDCA has been shown to normalise mPTP opening, SERCA2α and PLB activity as well as contractile dysfunction in the heart (Ceylan-Isik et al., 2011, Turdi et al., 2013). In the Otsuka Long-Evans Tokushima Fatty (OLETF) diabetic model, TUDCA normalised mitochondrial phosphorylation enzymes and the mPTP opening threshold in rat cardiomyocytes (Miki et al., 2009). In a study investigating a range of bile acids on rat cardiac mitochondria, glycol-conjugated UDCA was found to be the least toxic and had the least significant effect on mPTP opening and membrane potential (Ferreira et al., 2005).

Use of animal models has therefore supported the use of UDCA treatment for cardiac injury caused by myocardial infarction, obesity and diabetes. In addition to

the above animal experiments, clinical trials investigating UDCA treatment in adults have supported its use in cardiac disease. In a randomised placebo-controlled crossover study of 16 men with chronic heart failure, it was found that UDCA significantly improved post-ischaemic blood flow in the arm and there was a non-significant trend for improvement in the leg (von Haehling et al., 2012). It has also been demonstrated to reduce diastolic blood pressure in healthy participants (Schiedermaier et al., 2000). A study of 11 patients with coronary heart disease (CHD) demonstrated that UDCA improved endothelium-dependent nitric oxide-independent vasodilation in the arm, a function which is usually decreased in patients with CHD (Sinisalo et al., 1999). Moreover, an investigation on patients with atrial fibrillation showed they have lower levels of conjugated UDCA in their serum (Rainer et al., 2013).

UDCA has also been suggested to attenuate heart transplant rejection. In a retrospective study of cholestatic patients who were receiving cardiac allografts, adjuvant UDCA therapy lowered the number of acute rejection episodes in the first 6 months post-surgery (Bährle et al., 1998). It has demonstrated a protection against allograft rejection in murine models without cholestasis; UDCA treated mice had indefinite survival of mismatched cardiac allografts and increased generation of regulatory T cells which have a suppressive activity in leukocyte cultures (Zhang et al., 2009b). These outcomes are in agreement with an earlier study on rats that showed UDCA treatment with concomitant anti-thymocyte globulin administration prolongs cardiac allograft survival and increases allograft tolerance (Olausson et al., 1992).

Although UDCA treatment does not appear to clinically improve the risk of ICP-associated IUD in the small (and underpowered) studies that have been performed to date, further investigations are required to establish whether it is effective in severe cases of ICP. This is of particular interest as *in vitro* evidence from models of the fetal heart show it attenuates cardiac dysfunction caused by more hydrophobic bile acids.

1.6 Summary and aims

Intrahepatic cholestasis of pregnancy is disease that is commonly diagnosed through measurement of total serum bile acids (TSBA) concentrations and treated with ursodeoxycholic acid (UDCA). Evidence has shown there is a relatively high risk of spontaneous preterm labour (PTL) and intrauterine death (IUD) once maternal TSBA concentrations exceed 40 µmol/L and a markedly increased risk when TSBA concentrations are elevated above 100 µmol/L. Currently, many centres that treat patients with ICP operate infrequent and delayed measurement of TSBA concentrations, the most sensitive marker for predicting adverse outcomes. The exact mechanisms of ICP-associated spontaneous PTL and IUD are unknown and there is not enough data to confirm whether UDCA can successfully prevent these outcomes.

The following aims were created given the current knowledge of ICP and its outcomes:

1) Development of a bile-acid detecting biosensor that can sensitively detect serum concentrations of 100 µmol/L and can be eventually used in a point-of-care setting.
2) Creation and validation of an *in vitro* model of the PTL-complicated myometrium and to assess the effect of elevated bile acid exposure and UDCA therapy in order to elucidate mechanisms of ICP-associated PTL
3) Investigation of mechanisms of ICP-associated IUD using non-invasive fetal ECG monitoring and assessment of the efficacy of UDCA therapy

Chapter 2: Development of a point-of-care bile acid biosensor

2. Development of a point-of-care bile acid biosensor

2.1 Abstract

Rapid and accurate measurements of maternal bile acid concentrations would provide an immense clinical benefit to diagnosis and management of intrahepatic cholestasis of pregnancy (ICP), a disease characterised by elevated maternal total serum bile acid concentrations which are associated with adverse fetal outcomes. The work described in this chapter aimed to develop a point-of-care bile acid electrochemical biosensor. The bile acid-specific enzyme (3α-hydroxysteroid dehydrogenase) and coenzyme (nicotinamide adenine dinucleotide (NAD^+)) were used to measure 0-100 µmol/L of the bile acid taurocholic acid (TCA) using chronoamperometry on a methylene blue-modified screen-printed carbon electrode. A calibration assay of this biosensor showed a non-linear measurement of current vs. TCA concentration, a relative standard deviation ranging between 20.5% and 47.9% and a sensitivity of 1.1 nA per µmol/L of TCA. Additional development of this biosensor is required to improve the sensitivity and specificity to TCA as well as further modification for enzyme immobilisation.

2.2 Introduction

Intrahepatic cholestasis of pregnancy (ICP) is the most common pregnancy-specific liver disorder and is associated with increased fetal adverse outcomes, including intrauterine death (IUD) and spontaneous preterm labour (PTL). ICP is typically diagnosed in women who present with pruritus and have elevated maternal total serum bile acid (TSBA) concentrations, usually at a threshold of 10-14 µmol/L when the serum sample has been taken from a patient who hasn't fasted (Williamson and Geenes, 2014). Women often also have deranged liver function markers. It has been established that the most effective biomarker for predicting the likelihood of fetal adverse outcomes occurring is maternal TSBA concentrations (Ovadia et al., 2019). The risk of ICP-associated IUD and PTL is known to increase with severity of disease: studies have shown increased rates of these outcomes at TSBA concentrations of 40 µmol/L, and markedly more so when concentrations exceed 100 µmol/L (Geenes et al., 2014a, Glantz et al., 2004, Ovadia et al., 2019). The majority of ICP cases are known to present at ≥30 weeks of gestation and the risk of adverse

fetal outcomes increases with gestational age. There is currently no evidence that the current pharmacotherapies available to treat ICP attenuate the associated risk of fetal adverse outcomes, however active management i.e. early induction of labour, is commonly utilised alongside close monitoring of TSBA concentrations (Lee et al., 2008).

As discussed in section 1.2, there are numerous methods currently available for measuring TSBA concentrations, the most commonly available being an assay that utilises an enzymatic method; this reaction relies on the electrochemical measurement of reduced nicotinamide adenine dinucleotide (NADH) that has been generated by the oxidation of bile acids via the bile-acid specific enzyme 3α-hydroxysteroid dehydrogenase (3α-HSD). Whilst this method has proven to have high sensitivity and specificity, not all clinical sites have the assay available or conduct it frequently which can result in a delay in reporting real time TSBA measurements. This has an impact on clinical care as these results are time-sensitive in nature. A point-of-care (POC) method of detecting TSBA concentrations would therefore be the ideal solution to providing rapid and accurate results; electrochemical biosensors have been leaders at the forefront of techniques to monitor and diagnose diseases within a clinical setting (Pasinszki et al., 2017). Electrochemical biosensors that utilise the aforementioned enzymatic method have already demonstrated sensitivity to bile acids in serum using carbon screen-printed electrodes (CSPEs) that have been modified with the electron mediators Meldola's blue (MDB) and Ruthenium, the latter biosensor was able to measure taurocholic acid (TCA) at a sensitivity of 5-150 pmol/L in diluted human serum, however neither biosensor had been successfully modified to allow the immediate measurement of TSBA concentrations (Lawrance et al., 2015, Tian et al., 2018, Zhang et al., 2016a).

The aim of this project is therefore to develop a POC bile acid biosensor that can sensitively detect TSBA concentrations of 100 µmol/L in order to aid the monitoring and diagnosis of ICP.

2.3 Materials and Methods

2.3.1 Reagents for CSPE modification and chronoamperometry measurements

Methylene blue (MEB), MDB and sodium pyrophosphate powder for CSPE modification was purchased from Sigma-Aldrich (Sigma-Aldrich, Dorset, UK). βNADH, βNAD^+, ethylenediaminetetraacetic acid (EDTA), human serum (male, type AB), TCA, TRIZMA® (tris[hydroxymethyl]amino-methane) hydrochloride for chronoamperometry measurements were also purchased from Sigma-Aldrich (Sigma-Aldrich, Dorset, UK). Deionised water was obtained from a Triple Red (Triple Red Ltd., Bucks, UK) system.

2.3.2 CSPE modification

Carbon DRP-110 screen-printed electrodes (Dropsens Ltd, Spain) were modified by air-drying 10 µl of 1 mmol/L and 10 mmol/L solutions of MEB or MDB (made with deionised water) on the working electrode overnight (Figure 2.1). Modified CSPEs were kept at room temperature in the dark during modification and when not in use. Negative controls (electrodes that were not modified with an electron mediator) were made by air drying 10µl of deionised water to the working electrode overnight. Each modified CSPE was used for measurement once and disposed of after use.

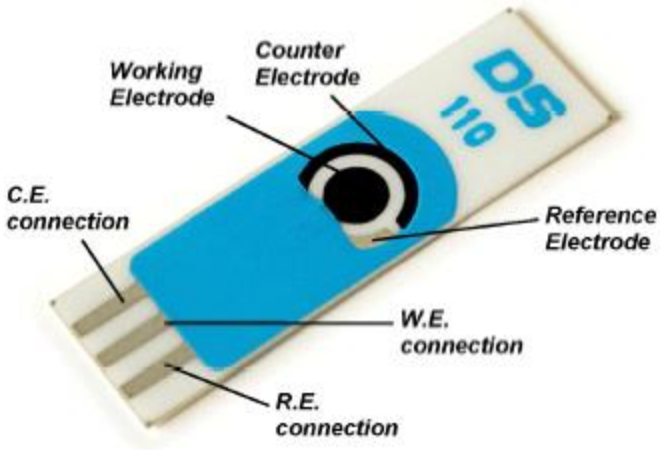

Figure 2.1: Photograph of the commercially available DRP-110 screen-printed electrode used for experiments prior to modification. Image provided by Dropsens Ltd.

2.3.3 Chronoamperometric measurement

In order to assess the ability of CSPE modification to aid electrooxidation at the surface of the working electrode, 0-100 µmol/L solutions of βNADH were made via serial dilutions with 0.1 mol/L sodium pyrophosphate buffer as the solvent (pH 9.5). Each chronoamperometric measurement was conducted using a 60 uL volume sample droplet on the CSPE which was connected to an EmStat3+ potentiostat (PalmSens, Netherlands) using custom CSPE connectors (Dropsens Ltd, Spain). Chronoamperometric measurements were made at room temperature and in the absence of a Faraday cage using a potential step of +0.1V that lasted for a period of 30 seconds at the working electrode. Data was sampled at a rate of 10 Hz and visualised using PSTrace V4.6 software (Palmsens, Netherlands).

Further experiments were conducted to assess whether the MEB-modified CSPEs could detect TCA in buffer and human serum-based solutions. To create the sample droplets for these experiments, stock solutions of 3α-HSD were made by dissolving 10 mg of 3α-HSD in 500 µl of 0.1 mol/L Tris-HCl containing 0.001 mol/L EDTA (pH 7.2). Stock solutions of 20 mmol/L βNAD^+ were made using 0.1 mol/L sodium pyrophosphate buffer (pH 9.5) as the solvent. A mixture of 150 µl of either pooled human serum or sodium pyrophosphate buffer (pH 9.5) was spiked with TCA at concentrations of 0, 10, 20, 30, 40, 50 and 100 µmol/L, to which 40 µl of βNAD^+ stock solution and 5 µl of 3α-HSD stock solution were added and mixed thoroughly to create test droplets for a calibration assay. The mixture was left to rest for 1 minute at room temperature before deposition onto the working electrode of the MEB-modified CSPE and chronoamperometeric measurement as described above. The three part reaction in this assay is described below:

$$\textbf{3α-hydroxy bile acid} + \beta\textbf{NAD}^+ \xrightarrow{\textit{3α-HSD}} \textbf{3-keto bile acid} + \beta\textbf{NADH} + \textbf{H}^+$$

$$\beta\textbf{NADH} + \textbf{MEB}^+ \longrightarrow \beta\textbf{NAD}^+ + \textbf{MEBH}^*$$

$$\textbf{MEBH}^* \longrightarrow \textbf{MEB}^+ + \textbf{H}^+ + 2\textbf{e}^-$$

***where MEBH is the reduced form of methylene blue**

2.3.4 Data visualisation and statistical analysis

Chronamperometry data and graphs of current vs. time were created using PSTrace V4.6 software (Palmsens, Netherlands) and exported into Microsoft Excel v2016 (Microsoft Corporation, WA, US). The calibration plot of current vs. TCA concentration in pooled serum was created and statistically analysed using GraphPad Prism v8.0 (GraphPad Software, US). Readings from the 5-second time point of the 30-second chronoamperometric measurement were taken and the mean current and standard deviation was calculated. Comparison of mean current generated from each TCA concentration was conducted via one-way analysis of variance with a post-hoc Bonferroni test. Significant differences in the current generated from each TCA concentration in comparison to baseline (0 µmol/L) have been reported. Relative standard deviation (RSD) was calculated by dividing standard deviation with the mean current for each TCA concentration tested. Linear regression was used to calculate the slope and y intercept of the calibration plot; these results were was used to ascertain sensitivity of the sensor.

A Cottrell plot of current vs. time$^{-1/2}$ was generated by taking the mean of all choroamperometric measurements for each of the 300 data points taken over 30 seconds. Statistical analysis to measure deviation of the fitted line for each concentration was conducted using a runs test using GraphPad Prism v8.0 (GraphPad Software, US).

2.4 Results

2.4.1 Methylene blue is a more effective electron mediator than meldola's blue

The electrode mediators MDB and MEB were used to modify bare CSPEs which were then used to detect the electrooxidation of varying concentrations of NADH via chronoamperometry. Both dyes used for CSPE modification resulted in a higher current measured than the CSPEs which were unmodified by a mediator (Figure 2.2A and B). Of the two mediators that were chosen, it was observed that CSPEs modified with 1 mmol/L of MDB generated a lower range of current values than 1mmol/L MEB (-0.06 – 0.32 µA vs. -0.01 – 0.83 µA, n=1) when measuring 0-100

µmol/L of NADH (Figure 2.2C and D respectively). Additionally, modification with MEB displayed clear incremental increases in current in response to increasing NADH concentrations which was not observed with MDB-modification (Figure 2.2A and D).

A

NADH Concentration (µmol/L)	Electrode modification		
	Water (µA)	MDB (µA)	MEB (µA)
0	0.015	-0.060	-0.005
5	-0.005	-0.036	0.108
10	0.003	-0.035	0.217
20	0.004	0.017	0.265
40	0.007	0.151	0.481
60	0.013	0.248	0.625
80	0.016	0.333	0.747
100	0.013	0.316	0.825

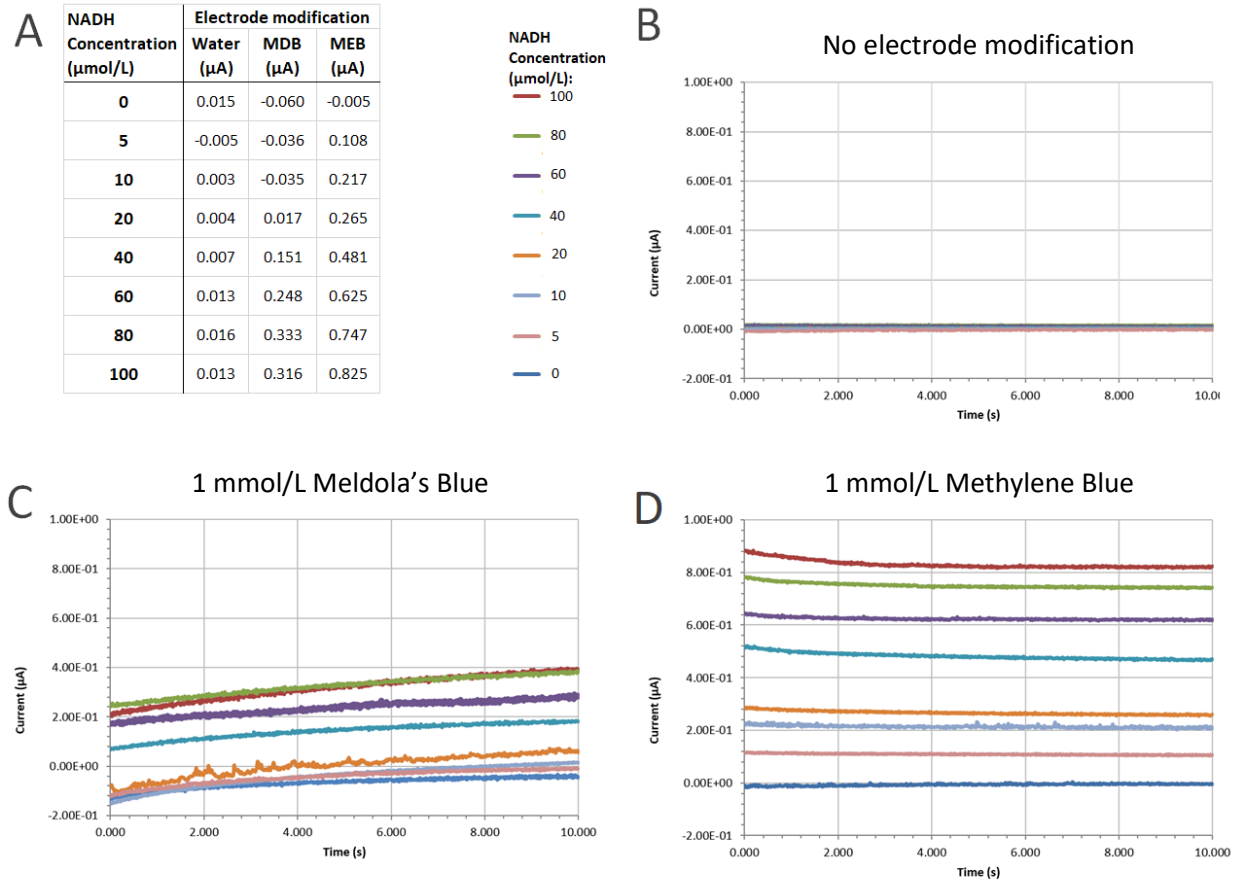

Figure 2.2: Investigation of different types of CSPE modification (A) Current values taken from the 5-second timepoint of chronoamperometric measurements of 0-100 µmol/L NADH (B-D) Chronoamperometric plots of CSPE medication with water, 1 mmol/L Meldola's Blue and 1 mmol/L Methylene Blue respectively. n=1 for each NADH concentration and electrode modification tested.

2.4.2 The optimal concentration for methylene blue modification is 1 mmol/L

Two concentrations of MEB were used to modify bare CSPEs in order to find the optimum concentration of electron mediator for the working electrode. 1 mmol/L of MEB generated larger current values than 10 mmol/L of MEB when measuring

concentrations of 250 (1.26 vs. 1.01 µA, n=1), 500 (1.95 vs. 1.52 µA, n=1) and 1000 (2.64 vs. 2.05 µA, n=1) µmol/L of NADH (Figure 2.3).

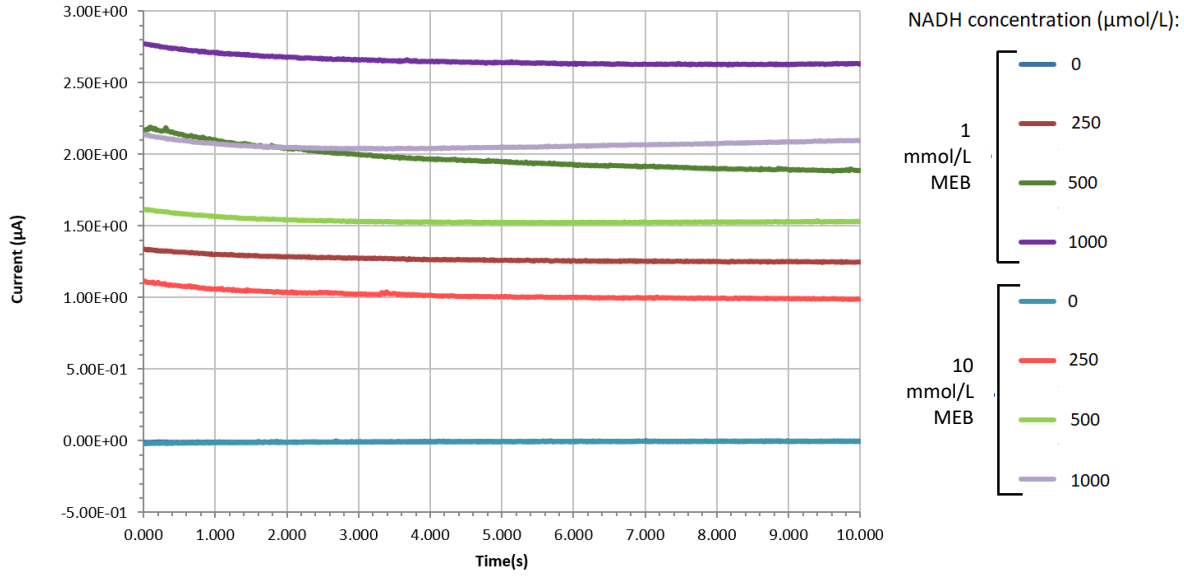

Figure 2.3: Comparison of 1 and 10 mmol/L of MEB solution used for CSPE modification using chronoamperometric measurement of 0, 250, 500 and 1000 µmol/L of NADH

2.4.3 Methylene blue-modified CSPEs can detect TCA in buffer

A mixture of βNAD$^+$ and 3α-HSD with varying concentrations of TCA was made in sodium pyrophosphate buffer and measured on the MEB-modified CSPE. When spiking the buffer mixture with 50 and 100 µmol/L of TCA, an incremental increase in current (0.07 and 0.14 µA respectively, n=1) was observed in comparison to the baseline (0 µmol/L) measurement (0.003 µA, n=1, Figure 2.4).

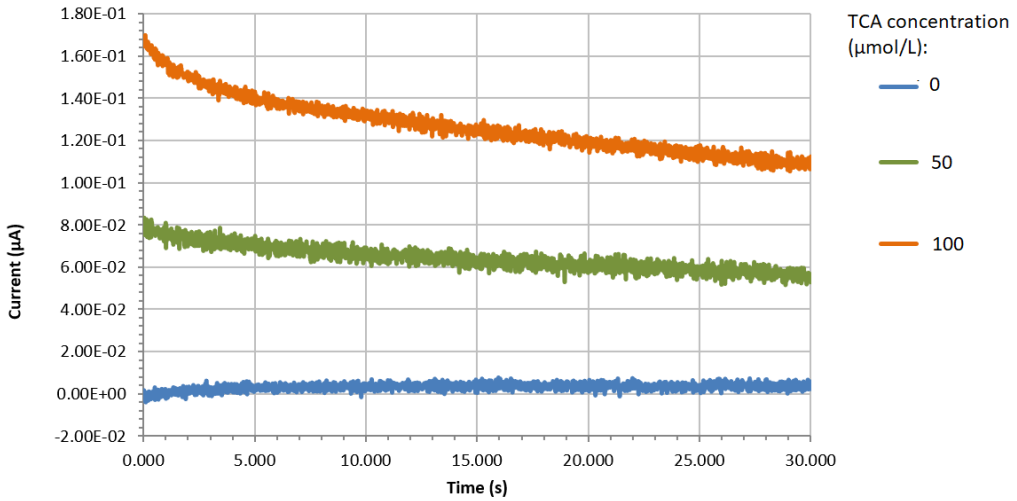

Figure 2.4: Chronoamperometric measurement of sodium pyrophosphate buffer spiked with NAD+, 3α-HSD and 0, 50 and 100 µmol/L of TCA

2.4.4 Methylene blue-modified CSPEs can detect TCA in pooled human serum

Pooled human serum was spiked with βNAD$^+$, 3α-HSD and 0-100 µmol/L of TCA. Increasing the concentration of TCA from 0 µmol/L (0.087 ± 0.03 µA, RSD 34.4%, n = 7) to 10 µmol/L (0.089 ± 0.02 µA, RSD 24.5%, n = 10), 30 µmol/L (0.091 ± 0.01 µA, RSD 13.2%, n = 6) 40 µmol/L (0.096 ± 0.02 µA, RSD 25.9%, n = 5) and 50 µmol/L (0.115 ± 0.03 µA, RSD 28.6%, n = 8) led to non-significant increases in current (Figure 2.5A). A significant increase was found between the mean current measurements of 100 µmol/L (0.187 ± 0.04 µA, 20.5%, n = 9, $p < 0.0099$) when compared to 0 µmol/L of TCA (Figure 2.5A). A non-significant decrease was found when comparing the mean current measurements of 20 µmol/L (0.085 ± 0.04 µA, RSD 47.9%, n = 12) and 0 µmol/L of TCA (Figure 2.5A). Linear regression analysis of the resulting calibration plot from these measurements resulted in a slope of $y = 0.001053X + 0.07069$ (Figure 2.5A). Cottrell analysis of the electrode response demonstrated that all concentrations of TCA had a linear regression best fit line that significantly deviated from the raw data ($p > 0.0001$ for all, Figure 2.5B).

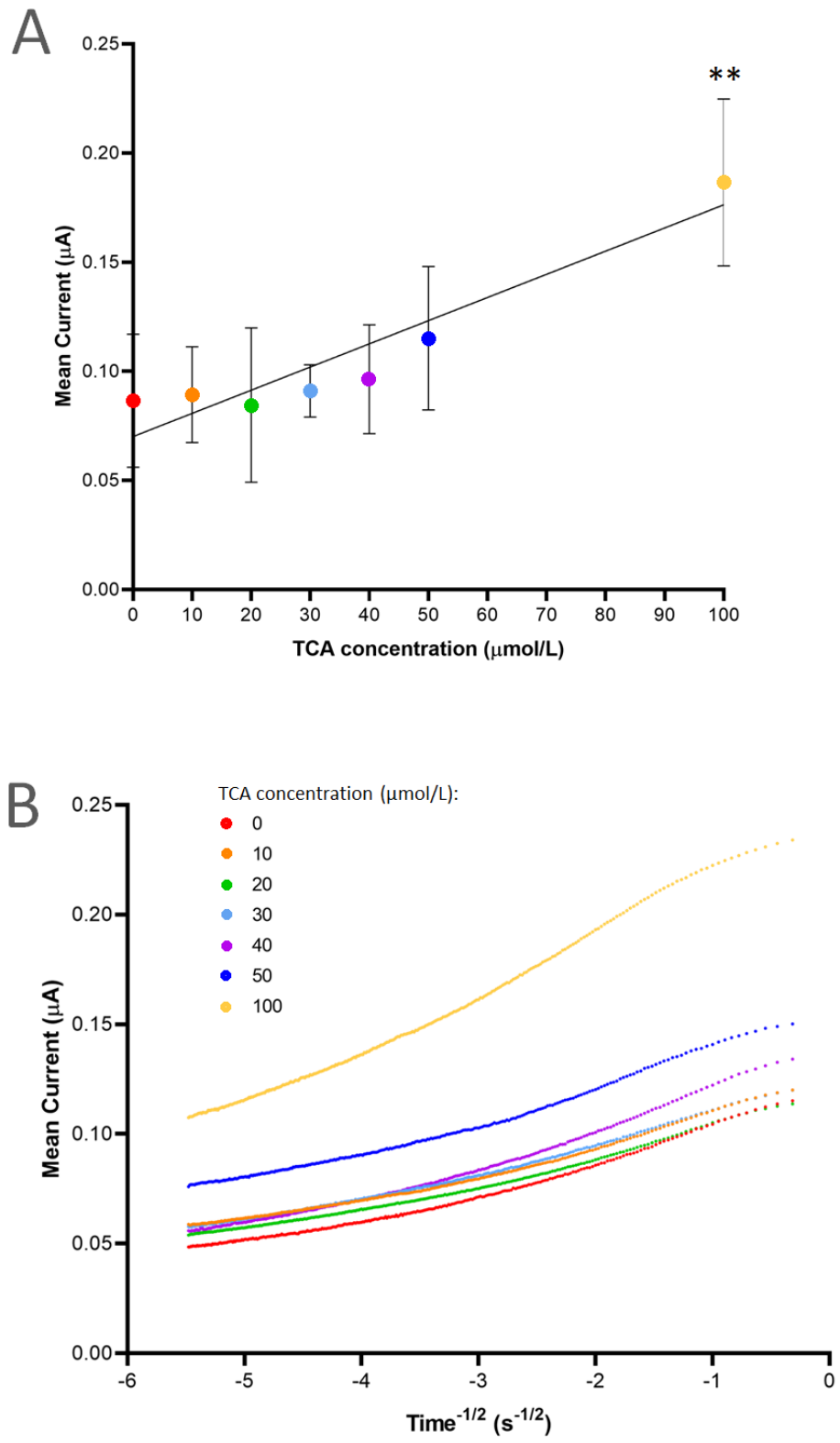

Figure 2.5: (A) Calibration plot of 0-100 µmol/L TCA-spiked pooled serum with linear regression best fit line. Asterisks demonstrate p value of 0.005 in comparison to baseline measurements of 0 µmol/L TCA. Results are presented as mean + SEM. (B) Cottrell plot of mean data generated from 30 second chronoamperometric measurement. Best fit lines are not displayed.

2.5 Discussion

2.5.1 Summary of findings

This project aimed to develop a biosensor that could accurately detect maternal TSBA concentrations of 100 µmol/L in a POC setting. In these experiments, the efficacy of modifying a CSPE were initially tested using two electron mediators, MEB and MDB, to investigate their ability to facilitate electrooxidation of NADH at the working electrode surface. A concentration of 1 mmol/L of MEB solution air dried onto the CSPE was found to be the more effective electron mediator modification. MEB-modified CSPEs were used to measure the current transients generated from the oxidation of the bile acid TCA within human pooled serum. Although current transients could be detected at concentrations between 0-100 µmol/L of TCA, the incremental increase in TCA concentration did not result in a linear relationship of current vs. concentration.

2.5.2 Comparison to previous work on CSPEs

There are relatively few bile acid biosensors that have been reported as successful in a research setting; currently three have demonstrated sensitivity using human serum on disposable CSPEs. Lawrance et al. (2015) used MDB-modified CSPEs to create a linear calibration of TCA-spiked serum at a range of 4.5-150 µmol/L with a relative standard deviation (RSD) of 8% and a sensitivity of 2.95 nA per µmol/L (Lawrance et al., 2015). Zhang et al. (2016) also used in-house manufactured MDB-modified CSPEs to detect TSBA concentrations at a range of 5-400 µmol/L in human serum samples from patients with hyperbilirubinemia using differential pulse voltammetry (Zhang et al., 2016a). Tian et al. (2018) of the same group developed a ruthenium-modified CSPE to detect TSBA concentrations 5-150 pmol/L in diluted human serum (Tian et al., 2018). It has therefore has been the most sensitive bile acid sensor reported so far, although ruthenium, NAD^+ or 3α-HSD were added to the diluted serum prior to measuring as immobilisation of these components to the CSPE was not successful (Tian et al., 2018).

The same method of using electron mediator modified-CSPEs was used in these experiments; screen-printed electrodes have the enormous advantage of being highly reproducible, amenable to miniaturisation, disposable and inexpensive, which increase their viability for commercial manufacture of biosensors for use in POC settings (Couto et al., 2016). Compared to the aforementioned bile acid biosensors, this biosensor had a higher RSD range (20.4 - 47.9%) and a lower sensitivity (1.053 µA per µmol/L of TCA). The RSD generally lowered as the concentration of TCA increased, which suggests that sensitivity is associated with TCA concentration, possibly due the background signal being overcome by the larger electrochemical signal generated with higher TCA concentrations.

Calculation of the Cottrell equation, which describes changes in current over time after a potential step and can give information about the diffusion and depletion of the electroactive species at the electrode surface, yielded non-linear plots for all concentrations of TCA that were tested. The shape of the curve eventually leads to a straight line towards the origin of the graph, suggesting that there is a higher rate of current generation and the beginning of the 30-second measurement that leads to a linear relationship by the end of the measurement. This is possibly due to a large amount of MEB generated upon the initial application of the potential step, therefore allowing increased electrooxidation at the electrode surface at the beginning of the measurement and a slower rate of current decline than expected. Future experiments to combat this could therefore attempt to further optimise the concentration of MEB solution used to modify the electrode as well as investigating the optimal concentrations of βNAD^+ and 3α-HSD in the reaction.

2.5.3 Potential causes of low sensitivity of the biosensor

Pooled human serum which had been spiked with TCA, βNAD^+ and 3α-HSD yielded a non-linear calibration plot and low sensitivity. Spiking sodium pyrophosphate buffer with the same components appeared to have a clearer signal to noise ratio which suggests that the serum itself may be obstructing the electrooxidation reaction. However, it must be stated that the buffer-based experiments were only conducted

once. The main component of serum is albumin, which bile acids are known to bind to and circulate, and have been known to cause biosensors to lose sensitivity (Sabaté Del Río et al., 2019). In order to reduce albumin-based reduction in sensitivity and an improve the signal to noise ratio, various dilutions of serum could be tested. A biosensor that had a higher sensitivity for bile acid concentrations in serum that was diluted 6-fold has already been demonstrated (Tian et al., 2018). Ascorbic acid, uric acid and paracetamol are known to be the main electroactive interferents present in human serum that interfere with NADH oxidation. To combat this, an electron mediator was used to lower the potential window of the working and electrode and minimise electroactivation of these components in the pooled serum, however this may have still allowed some electroactivation of unwanted species. This could be prevented via minimisation of electrode fouling as mentioned previously. The enzyme used for the biosensor, 3α-HSD, could have also catalysed the oxidation of other species in the serum such as sulphated progesterone metabolites which have coincidentally been implicated in the pathogenesis of ICP (Abu-Hayyeh et al., 2016). In future experiments, variations in serum composition could be accounted for via a standard addition of TCA which could be used for calibration of the measurement.

At the time of conducting experiments, the established threshold for the increased risk of IUD was at a maternal TSBA concentration of ≥40 μmol/L (Geenes et al., 2014a, Glantz et al., 2004). However, data has since shown that the IUD risk dramatically increases at TSBA concentrations of ≥100 μmol/L (Ovadia et al., 2019). Future experiments will therefore focus on developing the biosensor to have a high sensitivity around this concentration as this would be valuable for aiding clinical management of patients with severe ICP.

2.5.4 Use of electron mediator and method of modification

MEB was found to be the more favourable electron mediator in this study. MEB has demonstrated to be an efficient an electron mediator for NADH oxidation, and is most commonly used for sensing of nucleic acids (Dai et al., 2008, Komura et al., 2004, Wang et al., 2019b). The efficacy of MEB's ability to aid electrooxidation of

NADH depending on pH, mediator concentration, temperature and timing (Mark et al., 2010). When testing CSPEs which had been modified using 1 mmol/L and 10 mmol/L MEB solutions in this study, the former concentration was found to be optimal. This is not in agreement with the Langmuir model which demonstrates that MEB concentration is associated with adsorption capacity on CNTs (Yao et al., 2010). As the measurements of both concentrations were conducted on different days, ambient temperature could have played a role in the unexpected difference in current transients as well as the possibility of experimental error during the modification steps. Electrode fouling from the higher concentration of MEB could have also played a role in the unexpected results observed. Additionally, only one sensor was made and tested for each concentration of MEB and NADH, so results may have differed with repeat experiments.

In the above experiments, both electron mediators were adhered to the CSPE via air drying of solutions at room temperature. This resulted in some expected leaching of the water-soluble mediator dye upon the addition of both buffer- and serum-based samples. Leaching or diffusion of mediators into the sample can result in a loss of activity via denaturation, binding to other biological components in the sample or lowering of the volume of electron mediator at the working electrode surface. This in turn can result in a change in the required potential and the stability, sensitivity and specificity of the biosensor to be lost, and could have played a part in the low specificity of the MEB-modified CSPE in response to TCA-spiked human serum samples as well as the non-linear Cottrell plot. The ideal electron mediator would therefore not diffuse into the sample, and there are other more refined techniques of electrode modification which could potentially combat this. Modification of NADH-based biosensors to encompass mediators have been conducted via electropolymerisation, i.e. the growth of mediator polymers under electrochemical conditions, and entrapment, which are avenues to explore in future experiments (Prieto-Simón and Fàbregas, 2004). Electropolymerisation in particular is known to increase stability and sensitivity of the mediator with each added layer of the monomer; electropolymerisation of specifically MEB has been reported to be effective for sensing biological components such as haemoglobin, glucose and markers of cardiovascular disease (Brett et al., 1999, Silber et al., 1996, Li et al.,

2018). In addition, modification of MEB on multi-walled CNTs have been shown to reduce leaching due to the ability of CNTs' hollow structure to entrap MEB polymers (Moyo et al., 2012).

2.5.5 Alternative materials for working electrode fabrication

The working electrode on the CSPE was made using carbon, however there is evidence that modification of the working electrode with CNTs could result in a more effective biosensor for biomarkers, and particularly for sensing NADH (Rivas et al., 2007, Fanjul-Bolado et al., 2007). CNTs are constructed via flat sheets of graphene that are rolled into hollow tubes and can be single-walled (where a single layer forms the tube) or multi-walled (where several additional concentric layers are wrapped around the tube), the latter of which is more commonly used in biosensing due to its more successful ability to act as a scaffold for immobilisation of biological recognition elements and electron mediators (Georgakilas et al., 2015, Cho et al., 2018). The electroactive surface area and ability to transfer electrons is dramatically increased which results in an magnified electrical signal as a result of the highly active groups for electron transfer at the end of the tubes (Fortunati et al., 2019). Multi-walled CNTs could therefore could be used to entrap 3α-HSD, NAD^+ and MEB within the working electrode, which would aid direct electron transfer between the analyte and the electrode surface (Kumar et al., 2015). Experimental evidence from a glucose dehydrogenase-based biosensor has demonstrated the successful non-covalent attachment of NAD^+ in multi-walled CNTs (Zhou et al., 2010). Other graphene nanostructures, such as capsules and nanowires, have also demonstrated efficacy at immobilising enzymes on the working electrode (Kumar et al., 2015, Bagal-Kestwal et al., 2018). The use of CNT-modified CSPEs could even result in the lack of necessity for an electron mediator due to the high conductivity of the material. Both multi-walled and single-walled CNT-modified CSPEs are commercially available from the same company that manufactured the CSPEs used in these experiments and are therefore a potential avenue for increasing the sensitivity whilst sustaining the feasibility of commercial manufacture of the sensor.

2.5.6 Microfluidics for future experiments

Recently, microfluidics platforms, i.e. the manipulation of very small volumes of liquid, have been integrated with biosensors in order to form a "lab-on-a-chip" for use in the biomedical field (Mark et al., 2010). These systems tend to involve the continuous flow of liquids through multiple micro-channels and the occurrence of several processing techniques on the same platform; these can include sample separation, purification and the final biosensing steps. In theory, multiple samples can be measured for multiple analytes on the same chip (Prakash et al., 2012). One of the main advantages of microfluidics technology is the ability to encompass a high surface-to-volume ratio, therefore only requiring a minute volume of sample (as low as picolitres) for accurate measurements (Liu et al., 2010, Luka et al., 2015). They also increase sensitivity and specificity, have a rapid performance, are amenable to miniaturisation, portability and can provide real-time results, which would be ideal for a POC biosensor (Liu et al., 2010, Luka et al., 2015). Recently, "lab-on-a-chip" technology has been utilised to successfully extract and fluorescently label a panel of PTB biomarkers for detection (Bickham et al., 2020). In our case, microfluidics would be particularly useful to allow the bile acid biosensor to be truly POC as the manual separation of serum from whole blood prior to measurement would no longer be required, electroactive interferents could be removed and serum could be adequately diluted to increase sensitivity (Tian et al., 2018). In addition, the ability to separate and detect individual bile acids in serum would be particularly useful as conjugated CA in particular are known to be raised in women with ICP (Tribe et al., 2010).

Recent research advances have also created stretchable and wearable "lab-on-a-patch" biosensors which have proven effective in an experimental setting for continuous non-invasive monitoring of cortisol, glucose and lactate in sweat and interstitial fluid (Bae et al., 2019, Toi et al., 2019, Jia et al., 2013, Lee et al., 2020). Previous research has shown TSBA concentrations exhibit diurnal variation and increase after consumption of food (Gälman et al., 2005). Therefore, a "lab-on-a-patch" biosensor would be useful for research purposes to standardise the most appropriate methods of testing and optimal bile acid ranges for predicting outcomes

in women with ICP (depending on the type of biofluid being monitored) as well as for clinical purposes to aid effective monitoring and response, particularly in patients who have severe ICP and/or TSBA concentrations of ≥100 μmol/L. "Lab-on-a-patch" biosensors also take us one step towards personalised medicine, and are therefore likely to play a huge part in monitoring other diseases with known biomarkers that oscillate in a short period of time.

2.6 Conclusion

A successful electrochemical biosensor has the clear advantage over the current colorimetric assay used due to biosensors in general being cheap, having a high sensitivity and specificity for the target analyte and an ease of portability which make it ideal for use in a clinical or home setting (Rechnitz and Nakamura, 1988). Biosensors are defined in the simplest terms as a method of measuring one or more target analyte that uses a biological recognition element to generate a quantifiable signal (Turner et al., 1987). More recently, biosensors have been suggested to be devices where the biological recognition element is directly interfaced to the signal transducer and acts as the primary selective component (Kissinger, 2005). By this definition, a bile acid biosensor would require 3α-HSD and βNAD^+ immobilised onto the working electrode and this will be one of the next aims for further developing this biosensor. Recognition elements in a biosensor can be immobilised to the transducer using various methods, such as adsorption, entrapment, encapsulation and covalent- or cross-linkage (Malhotra and Chaubey, 2003). In order for this biosensor to eventually be used in a POC setting, future experiments to immobilise 3α-HSD and NAD^+ onto the CSPE will also be required, perhaps using CNTs and/or Nafion. The use of a microfluidics-based platform is a promising future direction for continuous monitoring of bile acid concentrations.

Chapter 3: Investigation of bile acid induced-contractions in human myometrial cells

3. Investigation of bile acid-induced contractions in human myometrial cells

3.1 Abstract

Intrahepatic cholestasis of pregnancy (ICP), commonly treated with the drug ursodeoxycholic acid (UDCA), is associated with an increased risk of spontaneous preterm labour which is positively correlated with maternal serum bile acid concentrations. We aimed to investigate how bile acids and UDCA affect uterine contractions via the investigation of intracellular calcium ($[Ca^{2+}]_i$) handling in primary human myometrial cells subjected to exogenous drug stimulation.

Primary human myometrial cells were isolated from biopsies of non-labouring myometrium and cultured until passage five or six. Cells were incubated with Fluo4-AM prior to 20-minute treatments of 10 nmol/L oxytocin (OT) (n=3), 100 µmol/L taurocholic acid (TCA) (n=3), a combination of OT and TCA (n=3), 10 nmol/L prostaglandin E_2 (PGE_2) (n=4) or $F_{2\alpha}$ ($PGF_{2\alpha}$) (n=7) with and without concomitant 100 µmol/L UDCA treatment. Time-lapse imaging was performed and the amplitude, time to peak, duration and time to decay of the $[Ca^{2+}]_i$ transients was measured.

Analysis of the $[Ca^{2+}]_i$ handling of myometrial cells after OT and OT+TCA administration resulted in an increase in the amplitude of $[Ca^{2+}]_i$ transients when compared to the vehicle control ($p = 0.003$ and $p < 0.0005$ respectively). Concomitant UDCA administration resulted in a significant decrease in amplitude ($p = 0.002$). Administration of OT and OT+UDCA resulted in a decrease in the time to peak, duration and time to decay of $[Ca^{2+}]_i$ transients ($p < 0.0005$ and $p = 0.001$ respectively for all three parameters). Administration of TCA alone did not affect $[Ca^{2+}]_i$ transients. Administration of PGE_2 resulted in an increase in the time to peak ($p = 0.011$), duration ($p = 0.023$) and time to decay ($p = 0.036$) of $[Ca^{2+}]_i$ transients. Concomitant UDCA administration resulted in a decrease in the time to decay ($p = 0.043$). Administration of $PGF_{2\alpha}$ resulted in a significant increase in amplitude of $[Ca^{2+}]_i$ transients ($p = 0.026$). Concomitant UDCA administration had no effect.

Based on these results, the action of TCA in inducing contractile activity in myometrial cells is via an increased sensitivity to OT which is consistent with previous data regarding ICP-associated spontaneous preterm labour. UDCA

administration attenuated this effect as well as attenuating the PGE_2-induced increase in the time to decay, suggesting further investigation of its use to protect against stimulation of myometrial contraction is warranted.

3.2 Introduction

Intrahepatic cholestasis of pregnancy (ICP) is the most common gestational liver disease. As evidenced by previous studies of Swedish and British cohorts, spontaneous preterm labour (PTL) is known to increase in women with severe ICP, which is defined by maternal TSBA concentrations of ≥40 μmol/L (Geenes et al., 2014a, Glantz et al., 2004). More recent analysis of global individual patient data has shown that this risk markedly increases in ICP-affected women with singleton pregnancies who have TSBA concentrations of ≥100 μmol/L (Ovadia et al., 2019). ICP is often treated with the drug ursodeoxycholic acid (UDCA), however evidence from the largest randomised controlled trial of this pharmacotherapy to date did not show a statistical difference in a composite result of fetal adverse outcomes, one of which included the incidence of spontaneous preterm birth (Chappell et al., 2019). Preterm birth (PTB) is known to be the leading cause of infant mortality and increases the risk of developing a disability in later life (Blencowe et al., 2012, Murray et al., 2012).

The mechanism for ICP-induced PTL is unknown, although there is evidence that bile acids can affect myometrial contractile activity. Chronic infusion of the bile acid cholic acid (CA) in sheep resulted in a 100% of lambs being spontaneously delivered prematurely (Campos et al., 1986). Experimental evidence has shown that rat myometrial strips increased contractile activity as a result of CA exposure *in vitro* (Germain et al., 2003). A potential mechanism of bile acid-induced myometrial contraction has been suggested to be via an upregulation of the oxytocin receptor (OTR) and therefore increased sensitivity to oxytocin (OT) as evidenced by protein expression studies of myometrial strips (Germain et al., 2003). Increased oxytocin sensitivity has also been demonstrated in ICP cases during parturition (Israel et al., 1986). Pathological findings from human placental tissue has also demonstrated that bile acid exposure induces placental oxidative stress and inflammation during

pregnancy which may also contribute to the induction of preterm labour (Geenes et al., 2011, Costoya et al., 1980, Du et al., 2014b, Wikström Shemer et al., 2012, Sepúlveda et al., 1991, Perez et al., 2006).

The aim of this project is to investigate how elevated bile acid concentrations affect the contractility of myometrial cells via the measurement of intracellular calcium ($[Ca^{2+}]_i$) handling in a 2D human myometrial cell model of PTL.

3.3 Patients and methods

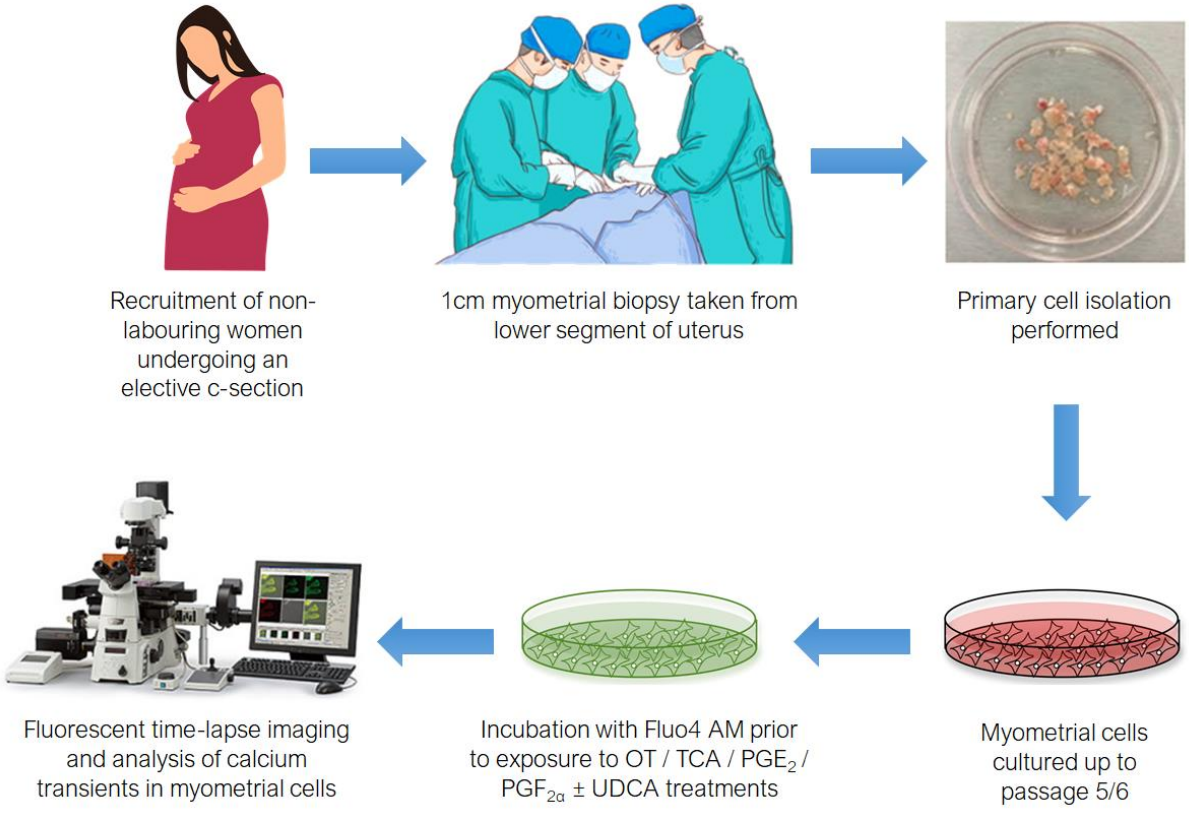

Figure 3.1: Schematic flowchart of the methods used for obtaining and investigating myometrial cells

3.3.1 Participant recruitment and myometrial biopsy

Women were recruited prior to undergoing an elective caesarean section procedure due to breech presentation or previous caesarean section at Queen Charlotte's and Chelsea Hospital (local ethics committee, REC 3357). After informed consent, a 1cm biopsy of the lower segment of the uterus was taken during the procedure by Vasso Terzidou (Institute of Reproductive and Developmental Biology, Imperial College London). Primary cell isolation of the biopsies was performed by Sung Hye Kim (Institute of Reproductive and Developmental Biology, Imperial College London).

3.3.2 Primary myometrial cell culture

Myometrial cells were cultured in high glucose full Dulbecco's Modified Eagle Medium (DMEM) containing 10% fetal calf serum, 1% L-Glutamine and 1% penicillin and streptomycin (Invitrogen, Paisley, UK) in T25 flasks (Corning, US) inside an incubator maintained at 37°C and 5% carbon dioxide. Cells were passaged upon full confluency and cultured until passage 5 or 6 for $[Ca^{2+}]_i$ handling assays. For each passage, flasks were washed in Dulbecco's Phosphate Buffered Saline (D-PBS) (Invitrogen, Paisley, UK) and trypsinised in 0.25% Trypsin-EDTA (Invitrogen, Paisley, UK) for 5 minutes before inhibition by full DMEM. Cells were pelleted, resuspended and split into new T25 flasks. Cells were split into round coverslips (MatTek Corp, US) prior to drug treatment and imaging for $[Ca^{2+}]_i$ handling experiments (Figure 3.1). Only one passage from the myometrial biopsy was used for each experiment.

3.3.3 Drug treatments

For $[Ca^{2+}]_i$ handling experiments, oxytocin (OT) (Sigma Aldrich, Gillingham, UK), Prostaglandin (PG) E_2 (Tocris Bioscience, Bristol, UK), and $F_{2\alpha}$ (Cayman Pharma, Czech Republic), taurocholic acid (TCA) (Sigma Aldrich, Gillingham, UK) and ursodeoxycholic acid (UDCA) (Sigma Aldrich, Gillingham, UK) were dissolved in non-sterile Hank's buffered saline solution (HBSS) to create stock solutions, and subsequently serially diluted with HBSS in order to obtain the final concentrations

used for treatments. HBSS was prepared by addition of a vial of Phenol Red-free Hank's balanced salts (Sigma Aldrich, Gillingham, UK), 0.35 g/L sodium bicarbonate (Sigma Aldrich, Gillingham, UK) and 2.38 g/L N-2-hydroxyethylpiperazine-N-ethanesulfonic acid (HEPES) (VWR, Lutterworth, UK) to 1L distilled water. OT, PGE_2 and $PGF_{2\alpha}$ were diluted to a concentration of 10 nmol/L whilst TCA and UDCA were diluted to a concentration of 100 µmol/L for treatments.

3.3.4 Optical recording of analysis of $[Ca^{2+}]_i$

Coverslips were incubated for 20 minutes in 1ml of full DMEM containing 20 mM Fluo4 acetoxymethyester (Fluo4 AM) (Invitrogen, Paisley, UK). After incubation the coverslip was washed in non-sterile HBSS and mounted on a holder. The holder was then mounted on an inverted microscope (Nikon Eclipse TI) with a MICAM Ultima Camera for optical recording at a x200 magnification. Images were taken at a frame rate of 1 frame/ms for 480 seconds. Three recordings were taken from different representative areas of the coverslip. One of five sets of drug treatments using OT, TCA, PGE_2 or $PGF_{2\alpha}$ were subsequently administrated to the cells and incubated for 20 minutes (Table 3.1).

(1)	20 minutes 10nmol/L oxytocin →	3 x 480 s optical recording →	20 minutes 100 µmol/L ursodeoxycholic acid →	3 x 480 s optical recording		
(2)	20 minutes 100 µmol/L taurocholic acid →	3 x 480 s optical recording →	20 minutes 100 µmol/L ursodeoxycholic acid →	3 x 480 s optical recording		
(3)	20 minutes 10nmol/L oxytocin →	3 x 480 s optical recording →	20 minutes 100 µmol/L taurocholic acid →	3 x 480 s optical recording →	20 minutes 100 µmol/L ursodeoxycholic acid →	3 x 480 s optical recording
(4)	20 minutes 10nmol/L prostaglandin E_2 →	3 x 480 s optical recording →	20 minutes 100 µmol/L ursodeoxycholic acid →	3 x 480 s optical recording		
(5)	20 minutes 10 nmol/L prostaglandin $F_{2\alpha}$ →	3 x 480 s optical recording →	20 minutes 100 µmol/L ursodeoxycholic acid →	3 x 480 s optical recording		

Table 3.1: Table depicting the order of drug administration in the five sets of composite drug treatments and their accompanying incubation times

Time-lapse imaging was subsequently repeated using the same protocol. UDCA was administered as the final treatment prior to another set of three time-lapse recordings

for each coverslip. Optical recording experiments were completed in collaboration with Francisca Schultz (Institute of Reproductive and Developmental Biology, Imperial College London).

Fiji software (Vale Lab, Schindelin et al, 2012) was used to create a stack of 480 images for each recording in order to analyse the intracellular $[Ca^{2+}]_i$ transients. The autocorrect tool was used to improve the brightness and contrast for the entire stack to a standard level and regions of interest were manually drawn around each visible myocyte from each stack. The fluorescence within each region of interest throughout the 480s period was exported as a Microsoft Excel spreadsheet and plotted as f mV vs. time using Clampfit v10 software (Molecular Devices, US). The time to peak, amplitude, time to decay and durations of $[Ca^{2+}]_i$ transients within each region of interest were measured using the callipers included in Clampfit software (Figure 3.2). The mean and standard deviation of all regions of interest was calculated from all three recordings taken from each post-treatment coverslip and subsequently used for statistical analysis.

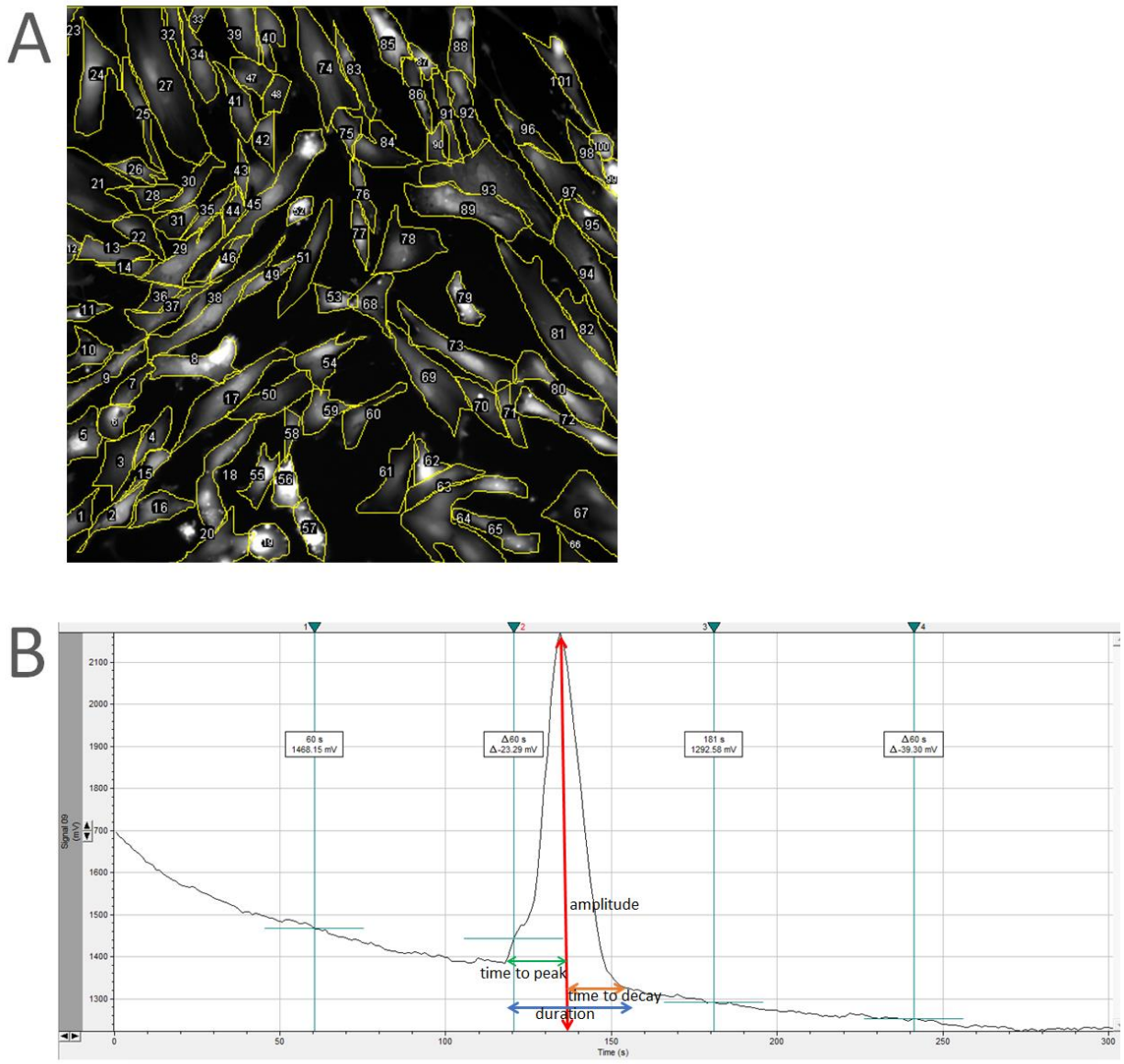

Figure 3.2: (A) Representative fluorescent image taken from a stack of 480 with regions of interest drawn around myometrial cells to be measured using Fiji software (B) Representative intracellular calcium transient of fluorescence vs. time in one cell visualised using Clampfit software, labels have been used to indicate which parameters were measured.

3.3.5 Statistical analysis

In order to perform statistical analysis on the $[Ca^{2+}]_i$ handling data, the mean of each parameter from the three stacks of images was calculated as the representative value for that experiment. Therefore, the mean of each experiment was calculated from

approximately 100-700 cells. Statistical differences between all the changes in parameters following administration of each drug was measured using a repeated measures ANOVA. Multiple comparisons between specific drug treatments were conducted using a Tukey test; differences between groups were considered statistically significant if $p > 0.05$. The mean and standard deviation of each $[Ca^{2+}]_i$ transient parameter in response to each drug treatment has been reported in the text along with the absolute p values from the aforementioned statistical analyses. Each $[Ca^{2+}]_i$ handling parameter which was measured has been plotted on a separate graph but displayed together in one panel for each set of treatment, each differently coloured line on the same graph is representative of a different experiment.

Statistical tests were conducted using Stata IC v.16 (Stata Corporation, TX, US). Graphs were created using GraphPad Prism v.8.0 (GraphPad Software, US).

3.4 Results

3.4.1 OT administration changes the parameters of $[Ca^{2+}]_i$ transients; concomitant UDCA treatment has no effect

Analysis of the effect of OT ± UDCA administration by repeated measures ANOVA showed that there was no significant difference in the amplitude of $[Ca^{2+}]_i$ transients between all treatment groups ($n = 3$, $p = 0.0857$, Figure 3.3A).

Repeated measures ANOVA revealed a significant difference in the time to peak of the $[Ca^{2+}]_i$ transients between all treatment groups ($n = 3$, $p = 0.0012$, Figure 3.3B). Further analysis using multiple comparison tests revealed that both OT administration (82.8 ± 23.9 s, $n = 3$, $p < 0.0005$, Figure 3.3B) and UDCA administration (97.7 ± 2.8 s, $n = 3$, $p = 0.0010$, Figure 3.3B) resulted in a significant decrease when compared to the vehicle control of HBSS (193.2 ± 9.8 s, n=3, Figure 3.3B).

The same trend was observed when analysing the duration and time to decay of $[Ca^{2+}]_i$ transients. Comparison of results by repeated measures ANOVA yielded significant values for the duration ($n = 3$, $p = 0.0003$, Figure 3.3C) and time to decay ($n = 3$, $p = 0.0031$, Figure 3.3D). Comparison of specific pairs of treatments using multiple comparisons tests revealed that OT administration (181.0 ± 34.2 s, $n = 3$, p

< 0.0005, Figure 3.3C) and UDCA administration (221.5 ± 14.9 s, n = 3, p = 0.0010, Figure 3.3C) significantly decreased the duration of $[Ca^{2+}]_i$ transients compared to HBSS alone (361.2 ± 11.1 s, n = 3, Figure 3.3C). An OT- (98.1 ± 12.4 s, n = 3, p < 0.0005, Figure 3.3D) and UDCA- (115.1 ± 3.0 s, n = 3, p = 0.0010, Figure 3.3D) induced decrease in the time to decay of $[Ca^{2+}]_i$ transients was also observed when compared to HBSS alone (177.8 ± 15.3 s, n = 3, Figure 3.3D).

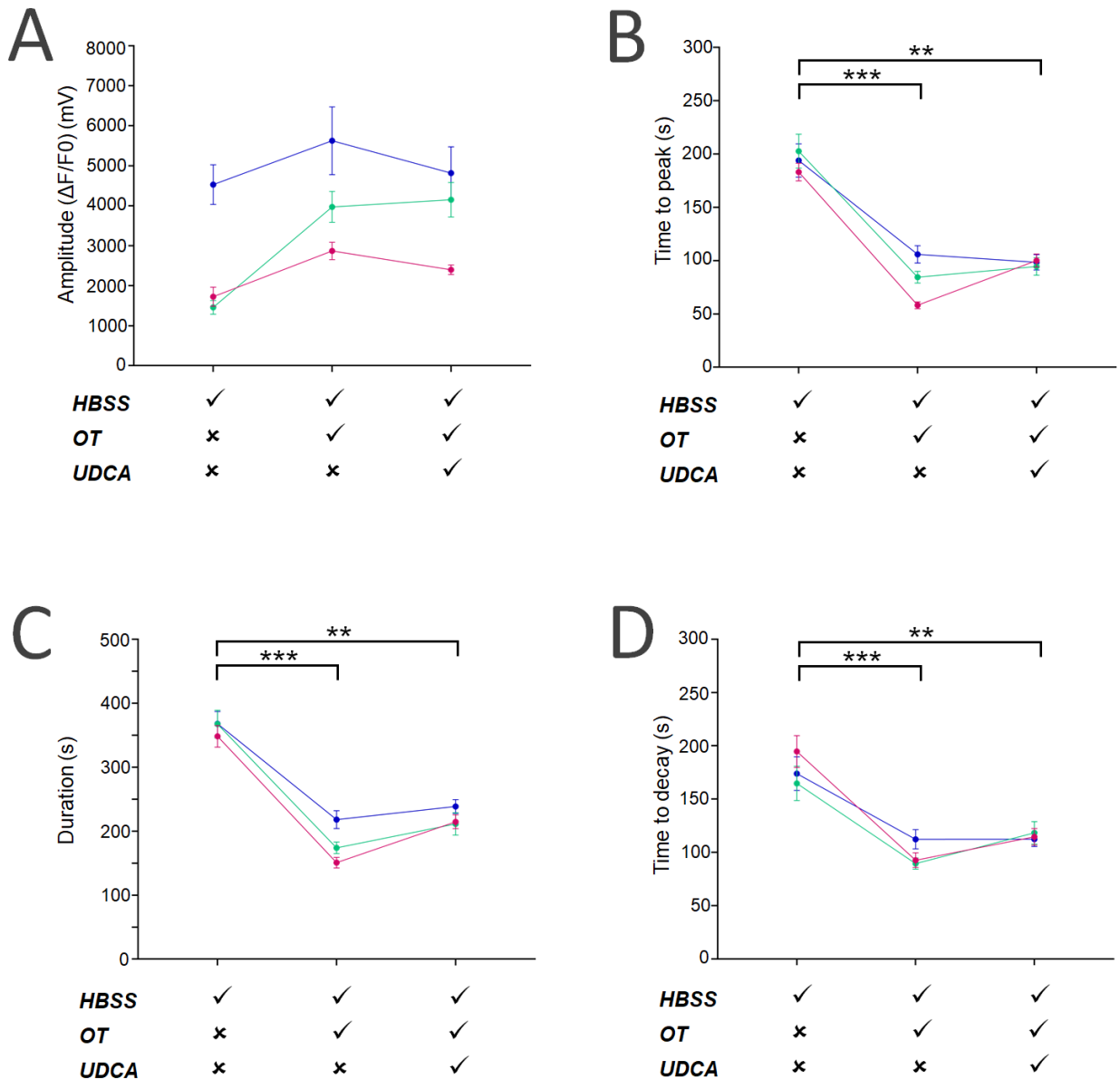

Figure 3.3: Measurements of the change in calcium transients in response to oxytocin (OT) and ursodeoxycholic acid (UDCA) administration (A) amplitude (B) time to peak (C) duration (D) time to decay. Data points signify mean values and

*error bars represent the standard error of means, each n is represented by a different colour, ** = p < 0.005, *** = p < 0.0005*

3.4.2 TCA administration with or without concomitant UDCA administration does not alter $[Ca^{2+}]_i$ transients

Analysis of the effect of TCA ± UDCA administration by repeated measures ANOVA showed that there were no significant differences between treatment groups when analysing the amplitude (n = 3, p = 0.9376, Figure 3.4A), time to peak (n = 3, p = 0.8487, Figure 3.4B), duration (n = 3, p = 0.8871, Figure 3.4C) and time to decay (n = 3, p = 0.1082, Figure 3.4D) of $[Ca^{2+}]_i$ transients. Multiple comparison testing also showed there were no significant differences between specific pairs of treatments.

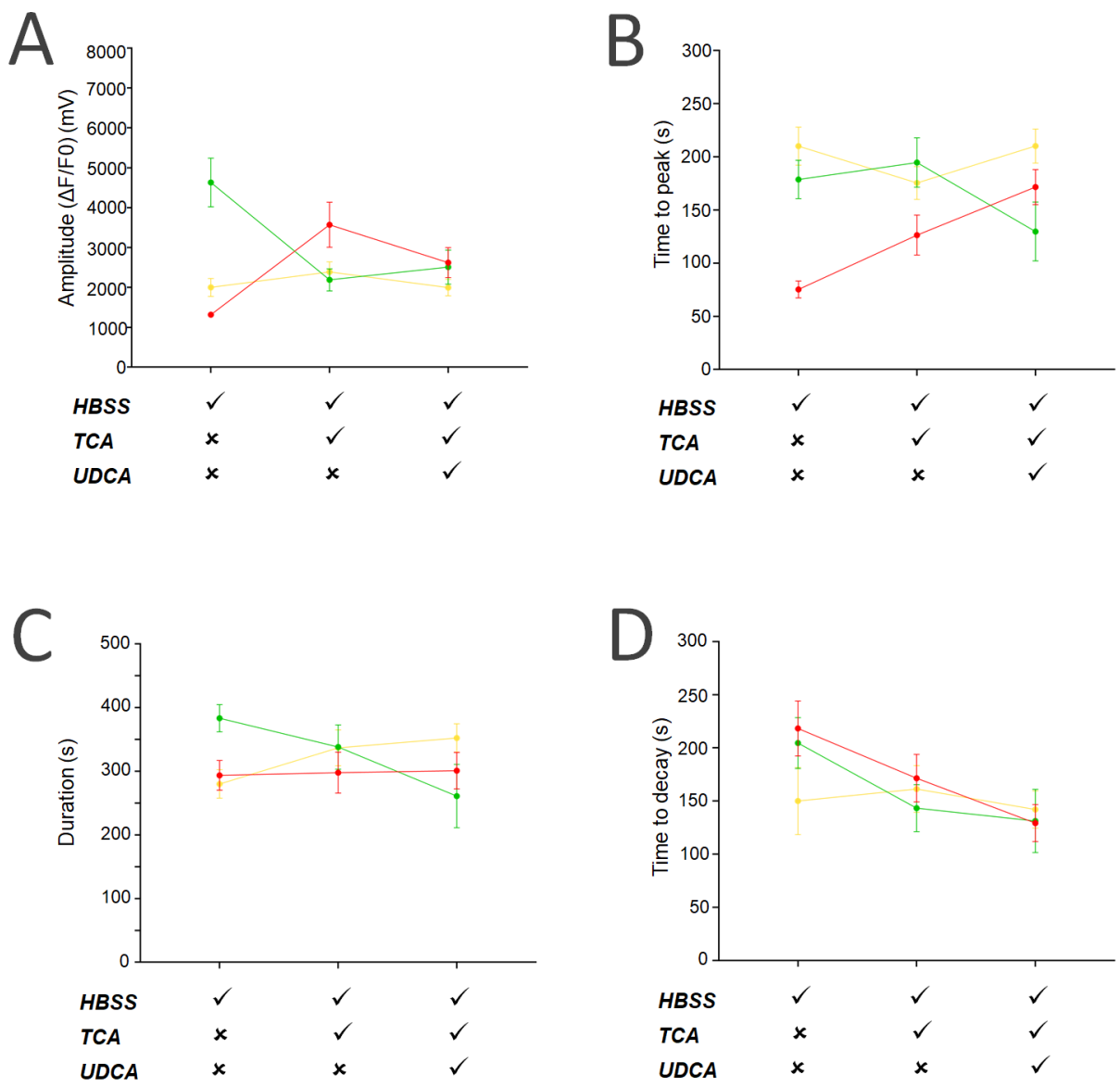

Figure 3.4: Measurements of the change in calcium transients in response to taurocholic acid (TCA) and ursodeoxycholic acid (UDCA) administration (A) amplitude (B) time to peak (C) duration (D) time to decay. Data points signify mean values and error bars represent the standard error of means, each n is represented by a different colour

3.4.3 TCA administration further increases the OT-induced increase in the amplitude of $[Ca^{2+}]_i$ transients; concomitant UDCA administration reduces this

Analysis of the effect of OT ± TCA ± UDCA administration by repeated measures ANOVA showed that there was a significant difference in the amplitude of $[Ca^{2+}]_i$ transients between all treatment groups (n = 3, p = 0.0010, Figure 3.5A). Multiple comparison tests showed significant differences in amplitude upon OT administration (1204.5 ± 236.1 mV, n=3, p = 0.003, Figure 3.5A) and OT + TCA administration (1533.1 ± 258.3 mV, n = 3, p < 0.0005, Figure 3.5A) in comparison to the HBSS control (404.2 ± 15.2 mV, n=3, Figure 3.5A). There was a non-significant increase in the amplitude of $[Ca^{2+}]_i$ transients when comparing the OT and OT + TCA administrations (n=3, p = 0.2100, Figure 3.5A). Upon UDCA administration, there was a significant reduction in amplitude compared to the OT + TCA administration (659.5 ± 119.2 mV, n = 3, p = 0.0020, Figure 3.5A). A significant reduction was also observed when comparing the amplitude after UDCA administration and OT administration alone (n = 3, p = 0.0280, Figure 3.5A).

Analysis by repeated measures ANOVA resulted in no significant changes in $[Ca^{2+}]_i$ transients between drug treatments for the other parameters of time to peak (n = 3, p = 0.4317, Figure 3.5B), duration (n = 3, p = 0.4476, Figure 3.5C) or time to decay (n = 3, p = 0.0988, Figure 3.5D).

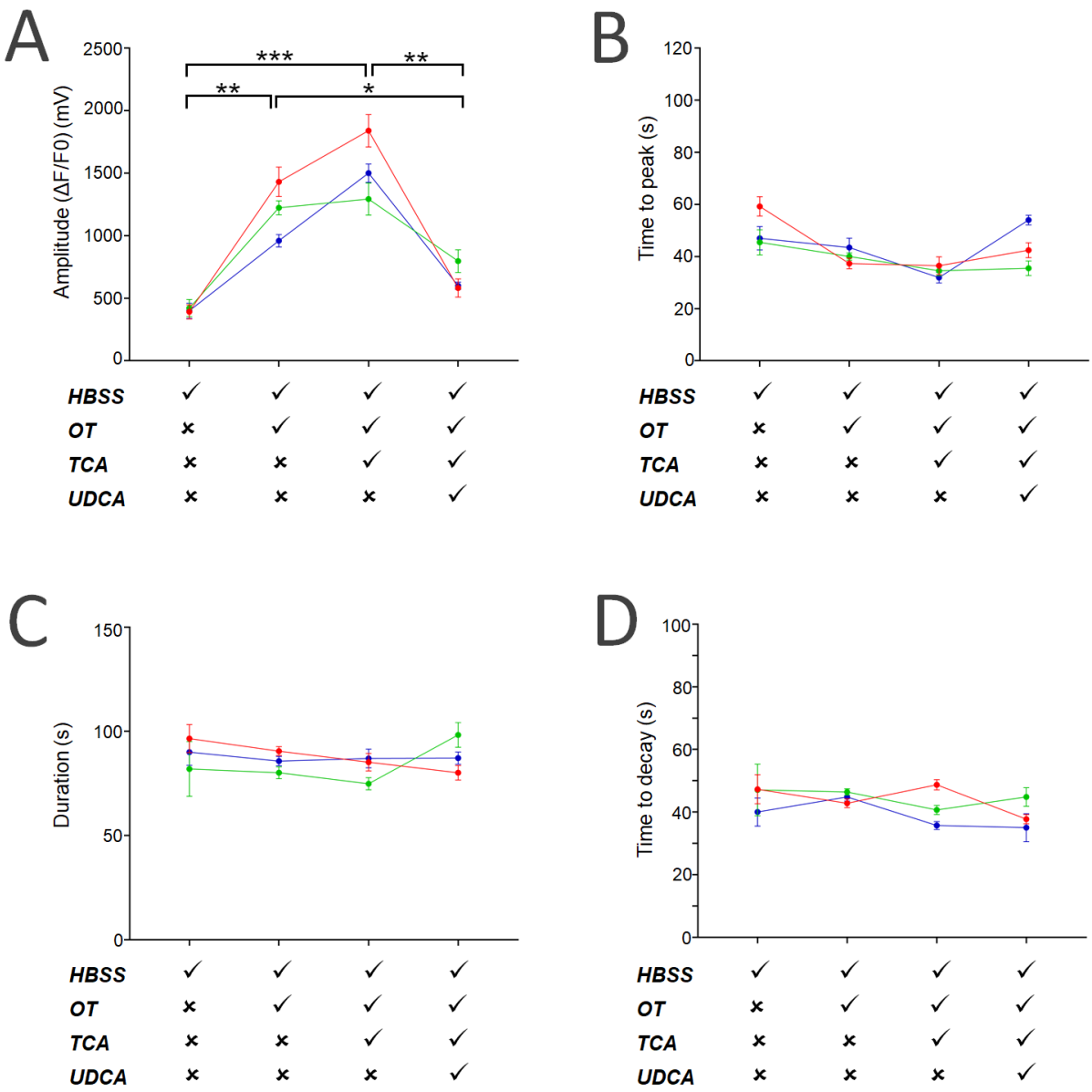

*Figure 3.5: Measurements of the change in calcium transients in response to cumulative oxytocin (OT), taurocholic acid (TCA) and ursodeoxycholic acid (UDCA) administration (A) amplitude (B) time to peak (C) duration (D) time to decay. Data points signify mean values and error bars represent the standard error of means, each experiment is represented by a different colour, * = $p < 0.05$, ** = $p < 0.005$, *** = $p < 0.0005$*

3.4.4 PGE_2 administration increases $[Ca^{2+}]_i$ transient parameters; UDCA administration partially reduces this

Analysis of the effect of PGE_2 ± UDCA administration on the amplitude of $[Ca^{2+}]_i$ transients by repeated measures ANOVA showed there were no significant differences between treatment groups (n = 4, p = 0.0568, Figure 3.6A).

There was a significant difference in the time to peak of $[Ca^{2+}]_i$ transients between treatment groups when analysed by repeated measures ANOVA (n = 4, p = 0.0146, Figure 3.6B). Multiple comparisons tests indicated that there was a significant increase in the time to peak upon PGE_2 administration (214.8 ± 38.0 s, n = 4, p = 0.011, Figure 3.6B) and UDCA administration (198.4 ± 26.6 s, n = 4, p = 0.025, Figure 3.6B) when compared to the HBSS control (116.9 ± 8.8 s, n = 4, Figure 3.6B).

A significant difference was also observed between treatment groups when analysing the duration of $[Ca^{2+}]_i$ transients when using a repeated measures ANOVA (n = 4, p = 0.0227, Figure 3.6C). Multiple comparisons tests showed that the duration of $[Ca^{2+}]_i$ transients significantly increased upon PGE_2 administration in comparison to the HBSS control (342.2 ± 46.5 vs. 208.3 ± 19.4 s, n = 4, p = 0.0070, Figure 3.6C).

No significant difference in the time to decay of $[Ca^{2+}]_i$ transients between treatment groups was found using repeated measures ANOVA (n = 4, p = 0.0649, Figure 3.6D). However, multiple comparisons tests indicated that there was a significant increase in the time to decay upon PGE_2 administration (127.3 ± 10.5 vs. 91.4 ± 10.6 s, n = 4, p = 0.036, Figure 3.6D). Subsequent administration of UDCA resulted in a reduction in the time to decay (92.9 ± 17.3 s, n = 4, p = 0.043, Figure 3.6D).

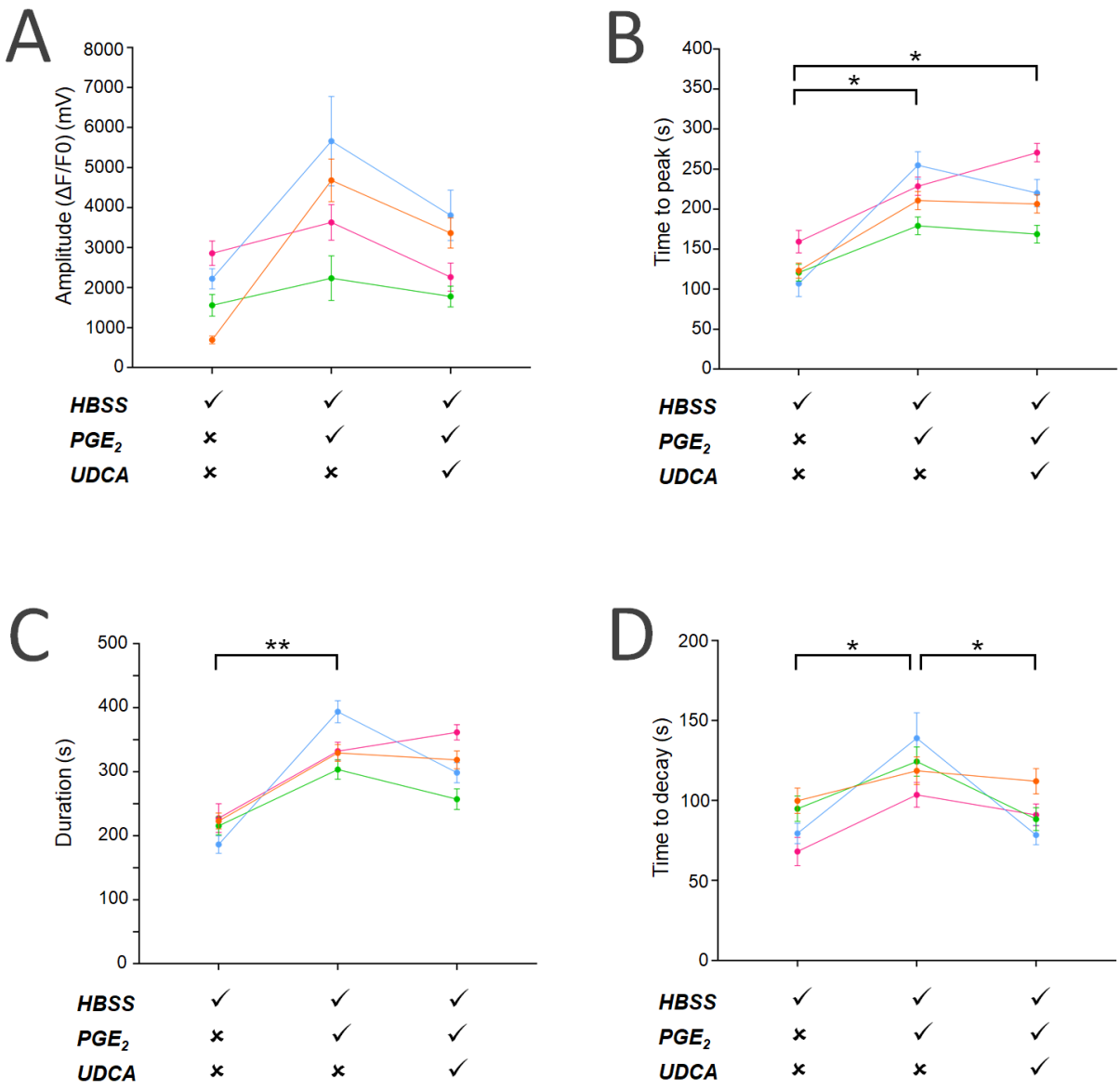

*Figure 3.6: Measurements of the change in calcium transients in response to prostaglandin E2 (PGE2) and ursodeoxycholic acid (UDCA) administration (A) amplitude (B) time to peak (C) duration (D) time to decay. Data points signify mean values and error bars represent the standard error of means, each n is represented by a different colour, * = $p < 0.05$, ** = $p < 0.005$*

3.4.5 $PGF_{2\alpha}$ administration increases the amplitude of $[Ca^{2+}]_i$ transients; this is not observed upon administration of UDCA

Analysis of the effect of $PGF_{2\alpha}$ ± UDCA administration on the amplitude of $[Ca^{2+}]_i$ transients by repeated measures ANOVA showed there was a significant differences

between treatment groups (n = 7, p = 0.0051, Figure 3.7A). Multiple comparisons tests indicated a significant increase in amplitude after $PGF_{2\alpha}$ administration in comparison to the HBSS control (5052.5 ± 1690.3 vs. 3156.5 ± 1088.7 mV, n = 7, p = 0.0260, Figure 3.7A). No significant differences in the time to peak (n = 7, p = 0.0771, Figure 3.7B) or duration (n = 7, p = 0.8931, Figure 3.7C) of $[Ca^{2+}]_i$ transients was found between treatment groups when analysed by a repeated measures ANOVA. A significant difference in the time to decay of $[Ca^{2+}]_i$ transients was observed between treatment groups (n = 7, p = 0.0444, Figure 3.7D), however multiple comparisons tests indicated no significant differences between specific pairs of treatments.

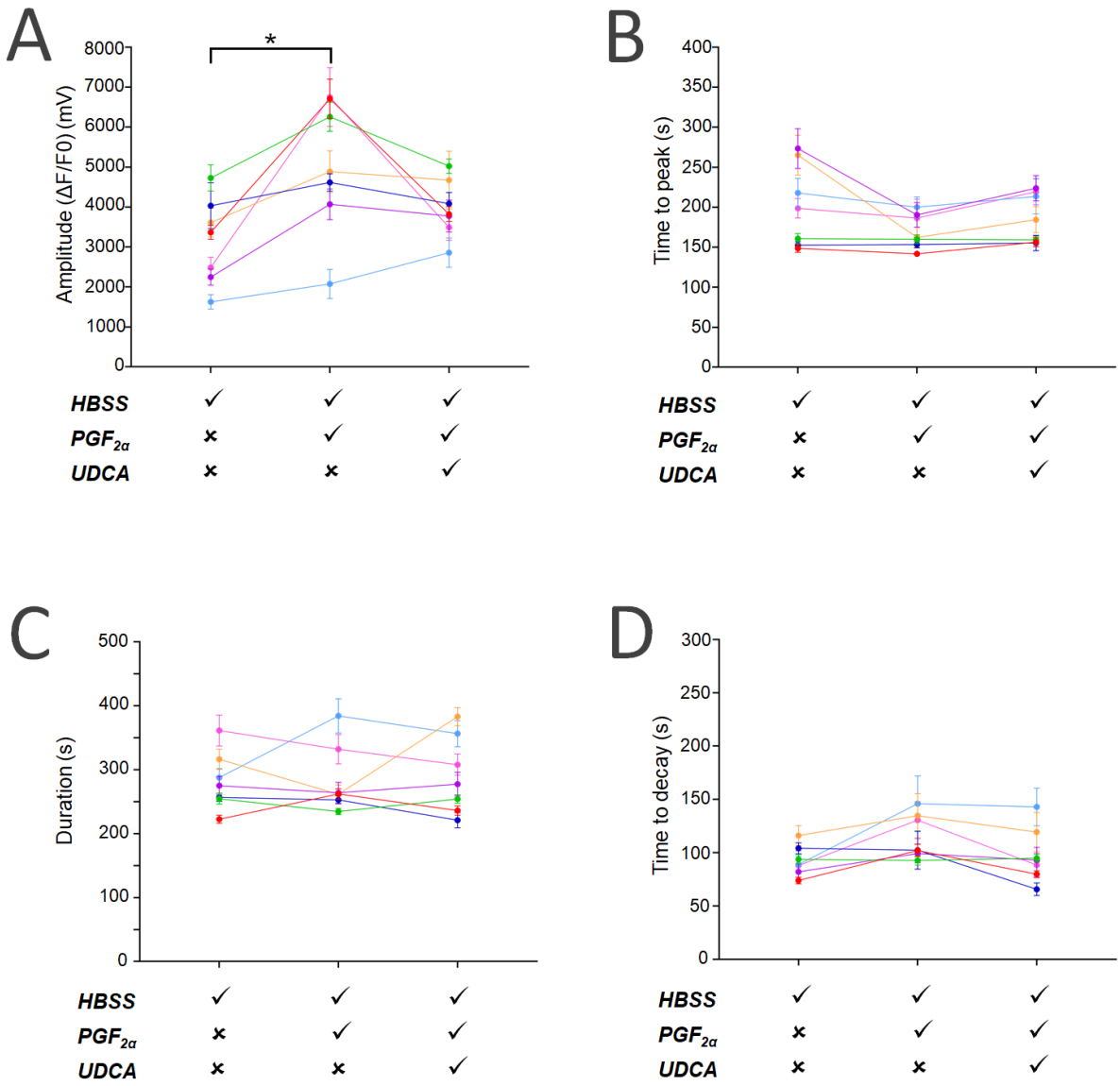

Figure 3.7: Measurements of the change in calcium transients in response to prostaglandin F2α (PGF2α) and ursodeoxycholic acid (UDCA) administration (A)

*amplitude (B) time to peak (C) duration (D) time to decay. Data points signify mean values and error bars represent the standard error of means, each n is represented by a different colour, * = $p < 0.05$*

3.5 Discussion

3.5.1 Summary of findings

This investigation measured the $[Ca^{2+}]_i$ handling and gene expression of primary human myometrial cells in response to OT, TCA, PGE_2 and $PGF_{2\alpha}$ administration with or without concomitant UDCA administration. It was observed that OT administration alone significantly decreased the time to peak, duration and time to decay of $[Ca^{2+}]_i$ transients in this model. Co-administration of UDCA also resulted in a significant decrease in the time to peak, duration and time to decay of $[Ca^{2+}]_i$ transients compared to the HBSS vehicle. In an experiment where additional TCA administration took place, OT administration significantly increased the amplitude of $[Ca^{2+}]_i$ transients. A further significant increase was observed after TCA administration. Subsequent UDCA administration resulted in the amplitude significantly decreasing. No change was observed in the $[Ca^{2+}]_i$ handling of myometrial cells after administration of TCA alone. Administration of PGE_2 significantly increased the time to peak, duration and time to decay of $[Ca^{2+}]_i$ transients. Co-administration of UDCA significantly decreased the time to decay. Administration of $PGF_{2\alpha}$ significantly increased the amplitude of $[Ca^{2+}]_i$ transients, an effect that was no longer observed after administration of UDCA.

These results demonstrate that TCA increases the size of $[Ca^{2+}]_i$ transients in human myometrial cells *in vitro* if it is co-administrated with OT. UDCA administration is associated with a partial attenuation of the OT + TC and prostaglandin-induced increase in $[Ca^{2+}]_i$ transient measurements.

3.5.2 Bile-acid induced effects on myometrial contractions

The $[Ca^{2+}]_{i.}$ handling of myometrial cells was assayed with the aim of assessing contractility; excitation-contraction coupling occurs via a membrane depolarisation and rapid increase of $[Ca^{2+}]_i$, which eventually leads to the formation of actomysosin crossbridges and contraction of the cell. This is the first study to examine the effect of bile acids on the $[Ca^{2+}]_i$ handling of primary human myometrial cells *in vitro*. The effect of the drug UDCA has not been studied on any assays of myometrial contractility.

The clinical context of this investigation was to evaluate potential mechanisms of ICP-associated spontaneous preterm labour (PTL). The risk of this adverse outcome has been associated with concentrations of maternal total serum bile acid (TSBA) concentrations, with a steep increase in risk once maternal TSBA concentrations rise above 100 µmol/L (Geenes et al., 2014a, Glantz et al., 2004, Ovadia et al., 2019). In this investigation, we observed that exposure to 100 µmol/L of the bile acid TCA resulted in increased the amplitude of $[Ca^{2+}]_i$ transients in human myometrial cells when administered with OT. The increase in amplitude of $[Ca^{2+}]_i$ transients upon TCA administration is consistent with data that shows that spontaneous preterm labour is more prevalent in women with ICP (Ovadia et al., 2019, Geenes et al., 2014a, Glantz et al., 2004).

This investigation also supports data from previous studies which observed that women with a diagnosis of ICP required a lower dose of OT to elicit uterine contractions during the induction of labour; this was also observed in contraction assays using myometrial strips from women with ICP incubated with oxytocin (Germain et al., 2003, Israel et al., 1986). The mechanism of this was stipulated to be via the increased expression of OTR which was evidenced by incubation of myometrial strips with cholic acid (CA) and subsequent protein quantification (Germain et al., 2003). In the above investigation, we have observed that a significant increase in the amplitude of $[Ca^{2+}]_i$ transients of primary myometrial cells is observed with a combination of OT and TCA treatment but not TCA alone, suggesting that the mechanism of ICP-induced PTL is at least partially via an

upregulation of OTR in the myometrium by increased bile acid concentrations and therefore increased sensitivity to OT. Increased circulating estradiol has also been reported in women with ICP that have had oxytocin-induced labour which suggests that bile acid effects on estrogen signalling should be investigated in the future (Kauppila et al., 1980).

Chronic infusion of sheep with CA also resulted in a shorter gestation period in comparison to untreated counterparts (Campos et al., 1986). More recently, there is evidence of liver dysfunction being associated with spontaneous PTL outside of ICP, with correlations observed in TSBA, alanine aminotransferase (ALT) and aspartate aminotransferase (AST) concentrations regardless of the cause or classification of disease (You et al., 2020). Estradiol, carbon tetrachloride and CA-induced cholestasis in mice also resulted in higher rates of spontaneous preterm birth which correlated with serum TSBA concentrations and reversed by FXR activation (You et al., 2020).

There is plentiful evidence to show that hydrophobic bile acids increase Ca^{2+} handling in other models. Ca^{2+} is an important cell signal for activation for various processes such as apoptosis, secretion and, in our interest, contraction (Berridge et al., 2000). Secretion of bile from the apical membrane of the hepatocyte to the canaliculus in cholestatic disease is thought to be facilitated by a hydrophobic bile acid-induced increase in $[Ca^{2+}]_{i..}$ This has been evidenced by chenodeoxycholic acid (CDCA), deoxycholic acid (DCA), taurodeoxycholic acid (TDCA), TCA and taurolithocholic acid (TLCA) interacting with the endoplasmic reticulum (ER) and golgi apparatus, mobilising $[Ca^{2+}]_i$ and causing an increase in cytoplasmic $[Ca^{2+}]_i$ in rat hepatocytes (Murray et al., 2012, Erlinger, 1990, Combettes et al., 1988, Gregory et al., 2004). Concomitant exposure to TUDCA was observed to attenuate this effect (Thibault and Ballet, 1993).

Models of other tissues have also documented hydrophobic bile acid-induced increases in $[Ca^{2+}]_{i.}$. Exposure of DCA in mouse oesophageal epithelial cells is

associated with an increase in $[Ca^{2+}]_{i.}$ (Yamada et al., 2011). In the pancreas, the Takeda G-Protein Receptor 5 (TGR5) agonist (INT-777) and sulphated TLCA also demonstrated the ability to induce $[Ca^{2+}]_i$ release via GPCR-induced cAMP activation of the ryanodine receptor and inositol triphosphate receptor (Husain et al., 2012, Kumar et al., 2012, Gerasimenko et al., 2006). In pancreatic acinar cells, CA, DCA and CDCA inhibited sarco/endoplasmic reticulum Ca^{2+}-ATPase (SERCA) leading to an increase in $[Ca^{2+}]_i$ and apoptosis due to impaired Ca^{2+} signalling (Kim et al., 2002). In a model of colon cancer, DCA treatment resulted in increased $[Ca^{2+}]_i$ which subsequently resulted in MAPK activation (Centuori et al., 2016). Rapid increases in $[Ca^{2+}]_{i.}$ induced by DCA and CDCA was also associated with the formation of pre-cancerous crypts in a model of colon cancer (Momen et al., 2002).

The functional association between a bile acid-induced increase in $[Ca^{2+}]_{i.}$ and contraction of cardiac muscle has also been investigated *in vitro*. In neonatal cardiomyocytes, TCA has been observed to bind to muscarinic 2 (M_2) receptors, causing dysfunctional Ca^{2+} dynamics via cAMP inhibition and arrhythmic activity (Sheikh Abdul Kadir et al., 2010, Gorelik et al., 2002, Williamson et al., 2001, Gao et al., 2014). Reduced activity of T-type voltage-dependent Ca^{2+} channels (VDCC) has also been stipulated to cause TCA-induced slowing of conduction velocity in the neonatal rat heart (Adeyemi et al., 2017). UDCA has a protective effect in models of the heart, restoring SERCA activity, improving markers of ER stress and preventing arrhythmia caused by hypertension, obesity or hydrophobic bile acid exposure (Ye et al., 1991, Bal et al., 2019, Schultz et al., 2016, Gorelik et al., 2003, Ceylan-Isik et al., 2011, Turdi et al., 2013).

Bile acid-induced contractile dysfunction via disruption of Ca^{2+} signalling has also been reported in other tissues. TDCA, taurochenodeoxycholic acid (TCDCA) and, to a lesser extent, tauroursodeoxycholic acid (TUDCA) causes a dose-dependent relaxation of vascular smooth muscle via the inhibition of VDCC-induced Ca^{2+} influx rather than release from intracellular stores (Pak et al., 1994). Evidence of the impact of bile acids on smooth muscle contraction include experimental data showing DCA induced relaxation in a model of the gallbladder via increasing $[Ca^{2+}]_i$

efflux (Sunagane et al., 1990). In rat bladder smooth muscle cells, lithocholic acid (LCA) was observed to decrease $[Ca^{2+}]_{i.}$ via the sodium-calcium exchanger (NCX) and therefore promoting relaxation (Zhu et al., 2016). In some studies, DCA has demonstrated to induce the increase of $[Ca^{2+}]_{i.}$ and therefore peristalsis in the colon, whilst others have demonstrated inhibition of colonic motility via blocking L-type VDCC activity (Hu et al., 2012, Kim et al., 2017). TCA was also demonstrated to reversibly inhibit contractions in ileum smooth muscle cells as a result of NCX activation (Laurence and Simmonds, 1963, Sparrow and Simmonds, 1965, Romero et al., 1993).

In this investigation, administration of UDCA induced a significant decline in the amplitude of $[Ca^{2+}]_i$ transients induced by the combination of OT and TCA treatment. The largest randomised controlled trial to date to assess the ability of UDCA therapy improve perinatal outcomes complicated by ICP demonstrated that UDCA therapy did not change the incidence of spontaneous preterm birth, although the majority of participants in the aforementioned trial had mild ICP with TSBA concentrations of <40 µmol/L (Chappell et al., 2019). However, in *in vitro* studies, TUDCA is protective against ER stress and inflammatory mediators in the fetal membranes and in myometrium (Liong and Lappas, 2014). UDCA in its unconjugated or taurine-conjugated form has been observed to improve dysfunctional Ca^{2+} signalling in other *in vitro* models. In rat vascular smooth muscle cells, UDCA inhibited hyperplasia and proliferation induced by activation of the AKT/mTOR signalling pathway (Huang et al., 2020). UDCA and TUDCA has also attenuated TLCA-induced increase in Ca^{2+} efflux in rat hepatocytes (Bouscarel et al., 1993). This suggests that there is a potential for UDCA therapy to be protective against ICP-induced spontaneous PTL, however more work is required to ascertain if it has any functional benefit in attenuating PTL-associated myometrial contractions in women with ICP. Additionally, the subset of women with ICP who would benefit from UDCA therapy requires more detailed investigation.

3.5.3 Effect of oxytocin and prostaglandin with or without UDCA treatment

Administration of OT alone non-significantly increased the amplitude and significantly decreased the time to peak, duration and time to decay of $[Ca^{2+}]_i$ transients. The oxytocin-induced peak in $[Ca^{2+}]_i$ of primary myometrial cells has previously been characterised, and oxytocin is known to increase amplitude of baseline $[Ca^{2+}]_i$ transients in these cells as well as induce a reversible oscillatory waveform which is consistent with what was observed in these data (Burghardt et al., 1999). UDCA treatment had no effect on OT-induced changes in $[Ca^{2+}]_i$ transients, this evidenced by a maintenance in the significance of reduction in the time to peak, duration and time to decay of $[Ca^{2+}]_i$ transients which was induced by OT administration. The only previous report of the effect of UDCA on OT is on isolated toad skin, and found that UDCA inhibited the OT-induced increase in sodium transport (Alonso et al., 1995). The data collected in this investigation is therefore novel and cannot be compared to previous literature. Further investigation of the effect of UDCA on OT in myometrial may be worthwhile.

The increase in amplitude of $[Ca^{2+}]_i$ transients observed in response to OT, PGE_2 and $PGF_{2\alpha}$ exposure is an expected observation based on multiple historical studies of the same drug treatments and fluorescent labelling of $[Ca^{2+}]_i$ on primary human myometrial cells and strips, causing a proportional increase in MLCK phosphorylation and a subsequent initiation of force and contractile activity in this cell or tissue type (Mackenzie et al., 1990, Luckas et al., 1999). However, evidence taken from Pregnant Human Myometrium (PHM) cell lines and primary myometrial cells has shown that Ca^{2+} mobilisation as a result of OT and PGE_2 treatment occurs from both intracellular and extracellular sources (Monga et al., 1996, Thornton et al., 1992).

3.5.4 Bile acid interactions with prostaglandin E_2

Although the effects of bile acids on PGE_2 synthesis in the myometrium has not been studied, there is now plentiful evidence that relatively hydrophobic bile acids induce PGE_2 production in other models. Colonic perfusion of LCA, CDCA, and DCA induced PGE_2 synthesis (Hikasa et al., 1989, Narisawa et al., 1987). This was also

observed in models of oesophageal cancer after exposure to CDCA and DCA (Kaur and Triadafilopoulos, 2002, Zhang et al., 1998, Kawabe et al., 2004). In pancreatic cancer models, CDCA and DCA caused dose-dependent stimulation of PGE_2 synthesis (Nakamura et al., 1994, Tucker et al., 2004). Exposure of rabbit gallbladders to TDCA led to increased prostacyclin and PGE_2 release (Myers et al., 1995). Contrastingly, DCA inhibited PGE_2 synthesis via binding to Farnesoid-X receptor (FXR) and inhibiting the enzyme phospholipase A2 in colon crypts (Jain et al., 2018). However, the majority of these data suggest that hydrophobic bile acids have a stimulatory effect on PGE_2 production. Prostaglandins also appear to have an inhibitory effect on bile acid circulation, as evidenced by $PGF_{2\alpha}$ and PGE_2 supressing bile flow and bile acid secretion in the rat liver, suggesting a negative feedback mechanism between the two signalling molecules (Beckh et al., 1994).

In this investigation, administration of UDCA concomitantly with PGE_2 resulted in a significant decrease of the time to decay of $[Ca^{2+}]_{i.}$ transients compared to PGE_2 administration alone. There also appeared to be non-significant attenuation of PGE_2- and $PGF_{2\alpha}$-induced increases in amplitudes of $[Ca^{2+}]_{i.}$ transients. Although the effect of UDCA on prostaglandins or their synthesis has not been investigated in the myometrium, it has been studied in other cells and tissues. UDCA reduced PGE_2 levels in the supernatant of lymphocytes collected from healthy controls in comparison to those which were incubated with CDCA (Nishigaki et al., 1996). In gallbladder smooth muscle collected form patients with symptomatic cholesterol gallstones, UDCA increased contractility whilst significantly decreasing production of PGE_2 (Behar et al., 2013, Guarino et al., 2007). It also supressed dysfunctional PGE_2-induced contraction of gallbladder muscle in guinea pigs which was not observed with CDCA treatment (Xiao et al., 2003). Patients with multiple cholesterol gallstones that had undergone long-term treatment with UDCA also had decreased levels of PGE_2 in the gallbladder (Kano et al., 1998). Mucosal concentrations of PGE_2 were lower in rat colons pre-treated with a carcinogen and subsequently treated with UDCA in comparison to colons without UDCA treatment (Ikegami et al., 1998, Earnest et al., 1994). UDCA attenuated CDCA-induced PGE_2 production in primary human gastric cancer cells *in vitro*, but it did not affect COX-2 expression (Wu et al., 2018). TUDCA treatment attenuated the ER stress-induced

increase in PGE_2 levels in rat livers (Aslan et al., 2018). In contrast to the aforementioned data, UDCA prevented the ethanol-induced fatty liver in rats from metabolising PGE_2 and therefore increased its circulating levels (Lukivskaya et al., 2001). The above data therefore highly suggests that UDCA attenuates dysfunctional PGE_2 synthesis.

A recent investigation of sphingolipid concentrations in a Polish cohort of women with who had been diagnosed with mild ICP found that circulating plasma concentrations of C16 Ceramide (C16-Cer) in these women were higher than controls and reduced in response to UDCA treatment (Mikucka-Niczyporuk et al., 2020). Ceramides are a class of sphingolipids that act as pro-inflammatory and –apoptotic signals, and have demonstrated to upregulate the synthesis of COX-2 and subsequent production of PGE2 in the amnion and cervix (Chalfant and Spiegel, 2005, Kishore et al., 2017, Nakamura et al., 2001, Subbaramaiah et al., 1998). C16-Cer levels in particular have also been significantly positively associated with the incidence of PTL (Signorelli et al., 2016, Laudanski et al., 2016). However, the median TSBA concentration of the untreated cohort of cases was 11.13 µmol/L and elevated TSBA concentrations were not mandatory for ICP diagnosis in the aforementioned study (Mikucka-Niczyporuk et al., 2020). Unfortunately, rates of PTL in these participants were not reported or analysed in relation to circulating TSBA and C16-Cer concentrations (Mikucka-Niczyporuk et al., 2020). However, the downregulation of C16-Cer by UDCA in the myometrium could provide a potential mechanism to explain the significant decrease in the PGE_2-induced increase in the time to decay and the non-significant decrease in the amplitude of $[Ca^{2+}]_{i.}$ transients observed in our study. Although the effect of TCA in combination with prostaglandin treatment was not studied in this investigation, this would certainly be an interesting avenue to investigate in future due to the indication that ceramides may be markers for ICP. Circulating concentrations of prostaglandins in women with ICP and their relation to TSBA concentrations could also be assayed as an observational study. In addition, the aforementioned data demonstrating the protective effect of UDCA against PGE_2 in other non-myometrial models that have not been exposed to high levels of hydrophobic bile acids suggests that UDCA could

be worth investigating as a tocolytic therapy in pregnancies that are not complicated by ICP.

3.5.5. Limitations of calcium handling assays

Fluo-4 AM has been demonstrated to effectively indicate $[Ca^{2+}]_i$ in primary human myometrial cells that have been stimulated by oxytocin exposure (Murtazina et al., 2011). Fluo-4 is one of several high-affinity Ca^{2+}-binding fluorescent indicators that can be loaded into cells using an acetoxymethyl (AM) ester derivative; the use of these have now become common methods of measuring dynamic movement of freely diffusible $[Ca^{2+}]_{i.}$ in living cells (Paredes et al., 2008). Although these methods have benefits, such as being non-invasive, they have limitations due to their ability to enter and their de-esterified form accumulate in the cell's organelles, particularly mitochondria (Paredes et al., 2008). Fluo-4 AM specifically has been demonstrated to accumulate in the sarcoplasmic reticulum more than the other high-affinity indicators fluo-2 AM and fluo-3 AM (Terentyev et al., 2002). This in turn leads to a slower recovery rate and higher peak of $[Ca^{2+}]_{i.}$ transients (Terentyev et al., 2002). In order to combat this, an alternative fluo-AM could be used as a $[Ca^{2+}]_{i.}$ indicator in future experiments. Loading of a $[Ca^{2+}]_i$ indicator via a patch pipette for localised delivery can also be used which has been demonstrated to successfully deliver dextran-conjugated $[Ca^{2+}]_{i.}$ indicators (Hagen et al., 2012).

3.5.6 Alternative models of the myometrium to investigate preterm labour

In this investigation, primary cells were isolated from the lower segment of the non-labouring pregnant uterus and cultured until confluent enough for experiments. There is contrasting evidence of whether the location of uterine biopsy is relevant, as both lower and upper segments of the uterus have been demonstrated to have the same functional physiology in contraction experiments of myometrial strips which suggests that the location of biopsy did not have an effect on the contractile properties of the cells in our investigations (Luckas and Wray, 2000). However, the expression of Cx43, vimentin and PTGS2 were found to be higher in cells from the lower segment suggesting that biopsies from both sections have transcriptome

differences and the bile acid response to both types of tissue should be investigated (Mosher et al., 2013).

An *in vitro* primary cell model holds many advantages due to the ability to use a relatively simple technique to study the physiological processes of the myometrium, however due to the requirement to culture the cells to their fifth or sixth passage to obtain the appropriate confluency for investigation, there are legitimate concerns of how well the cells represent the response of the original tissue they were obtained from. However, data from primary myometrial cells showed stable expression of smooth muscle cell markers and response to inflammatory stimuli for ten passages (Mosher et al., 2013). Modified models of primary myometrial cells have previously been utilised to investigate contraction, e.g. primary myometrial cells from non-labouring tissue have been cultured on top of a layer of flexible collagen in order to simulate stretching of the myometrium. This *in vitro* model has demonstrated that consistent stretching induces COX2 activity which led to higher concentrations of PGE_2 and prostacyclin and lower concentrations of $PGF_{2\alpha}$ in the surrounding medium and can be considered as an alternative method in lieu of drug-induced contractions in this investigation (Sooranna et al., 2004).

Primary cell models also have the experimental disadvantages of a lower life span and proliferative capacity as well as decreased contractility in response to agonists (Campbell et al., 1974). In addition, biopsies from caesarean sections are required which can be difficult to obtain due to ethical considerations and dependency on a non-essential procedure during invasive surgery. To combat these difficulties, an immortalised cell line may be useful to do an investigation of treatments on large sample numbers with ease. The PHM cell line, a human pregnancy-derived immortalised myometrial cell line, is commercially available and has been demonstrated to be OT-sensitive and effective for contractile studies on myometrial cells with the use of Fluo-4 AM as a $[Ca^{2+}]_i$ indicator (Monga et al., 1996, Makieva et al., 2016, Murtazina et al., 2011). A cell line using immortalised non-pregnancy human myometrial cells which were transfected with human telomerase reverse transcriptase (hTERT) has been developed and is also commercially available and

has been extensively used to study the myometrium (Condon et al., 2002, Shay and Wright, 2005). Comparative assays between PHM-1 and hTERT cells to primary myometrium cells showed that the transcriptome OT-induced $[Ca^{2+}]_{i.}$ increase of PHM-1 cells was most similar to the primary myometrial cells, however hTERT cells exhibited the most similar responses to a panel of 61 inhibitory and excitatory drugs overall (Siricilla et al., 2019). Both of these cell lines could therefore be an alternative to primary cell culture of human myometrium in order to investigate the effect of bile acids and drug treatments on a larger sample size.

However, 2D culturing systems do not mimic the cell-to-cell interactions that would occur *in vivo*. 3D culturing systems of the human myometrium have therefore been developed as an alternative technique, although these will not mimic a true biochemical environment *in vivo* as well as the inability to replicate the mechanical pressure that occurs during parturition (Drover and Casper, 1983). These have the benefit over 2D systems in that they improve the ability to study and mimic the physiological mechanisms of parturition and responsiveness to drugs *in vivo* (Ravi et al., 2015). 3D human myometrial cell culture systems have been developed via scaffold, bioengineering and 3D-bioprinting methods (Malik and Catherino, 2012, Souza et al., 2017, Heidari Kani et al., 2017, Vidimar et al., 2018, Yochum et al., 2018). Stem cell differentiation to create functional myometrial cells has also been explored to combat the limited proliferative capacity of primary myometrial cells in order to form a 3D model (Heidari Kani et al., 2017, Xiao et al., 2010). Although these type of culture systems require a much larger scope of technical expertise, specialised equipment and a larger expense, use of these techniques could be a possibility in future studies to investigate ICP-associated parturition.

Myometrial strips connected to force transducers in an organ bath *ex vivo* are possibly the most frequently used model for contractility and drug discovery assays of the pregnant myometrium; this was the technique used to demonstrate that bile acids induce a higher sensitive of OT via upregulation of OTR (Germain et al., 2003). Myometrial strips are thought to provide a closer representation to *in vivo* responses due to being investigated whilst freshly isolated and in addition to

allowing real-time observation of contractile properties in response to different environments, the same strips can be assayed afterwards for histology, mRNA and protein expression analyses to elucidate on mechanisms of contraction (Anderson et al., 2009). Myometrial explants or tissue pieces that are biopsied and subsequently incubated with different treatments have also been utilised as an *ex vivo* model (Welsh et al., 2012). Comparisons between snap-frozen fresh myometrial biopsies, *ex vivo* myometrial pieces, *in vitro* primary myometrial cells at passage 4 and hTERT cells has shown that the transcriptomes of the *ex vivo* myometrial pieces resembled the fresh biopsies the closest, with the mRNA expression of parturition-associated key genes such as *PGR*, *OXTR* and *GJA1* being significantly higher or lower than fresh biopsies (Georgiou et al., 2016). Although a pro-inflammatory phenotype was observed in all 3 models compared to the fresh biopsies, the study showed that *ex vivo* models were more likely to represent a fresh biopsy than in vitro models (Georgiou et al., 2016). However, there is also evidence that pregnant non-labouring myometrial tissue undergo rapid phenotypic changes during their incubation *ex situ*; transcriptome analysis has shown that the progesterone (P4) receptor PRA:PRB ratio significantly increases after 6 hours of incubation, which is consistent with the transition from phase 0 of labour (quiescence) to phase 1 (initiation) (Ilicic et al., 2017). Furthermore, mRNA quantification of this tissue also observed significant culture-induced changes in expression of *ESR1*, *PTGS2* and *OTR* and a non-responsiveness of *ESR1* and *PTGS2* expression to P4 and estrogen treatments (Ilicic et al., 2017).

Manipulation of the myometrium *in vivo* can be conducted using animal models, although there are barriers regarding translational applicability to human parturition (Mitchell and Taggart, 2009). Induction of cholestasis and investigation of spontaneous preterm birth has been investigated via utilisation of estradiol, CCl4 and CA in animal models [18]. Such models can also be used to investigate whether other mechanistic pathways are involved in bile acid-induced PTL, particularly via the inhibition or activation of receptors that bile acids are known to mediate.

3.5.7 Further investigation of this model

Future investigations using this model will include mRNA and protein expression studies. The aim of these studies will be to investigate the expression of genes and proteins which are upregulated in PTL, such Tumour Protein 53, interleukin-9, PTGS2 and calmodulin as well as other myometrial markers such as alpha-smooth muscle actin and estrogen receptor (Charpigny et al., 2003). Quantification of mRNA will be via RT-qPCR. Measurements of mRNA will allow us to observe which genes have an upregulated transcription in myometrial cells, however, they may not necessarily reflect the level of protein translation and expression (Vogel and Marcotte, 2012). Therefore, a common and relatively simple method for quantification of protein levels in cells that could also be conducted in addition to mRNA measurement is western blotting (or immunoblotting) (Towbin et al., 1979).

3.5.8 Other limitations

The main limitation of the data presented in this chapter is the low number of samples in each experiment. Due to the time-consuming nature of the time-lapse imaging of $[Ca^{2+}]_i$ handling and subsequent measurement, the majority of treatment sets were only replicated three times. Ideally, a larger number of replicate experiments would have been conducted in order to get a more representative set of data about the responses to the different drug treatments used. In addition, since performing these experiments, it was discovered that the risk of spontaneous PTL dramatically increases at maternal TSBA concentrations of ≥100 μmol/L (Ovadia et al., 2019). TCA has the most substantial elevation in concentration in untreated ICP compared to the other bile acids present in the maternal and fetal bile acid pool, however, only one concentration of TCA and UDCA was used in these experiments. Using a larger range of bile acids and concentrations would provide more insight in the association between severity of ICP and ICP-induced PTL.

The experiments in which both OT and TCA were exposed to the myometrial cells concomitantly resulted in $[Ca^{2+}]_i$ handling data measurements that were relatively lower than measurements captured with OT and TCA treatment alone. It is difficult

to ascertain exactly why this was, however, due to all these particular experiments being conducted during a small time period, an ineffective/expired batch of Fluo-4AM could provide a likely explanation for the lower levels of fluorescence observed. Ideally, these experiments would be repeated to obtain measurements which are more comparable to the rest of the optical recordings.

3.6 Conclusion

This is the first investigation to measure the $[Ca^{2+}]_i$ handling of primary human myometrial cells in response to bile acid exposure. We observed that exposure to TCA, in addition to OT, significantly increased the amplitude of $[Ca^{2+}]_{i.}$ transients which was not observed with OT alone which provides support to the hypothesis that raised maternal TSBA concentrations as a result of ICP induce spontaneous preterm labour via increasing the sensitivity of oxytocin in the myometrium. UDCA was demonstrated to reduce the increased amplitude of $[Ca^{2+}]_i$ transients induced by the combination of oxytocin and taurocholic acid as well as PGE_2 and $PGF_{2\alpha}$ treatments; this a novel finding as the myometrial response to UDCA has not been measured in any models or observational studies.

Future investigations will concentrate on investigating the mechanisms by which the above drug treatments affect $[Ca^{2+}]_i$ handling in the myometrium via assays of mRNA and protein quantification. The data in this study is suggestive that UDCA should be further investigated as a potentially useful pharmacotherapy for bile acid-induced $[Ca^{2+}]_i$ dysregulation in the myometrium.

Chapter 4: Observations of fetal cardiac dysfunction in intrahepatic cholestasis of pregnancy

4. Observations of fetal cardiac dysfunction in intrahepatic cholestasis of pregnancy

4.1 Abstract

Intrahepatic cholestasis of pregnancy (ICP) is associated with increased IUD risk. This study aimed to assess the relationship between bile acid concentrations and fetal cardiac dysfunction in ICP with or without ursodeoxycholic acid (UDCA) treatment.

Bile acid profiles and NT-proBNP, a marker of ventricular dysfunction, were assayed in umbilical venous serum from 15 controls and 76 ICP cases (36 untreated, 40 UDCA-treated). Fetal ECG traces were obtained from 43 controls and 48 ICP cases (26 untreated, 22 UDCA-treated). PR interval length and heart rate variability parameters (RMSSD, SDNN) were measured in two behavioural states (quiet and active sleep). Partial correlation coefficients (r) and median [IQR] are reported.

In untreated ICP, fetal total serum bile acids (TSBA, r=0.49, p = 0.019), their hydrophobicity index (r=0.20, p = 0.039), glycocholate (r=0.56, p = 0.007) and taurocholate (r=0.44, p = 0.039) positively correlated with fetal NT-proBNP. Maternal TSBA (r=0.40, p = 0.026) and alanine aminotransferase (r=0.40, p = 0.046) also positively correlated with fetal NT-proBNP. No significant correlations to NT-proBNP were observed in the UDCA-treated cohort. Fetal PR interval length positively correlated with maternal TSBA in untreated (r=0.46, p = 0.027) and UDCA-treated ICP (r=0.54, p = 0.026). Fetal RMSSD in active sleep (9.6 [8.8,11.3] vs. 8.7 [7.6,9.6] ms, p = 0.028) and SDNN in quiet sleep (11.0 [9.5,14.9] vs. 7.9 [5.1,9.7] ms, p = 0.013) and active sleep (25.4 [21.0,32.4] vs. 18.2 [14.7,25.7] ms, p = 0.003) were significantly higher in untreated ICP cases than controls. UDCA treatment was associated with a significant reduction in RMSSD in active sleep (8.5 [7.4, 9.7] ms, p = 0.030).

An elevated fetal and maternal serum bile acid concentrations in untreated ICP are associated with an abnormal fetal cardiac phenotype characterised by increased NT-proBNP concentration, PR interval length and heart rate variability. UDCA treatment partially attenuates this phenotype.

4.2 Introduction

Intrahepatic cholestasis of pregnancy (ICP), the most common gestational liver disease, is diagnosed in women with pruritus and elevated maternal total serum bile acid (TSBA) concentrations (Geenes et al., 2014b, Glantz et al., 2004). ICP is associated with adverse pregnancy outcomes; maternal TSBA concentrations ≥40 μmol/L resulted in the increased likelihood of spontaneous preterm birth, prolonged neonatal unit (NNU) admission and fetal asphyxia in a prospective Swedish cohort, and intrauterine death (IUD) was also increased in a UK cohort (Glantz et al., 2004, Geenes et al., 2014a). More recently, maternal TSBA concentrations were found to be the most useful predictive biomarker for ICP-associated IUD (Ovadia et al., 2019). The prevalence of IUD was shown to increase from 0.28% to 3.44% in singleton pregnancies with maternal TSBA concentrations of ≥100 μmol/L; the prevalence of IUD in the control cohort of this study was found to be 0.31% (Ovadia et al., 2019).

The mechanism of ICP-associated IUD is unknown, post-mortem evidence has shown that infants are appropriately grown after an IUD event (Fisk and Storey, 1988). However, there is evidence of fetal cardiac dysfunction in pregnancies complicated by ICP, with speculation of a sudden arrhythmic event causing fetal demise (Williamson et al., 2001). Echocardiography has demonstrated fetal atrial flutter and supraventricular tachycardia in ICP and cardiotocography (CTG) monitoring has detected bradycardia preceding an IUD (Al Inizi et al., 2006, Shand et al., 2008, Altug et al., 2015, Lee et al., 2009). Women with both ursodeoxycholic acid (UDCA) -treated and untreated ICP have impaired fetal left ventricular function, evidenced by increased left ventricular myocardial performance index (LMPI), increased myocardial tissue velocities, reduced left ventricular (LV) global strain rate and increased isovolumetric contraction and relaxation times via echocardiography, all of which are more pronounced in severe ICP (Henry and Welsh, 2015, Sanhal et al., 2017, Ozel et al., 2018, Ataalla et al., 2016, Fan et al., 2014). In addition, concentrations of N-terminal pro-B-type natriuretic peptide (NT-proBNP) and cardiac troponin I, markers used for diagnosis of heart failure and left ventricular systolic dysfunction, are increased in fetal umbilical venous blood from ICP pregnancies (Fan et al., 2014, Zhang et al., 2009a).

There is evidence of increased fetal PR interval length in both UDCA-treated and untreated ICP which is associated with disease severity (Strehlow et al., 2010, Rodríguez et al., 2016, Kadriye et al., 2019). Although there is currently no evidence to suggest ICP prolongs fetal QTc interval length, maternal QTc interval prolongation has been reported in women with mild ICP (Kirbas et al., 2015).

Investigation of the cardiac time intervals (CTIs) mentioned above are useful for diagnosis of various disorders. A prolonged QTc interval (a QT interval that has been corrected for heart rate) length is an electrophysiological anomaly observed in Long QT Syndrome and Torsades De Pointes and associated with arrythmia-induced sudden death in adults (Moss et al., 1985, Myerburg et al., 1997). A prolonged PR interval length is a clinical indicator for atrioventricular (AV) block, which has been shown to lead to the development of atrial fibrillation and a higher risk of mortality (Cheng et al., 2009).

There are no conclusive data about the effect of ICP on fetal heart rate variability (fHRV), an established indicator of fetal autonomic nervous system function and wellbeing *in utero*, or the effect of UDCA treatment on this parameter (Van Leeuwen et al., 2013). Fetal heart rate activity exists in four different behavioural states (1F-4F), defined based on specific heart rate patterns, eye and body movements (Nijhuis et al., 1982). The fetus spends the majority of the time in 1F and 2F, thought to resemble non-REM (quiet) sleep and REM (active sleep), respectively (Pillai and James, 1990). Analysing fHRV in the context of behavioural state is necessary in order to differentiate between normal and abnormal activity. For example, state 1F has a reduced heart rate variability and movement activity compared to state 2F (Nijhuis et al., 1982).

UDCA marginally reduces maternal pruritus and most studies have shown improved concentrations of maternal and fetal TSBA in ICP (Chappell et al., 2012, Chappell et al., 2019). UDCA has a demonstrably lower bile acid hydrophobicity index (HI), a measure associated with bile acid-induced intra- and extracellular cytotoxicity

(Heuman, 1989, Hofmann, 1999). It has a protective effect in *in vitro* fetal heart models, attenuating taurocholic acid (TCA)-induced slowing of ventricular conduction velocity in neonatal rat hearts and inhibiting TCA-induced conduction abnormalities in human fetal and adult heart models (Rainer et al., 2013, Adeyemi et al., 2017, Schultz et al., 2016). The impact of UDCA on human fetal cardiac dysfunction *in vivo*, however, is yet to be fully established. There have been reports of fetal demise and CTG abnormalities occurring in UDCA-treated pregnancies and fetuses of UDCA-treated cohorts have displayed left ventricular dysfunction and prolonged mechanical PR interval length (Lee et al., 2009, Sanhal et al., 2017, Strehlow et al., 2010, Schultz et al., 2016, Miragoli et al., 2011, Sentilhes et al., 2006), however most of the aforementioned studies do not adjust for severity of hypercholanaemia.

The aim of this project is to establish whether untreated severe ICP causes a fetal cardiac phenotype that predisposes to potentially fatal cardiac arrhythmia using measurement of fetal cardiac time intervals (CTI), fHRV and NT pro-BNP concentrations in the umbilical venous blood. We also aim to evaluate the impact of UDCA treatment on fetal cardiac parameters.

4.3 Patients and Methods

4.3.1 Recruitment for umbilical venous blood assays

Umbilical venous blood was collected from ICP participants ± UDCA treatment and matched controls after informed consent from St. Thomas' and Queen Charlotte's Hospitals, UK, between September 2009 and January 2019 (ethical approval REC numbers 15/WM/0017 and 08/H0707/21) (Figure 4.1). Some participants were also recruited from the PITCHES trial (n=14) (EudraCT number: 2014-004478-41) (Chappell et al., 2019). Recruitment of participants was conducted by the NIHR Clinical Research Network team at each site.

ICP was diagnosed in women with pruritus and non-fasting serum TSBA concentrations ≥10 μmol/L. Peak maternal TSBA concentrations taken during pregnancy were used to classify women as having mild (10-39 μmol/L) or severe (≥40 μmol/L) ICP. Women treated with UDCA (500-2500 mg per day) were analysed separately to untreated cases. Women recruited as controls had uncomplicated pregnancies with no symptoms of ICP and no diagnosis of ICP in previous pregnancies. Maternal and fetal demographic and delivery details for these participants are summarised in Table 4.1.

Umbilical venous blood was collected immediately after delivery in plain vacutainers, centrifuged for 15 minutes at 3500rpm and umbilical serum frozen within 30 minutes at -80°C. Umbilical venous blood was collected by the clinical staff on call at the time of delivery and processing and freezing steps were conducted by the laboratory research staff. NT-proBNP concentrations were measured using a human proBNP enzyme linked immunosorbant assay (ELISA) kit (Raybiotech, GA, USA) as per manufacturer's instructions. Individual bile acids were measured using ultra-performance liquid chromatography tandem mass spectrometry (UPLC-MS/MS) by Anita Lövgren-Sandblom and Hanns-Ulrich Marschall (Karolinska Institute, Sweden). The HI of fetal bile acids in each serum sample was calculated using the mole fraction and the previously reported hydrophobicity of individual bile acids by Heuman et al (Heuman, 1989).

4.3.2 Recruitment for ECG recording

Prospective cohorts of women with ICP or uncomplicated pregnancy who were >20 weeks of gestation were recruited after informed consent from Nottingham City Hospital between October 2007 and January 2011 and St. Thomas', Queen Charlotte's and St. Richard's Hospitals in the UK between January 2015 and June 2019 (REC numbers 08/H0707/21 and 15/WM/0017) (Figure 4.1). Some participants were also recruited from the PITCHES trial (n=3) (Chappell et al., 2019). Initial ethics applications at the beginning of the study were written by Victoria Geenes and Jenny Chambers (King's College London). Recruitment of participants and fitting

of the ECG monitor was conducted by the NIHR Clinical Research Network team at St. Thomas', Queen Charlotte's and St. Richard's Hospitals. Some participants were also recruited and had the monitor fitted by Sahil Deepak (King's College London). Recruitment and fitting of the monitor at Nottingham City Hospital was conducted by Indu Asanka Jayawardane (Nottingham City Hospital).

Although ethical permission was granted to collect umbilical venous blood in women who underwent ECG recording, a separate cohort was required due to the low number of women who gave both types of sample. ICP was diagnosed as described in section 4.3.1. Maternal TSBA concentrations were tested via enzymatic assay within 3 days of participation to obtain a measurement close to the time of fECG recording. ICP cases treated with UDCA (500-2500 mg per day) at the time of fECG acquisition were analysed separately to untreated cases. Demographic and delivery details of participants are shown in Table 4.2.

Women were not eligible for recruitment if they had a multifetal pregnancy, were in active labour, had diabetes mellitus, hypertension or any cardiac/liver disorders or if the fetus had identified congenital abnormalities. Birth weight centile for fetuses who underwent ECG and umbilical venous blood sample collection was calculated using GROW software and based on the mean birth weight reported in 2012 in England and Wales (Ghosh et al., 2018).

Based on questionnaires submitted after ECG recordings, no women felt unwell or had decreased fetal movements at the time of recording or up to 24 hours afterwards.

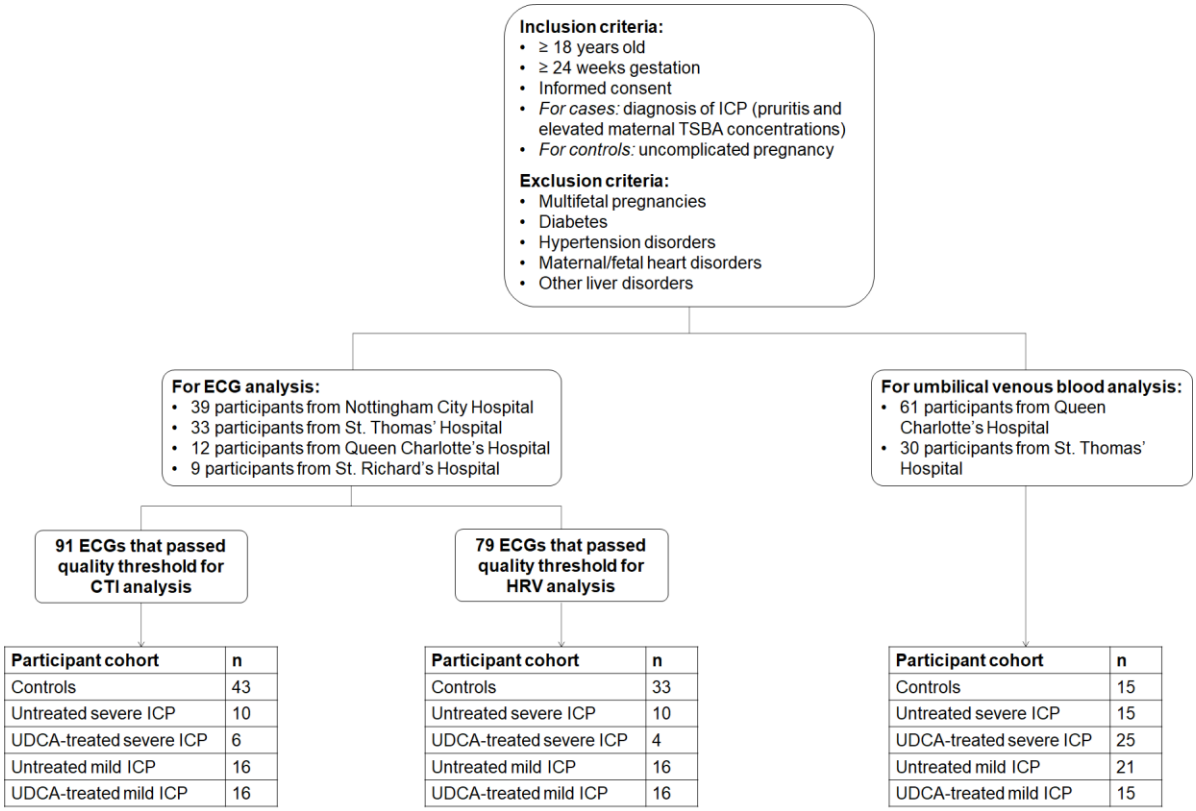

Participant cohort	n
Controls	43
Untreated severe ICP	10
UDCA-treated severe ICP	6
Untreated mild ICP	16
UDCA-treated mild ICP	16

Participant cohort	n
Controls	33
Untreated severe ICP	10
UDCA-treated severe ICP	4
Untreated mild ICP	16
UDCA-treated mild ICP	16

Participant cohort	n
Controls	15
Untreated severe ICP	15
UDCA-treated severe ICP	25
Untreated mild ICP	21
UDCA-treated mild ICP	15

Figure 4.1: Flowchart depicting numbers of participants in each analysed cohort and the sites they were recruited from.

4.3.3 ECG recording and processing

The Monica AN24 (Monica Healthcare Limited, Nottingham, UK) was used to obtain overnight fECG recordings as previously described (Graatsma et al., 2009, Piéri et al., 2001). Monica DK v1.9 software (Monica Healthcare Limited, Nottingham UK) was used to obtain a trace of fetal heart rate (FHR), maternal heart rate (MHR) and maternal movement over the recording period, as previously described (Figure 4.2). In order to remove probably periods of maternal wakefulness, the first and last hour of the recording were excluded from analysis. A two-hour period of the recording was chosen where there was a low indication of maternal movement through observation of the Monica AN24 inbuilt accelerometer and acceleration patterns in the MHR as well as ensuring the chosen period had a minimal loss of FHR signal. This 2-hour period was used for PR and QT interval length measurement and heart rate variability (HRV) analysis.

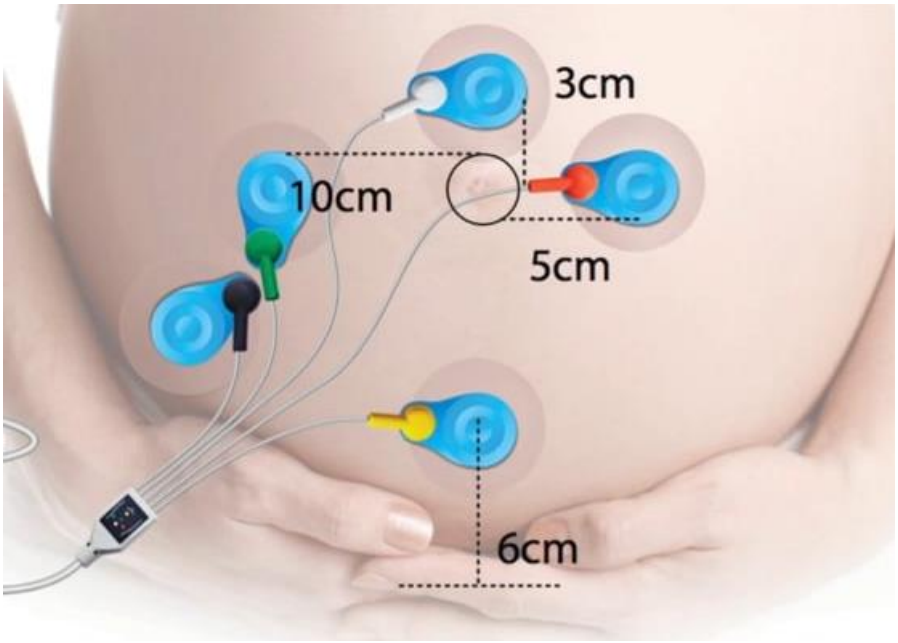

Figure 4.2: Image displaying the correct electrode placement for the Monica AN24. Image courtesy of Monica Healthcare Limited (Nottingham UK).

4.3.4 Analysis of cardiac time intervals

The PR and QT interval lengths were measured by two independent observers who were familiar with ECG waveform analysis. Monica DK v1.9 was used to extract the raw ECG waveform from the recordings (sample frequency 1kHz), with an inbuilt algorithm that detects R peak frequency and amplitude. Monica DK v1.9 was used to create an averaged waveform of all identified cardiac cycles that lay within a specified heart rate range in the two-hour period. An averaged waveform created from the FHRs of 110 to 169 beats per minute (bpm) was used to mark cardiac time intervals. The P, Q, R, S and T of each averaged fECG waveform were marked and the PR and QT interval automatically calculated by the Monica DK v1.9. Analysis of the maternal ECG (mECG) used the same two-hour period as the fECG. Averaged waveforms that did not have a clearly identifiable P and T wave were excluded from analysis; all other morphological abnormalities were also noted. QT intervals were corrected for FHR or MHR using Bazett's formula.

4.3.5 Fetal behavioural state coding

MATLAB vR2017a software (Mathworks Inc, US) was used to plot the FHR in bpm (sampled at 0.25s intervals) vs. time in the selected two-hour analysis period. The behavioural state of the fetus was assessed prior to HRV analysis in order to ensure equivalent behavioural states were compared during statistical analysis of HRV. Behavioural state, classed as 1F (quiet sleep), 2F (active sleep), 3F (quiet awake), 4F (active awake) or "indeterminable" was allocated for the entirety of the selected two-hour analysis period as previously described; each determinable state was required to have a minimum duration of 3 minutes (Nijhuis et al., 1982).

4.3.6 Heart rate variability analysis

Time-domain HRV analysis was conducted on the fetal and maternal ECG files through the calculation of the root mean squared of successive differences (RMSSD), standard deviation of normal to normal intervals (SDNN) and median heart rate. A .csv file containing measurements of maternal and fetal R-R intervals was extracted from the raw ECG waveform file using Monica DK v1.9. MATLAB was used to calculate the quality of the ECG per 30 second epoch based on a standard length and absolute difference between consecutive intervals (Lucchini et al., 2020). Epochs which were ≤70% quality within the chosen two-hour window were excluded from analysis. The mean R-R interval value of each 30 second epoch was determined using MATLAB; these values were subsequently used to calculate the median RMSSD and SDNN after fetal behavioural state for each epoch was allocated using the method described above. MATLAB scripts were written and edited by Maristella Lucchini, Joel Yang and William Fifer (Columbia University, US).

4.3.7 Statistical analyses

Initial investigation of differences between laboratory, clinical and delivery details of women who had ECG recording or NT-proBNP measurements was performed via a Kruskal Wallis analysis of variance (ANOVA) after participants were designated

into control, untreated and UDCA-treated cohorts of mild or severe ICP. Multiple comparison tests to compare significance between specific pairs of cohorts were not conducted for this data. Missing delivery data is indicated as "unknown" in Tables 4.1 and 4.2; these data were excluded from statistical analyses. A p value of < 0.05 was considered statistically significant and data are presented as median [IQR] or n (%).

Partial correlation analysis was used to investigate the strength of association between fetal NT-proBNP concentration and fetal bile acid profiles or maternal TSBA, alanine aminotransferase (ALT) and bilirubin concentrations in untreated and UDCA-treated ICP. Partial correlations investigating fetal NT-proBNP concentrations were controlled for the co-variates of mode of delivery, induction of labour, gestational age at delivery and fetal sex. Due to the low numbers of data available for neonatal unit admission, this covariate was omitted from all correlation analyses.

Partial correlation analysis was also used to investigate the strength of associations between cardiac time intervals or HRV measurements and maternal TSBA concentrations at the time of ECG recording in untreated and UDCA-treated ICP. Correlations investigating fetal cardiac data were controlled for the covariates of gestational age and fetal sex. Correlations investigating maternal cardiac data were controlled for the covariates of maternal BMI and maternal age. Information on maternal bilirubin concentrations of participants who underwent ECG analysis was not collected due to the lack of association with bilirubin in the previous umbilical venous blood assays. Correlation analyses between maternal ALT concentrations and ECG parameters were not conducted due to a lack of a significant difference in concentration between groups as measured by Kruskal-Wallis ANOVA. Skewness and kurtosis tests confirmed all continuous variables were abnormally distributed and were therefore log-transformed (using natural logarithm) prior to analysis.

Fetal HRV data were separated by behavioural state; the small sample size and lower likelihood of finding the fetus in behavioural states 3F or 4F prevented the statistical analysis of these data and they were therefore excluded. Due to low numbers of cases for the HRV analysis, Kruskal Wallis ANOVA with post-hoc Dunn's test was conducted between case and control cohorts instead of a separate partial correlation to assess the effect of UDCA treatment.

Individual dot plots and box and whisker plots have been presented to report the results of the one-way ANOVA analyses. Added variable scatter plots of the aforementioned partial correlation analyses are presented with adjusted data points based on covariates; fitted lines have been drawn in plots that reported statistically significant correlation coefficients (r). Partial correlation analysis was initially conducted between control and untreated cases as one cohort to establish the impact of a range of TSBA concentrations on parameters of interest. Subsequent analyses investigated only untreated and UDCA-treated ICP cases if the initial correlation was significant. Statistical analysis and figures were created using Stata IC v15.0 (Stata Corporation, TX, USA). Statistical advice was provided by Paul Seed (King's College London).

4.4 Results

4.4.1 Clinical and demographic details of participants

Demographic and delivery details of participants who underwent umbilical venous assays are presented in Table 4.1 Clinical and demographic details of participants who underwent ECG recording are presented in Table 4.2. Participants with ICP had increased rates of induced labour in both groups compared to controls with uncomplicated pregnancy, and infants from participants with severe ICP, in whom fetal ECG was collected, had increased neonatal unit admission.

		Control	Untreated Severe ICP	UDCA-treated Severe ICP	Untreated Mild ICP	UDCA-treated Mild ICP	*p*
n		**15**	**15**	**25**	**21**	**15**	
Maternal ethnicity (n)	White British	7 (47)	6 (40)	15 (60)	6 (29)	6 (40)	*0.258*
	White other	3 (20)	6 (40)	6 (24)	11 (52)	3 (20)	
	Asian or Asian other	3 (20)	2 (13)	2 (8)	1 (5)	1 (7)	
	Black or Black other	1 (7)	1 (7)	0 (0)	3 (14)	3 (20)	
	Other / Unknown	1 (7)	0 (0)	2 (8)	0 (0)	2 (13)	
Induction of labour (n)	Yes	0 (0)	9 (60)	13 (52)	18 (86)	11 (73)	***<0.001 ******
	No	10 (67)	5 (33)	11 (44)	2 (10)	4 (27)	
	Unknown	5 (33)	1 (7)	1 (4)	1 (5)	0 (0)	
Mode of delivery (n)	SVD	1 (7)	9 (60)	11 (44)	11 (52)	9 (60)	***0.011 ****
	ELCS	1 (7)	1 (7)	3 (12)	6 (29)	3 (20)	
	EMCS	9 (60)	4 (27)	9 (36)	1 (5)	1 (7)	
	Instrumental	2 (13)	1 (7)	2 (8)	2 (10)	2 (13)	
	Unknown	2 (13)	0 (0)	0 (0)	1 (5)	0 (0)	
Sex (n)	Female	8 (53)	5 (33)	15 (60)	8 (38)	5 (33)	*0.270*
	Male	5 (33)	10 (67)	10 (40)	11 (52)	10 (67)	
	Unknown	2 (13)	0 (0)	0 (0)	2 (10)	0 (0)	
Gestational age at delivery (weeks^{+days})		39^{+2} [39^{+0},40^{+2}]	38^{+0} [37^{+1},38^{+2}]	37^{+1} [35^{+6},37^{+4}]	38^{+2} [38^{+1},39^{+4}]	38^{+0} [37^{+3},38^{+5}]	***0.0001 ******
Birth weight (g)		3948 [3495,4330]	3302 [3050,3402]	3070 [2428,3308]	3270 [2975,3468]	3340 [3050,3645]	***0.0001 ******
Birth weight centile (%)		93.0 [75.3,100.0]	79.0 [49.0,98.0]	69.0 [26.0,94.8]	57.0 [36.0,90.8]	77.0 [56.0,94.0]	*0.109*
APGAR 1 minute ≤ 7 (n)		1 (7)	2 (13)	2 (8)	3 (14)	0 (0)	*n/a*
APGAR 5 minutes ≤ 7 (n)		0 (0)	0 (0)	1 (4)	0 (0)	0 (0)	*n/a*
Arterial pH ≤ 7.0 (n)		0 (0)	0 (0)	0 (0)	0 (0)	0 (0)	*n/a*
Venous pH ≤ 7.0 (n)		0 (0)	0 (0)	0 (0)	0 (0)	0 (0)	*n/a*
Non-reassuring CTG during labour (n)		0 (0)	4 (27)	1 (4)	5 (24)	6 (40)	*0.661*
Presence of meconium-stained amniotic fluid (n)		1 (7)	3 (20)	4 (16)	2 (10)	0 (0)	*0.309*
Admission to NNU (n)		0 (0)	1 (7)	6 (24)	0 (0)	0 (0)	***0.006 *****

*Table 4.1: Demographic and delivery details of the participants from whom umbilical venous blood was collected for NT-proBNP measurement and UPLC-MS/MS measurement of bile acid profiles. Results are presented as median [IQR] or n (%). Significant p values are presented in bold. *=p<0.05, **=p<0.005, ***=p<0.0005.*

n		Control	Untreated Severe ICP	UDCA-treated Severe ICP	Untreated Mild ICP	UDCA-treated Mild ICP	*p*
		43	**10**	**6**	**16**	**16**	
Maternal age (years)		34.0 [30.5,36.0]	37.0 [32.0, 39.0]	30.5 [26.0, 35.0]	36.0 [26.0,37.0]	33.5 [30.3,39.8]	*0.720*
Gestatational age at recording (weeks^{+days})		34^{+0} [30^{+2},37^{+0}]	35^{+0}, [31^{+6}, 36^{+6}]	33^{+5} [28^{+0},36^{+2}]	35^{+0} [34^{+5},36^{+3}]	35^{+5} [34^{+6},36^{+5}]	*0.433*
Maternal ethnicity (n)	White British	26 (59.1)	5 (50.0)	5 (83.3)	9 (56.3)	10 (62.5)	*0.203*
	White other	9 (20.5)	1 (10.0)	1 (16.6)	4 (25.0)	5 (31.3)	
	Asian or Asian other	1 (2.3)	1 (10.0)	0 (0)	1 (6.3)	1 (6.3)	
	Black or Black other	1 (2.3)	0 (0)	0 (0)	0 (0)	0 (0)	
	Other / Unknown	7 (15.9)	3 (30.0)	0 (0)	2 (12.5)	0 (0)	
BMI (kg/m^2)		23.0 [21.7,28.8]	22.2 [21.0,25.8]	20.0 [17.8,24.0]	22.6 [20.7,25.8]	24.3 [20.5,26.8]	*0.339*
Induction of labour (n)	Yes	4 (9.0)	5 (50.0)	2 (33.3)	10 (62.5)	9 (56.3)	***<0.001*** ***
	No	21 (47.7)	3 (30.0)	0 (0)	5 (31.3)	4 (25.0)	
	Unknown	19 (43.2)	2 (20.0)	4 (66.7)	1 (6.3)	3 (18.8)	
Mode of delivery (n)	SVD	23 (52.3)	5 (50.0)	1 (16.7)	10 (62.5)	7 (43.8)	*0.739*
	ELCS	11 (25.0)	2 (20.0)	2 (33.3)	2 (12.5)	3 (18.8)	
	EMCS	3 (6.8)	1 (10.0)	0 (0)	2 (12.5)	3 (18.8)	
	Instrumental	2 (4.5)	1 (10.0)	1 (16.7)	2 (12.5)	3 (18.8)	
	Unknown	5 (11.4)	1 (10.0)	2 (33.3)	0 (0)	0 (0)	
Sex (n)	Female	19 (43.2)	6 (60.0)	0 (0)	8 (50.0)	7 (43.8)	*0.292*
	Male	21 (47.7)	3 (30.0)	4 (66.7)	8 (50.0)	8 (50.0)	
	Unknown	4 (9.0)	1 (10.0)	2 (33.3)	0 (0)	1 (6.3)	
Gestational age at delivery (weeks^{+days})		39^{+4} [38^{+2},40^{+3}]	38^{+0} [37^{+2},39^{+2}]	36^{+2} [34^{+5},38^{+1}]	37^{+5} [36^{+5},38^{+4}]	37^{+5} [37^{+3},39^{+3}]	***<0.001*** ***
Birth weight (g)		3345 [3014,3765]	2690 [2590,3235]	2760 [2573,2993]	3175 [2883,3438]	3255 [2970,3603]	***0.029*** *
Birth weight centile (%)		63.0 [26.5,83.5]	34.0 [23.0,69.0]	71.0 [17.0,95.8]	84.0 [43.3,94.8]	71.0 [61.8,90.8]	*0.121*
APGAR 1 minute ≤ 7 (n)		2 (5.3)	0 (0)	0 (0)	0 (0)	0 (0)	*0.895*
APGAR 5 minutes ≤ 7 (n)		0 (0)	0 (0)	0 (0)	0 (0)	0 (0)	*n/a*
Arterial pH ≤ 7.0 (n)		0 (0)	0 (0)	0 (0)	0 (0)	0 (0)	*n/a*
Venous pH ≤ 7.0 (n)		0 (0)	0 (0)	0 (0)	0 (0)	0 (0)	*n/a*
Non-reassuring CTG during labour (n)		0 (0)	0 (0)	0 (0)	1 (6.3)	1 (6.3)	*0.107*
Presence of meconium-stained amniotic fluid (n)		3 (6.8)	1 (10)	0 (0)	1 (6.3)	1 (6.3)	*0.870*
Admission to NNU (n)		0 (0)	0 (0)	0 (0)	1 (6.3)	2 (12.5)	*0.590*

*Table 4.2: Demographic and delivery details of the participants who underwent ECG recording and analysis. Results are presented as median [IQR] or n (%). Significant p values are presented in bold. *=p<0.05, ***=p<0.0005.*

4.4.2 Maternal and fetal TSBA concentrations and fetal bile acid hydrophobicity index positively correlate with fetal NT-proBNP concentrations

One-way ANOVA demonstrated significant differences in peak maternal and fetal TSBA concentrations, and fetal NT-proBNP concentrations at delivery between participant cohorts (Figures 4.3A-C). Multiple comparison tests indicated maternal and fetal TSBA concentrations in severe ICP were significantly higher than in controls (Figures 2A and B). Similarly, fetal NT-proBNP concentrations were significantly higher in untreated severe ICP than in controls (Figure 4.3C).

One-way ANOVA of individual bile acids in umbilical venous blood demonstrated significant differences between fetal concentrations of TSBA, CA, GCA, TCA, CDCA, GCDCA, LCA, UDCA and GUDCA between cohorts (Table 4.3).

There were significant positive correlations between fetal NT-proBNP and HI of the fetal bile acids (Figure 4.4A) and with concentrations of fetal TSBA, GCA and TCA in the untreated ICP cohort (Figure 4.4B). No correlations were observed between fetal NT-proBNP concentrations and fetal TSBA in the UDCA-treated cohort (Figure 4.4B).

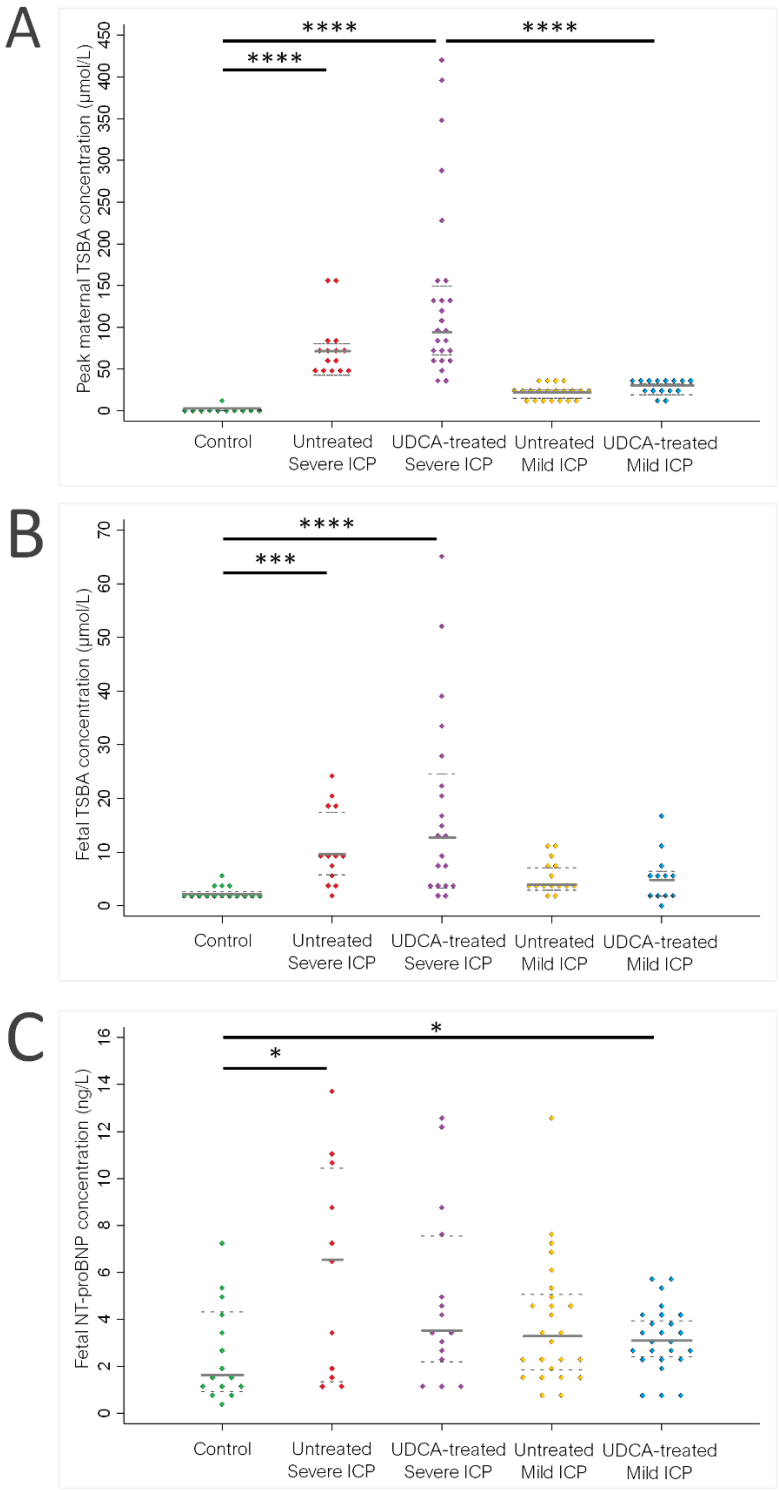

*Figure 4.3: TSBA and NT-proBNP concentrations of control (n=15), severe untreated ICP (n=15), severe UDCA-treated ICP (n=25), mild untreated ICP (n=21) and UDCA-treated mild ICP (n=15) (A) Peak maternal TSBA concentrations measured during pregnancy (B) corresponding fetal TSBA concentrations measured using umbilical venous blood (C) Fetal NT-proBNP concentrations measured using umbilical venous blood. *=p<0.05, ***=p<0.001, ****=p<0.0001.*

			Control	Untreated Severe ICP	UDCA-treated Severe ICP	Untreated Mild ICP	UDCA-treated Mild ICP	*p*
n			**15**	**15**	**25**	**21**	**15**	
Fetal NT-proBNP concentration (pg/L)			1634 [981,4378]	6536 [1408,10500]	3511 [2243,7600]	3422 [1688,5186]	3108 [2374,4069]	***0.015*** *
Fetal TSBA concentration at delivery (µmol/L)			2.180 [1.75,2.85]	9.590 [5.20,18.12]	12.630 [3.45,26.50]	3.910 [3.19,7.31]	4.910 [2.01,7.39]	***<0.0001*** ****
Individual fetal serum bile acid concentrations at delivery (µmol/L)	**CA**	unconjugated	0.03 [0.03,0.04]	0.06 [0.03,0.07]	0.06 [0.04,0.13]	0.05 [0.03,0.10]	0.05 [0.03,0.08]	***0.013*** *
		G-conjugated	0.25 [0.20,0.42]	1.84 [1.22,4.68]	1.31 [0.43,3.27]	0.83 [0.35,2.15]	0.36 [0.26,0.10]	***<0.0001*** ****
		T-conjugated	0.39 [0.34,0.65]	2.03 [1.20,6.27]	1.13 [0.44,2.28]	0.97 [0.63,1.78]	0.70 [0.26,0.78]	***0.001*** ***
	CDCA	unconjugated	0.02 [0.01,0.02]	0.02 [0.01,0.02]	0.02 [0.02,0.06]	0.02 [0.01,0.02]	0.02 [0.01,0.02]	***0.002*** **
		G-conjugated	0.51 [0.40,0.58]	1.72 [0.63,2.68]	2.05 [0.80,4.29]	0.72 [0.56,1.15]	0.98 [0.33,1.96]	***0.001*** ***
		T-conjugated	0.80 [0.49,1.19]	1.41 [1.03,2.26]	0.87 [0.69,1.63]	1.01 [0.64,1.90]	0.76 [0.32,1.85]	*0.167*
	DCA	unconjugated	0.01 [0.00,0.01]	0.01 [0.00,0.02]	0.01 [0.00,0.02]	0.01 [0.00,0.04]	0.01 [0.00,0.01]	*0.835*
		G-conjugated	0.01 [0.01,0.02]	0.01 [0.01,0.04]	0.02 [0.01,0.03]	0.01 [0.01,0.02]	0.01 [0.01,0.02]	*0.677*
		T-conjugated	0.00 [0.00,0.01]	0.01 [0.00,0.04]	0.00 [0.00,0.02]	0.01 [0.00,0.02]	ND	*n/a*
	LCA	unconjugated	0.01 [0.00,0.01]	0.01 [0.00,0.01]	0.02 [0.01,0.02]	0.01 [0.00,0.02]	0.01 [0.01,0.02]	***0.001*** ***
		G-conjugated	ND	ND	ND	ND	ND	*n/a*
		T-conjugated	ND	0.00 [0.00,0.01]	0.00 [0.00,0.01]	ND	0.00 [0.00,0.01]	*n/a*
	UDCA	unconjugated	0.00 [0.00,0.01]	0.00 [0.00,0.01]	0.87 [0.35,2.68]	0.00 [0.00,0.02]	0.20 [0.04,0.69]	***<0.0001*** ****
		G-conjugated	ND	ND	2.33 [0.43,5.20]	0.00 [0.00,0.01]	0.36 [0.11,0.82]	*n/a*
		T-conjugated	ND	ND	0.24 [0.07,0.50]	ND	0.03 [0.02,0.09]	*n/a*
Peak maternal TSBA concentration during pregnancy (µmol/L)			3.0 [2.0,4.0]	71.0 [44.0,82.0]	94.0 [65.0,156.0]	22.0 [16.5,27.5]	31.0 [21.0,34.0]	***<0.0001*** ****
Peak maternal ALT concentration during pregnancy (IU/L)			13.0 [10.0,21.0]	147.0 [52.0,361.0]	129.0 [95.0,256.0]	92.0 [34.5,201.0]	181.5 [33.0,290.5]	***<0.0001*** ****
Peak maternal bilirubin concentration during pregnancy (µmol/L)			7.0 [5.0,8.0]	11.0 [7.0,12.0]	16.0 [13.0,23.0]	7.0 [5.0,8.5]	8.0 [6.0,12.5]	***<0.0001*** ****
Time between ICP onset and delivery (days)			n/a	5.0 [3.0,24.0]	36.0 [27.5,58.5]	10.0 [5.5,30.0]	23.0 [11.0,33.0]	*n/a*
UDCA dosage (mg)			n/a	n/a	2000 [1250,2000]	n/a	1000 [1000,1500]	*n/a*
Duration of UDCA treatment (days)			n/a	n/a	36 [26,65]	n/a	12 [6,31]	*n/a*

*Table 4.3: Fetal and maternal laboratory and treatment details of the participants from whom umbilical venous blood was collected for NT-proBNP measurement. Results are presented as median [IQR] or n (%). Significant p values are presented in bold. *=p<0.05, **= p<0.005, ***=p<0.0005, ****=p<0.0001. ND signifies "not detected".*

A fetal NT-proBNP vs. fetal bile acid hydrophobicity index

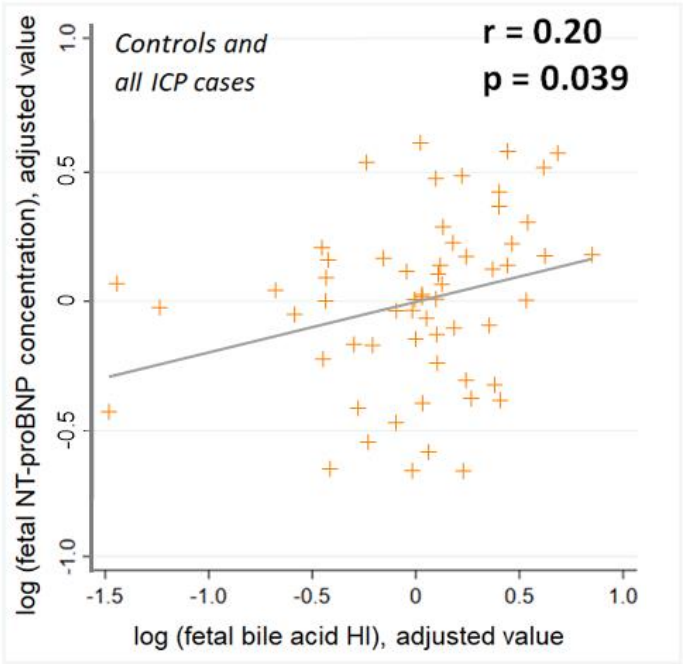

B fetal NT-proBNP vs. individual fetal bile acids

Bile acid		Untreated ICP		UDCA-treated ICP	
		r	p	r	p
Total		**0.49**	***0.019 ****	0.23	*0.232*
Cholic acid (CA)	unconjugated	0.29	*0.187*	0.20	*0.297*
	G-conjugated	**0.56**	***0.007 *****	0.33	*0.079*
	T-conjugated	**0.44**	***0.039 ****	0.33	*0.077*
Chenodeoxycholic acid (CDCA)	unconjugated	0.06	*0.785*	0.12	*0.520*
	G-conjugated	0.19	*0.404*	0.26	*0.179*
	T-conjugated	0.02	*0.931*	0.12	*0.532*
Deoxycholic acid (DCA)	unconjugated	0.1	*0.661*	0.05	*0.802*
	G-conjugated	-0.36	*0.099*	-0.05	*0.787*
	T-conjugated	-0.04	*0.865*	0.16	*0.397*
Lithocholic acid (LCA)	unconjugated	0.02	*0.914*	0.02	*0.879*
	G-conjugated	n/a	*n/a*	n/a	*n/a*
	T-conjugated	n/a	*n/a*	n/a	*n/a*
Ursodeoxycholic acid (UDCA)	unconjugated	-0.26	*0.230*	-0.02	*0.898*
	G-conjugated	-0.33	*0.130*	0.11	*0.572*
	T-conjugated	n/a	*n/a*	n/a	*n/a*

(G-conjugated = Glycine-conjugated, T-conjugated = Taurine-conjugated)

*Figure 4.4: (A) Added variable plot of partial correlation analysis between fetal NT-proBNP concentration and fetal bile acid hydrophobicity index (HI) measured using umbilical venous blood samples taken from controls, untreated and UDCA-treated ICP (B) Table demonstrating partial correlation analysis of individual fetal serum bile acids and NT-proBNP concentrations from women with untreated or UDCA-treated ICP only. r=correlation coefficient. Significant p values are presented in bold. *=p<0.05, **=p<0.01*

4.4.3 Maternal peak TSBA and ALT concentrations positively correlate with fetal NT-proBNP concentrations

No correlation was found between fetal NT-proBNP and maternal bilirubin concentrations (Figure 4.5). A significant positive partial correlation was observed between concentrations of fetal NT-proBNP and maternal TSBA and ALT when analysing untreated ICP cases and controls together (Figure 4.6A and B). Analysis of untreated ICP cases demonstrated significant positive correlations between fetal NT-proBNP and maternal TSBA and ALT concentrations (Figure 4.6C and E). No correlations were observed in the UDCA-treated group (Figure 4.5D and F).

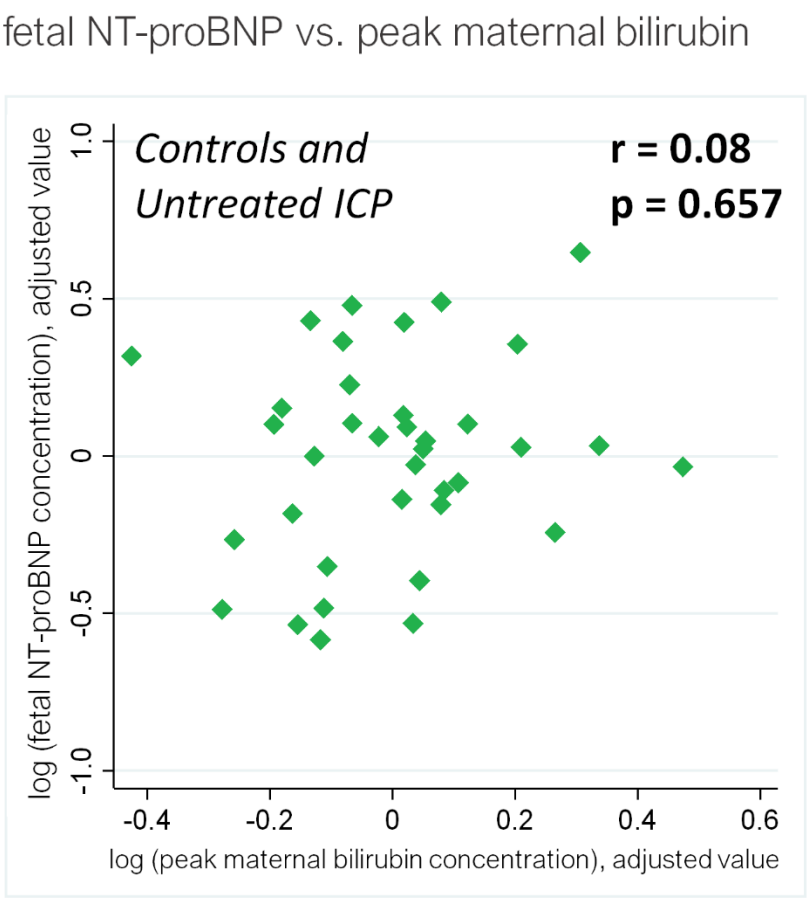

Figure 4.5: Added variable plots demonstrating the lack of partial correlation between fetal NT-proBNP and peak maternal bilirubin concentrations in control participants (n=15) and participants with untreated ICP (n=36).

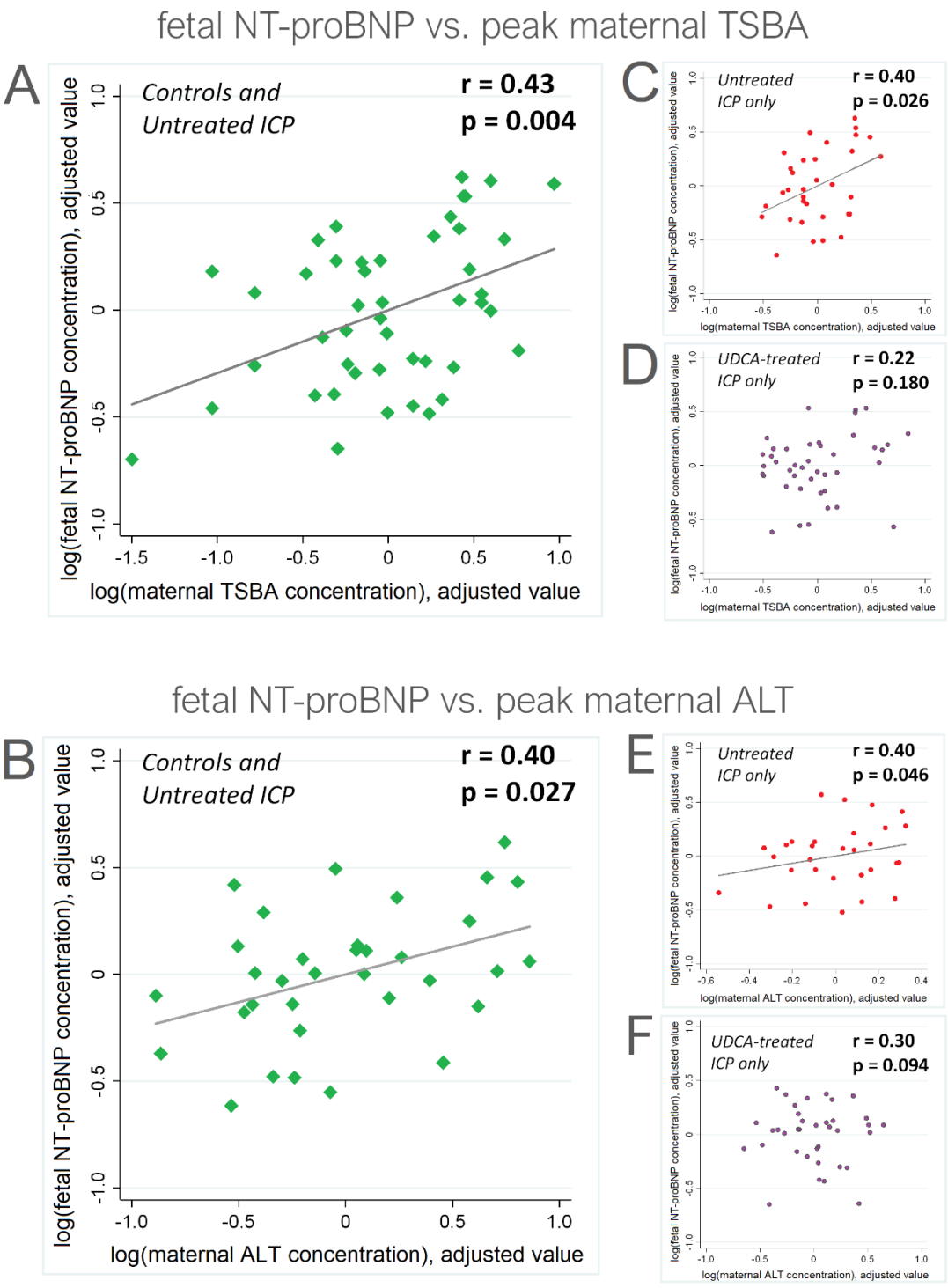

Figure 4.6: Partial correlation between fetal NT-proBNP concentration and maternal TSBA or ALT concentrations (A & D) in both controls (n=15) and women with untreated ICP (n=36) (B & E) in women with untreated ICP only (n=36) (C & F) in women with UDCA-treated ICP only (n=40). Plots with both controls and cases on the same graph have diamond-shaped green data points, plots with untreated ICP cases only have circle-shaped red data points and plots with UDCA-treated cases only have circle-shaped purple data points.

4.4.4 Maternal TSBA concentrations positively correlate with the prolongation of the fetal PR interval length, but not the length of the QTc interval or QRS duration

One-way ANOVA demonstrated significant differences in fetal PR interval length between cohorts (Table 4.4). Partial correlation analysis demonstrated a significant positive correlation between maternal TSBA and fetal PR interval length measurements when analysing untreated ICP cases and controls together (Figure 4.7C). Analysis of ICP cases demonstrated significant positive correlations between maternal TSBA concentrations and fetal PR interval length for both untreated and UDCA-treated cases (Figure 4.7D and E respectively). No significant correlations with maternal TSBA concentration were observed when analysing fetal QTc interval length or QRS duration (Figure 4.8A and B respectively). There were no significant correlations between maternal TSBA concentrations and maternal CTI (Figure 4.10A-C).

n			Control	Untreated Severe ICP	UDCA-treated Severe ICP	Untreated Mild ICP	UDCA-treated Mild ICP	*p*
			43	10	6	16	16	
TSBA concentration at recording (µmol/L)			1.0 [1.0,6.0]	53.5 [42.5,63.3]	78.5 [50.5,123.0]	19.5 [14.3,27.3]	21.5 [18.0,24.8]	***<0.001 ******
ALT concentration at recording (IU/L)			12.0 [11.0,15.0]	165.0 [95.8,350.0]	43.5 [10.8,116.0]	102.0 [75.3,200.3]	79.0 [33.3,120.0]	*0.072*
Fetal cardiac time interval measurements (ms)		PR interval length	117.0 [111.0,127.0]	133.0 [120.8,143.5]	128.5 [114.3,137.3]	119.5 [107.8,130.3]	79.0 [33.3,120.0]	***0.021 ****
		QTc interval length	409.9 [384.2,426.3]	390.5 [352.2,425.0]	400.6 [357.2,418.5]	411.6 [372.6,428.2]	397.5 [357.0,422.1]	*0.680*
		QRS Duration	30.0 [26.0,34.0]	31.5 [28.8,34.0]	30.0 [28.8,33.0]	31.5 [30.0,33.0]	31.5 [30.0,33.8]	*0.758*
Fetal heartrate variability measurements	Behavioural state 1F (quiet sleep)	RMSSD (ms)	7.9 [6.7,9.6]	7.8 [6.7,8.9]	8.8 [7.1,10.4]	8.6 [6.9,10.5]	8.0 [7.0,8.7]	*0.763*
		SDNN (ms)	7.9 [5.0,9.7]	10.4 [9.2,17.5]	9.0 [5.8,12.2]	12.4 [9.5,14.5]	11.0 [7.3,13.5]	*0.062*
		Median heartrate (bpm)	129.9 [125.0,135.3]	128.1 [121.2,129.8]	121.9 [114.0,129.8]	126.9 [125.9,131.1]	128.5 [121.4,133.3]	*0.721*
	Behavioural state 2F (active sleep)	RMSSD (ms)	8.7 [7.6,9.6]	10.6 [8.8,11.4]	8.7 [7.1,11.0]	9.4 [8.8,11.1]	8.5 [7.6,9.7]	***0.049 ****
		SDNN (ms)	18.2 [14.7,25.7]	26.2 [21.6,34.6]	19.1 [12.7,29.1]	25.4 [20.6,31.8]	21.9 [17.7,25.9]	***0.021 ****
		Median heartrate (bpm)	134.5 [130.4,140.3]	130.5 [129.2,139.1]	132.1 [126.4,134.0]	133.2 [129.6,138.9]	133.4 [130.2,140.7]	*0.913*
Maternal cardiac time interval measurements (ms)		PR interval length	152.0 [139.0,170.5]	124.0 [117.5,152.5]	145.0 [140.5,154.8]	159.0 [143.3,166.8]	151.5 [140.8,166.5]	*0.087*
		QTc interval length	409.6 [396.1,433.3]	402.9 [357.1,415.8]	427.7 [373.3,452.7]	408.0 [382.6,415.6]	412.6 [388.8,425.2]	*0.357*
		QRS Duration	54.0 [49.5,59.5]	55.0 [49.5,70.0]	53.0 [48.0,62.0]	53.0 [46.8,56.5]	58.0 [52.5,61.8]	*0.320*
Maternal heartrate variability measurements		RMSSD (ms)	26.1 [16.6,37.2]	27.0 [19.9,38.7]	39.5 [29.6,53.9]	34.5 [24.2,42.0]	25.6 [19.5,43.1]	*0.208*
		SDNN (ms)	50.0 [41.7,59.2]	47.9 [34.9,61.6]	71.5 [43.7,77.9]	56.2 [36.3,66.7]	44. [27.6,59.9]	*0.189*
		Median heartrate (bpm)	74.9 [67.4,82.0]	73.2 [65.0,84.4]	72.3 [64.9,77.8]	72.7 [67.7,79.6]	69.1 [66.4,76.4]	*0.679*

*Table 4.4: Laboratory details, cardiac time interval measurements and heart rate variability measurements of participants who underwent ECG recording and analysis. Results are presented as median [IQR]. Significant p values are presented in bold. *=p<0.05, ***=p<0.0005.*

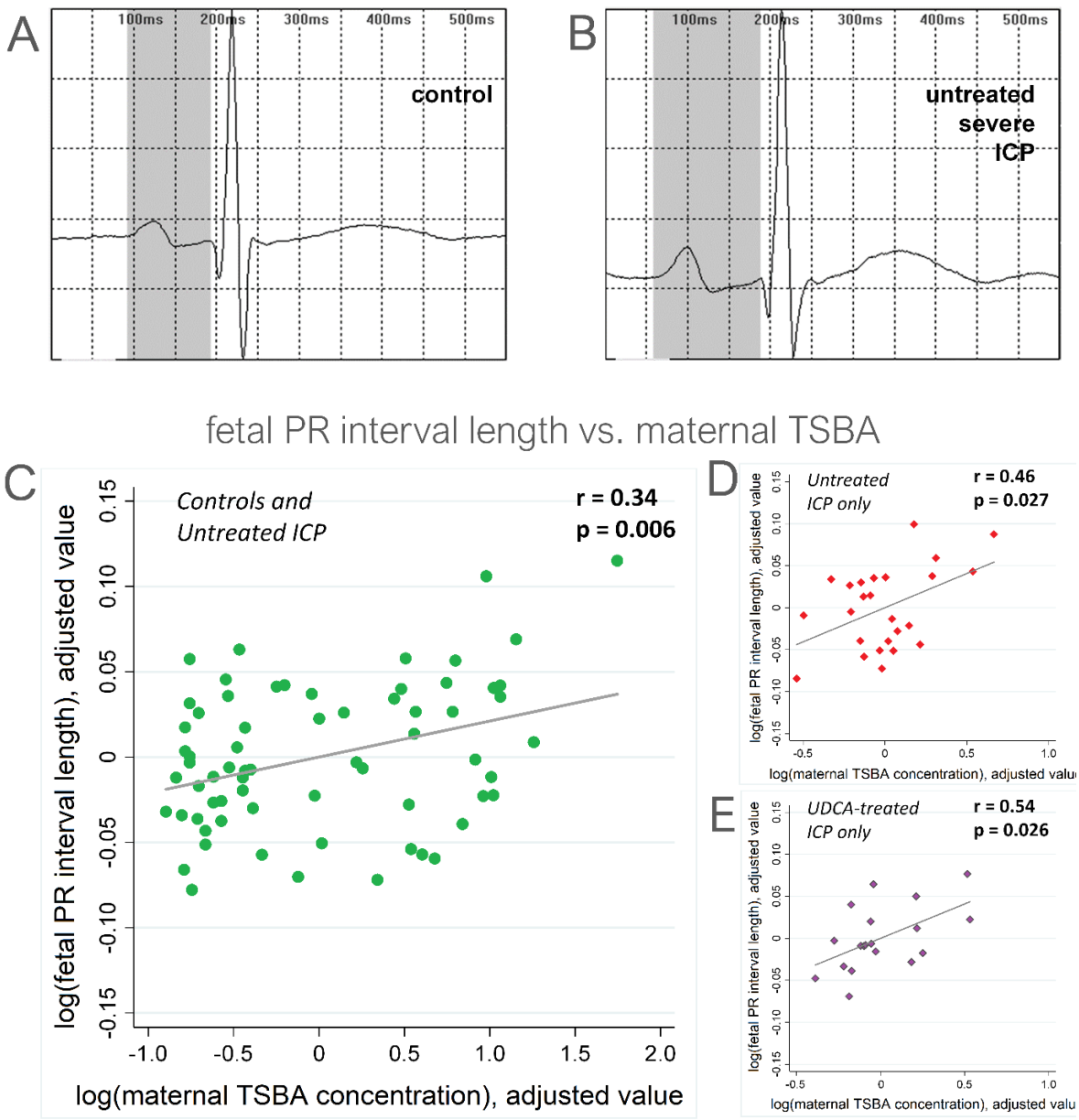

Figure 4.7: (A & B) Representative averaged fECG waveforms taken from Monica DK software of a control and untreated severe ICP participant. PR intervals have been shaded in grey. (C-E) added variable plot demonstrating the partial correlation between maternal TSBA concentration and fetal PR interval length in control participants (C) In both controls (n=43) and women with untreated ICP (n=26) (D) in women with untreated ICP only (n=26) (E) in women with UDCA-treated ICP only (n=22). Plots with both controls and cases on the same graph have circle-shaped green data points, plots with untreated ICP cases only have diamond-shaped red data points and plots with UDCA-treated cases only have diamond-shaped purple data points.

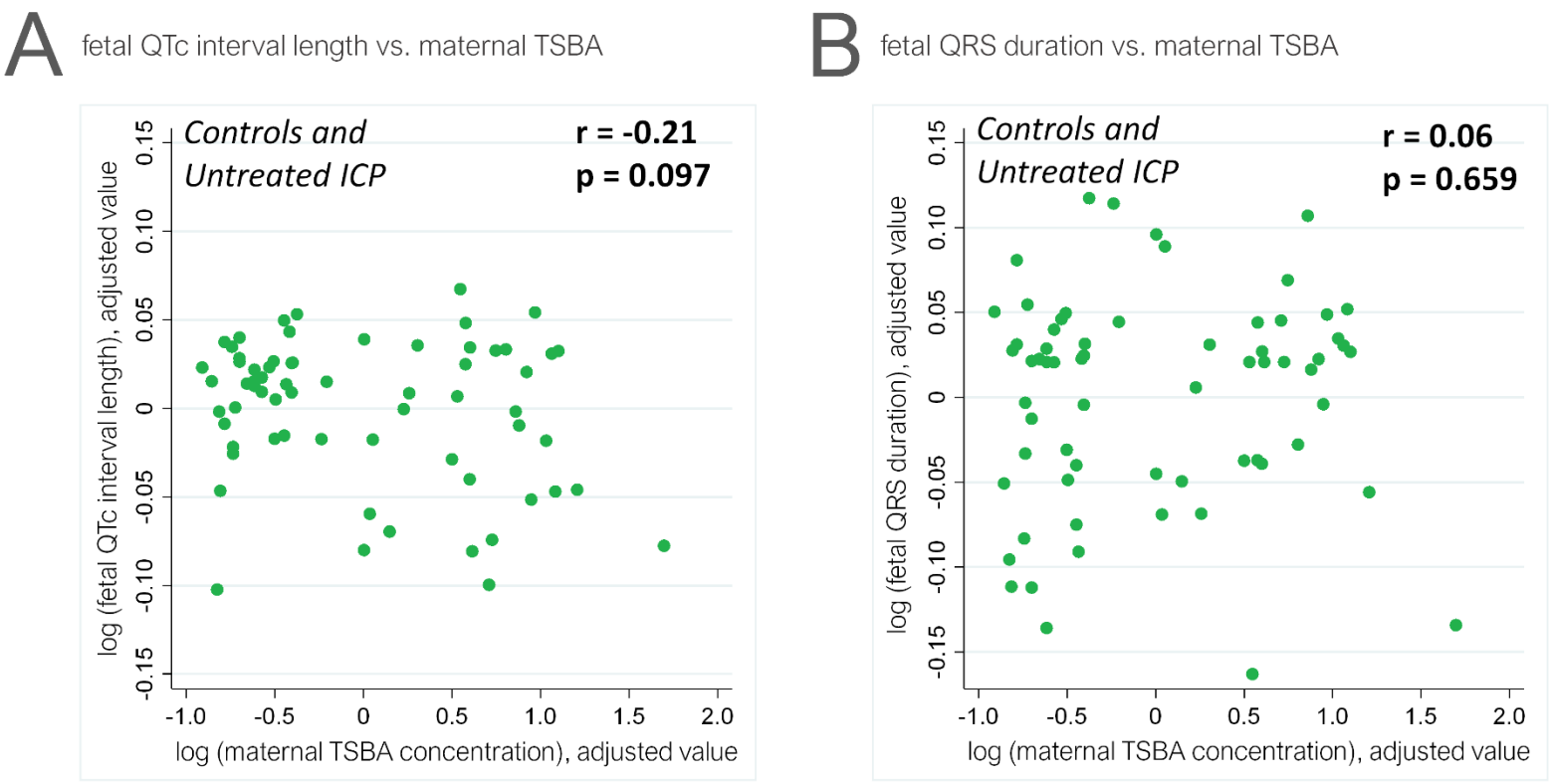

Figure 4.8: (A&B) Added variable plots demonstrating the lack of partial correlation between fetal QTc and QRS interval lengths and maternal TSBA concentrations in control participants (n=43) and participants with untreated ICP (n=26).

4.4.5 Maternal TSBA concentrations positively correlate with fetal heart rate variability

To investigate ICP-induced changes in fHRV, we performed time domain analysis on the RR intervals derived from fetal ECGs of women with untreated ICP. One-way ANOVA demonstrated significant differences in RMSSD and SDNN values in behavioural state 2F (Table 4.4).

Partial correlation analysis demonstrated a lack of correlation between maternal TSBA concentrations and fetal RMSSD values from behavioural state 1F (quiet sleep), while a significant positive correlation was observed in values from behavioural state 2F (active sleep) (Figure 4.9A and C respectively). Positive correlations were also observed between maternal TSBA concentrations and fetal SDNN values in both behavioural states (Figure 4.9B and D respectively).

When all untreated cases were compared using one-way ANOVA, there was a significant increase of RMSSD values in behavioural state 2F (active sleep) (9.6 [8.8,11.3] vs. 8.7 [7.6,9.6] ms, p = 0.028 (Figure 4.9G) and SDNN values in behavioural state 1F (quiet sleep) (11.0 [9.5,14.9] vs. 7.9 [5.1,9.7] ms, p = 0.013 (Figure 4.9F) and active sleep 2F (25.4 [21.0,32.4] vs. 18.2 [14.7,25.7] ms, p = 0.003 (Figure 4.9H). UDCA treatment was associated with a significant reduction in RMSSD in behavioural state 2F (8.5 [7.4, 9.7] ms, p = 0.030, Figure 4.9G), and there were a non-significant attenuation of the ICP-associated increase in SDNN values in UDCA-treated cases (Figure 4.9F and H). There were no significant correlations between maternal TSBA concentrations and maternal HRV values (Figure 4.10D-F).

.

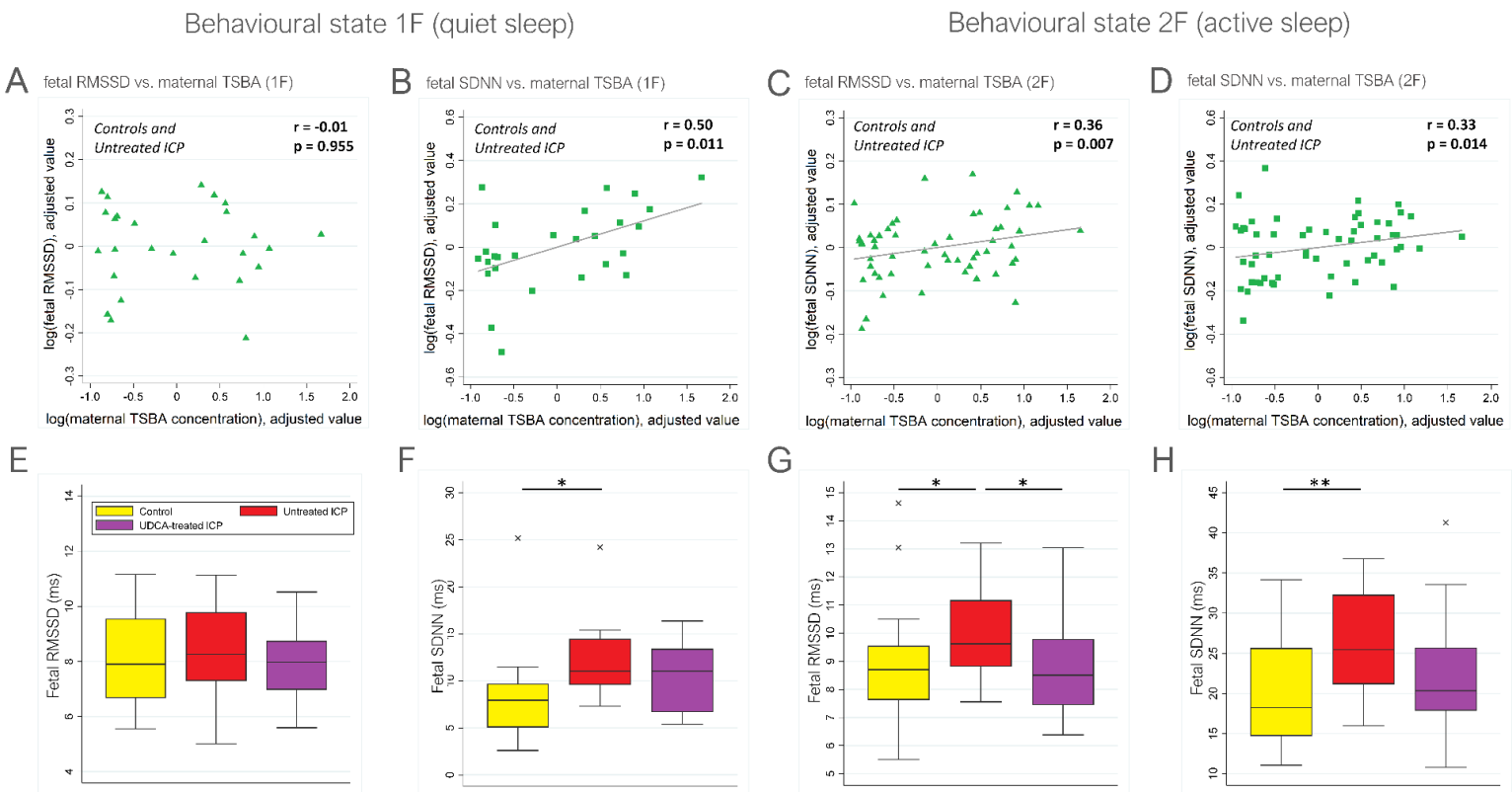

*Figure 4.9: Added variable plots demonstrating the partial correlation between maternal TSBA concentration and fetal time domain fHRV measurements of behavioural states 1F and 2F in controls (n=16 in 1F and n=33 in 2F) and untreated ICP (n=13 in 1F and n=26 in 2F) (E-H) Box and whisker plots demonstrating the medians and IQRs of fetal RMSSD and SDNN values of control, untreated ICP and UDCA-treated ICP cohorts in behavioural states 1F and 2F respectively. RMSSD data points are displayed as triangles whilst SDNN data points are displayed as squares. *=p<0.05, **=p<0.005*

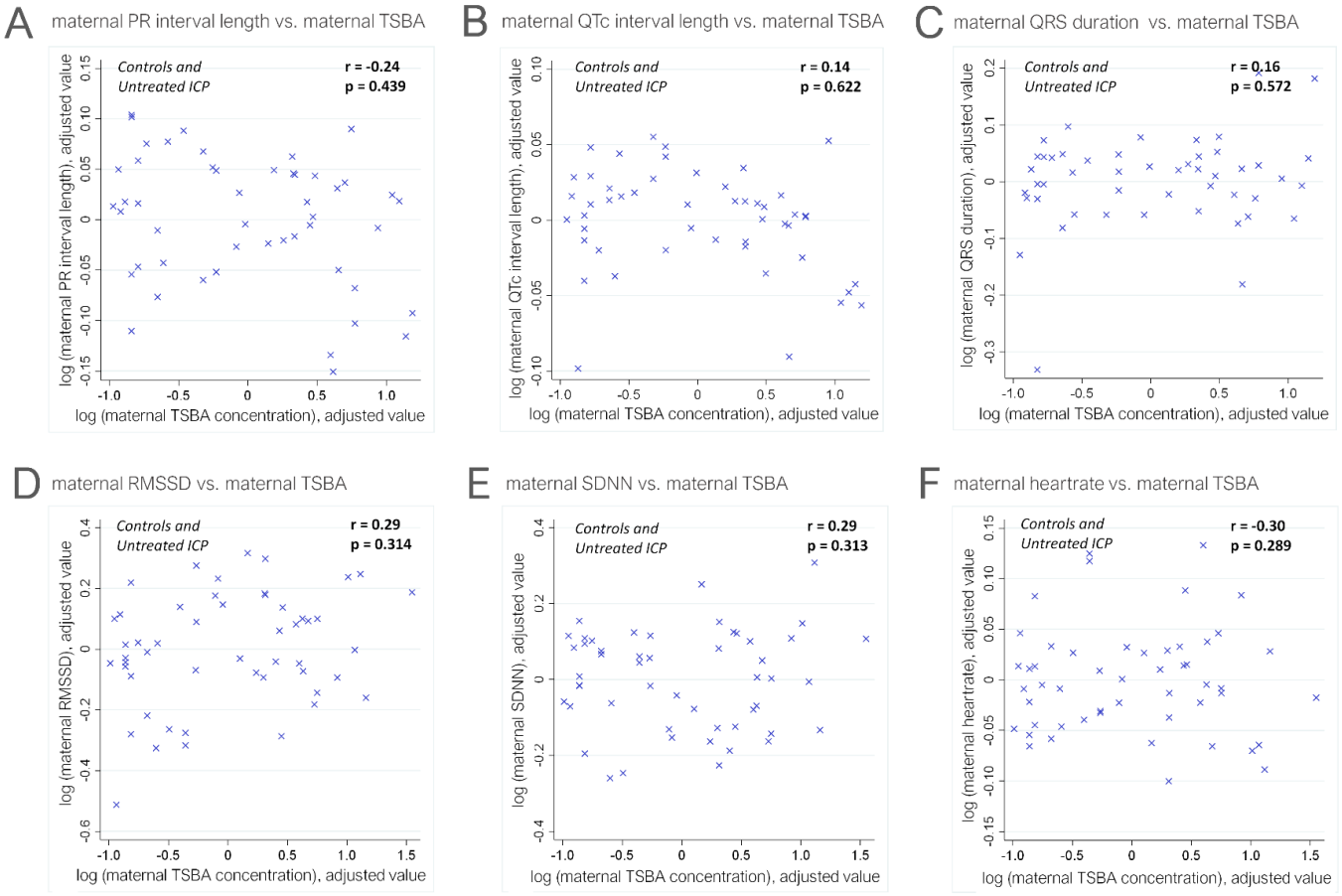

Figure 4.10: Added variable plots demonstrating the lack of partial correlation between maternal TSBA concentration and maternal ECG parameters of controls (n = 43) and participants with untreated ICP (n = 26). (A-C) Maternal cardiac time interval measurements, (D-F) Maternal heart rate variability parameters.

4.5 Discussion

4.5.1 Summary of findings

In this study, we have demonstrated that untreated ICP is associated with a fetal cardiac phenotype that positively correlates with fetal and maternal serum bile acid concentrations. Fetal TSBA, and conjugated CA concentrations and bile acid HI positively correlated with fetal NT-proBNP concentrations. Additionally, maternal TSBA concentrations positively correlated with fetal PR interval length, fHRV and fetal NT-proBNP concentrations. Peak maternal ALT concentrations in untreated ICP also positively correlated with fetal NT-proBNP concentrations. Using a matched cohort of participants with UDCA-treated ICP, we found that the fetuses of women taking UDCA treatment did not have the same dysfunctional cardiac phenotype for most parameters, suggesting that UDCA may be cardioprotective.

4.5.2 Importance of bile acid hydrophobicity and severity of elevation

The fetal cardiac phenotype observed in untreated ICP constituted, in part, an elevated fetal NT-proBNP concentration in umbilical venous blood, which is an indicator of fetal distress, tachy- and bradyarrhythmia and heart failure in fetuses with congenital heart defects (Miyoshi et al., 2018). The range of NT-proBNP concentrations obtained from control participants was similar to previous reports, therefore elevated NT-proBNP concentrations suggest that ICP fetuses have a cardiac phenotype concordant with arrhythmic activity and fetal distress (Schwachtgen et al., 2005).

Measurement of total and individual serum bile acids in umbilical venous blood demonstrated that fetal TSBA, GCA and TCA concentrations and bile acid HI are positively correlated with fetal NT-proBNP concentrations. This is the first study to report this association in untreated ICP. GCA and TCA form the majority of the maternal serum bile acid pool in ICP (Tribe et al., 2010). CA and TCA administration causes cardiac dysfunction in experimental models and both are demonstrably deleterious in comparison to UDCA (Adeyemi et al., 2017, Schultz et

al., 2016, Miragoli et al., 2011, Zavecz and Battarbee, 2010). This suggests that fetal cardiotoxicity may be an explanation for the novel finding of a correlation between elevated NT-proBNP concentration and increased fetal bile acid HI, an established indicator of bile acid cytotoxicity (Hofmann, 1999). The association of the severity of fetal cardiac phenotype with increasing serum concentrations of maternal and/or fetal TSBA is in agreement with previous studies (Henry and Welsh, 2015, Ataalla et al., 2016, Fan et al., 2014, Kadriye et al., 2019). Severity of hypercholanaemia is associated with adverse fetal outcomes, e.g. IUD when maternal TSBA concentrations exceed 40 μmol/L and markedly so at ≥100 μmol/L (Geenes et al., 2014a, Glantz et al., 2004, Ovadia et al., 2019). No IUD events occurred in this study, although only three participants had TSBA concentrations of ≥100 μmol/L; one untreated fECG study participant had a TSBA concentration of 187 μmol/L and two untreated NT-proBNP assay participants had TSBA concentrations of 100 μmol/L and 151 μmol/L.

4.5.3 Relevance of findings in UDCA-treated participants

UDCA-treated participants did not have the same fetal cardiac phenotype as untreated ICP which may be explained by the alterations in the fetal bile acid composition and HI, which has previously been demonstrated in studies of both healthy and hypercholanaemic patients (Setchell et al., 2005, Takano et al., 1994). The bile acid HI may be of more relevance than the TSBA concentration, as it is noteworthy that the TSBA concentrations were not lower in the maternal or fetal serum samples following UDCA treatment. Although higher NNU admission rates were observed in UDCA-treated severe participants (24%) compared to untreated severe participants (7%) in this study, other fetal outcomes showed association with the bile acid HI rather than the TSBA concentration itself . Consistent with this observation, UDCA treatment alters the concentration of individual bile acids in maternal serum; specifically the proportion of UDCA rises from <0.5% to 60% whilst CA reduces from 51% to <20% in the serum of women with ICP after UDCA treatment (Manna et al., 2019). Unlike untreated participants, fetal TSBA and GCA concentrations in UDCA-treated participants did not correlate with fetal NT-proBNP

concentrations, which is in line with the calculated HI and their association with fetal NT-proBNP concentration.

The recent PITCHES trial did not demonstrate an impact of UDCA treatment on a composite measure of adverse pregnancy outcome that included IUD, preterm birth and NNU admission (Chappell et al., 2019). This is not contradictory to our data related to an ICP-associated fetal cardiac phenotype as this study of fECG is of particular relevance to the aetiology of IUD. There were three IUDs in the PITCHES trial cohort (two did not receive UDCA treatment) from a total of 604 participants (Chappell et al., 2019). Furthermore, 76% of the 605 PITCHES participants had TSBA concentrations <40 μmol/L, and only 7% participants had concentrations ≥100 μmol/L at the time of randomisation (Chappell et al., 2019).

4.5.4 Abnormal cardiac time intervals in ICP

The positive correlation between maternal TSBA concentrations and fetal PR interval length is in agreement with findings from previous studies which have reported ICP-induced changes in fetal mechanical PR interval, however UDCA-treated mothers were used as participants in these studies with no matched untreated cases investigated (Strehlow et al., 2010, Rodríguez et al., 2016).

PR interval prolongation is typically used as a diagnostic tool for first-degree atrioventricular (AV) block (Cheng et al., 2009). According to the PRIDE study which used echocardiography to measure fetal PR intervals, an average length of >150ms was considered long enough to warrant further investigation of first-degree AV block (Friedman et al., 2008). Other studies which have used non-invasive fECG have demonstrated mean lengths of 105-135 ms at term (Smith et al., 2018). The above data corresponds with the mean PR interval lengths from our cohorts, however two participants from the severe untreated ICP group would warrant further screening for AV block if using the above diagnostic criteria. (Taylor et al., 2003).

Experimental data has demonstrated that bile acid-induced PR interval prolongation occurs via TCA activation of muscarinic acetylcholine M_2 receptors, resulting in intracellular calcium dynamic disruption via T-type voltage-dependent calcium channels and slowing of conduction velocity at the AV node (Adeyemi et al., 2017, Sheikh Abdul Kadir et al., 2010). Expression and activation of these receptors have been established to affect impulse conduction at the AV node in the human heart (Martin, 1977). This suggests a mechanism by which higher circulating TCA concentrations causes fetal PR interval length prolongation in untreated ICP.

Fetal PR interval prolongation has previously been reported in both untreated and UDCA-treated cohorts, suggesting that UDCA is not completely protective (Rodríguez et al., 2016). However, UDCA has a cardioprotective effect in experimental fetal heart models (Rainer et al., 2013, Adeyemi et al., 2017, Schultz et al., 2016, Miragoli et al., 2011). TCA-induced PR interval prolongation observed in an *in vitro* model of the fetal heart was attenuated by UDCA, although 400 μM of TCA was used which is rarely physiologically observed in ICP (Adeyemi et al., 2017). UDCA hyperpolarised the membrane voltage of *in vitro* myofibroblasts via the sulphonylurea receptors, thereby increasing potassium conductance and counteracting the effects of TCA (Miragoli et al., 2011). UDCA acted as an agonist for the bile acid receptor Tgr5 (GPBAR1) in murine ventricular cardiomyocytes although it did not elicit contractile changes in this cell type (Ibrahim et al., 2018). Cardioprotective effects of UDCA in non-cholestatic adults with cardiac disease has also been reported and serum concentrations of conjugated UDCA are lower in patients who have had atrial fibrillation events (Rainer et al., 2013, Bährle et al., 1998, von Haehling et al., 2012). The tauro-conjugated form of UDCA (TUDCA) has also been shown to reduce markers of hypoxia as well as high fat or obesity-induced intracellular calcium dysregulation in murine cardiomyocytes (Ceylan-Isik et al., 2011, Turdi et al., 2013, Mohamed et al., 2017). UDCA perfusion in isolated rat hearts reduces ischaemia-induced injury and protects against apoptosis associated with myocardial infarction (Rajesh et al., 2005, Lee et al., 1999). In addition to the evidence of its beneficial effect in animal models and *in vitro* models of human hearts, UDCA has been shown to improve post-ischaemic blood flow in adults with chronic heart failure (von Haehling et al., 2012).

A lack of association between fetal QTc interval length and ICP was found in our study, which is agreement with recent data, however this study mainly utilised data from UDCA-treated participants (Joutsiniemi et al., 2019). Investigations using the Monica AN24 as well as fetal magnetocardiograms in uncomplicated pregnancies have demonstrated the fetal T-wave has a low amplitude and is difficult to discern, which is thought to be attributed to opposing directions of ventricular repolarisation in different areas of the heart (Strand et al., 2019, Wacker-Gussmann et al., 2018). Flat and low amplitude fetal T-waves were observed in the ECG data collected for this study which suggests an alternative method to accurately measure the fetal QT interval is required.

4.5.5 Maternal vs. fetal cardiac susceptibility to bile acid-induced dysregulation

Our data has shown a lack of correlation between maternal TSBA concentrations and maternal ECG parameters in comparison to control pregnancies. Maternal QTc interval lengths were found to be within normal range which is contrary to a previous study using an adult 12-lead ECG device (Kirbas et al., 2015). Whilst TCA caused a disruption in calcium signalling in *in vitro* models of the fetal heart, it is important to note that the effect of calcium dynamic disruption was not observed in the adult heart models from these studies which is reflective of the absence in maternal ECG anomalies observed in our data and suggests a fetus-specific receptivity to bile acid induced disruption (Miragoli et al., 2011). The lack of effect on the adult heart could simply be due to the specific physiology of the fetal heart; it is known that the fetal heart lies in a relatively hypoxic state *in utero* which leads to a transient development of cardiac myofibroblasts, a cell type which is associated with ischaemic injury in the adult heart and has been shown to be hyperpolarised by UDCA (Schultz et al., 2016). However, when observing cholestasis outside of pregnancy, it has been shown that elevated bile acids can lead to PR interval prolongation via a disorder known as cirrhotic cardiomyopathy; this has been documented in adults with liver cirrhosis and models of cholestasis showing that the adult heart is not in fact protected from and increased concentration of bile acids outside of pregnancy (Vasavan et al., 2018).

4.5.6 Importance of measuring fetal heart rate variability

The behavioural state of the fetus is indicative of fetal wellbeing and is closely associated with fetal movement, FHR and fHRV (Van Leeuwen et al., 2013). This is the first study to our knowledge that investigates behavioural state-specific time domain measurements of fHRV in women with untreated and UDCA-treated ICP. Statistically significant differences were more prominent in behavioural state 2F (active sleep), likely due to fetuses spending more time in this behavioural state, resulting in a larger number of data points, as well as the wider scope of fHRV fluctuation when the fetus is in an active state (Nijhuis et al., 1982). Median SDNN and RMSSD values from case cohorts were within the normal range cited in previous literature and no infants in our study had clinical indicators of fetal hypoxia at delivery, although there are reports of ICP-induced fetal hypoxia in other cohorts (Oztekin et al., 2009, Sterrenburg et al., 2014, Laatikainen, 1975). Based on the limited literature available which has investigated fHRV in ICP, our data does not agree with a previous study demonstrating the lowering of fHRV in women with via measurement of differential index (Ammälä and Kariniemi, 1981). However, our data is consistent with spectral analysis of rats with ICP which showed an increase in fHRV in the 15 minutes prior to arrhythmic events (Shao et al., 2007).

Interpreting changes in fHRV is difficult as it is a complex phenomenon affected by multiple factors and patterns tend to have a high variation between individuals. Governed by the parasympathetic and sympathetic branches of the ANS, fHRV and is known to increase with gestational age in accordance with the associated maturation of the ANS and its ability to maintain homeostasis. The relatively high fHRV in our gestationally matched cohort of ICP women suggests either withdrawal of activity from the sympathetic branch of the ANS or an increase in parasympathetic activity in comparison to controls. This relative autonomic imbalance appears to be restored in ICP participants who have had UDCA treatment. An increased fHRV is directly associated with increased vagal tone, a signal of efficient parasympathetic response and respiratory sinus arrythmia, the latter of which refers to the normal variation in heart rate caused by breathing. However,

vagal tone has also been demonstrated to increase prior to the onset of atrial fibrillation in adults, although research on using HRV or vagal tone as a predictive marker for atrial fibrillation has had conflicting results and the relationship is still not fully understood (van den Berg et al., 1997, Huang et al., 1998, Lombardi et al., 2004, Zimmermann and Kalusche, 2001, Perkiömäki et al., 2014).

HRV in the fetus has also been known to increase with maternal physical activity (Dietz et al., 2016, Stone et al., 2017). Although we deliberately analysed periods of the fetal ECG where the maternal movement was observed to be low, ICP is known to cause pruritis which typically worsens during the night (Ovadia and Williamson, 2016). It is possible that the movement caused by itching or a change in maternal sleep position which may not have been picked up by the Monica AN24's inbuilt accelerometer could have affected the fHRV in the untreated participants. It has been observed that fHRV reduces in the semi-recumbent and supine sleeping positions of the mother, and increase in periods of changing sleep position (Stone et al., 2017).

Uterine activity has also been shown to heavily influence fHR, whereby fHRV increases during uterine contractions in comparison to "rest" periods during active labour, and it has been shown that fHRV is more indicative of fetal distress when contractions are taken into account (Romano et al., 2006, Warmerdam et al., 2018). This is particularly interesting, as it is known the incidence of spontaneous preterm labour is increased in women with ICP and there is supporting evidence of bile acid perfusions inducing contractions via an increased receptivity to the contraction hormone oxytocin in sheep and *in vitro* models of human myometrium (Campos et al., 1986, Campos et al., 1988, Israel et al., 1986, Germain et al., 2003). This suggests further studies are required investigating the relationship between fHRV, uterine activity and exposure to a high concentration of bile acids in women with ICP. In this study we have used the statistical (also known as time domain) method of RMSSD analysis to ascertain HRV in the fetus as opposed to spectral or frequency domain measures of fHRV. Although each method has its limitations, frequency domain analysis of fHRV will be particularly useful in investigating

women with ICP as this technique is more likely to identify transient or periodic changes in the heart rate (Huikuri et al., 2003, Van Leeuwen et al., 2007).

Our data therefore does suggest an autonomic imbalance in women with ICP and a higher fHRV which may predispose the fetal heart to an arrythmia, however the clinical significance of this finding is likely to be minor due to the lack of hypoxic phenotypes of these fetuses at delivery as well as the other influencing factors which could have caused the rise in variability.

4.5.6 Limitations

A limitation of this study is the fact that the UDCA-treated and untreated participants were not matched for severity of hypercholanaemia. In future, if it were feasible to study a prospectively recruited cohort of untreated vs UDCA-treated women with TSBA concentrations of ≥100 μmol/L, this would enable comparison of fetal cardiac parameters and markers of bile acid synthesis to establish the association between fetal cardiac function and highly elevated TSBA concentrations. The optimal experimental design would have taken both umbilical venous blood and fECG samples from the same participants to avoid differences in demographic data between severe ICP cohorts. Additionally, data on the duration of delivery would also be collected as part of multivariate statistical analysis of fetal NT-proBNP concentrations. To eliminate the potential effect of individual differences in HRV, this study should be repeated with a larger cohort of ICP participants prior to and after UDCA treatment with responsiveness to the drug also assessed. Ideally, diurnal post-prandial fluctuations in TSBA concentrations and their relationship to fetal cardiac dysfunction would also be evaluated, but the requirement for hourly venepuncture from pregnant women and the inability to obtain good quality fECG data during wakefulness precluded this approach.

4.6 Conclusion

This study has demonstrated a fetal cardiac phenotype that is associated with severity of ICP in untreated pregnancies. Although further investigation is required to assess the impact and importance of these anomalies, these data provide a step towards

understanding the mechanisms of ICP-associated fetal cardiac pathologies and support the hypothesis that elevated circulating fetal bile acids may predispose the fetal heart to a sudden arrhythmic event. Further studies measuring fetal cardiac parameters in a larger cohort, particularly in women who have serum bile acid concentrations ≥100 μmol/L, are required to establish the risk of elevated serum bile acid concentrations, to stratify those who would benefit most from increased fetal heart monitoring, and to clarify whether UDCA treatment is protective for these high-risk pregnancies.

Chapter 5: Conclusion

5. Conclusion

Intrahepatic cholestasis of pregnancy (ICP) is a disorder that is characterised by elevated maternal total serum bile acid (TSBA) concentrations resulting in an abnormal feto-maternal placental bile acid gradient and increased TSBA concentrations in the fetus (Geenes et al., 2014b). ICP is associated with an increased risk of adverse fetal outcomes, including spontaneous preterm labour (PTL) and intrauterine death (IUD), both of which are directly correlated with maternal TSBA concentrations with a substantially increased odds ratio at concentrations of ≥100 μmol/L (Ovadia et al., 2019) . The exact mechanisms of these fetal adverse outcomes are largely unknown, although there is experimental and observational evidence to suggest that ICP-associated PTL is due to an increase in the pregnant myometrium's responsiveness to oxytocin (OT), and ICP-associated IUD is due to a sudden fetal arrhythmia (Israel et al., 1986, Germain et al., 2003, Ataalla et al., 2016, Fan et al., 2014, Sanhal et al., 2017, Shand et al., 2008, Lee et al., 2009). ICP is currently commonly treated by the drug ursodeoxycholic acid (UDCA); although UDCA is protective in *in vitro* models of the fetal heart, there is currently no data on its effect on the myometrium nor evidence that UDCA treatment decreases the likelihood of PTL or IUD in pregnancies complicated by ICP (Adeyemi et al., 2017, Schultz et al., 2016, Miragoli et al., 2011, Chappell et al., 2019).

The overall aim of this project was to improve the monitoring of ICP and mechanistic understanding of ICP-associated PTL and IUD. As a starting point, we aimed to better diagnosis and monitoring of ICP via the development of a novel bile acid biosensor that could be utilised in a point-of-care (POC) setting and yield immediate measurements of TSBA concentrations. Next, we aimed to investigate the mechanisms of ICP-associated spontaneous preterm labour (PTL) via exposure of contractile agonists and bile acids to *in vitro* primary human myometrial cell culture model. Finally, we aimed to investigate the mechanism of ICP-associated intrauterine death (IUD) via non-invasive fetal ECG monitoring.

Measurement of TSBA concentrations in the clinical laboratory for diagnostic or monitoring purposes occurs via a colorimetric assay that utilises an enzymatic reaction that accumulates NADH at concentrations analogous to the TSBA present in the sample (Zhang et al., 2005). This assay, although high in sensitivity and specificity, is not necessarily available at all sites that manage women with ICP nor are the results always immediately provided (Danese et al., 2017). In order to fulfil the first aim of this project, an electrochemical biosensor was developed with the use of the aforementioned enzymatic reaction which measured NADH accumulation from taurocholic acid (TCA)-spiked samples on a commercially available carbon screen-printed electrode (CSPE) via chronoamperometry. The CSPE biosensor was subsequently manually modified with various concentrations of the electron mediators Meldola's blue and methylene blue (MEB). Although the MEB-modified biosensor was able to detect NADH concentrations generated from TCA concentrations of up to 100 µmol/L, there was a high relative standard deviation between the each biosensor measurement and a non-linear relationship between the TCA concentration and the current generated from NADH accumulation.

Although the field of biosensor development is expansive, research and development into bile acid biosensing is relatively niche. As it has now been established that maternal TSBA concentrations are the most effective biomarker for determining the risk of IUD in ICP-complicated pregnancies, the necessity to develop a sensitive POC biosensor for TSBA measurement is paramount in order to quickly assess and identify the subset of patients who are most at risk of an adverse outcome (Ovadia et al., 2019). Although this work has not yet fulfilled this aim, there has been substantial progress towards optimising and establishing the correct experimental protocols for future work. Additionally, we have shown MEB is a successful electron mediator for detection of TCA which had not been validated prior to this work. The aims for this project in the near future are to optimise the biosensor to accurately test TCA-spiked pooled human serum around and above concentrations of 100 µmol/L and, following on from this, validate the biosensor using serum samples collected from women with ICP which have been previously tested via colorimetric assay in a clinical laboratory. The main focus, and perhaps the greatest difficulty, to fulfil these aims will be the successful modification of the biosensor which has not

yet been achieved by any research groups that are investigating bile acid biosensing (Tian et al., 2018). Future work will also involve making the first steps towards development of a "lab-on-a-chip" biosensor for TSBA concentrations via microfluidics technology, which will be particularly useful as circulating TSBA concentrations are susceptible to diurnal variation (Gälman et al., 2005).

There is currently a paucity of data regarding the mechanism of ICP-associated PTL, however there is evidence that bile acids cause the myometrium to be more responsive to exogenous OT via upregulation of the oxytocin receptor (Germain et al., 2003, Israel et al., 1986). The effect of UDCA treatment on the myometrium is unknown. In order to fulfil the second aim of this project, we used a primary myometrial cell model to investigate ICP-associated PTL. This model was exposed to a combination of elevated bile acids and/or uterotonic drugs and the subsequent contractile response was measured via the optical recording of intracellular calcium ($[Ca^{2+}]_i$) transients. We found that TCA further increases the OT-induced changes in $[Ca^{2+}]_i$ transients and co-administration of UDCA results in the attenuation of this effect. UDCA also appeared to attenuate prostaglandin-induced changes in $[Ca^{2+}]_i$ transients.

There is currently no literature that has measured the effect of elevated bile acids on the $[Ca^{2+}]_i$ of myometrial cells, nor the effect of UDCA on myometrial contractility. The results from this study are therefore novel and provide a step towards understanding the mechanisms of ICP-associated PTL and the potential benefit of UDCA treatment. Although it has been suggested that bile acids increase myometrial sensitivity to OT and therefore increase the likelihood of spontaneous PTL in women with ICP, there is still relatively little supporting evidence for this theory. Here, we have provided data that agrees with this hypothesis as well as showing that exposure of myometrial cells to TCA alone does not elicit any changes to $[Ca^{2+}]_i$ transients, therefore further reinforcing the assumption that its mechanism of action is via the oxytocin receptor. Perhaps the most interesting result is the response of the model to UDCA administration following exposure to the uterotonic drugs or TCA. The ability of UDCA to attenuate TCA and prostaglandin-induced

changes to $[Ca^{2+}]_I$ transients suggests it may be worthwhile investigating its ability to act as a tocolytic therapy for both ICP- and non ICP-associated spontaneous PTL.

Further experiments in the near future that will utilise this cell model will involve measurement of mRNA and proteins that are known to be markers of spontaneous PTL in the myometrium. One of the main limitations of the optical recording experiments was the low number of experiments; this was mainly due to the time-intensive nature of the experiments and analysis. Future investigations could explore other models to examine myometrial contractility such as cell lines or myometrial strips. It would also be valuable to investigate the effect of a larger range of concentrations of TCA due to the relationship between TSBA concentrations and rate of PTL in pregnancies complicated by ICP. In addition, the effect of TCA in combination with prostaglandin administration was not investigated in these experiments so this would also be interesting to study as there is evidence that hydrophobic bile acids stimulate prostaglandin E_2 synthesis in other tissues (Jain et al., 2018, Hikasa et al., 1989, Nakamura et al., 2001).

Although the mechanisms of ICP-associated IUD have not been fully elucidated, there is now a large amount of evidence pointing to a sudden fetal cardiac arrythmia as the cause; this is evidenced by the observation of cardiotocography and echocardiography abnormalities such as bradycardia and left ventricular dysfunction, and *in vitro* studies demonstrating TCA-induced arrythmia in fetal heart models (Lee et al., 2009, Ataalla et al., 2016, Fan et al., 2014, Sanhal et al., 2017, Strehlow et al., 2010, Gorelik et al., 2002, Sheikh Abdul Kadir et al., 2010). The last aim of this project was to investigate the mechanisms of ICP-associated IUD via the assessment of the fetal heart in ICP-complicated pregnancies. In order to fulfil this aim, we conducted an observational study to study the fetal cardia phenotype in women with mild or severe ICP who had either been untreated or treated with UDCA. A novel transabdominal fetal ECG (fECG) monitor, the Monica AN24, was used to record the ECG of these participants and umbilical venous serum samples were collected after delivery to measure the concentration of NT-proBNP, a marker of heart failure. We found that maternal and fetal TSBA concentrations were associated with the

degree of PR interval prolongation, heart rate variability and NT-proBNP concentration respectively. We also found that conjugated cholic acid, the main bile acid raised in ICP, and hydrophobicity index are associated with the increase in fetal NT-proBNP concentrations observed in ICP. Importantly, we found that participants from a matched UDCA-treated cohort did not have the same abnormal cardiac phenotype.

This work has added to the evidence which suggests that ICP-associated IUD is caused by a fetal arrhythmia. Although there have already been studies suggesting ICP causes fetal PR interval prolongation and elevated NT-proBNP concentrations, the analysis of fetal heart rate variability in ICP-complicated pregnancies is completely novel and supports the hypothesis that ICP causes a pro-arrhythmogenic phenotype in the fetal heart (Rodríguez et al., 2016, Strehlow et al., 2010, Fan et al., 2014). Importantly, the association between hydrophobicity index and conjugated cholic acid with fetal NT-proBNP concentration has not been explored before and supports *in vitro* evidence that TCA causes arrhythmic activity in fetal heart models via activation of M_2 receptors (Sheikh Abdul Kadir et al., 2010). This work also demonstrates that the severity of hypercholanemia in ICP is directly correlated with the degree of fetal cardiac dysfunction which is in line with observations of the rate of IUD in women with extremely elevated maternal TSBA concentrations (Ovadia et al., 2019). We observed that fetuses from pregnancies where the mother had received UDCA treatment did not have the same associations between TSBA concentration and fetal heart rate variability or NT-proBNP concentration. Although there is *in vitro* evidence to suggest that UDCA is cardioprotective in the fetal heart, the largest randomised controlled trial investigating the effect of UDCA on fetal outcomes to date did not show that UDCA treatment prevented a composite of adverse outcomes in ICP that included ICP-associated IUD (Adeyemi et al., 2017, Miragoli et al., 2011, Schultz et al., 2016, Chappell et al., 2019). However, 76% of participants in this trial had mild ICP and only 7% had maternal TSBA concentrations of ≥100 μmol/L which suggests that further investigation of the fetal heart in a subset of women with substantially elevated TSBA concentrations is warranted.

The relatively low proportion of women with TSBA concentrations of ≥100 μmol/L was also a limitation in our study, as only three participants from the untreated ICP cohort had maternal TSBA concentrations above this threshole. Future investigations will focus on recruiting a larger number of participants with severe hypercholanemia as this appears to be the population that is most at risk of fetal cardiac dysfunction. Ideally, a future study in these participants would also take longitudinal fECG measurements pre- and post-UDCA treatment to eliminate the effect of individual variability and robustly assess whether UDCA treatment is beneficial.

This project has utilised a range of novel approaches from several different academic disciplines in order to improve the monitoring and mechanistic understanding of ICP. Biosensor technology was used to develop a device to improve monitoring of ICP, a novel myometrial cell model of ICP-associated PTL was subjected to $[Ca^{2+}]_i$ handling assays and a novel transabdominal fECG monitor was used to assess fetal cardiac dysfunction associated with ICP. Moreover, novel data analysis techniques, particular for heart rate variability analysis, have been utilised to fulfil the aims of this project.

We have demonstrated that the development of a POC bile acid biosensor is feasible and worthwhile, particularly due to findings of the adverse effect of relatively hydrophobic bile acids on the pregnant myometrium and fetal heart as well as the importance of severity of hypercholanemia. In addition, development of this biosensor is important due the current lag between taking a blood sample and receiving TSBA measurements from the assays commonly utilised in clinical laboratories, which can delay clinical decisions in managing women with ICP. We have also shown that UDCA treatment may be protective against adverse fetal outcomes in pregnancies with substantially elevated maternal TSBA concentrations, suggesting that further investigation into its benefit is required.

6. References

ABEDIN, P., WEAVER, J. B. & EGGINTON, E. 1999. Intrahepatic cholestasis of pregnancy: prevalence and ethnic distribution. *Ethn Health,* 4**,** 35-7.

ABRAMOVITZ, M., BOIE, Y., NGUYEN, T., RUSHMORE, T. H., BAYNE, M. A., METTERS, K. M., SLIPETZ, D. M. & GRYGORCZYK, R. 1994. Cloning and expression of a cDNA for the human prostanoid FP receptor. *J Biol Chem,* 269**,** 2632-6.

ABU-HAYYEH, S., OVADIA, C., LIEU, T., JENSEN, D. D., CHAMBERS, J., DIXON, P. H., LÖVGREN-SANDBLOM, A., BOLIER, R., TOLENAARS, D., KREMER, A. E., SYNGELAKI, A., NOORI, M., WILLIAMS, D., MARIN, J. J., MONTE, M. J., NICOLAIDES, K. H., BEUERS, U., OUDE-ELFERINK, R., SEED, P. T., CHAPPELL, L., MARSCHALL, H. U., BUNNETT, N. W. & WILLIAMSON, C. 2016. Prognostic and mechanistic potential of progesterone sulfates in intrahepatic cholestasis of pregnancy and pruritus gravidarum. *Hepatology,* 63**,** 1287-98.

ADEYEMI, O., ALVAREZ-LAVIADA, A., SCHULTZ, F., IBRAHIM, E., TRAUNER, M., WILLIAMSON, C., GLUKHOV, A. V. & GORELIK, J. 2017. Ursodeoxycholic acid prevents ventricular conduction slowing and arrhythmia by restoring T-type calcium current in fetuses during cholestasis. *PLoS One,* 12**,** e0183167.

AL INIZI, S., GUPTA, R. & GALE, A. 2006. Fetal tachyarrhythmia with atrial flutter in obstetric cholestasis. *Int J Gynaecol Obstet,* 93**,** 53-4.

AL SHOBAILI, H. A., HAMED, H. O., AL ROBAEE, A., ALZOLIBANI, A. A., AMIN, A. F. & AHMAD, S. R. 2011. Obstetrical and fetal outcomes of a new management strategy in patients with intra-hepatic cholestasis of pregnancy. *Arch Gynecol Obstet,* 283**,** 1219-25.

ALBERY, W. J., BARTLETT, P. N. & CASS, A. E. 1987. Amperometric enzyme electrodes. *Philos Trans R Soc Lond B Biol Sci,* 316**,** 107-19.

ALEMDAROĞLU, S., YILMAZ BARAN, Ş., DURDAĞ, G. D., YUKSEL ŞIMŞEK, S., YETKINEL, S., ALKAŞ YAĞINÇ, D., KALAYCI, H. & ŞIMŞEK, E. 2020. Intrahepatic cholestasis of pregnancy: are. *J Matern Fetal Neonatal Med***,** 1-6.

ALONSO, C. E., GAMUNDI, S. S., CASTILLO, G., ORCE, G. & COVIELLO, A. 1995. Inhibitory effect of sodium ursodeoxycholate on basal and stimulated short-circuit current across the isolated toad skin. *Comp Biochem Physiol C Pharmacol Toxicol Endocrinol,* 110**,** 321-7.

ALSULYMAN, O. M., OUZOUNIAN, J. G., AMES-CASTRO, M. & GOODWIN, T. M. 1996. Intrahepatic cholestasis of pregnancy: perinatal outcome associated with expectant management. *Am J Obstet Gynecol,* 175**,** 957-60.

ALTUG, N., KIRBAS, A., DAGLAR, K., BIBEROGLU, E., UYGUR, D. & DANISMAN, N. 2015. Drug resistant fetal arrhythmia in obstetric cholestasis. *Case Rep Obstet Gynecol,* 2015**,** 890802.

AMANO, M., ITO, M., KIMURA, K., FUKATA, Y., CHIHARA, K., NAKANO, T., MATSUURA, Y. & KAIBUCHI, K. 1996. Phosphorylation and activation of myosin by Rho-associated kinase (Rho-kinase). *J Biol Chem,* 271**,** 20246-9.

AMBROS-RUDOLPH, C. M., GLATZ, M., TRAUNER, M., KERL, H. & MÜLLEGGER, R. R. 2007. The importance of serum bile acid level analysis and treatment with ursodeoxycholic acid in intrahepatic cholestasis of pregnancy: a case series from central Europe. *Arch Dermatol,* 143**,** 757-62.

AMMÄLÄ, P. & KARINIEMI, V. 1981. Short-term variability of fetal heart rate in cholestasis of pregnancy. *Am J Obstet Gynecol,* 141**,** 217-20.

ANDERSON, L., MARTIN, W., HIGGINS, C., NELSON, S. M. & NORMAN, J. E. 2009. The effect of progesterone on myometrial contractility, potassium channels, and tocolytic efficacy. *Reprod Sci,* 16**,** 1052-61.

ARAKI, S., ITO, M., KUREISHI, Y., FENG, J., MACHIDA, H., ISAKA, N., AMANO, M., KAIBUCHI, K., HARTSHORNE, D. J. & NAKANO, T. 2001. Arachidonic acid-induced Ca2+ sensitization of smooth muscle contraction through activation of Rho-kinase. *Pflugers Arch,* 441**,** 596-603.

ARIAS DE FUENTES, O., CAMPANELLA, L., CRESCENTINI, G., FALCIONI, A., SAMMARTINO, M. P. & TOMASSETTI, M. 2000. Flow injection analysis of cholic acids in pharmaceutical preparations using a polymeric membrane ISE as detector. *J Pharm Biomed Anal,* 23**,** 89-98.

ARROWSMITH, S. & WRAY, S. 2014. Oxytocin: its mechanism of action and receptor signalling in the myometrium. *J Neuroendocrinol,* 26**,** 356-69.

ASBÓTH, G., PHANEUF, S., EUROPE-FINNER, G. N., TÓTH, M. & BERNAL, A. L. 1996. Prostaglandin E2 activates phospholipase C and elevates intracellular calcium in cultured myometrial cells: involvement of EP1 and EP3 receptor subtypes. *Endocrinology,* 137**,** 2572-9.

ASLAN, M., KIRAÇ, E., YILMAZ, Ö., ÜNAL, B., KONUK, E. K., ÖZCAN, F. & TUZCU, H. 2018. Effect of tauroursodeoxycholic acid on PUFA levels and inflammation in an animal and cell model of hepatic endoplasmic reticulum stress. *Hum Exp Toxicol,* 37**,** 803-816.

ASTLE, S., THORNTON, S. & SLATER, D. M. 2005. Identification and localization of prostaglandin E2 receptors in upper and lower segment human myometrium during pregnancy. *Mol Hum Reprod,* 11**,** 279-87.

ATAALLA, W. M., ZIADA, D. H., GABER, R., OSSMAN, A., BAYOMY, S. & ELEMARY, B. R. 2016. The impact of total bile acid levels on fetal cardiac function in intrahepatic cholestasis of pregnancy using fetal echocardiography: a tissue Doppler imaging study. *J Matern Fetal Neonatal Med,* 29**,** 1445-50.

AZZAROLI, F., RASPANTI, M. E., SIMONI, P., MONTAGNANI, M., LISOTTI, A., CECINATO, P., ARENA, R., SIMONAZZI, G., FARINA, A., RIZZO, N. & MAZZELLA, G. 2013. High doses of ursodeoxycholic acid up-regulate the expression of placental breast cancer resistance protein in patients affected by intrahepatic cholestasis of pregnancy. *PLoS One,* 8**,** e64101.

BACQ, Y. & SENTILHES, L. 2014. Intrahepatic cholestasis of pregnancy: Diagnosis and management. *Clin Liver Dis (Hoboken),* 4**,** 58-61.

BAE, C. W., TOI, P. T., KIM, B. Y., LEE, W. I., LEE, H. B., HANIF, A., LEE, E. H. & LEE, N. E. 2019. Fully Stretchable Capillary Microfluidics-Integrated Nanoporous Gold Electrochemical Sensor for Wearable Continuous Glucose Monitoring. *ACS Appl Mater Interfaces,* 11**,** 14567-14575.

BAGAL-KESTWAL, D. R., PAN, M. H. & CHIANG, B. H. 2018. Electrically nanowired-enzymes for probe modification and sensor fabrication. *Biosens Bioelectron,* 121**,** 223-235.

BAIN, E., HEATLEY, E., HSU, K. & CROWTHER, C. A. 2013. Relaxin for preventing preterm birth. *Cochrane Database Syst Rev***,** CD010073.

BAL, N. B., HAN, S., KIREMITCI, S., SADI, G., ULUDAG, O. & DEMIREL-YILMAZ, E. 2019. Hypertension-induced cardiac impairment is reversed by the inhibition of endoplasmic reticulum stress. *J Pharm Pharmacol,* 71**,** 1809-1821.

BALDUCCI, J., RISEK, B., GILULA, N. B., HAND, A., EGAN, J. F. & VINTZILEOS, A. M. 1993. Gap junction formation in human myometrium: a key to preterm labor? *Am J Obstet Gynecol,* 168**,** 1609-15.

BARTLING, B., LI, L. & LIU, C. C. 2009. Determination of total bile acid levels using a thick-film screen-printed Ir/C sensor for the detection of liver disease. *Analyst,* 134**,** 973-9.

BASILE, F., SANTAMARIA, A., MANNUCCI, C., RIZZO, L., GANGEMI, S., D'ANNA, R. & ARCORACI, V. 2017. Interleukin 31 is involved in intrahepatic cholestasis of pregnancy. *J Matern Fetal Neonatal Med,* 30**,** 1124-1127.

BATRA, A. S. & BALAJI, S. 2019. Fetal arrhythmias: Diagnosis and management. *Indian Pacing Electrophysiol J,* 19**,** 104-109.

BATSRY, L., ZLOTO, K., KALTER, A., BAUM, M., MAZAKI-TOVI, S. & YINON, Y. 2019. Perinatal outcomes of intrahepatic cholestasis of pregnancy in twin versus singleton pregnancies: is plurality associated with adverse outcomes? *Arch Gynecol Obstet,* 300**,** 881-887.

BEATH, S. V. 2003. Hepatic function and physiology in the newborn. *Semin Neonatol,* 8**,** 337-46.

BEBLO, D. A., WANG, H. Z., BEYER, E. C., WESTPHALE, E. M. & VEENSTRA, R. D. 1995. Unique conductance, gating, and selective permeability properties of gap junction channels formed by connexin40. *Circ Res,* 77**,** 813-22.

BECKH, K., KNEIP, S. & ARNOLD, R. 1994. Direct regulation of bile secretion by prostaglandins in perfused rat liver. *Hepatology,* 19**,** 1208-13.

BEHAR, J., MAWE, G. M., MAWE, G., CAREY, M. C. & CAREY, M. 2013. Roles of cholesterol and bile salts in the pathogenesis of gallbladder hypomotility and inflammation: cholecystitis is not caused by cystic duct obstruction. *Neurogastroenterol Motil,* 25**,** 283-90.

BERG, B., HELM, G., PETERSOHN, L. & TRYDING, N. 1986. Cholestasis of pregnancy. Clinical and laboratory studies. *Acta Obstet Gynecol Scand,* 65**,** 107-13.

BERKANE, N., COCHETON, J. J., BREHIER, D., MERVIEL, P., WOLF, C., LEFÈVRE, G. & UZAN, S. 2000. Ursodeoxycholic acid in intrahepatic cholestasis of pregnancy. A retrospective study of 19 cases. *Acta Obstet Gynecol Scand,* 79**,** 941-6.

BERRIDGE, M. J., LIPP, P. & BOOTMAN, M. D. 2000. The versatility and universality of calcium signalling. *Nat Rev Mol Cell Biol,* 1**,** 11-21.

BHALLA, N., JOLLY, P., FORMISANO, N. & ESTRELA, P. 2016. Introduction to biosensors. *Essays Biochem,* 60**,** 1-8.

BIBEROGLU, E., KIRBAS, A., DAGLAR, K., KARA, O., KARABULUT, E., YAKUT, H. I. & DANISMAN, N. 2016. Role of inflammation in intrahepatic cholestasis of pregnancy. *J Obstet Gynaecol Res,* 42**,** 252-7.

BICKHAM, A. V., PANG, C., GEORGE, B. Q., TOPHAM, D. J., NIELSEN, J. B., NORDIN, G. P. & WOOLLEY, A. T. 2020. 3D Printed Microfluidic Devices for Solid-Phase Extraction and On-Chip Fluorescent Labeling of Preterm Birth Risk Biomarkers. *Anal Chem,* 92**,** 12322-12329.

BINAH, O., RUBINSTEIN, I., BOMZON, A. & BETTER, O. S. 1987. Effects of bile acids on ventricular muscle contraction and electrophysiological properties: studies in rat papillary muscle and isolated ventricular myocytes. *Naunyn Schmiedebergs Arch Pharmacol,* 335**,** 160-5.

BINDER, T., SALAJ, P., ZIMA, T. & VÍTEK, L. 2006. Randomized prospective comparative study of ursodeoxycholic acid and S-adenosyl-L-methionine in the treatment of intrahepatic cholestasis of pregnancy. *J Perinat Med,* 34**,** 383-91.

BLANKS, A. M. & THORNTON, S. 2003. The role of oxytocin in parturition. *BJOG,* 110 Suppl 20**,** 46-51.

BLENCOWE, H., COUSENS, S., OESTERGAARD, M. Z., CHOU, D., MOLLER, A. B., NARWAL, R., ADLER, A., VERA GARCIA, C., ROHDE, S., SAY, L. & LAWN, J. E. 2012. National, regional, and worldwide estimates of preterm birth rates in the year 2010 with time trends since 1990 for selected countries: a systematic analysis and implications. *Lancet,* 379**,** 2162-72.

BOUSCAREL, B., FROMM, H. & NUSSBAUM, R. 1993. Ursodeoxycholate mobilizes intracellular Ca2+ and activates phosphorylase a in isolated hepatocytes. *Am J Physiol,* 264**,** G243-51.

BRAINARD, A. M., KOROVKINA, V. P. & ENGLAND, S. K. 2007. Potassium channels and uterine function. *Semin Cell Dev Biol,* 18**,** 332-9.

BRAVO-VALENZUELA, N. J., ROCHA, L. A., MACHADO NARDOZZA, L. M. & JÚNIOR, E. A. 2018. Fetal cardiac arrhythmias: Current evidence. *Ann Pediatr Cardiol,* 11**,** 148-163.

BRETT, C. M., INZELT, G. & KERTESZ, V. 1999. Poly (methylene blue) modified electrode sensor for haemoglobin. *Analytica Chimica Acta,* 385**,** 119-123.

BREUILLER-FOUCHÉ, M., TERTRIN-CLARY, C., HÉLUY, V., FOURNIER, T. & FERRÉ, F. 1998. Role of protein kinase C in endothelin-1-induced contraction of human myometrium. *Biol Reprod,* 59**,** 153-9.

BRITES, D. 2002. Intrahepatic cholestasis of pregnancy: changes in maternal-fetal bile acid balance and improvement by ursodeoxycholic acid. *Ann Hepatol,* 1**,** 20-8.

BRITES, D., RODRIGUES, C. M., OLIVEIRA, N., CARDOSO, M. & GRAÇA, L. M. 1998. Correction of maternal serum bile acid profile during ursodeoxycholic acid therapy in cholestasis of pregnancy. *J Hepatol,* 28**,** 91-8.

BROUWERS, L., KOSTER, M. P., PAGE-CHRISTIAENS, G. C., KEMPERMAN, H., BOON, J., EVERS, I. M., BOGTE, A. & OUDIJK, M. A. 2015. Intrahepatic cholestasis of pregnancy: maternal and fetal outcomes associated with elevated bile acid levels. *Am J Obstet Gynecol,* 212**,** 100.e1-7.

BRUZZONE, R., WHITE, T. W. & PAUL, D. L. 1996. Connections with connexins: the molecular basis of direct intercellular signaling. *Eur J Biochem,* 238**,** 1-27.

BRYANT-GREENWOOD, G. D. 1991. The human relaxins: consensus and dissent. *Mol Cell Endocrinol,* 79**,** C125-32.

BURGHARDT, R. C., BARHOUMI, R., SANBORN, B. M. & ANDERSEN, J. 1999. Oxytocin-induced Ca2+ responses in human myometrial cells. *Biol Reprod,* 60**,** 777-82.

BÄHRLE, S., SZABÓ, G., STIEHL, A., THEILMANN, L., DENGLER, T. J., ZIMMERMANN, R. & KÜBLER, W. 1998. Adjuvant treatment with ursodeoxycholic acid may reduce the incidence of acute cardiac allograft rejection. *J Heart Lung Transplant,* 17**,** 592-8.

CAMPANELLA, L., FAVERO, G., MASTROFINI, D. & TOMASSETTI, M. 1996. Toxicity order of cholanic acids using an immobilised cell biosensor. *J Pharm Biomed Anal,* 14**,** 1007-13.

CAMPBELL, G. R., CHAMLEY, J. H. & BURNSTOCK, G. 1974. Development of smooth muscle cells in tissue culture. *J Anat,* 117**,** 295-312.

CAMPOS, G. A., CASTILLO, R. J. & TORO, F. G. 1988. [Effect of bile acids on the myometral contractility of the isolated pregnant uterus]. *Rev Chil Obstet Ginecol,* 53**,** 229-33.

CAMPOS, G. A., GUERRA, F. A. & ISRAEL, E. J. 1986. Effects of cholic acid infusion in fetal lambs. *Acta Obstet Gynecol Scand,* 65**,** 23-6.

CENTUORI, S. M., GOMES, C. J., TRUJILLO, J., BORG, J., BROWNLEE, J., PUTNAM, C. W. & MARTINEZ, J. D. 2016. Deoxycholic acid mediates non-canonical EGFR-MAPK activation through the induction of calcium signaling in colon cancer cells. *Biochim Biophys Acta,* 1861**,** 663-70.

CEYLAN-ISIK, A. F., SREEJAYAN, N. & REN, J. 2011. Endoplasmic reticulum chaperon tauroursodeoxycholic acid alleviates obesity-induced myocardial contractile dysfunction. *J Mol Cell Cardiol,* 50**,** 107-16.

CHALFANT, C. E. & SPIEGEL, S. 2005. Sphingosine 1-phosphate and ceramide 1-phosphate: expanding roles in cell signaling. *J Cell Sci,* 118**,** 4605-12.

CHALLIS, J. R., SLOBODA, D. M., ALFAIDY, N., LYE, S. J., GIBB, W., PATEL, F. A., WHITTLE, W. L. & NEWNHAM, J. P. 2002. Prostaglandins and mechanisms of preterm birth. *Reproduction,* 124**,** 1-17.

CHAO, S., XIAOJUN, L., HAIZHEN, W., LUDI, F., SHAOZHEN, L., ZHIWEN, S., WEILIANG, H., CHUNHONG, J., YING, W., FAN, W. & YUNFEI, G. 2019. Lithocholic acid activates mTOR signaling inducing endoplasmic reticulum stress in placenta during intrahepatic cholestasis of pregnancy. *Life Sci,* 218**,** 300-307.

CHAPLIN, M. F. 1995. Analysis of bile acids and their conjugates using high-pH anion-exchange chromatography with pulsed amperometric detection. *J Chromatogr B Biomed Appl,* 664**,** 431-4.

CHAPPELL, L. C., BELL, J. L., SMITH, A., LINSELL, L., JUSZCZAK, E., DIXON, P. H., CHAMBERS, J., HUNTER, R., DORLING, J., WILLIAMSON, C., THORNTON, J. G. & GROUP, P. S. 2019. Ursodeoxycholic acid versus placebo in women with intrahepatic cholestasis of pregnancy (PITCHES): a randomised controlled trial. *Lancet*.

CHAPPELL, L. C., GURUNG, V., SEED, P. T., CHAMBERS, J., WILLIAMSON, C., THORNTON, J. G. & CONSORTIUM, P. S. 2012. Ursodeoxycholic acid versus placebo, and early term delivery versus expectant management, in women with intrahepatic cholestasis of pregnancy: semifactorial randomised clinical trial. *BMJ,* 344**,** e3799.

CHARPIGNY, G., LEROY, M. J., BREUILLER-FOUCHÉ, M., TANFIN, Z., MHAOUTY-KODJA, S., ROBIN, P., LEIBER, D., COHEN-TANNOUDJI, J., CABROL, D., BARBERIS, C. & GERMAIN, G. 2003. A functional genomic study to identify differential gene expression in the preterm and term human myometrium. *Biol Reprod,* 68**,** 2289-96.

CHAUBEY, A. & MALHOTRA, B. D. 2002. Mediated biosensors. *Biosens Bioelectron,* 17**,** 441-56.

CHEN, J., LI, Q. & MA, J. 2019a. Maternal serum, placental, and umbilical venous blood irisin levels in intrahepatic cholestasis of pregnancy. *J Matern Fetal Neonatal Med***,** 1-8.

CHEN, W., GAO, X. X., MA, L., LIU, Z. B., LI, L., WANG, H., GAO, L., XU, D. X. & CHEN, Y. H. 2019b. Obeticholic Acid Protects against Gestational Cholestasis-Induced Fetal Intrauterine Growth Restriction in Mice. *Oxid Med Cell Longev,* 2019**,** 7419249.

CHENG, S., KEYES, M. J., LARSON, M. G., MCCABE, E. L., NEWTON-CHEH, C., LEVY, D., BENJAMIN, E. J., VASAN, R. S. & WANG, T. J. 2009. Long-term outcomes in individuals with prolonged PR interval or first-degree atrioventricular block. *JAMA,* 301**,** 2571-7.

CHIANG, J. Y. 1998. Regulation of bile acid synthesis. *Front Biosci,* 3**,** d176-93.

CHIANG, J. Y. 2013. Bile acid metabolism and signaling. *Compr Physiol,* 3**,** 1191-212.

CHIBBAR, R., MILLER, F. D. & MITCHELL, B. F. 1993. Synthesis of oxytocin in amnion, chorion, and decidua may influence the timing of human parturition. *J Clin Invest,* 91**,** 185-92.

CHIN-SMITH, E. C., SLATER, D. M., JOHNSON, M. R. & TRIBE, R. M. 2014. STIM and Orai isoform expression in pregnant human myometrium: a potential role in calcium signaling during pregnancy. *Front Physiol,* 5**,** 169.

CHO, I. H., LEE, J., KIM, J., KANG, M. S., PAIK, J. K., KU, S., CHO, H. M., IRUDAYARAJ, J. & KIM, D. H. 2018. Current Technologies of Electrochemical Immunosensors: Perspective on Signal Amplification. *Sensors (Basel),* 18.

CHOW, L. & LYE, S. J. 1994. Expression of the gap junction protein connexin-43 is increased in the human myometrium toward term and with the onset of labor. *Am J Obstet Gynecol,* 170**,** 788-95.

CHUNG, D., KIM, Y. S., PHILLIPS, J. N., ULLOA, A., KU, C. Y., GALAN, H. L. & SANBORN, B. M. 2010. Attenuation of canonical transient receptor potential-like channel 6 expression specifically reduces the diacylglycerol-mediated increase in intracellular calcium in human myometrial cells. *Endocrinology,* 151**,** 406-16.

CHWALISZ, K. & GARFIELD, R. E. 1997. Regulation of the uterus and cervix during pregnancy and labor. Role of progesterone and nitric oxide. *Ann N Y Acad Sci,* 828**,** 238-53.
CLARK, L. C. & LYONS, C. 1962. Electrode systems for continuous monitoring in cardiovascular surgery. *Ann N Y Acad Sci,* 102**,** 29-45.
COMBETTES, L., DUMONT, M., BERTHON, B., ERLINGER, S. & CLARET, M. 1988. Release of calcium from the endoplasmic reticulum by bile acids in rat liver cells. *J Biol Chem,* 263**,** 2299-303.
CONDON, J., YIN, S., MAYHEW, B., WORD, R. A., WRIGHT, W. E., SHAY, J. W. & RAINEY, W. E. 2002. Telomerase immortalization of human myometrial cells. *Biol Reprod,* 67**,** 506-14.
COSTOYA, A. L., LEONTIC, E. A., ROSENBERG, H. G. & DELGADO, M. A. 1980. Morphological study of placental terminal villi in intrahepatic cholestasis of pregnancy: histochemistry, light and electron microscopy. *Placenta,* 1**,** 361-8.
COUTO, R. A., LIMA, J. L. & QUINAZ, M. B. 2016. Recent developments, characteristics and potential applications of screen-printed electrodes in pharmaceutical and biological analysis. *Talanta,* 146**,** 801-14.
CSAPO, A., ERDOS, T., DE MATTOS, C. R., GRAMSS, E. & MOSCOWITZ, C. 1965. Stretch-induced uterine growth, protein synthesis and function. *Nature,* 207**,** 1378-9.
CSAPO, A. I. & PINTO-DANTAS, C. A. 1965. The effect of progesterone on the human uterus. *Proc Natl Acad Sci U S A,* 54**,** 1069-76.
CUI, D., ZHONG, Y., ZHANG, L. & DU, H. 2017. Bile acid levels and risk of adverse perinatal outcomes in intrahepatic cholestasis of pregnancy: A meta-analysis. *J Obstet Gynaecol Res,* 43**,** 1411-1420.
CURLEY, M., CAIRNS, M. T., FRIEL, A. M., MCMEEL, O. M., MORRISON, J. J. & SMITH, T. J. 2002. Expression of mRNA transcripts for ATP-sensitive potassium channels in human myometrium. *Mol Hum Reprod,* 8**,** 941-5.
CZUL, F., PEYTON, A. & LEVY, C. 2013. Primary biliary cirrhosis: therapeutic advances. *Clin Liver Dis,* 17**,** 229-42.
DAI, Z.-H., LIU, F.-X., LU, G.-F. & BAO, J.-C. 2008. Electrocatalytic detection of NADH and ethanol at glassy carbon electrode modified with electropolymerized films from methylene green. *Journal of Solid State Electrochemistry,* 12**,** 175-180.
DALRYMPLE, A., MAHN, K., POSTON, L., SONGU-MIZE, E. & TRIBE, R. M. 2007. Mechanical stretch regulates TRPC expression and calcium entry in human myometrial smooth muscle cells. *Mol Hum Reprod,* 13**,** 171-9.
DAMBORSKÝ, P., ŠVITEL, J. & KATRLÍK, J. 2016. Optical biosensors. *Essays Biochem,* 60**,** 91-100.
DANESE, E., SALVAGNO, G. L., NEGRINI, D., BROCCO, G., MONTAGNANA, M. & LIPPI, G. 2017. Analytical evaluation of three enzymatic assays for measuring total bile acids in plasma using a fully-automated clinical chemistry platform. *PLoS One,* 12**,** e0179200.
DANN, A. T., KENYON, A. P., WIERZBICKI, A. S., SEED, P. T., SHENNAN, A. H. & TRIBE, R. M. 2006. Plasma lipid profiles of women with intrahepatic cholestasis of pregnancy. *Obstet Gynecol,* 107**,** 106-14.
DAS, P., DAS, M., CHINNADAYYALA, S. R., SINGHA, I. M. & GOSWAMI, P. 2016. Recent advances on developing 3rd generation enzyme electrode for biosensor applications. *Biosens Bioelectron,* 79**,** 386-97.
DAVIES, M. H., DA SILVA, R. C., JONES, S. R., WEAVER, J. B. & ELIAS, E. 1995. Fetal mortality associated with cholestasis of pregnancy and the potential benefit of therapy with ursodeoxycholic acid. *Gut,* 37**,** 580-4.

DE BELLE, R. C., VAUPSHAS, V., VITULLO, B. B., HABER, L. R., SHAFFER, E., MACKIE, G. G., OWEN, H., LITTLE, J. M. & LESTER, R. 1979. Intestinal absorption of bile salts: immature development in the neonate. *J Pediatr,* 94**,** 472-6.

DEKKER, R., VAN DER MEER, R. & OLIEMAN, C. 1991. Sensitive pulsed amperometric detection of free and conjugated bile acids in combination with gradient reversed-phase HPLC. *Chromatographia,* 31**,** 549-553.

DELICONSTANTINOS, G. & FOTIOU, S. 1986. Effect of prostaglandins E2 and F2 alpha on membrane calcium binding, Ca2+/Mg2+-ATPase activity and membrane fluidity in rat myometrial plasma membranes. *J Endocrinol,* 110**,** 395-404.

DERYABINA, E. G., YAKORNOVA, G. V., PESTRYAEVA, L. A. & SANDYREVA, N. D. 2016. Perinatal outcome in pregnancies complicated with gestational diabetes mellitus and very preterm birth: case-control study. *Gynecol Endocrinol,* 32**,** 52-55.

DESAI, M. S., EBLIMIT, Z., THEVANANTHER, S., KOSTERS, A., MOORE, D. D., PENNY, D. J. & KARPEN, S. J. 2015. Cardiomyopathy reverses with recovery of liver injury, cholestasis and cholanemia in mouse model of biliary fibrosis. *Liver Int,* 35**,** 1464-77.

DESAI, M. S., MATHUR, B., EBLIMIT, Z., VASQUEZ, H., TAEGTMEYER, H., KARPEN, S. J., PENNY, D. J., MOORE, D. D. & ANAKK, S. 2017. Bile acid excess induces cardiomyopathy and metabolic dysfunctions in the heart. *Hepatology,* 65**,** 189-201.

DEVEER, R., ENGIN-USTUN, Y., CELEN, S., ERYILMAZ, O. G., TONGUÇ, E., MOLLAMAHMUTOĞLU, L., OKSUZOGLU, A. & DANISMAN, N. 2011. Two-year experience of obstetric cholestasis: outcome and management. *Clin Exp Obstet Gynecol,* 38**,** 256-9.

DI MASCIO, D., QUIST-NELSON, J., RIEGEL, M., GEORGE, B., SACCONE, G., BRUN, R., HASLINGER, C., HERRERA, C., KAWAKITA, T., LEE, R. H., BENEDETTI PANICI, P. & BERGHELLA, V. 2019. Perinatal death by bile acid levels in intrahepatic cholestasis of pregnancy: a systematic review. *J Matern Fetal Neonatal Med***,** 1-9.

DIAFERIA, A., NICASTRI, P. L., TARTAGNI, M., LOIZZI, P., IACOVIZZI, C. & DI LEO, A. 1996. Ursodeoxycholic acid therapy in pregnant women with cholestasis. *Int J Gynaecol Obstet,* 52**,** 133-40.

DIETZ, P., WATSON, E. D., SATTLER, M. C., RUF, W., TITZE, S. & VAN POPPEL, M. 2016. The influence of physical activity during pregnancy on maternal, fetal or infant heart rate variability: a systematic review. *BMC Pregnancy Childbirth,* 16**,** 326.

DIPIETRO, J. A., COSTIGAN, K. A. & VOEGTLINE, K. M. 2015. STUDIES IN FETAL BEHAVIOR: REVISITED, RENEWED, AND REIMAGINED. *Monogr Soc Res Child Dev,* 80**,** vii;1-94.

DIXON, P. H. & WILLIAMSON, C. 2016. The pathophysiology of intrahepatic cholestasis of pregnancy. *Clin Res Hepatol Gastroenterol,* 40**,** 141-53.

DOELLING, R. March 2000. *Potentiostats*, Bank Elektronik Intelligent Controls GmBA.

DONET, A., GIRAULT, A., PINTON, A. & LEPERCQ, J. 2020. Intrahepatic cholestasis of pregnancy: Is a screening for differential diagnoses necessary? *J Gynecol Obstet Hum Reprod***,** 101907.

DONG, X., YU, C., SHYNLOVA, O., CHALLIS, J. R., RENNIE, P. S. & LYE, S. J. 2009. p54nrb is a transcriptional corepressor of the progesterone receptor that modulates transcription of the labor-associated gene, connexin 43 (Gja1). *Mol Endocrinol,* 23**,** 1147-60.

DONOFRIO, M. T., MOON-GRADY, A. J., HORNBERGER, L. K., COPEL, J. A., SKLANSKY, M. S., ABUHAMAD, A., CUNEO, B. F., HUHTA, J. C., JONAS, R. A., KRISHNAN, A., LACEY, S., LEE, W., MICHELFELDER, E. C., REMPEL, G. R., SILVERMAN, N. H., SPRAY, T. L., STRASBURGER, J. F., TWORETZKY, W., RYCHIK, J. & AMERICAN HEART ASSOCIATION ADULTS WITH CONGENITAL HEART DISEASE JOINT COMMITTEE OF THE COUNCIL ON CARDIOVASCULAR DISEASE IN THE YOUNG AND COUNCIL ON CLINICAL

CARDIOLOGY, C. U. O. C. S. A. A. 2014. Diagnosis and treatment of fetal cardiac disease: a scientific statement from the American Heart Association. *Circulation,* 129**,** 2183-242.

DROVER, J. W. & CASPER, R. F. 1983. Initiation of parturition in humans. *Can Med Assoc J,* 128**,** 387-92.

DU, Q., PAN, Y., ZHANG, Y., ZHANG, H., ZHENG, Y., LU, L., WANG, J., DUAN, T. & CHEN, J. 2014a. Placental gene-expression profiles of intrahepatic cholestasis of pregnancy reveal involvement of multiple molecular pathways in blood vessel formation and inflammation. *BMC Med Genomics,* 7**,** 42.

DU, Q., ZHANG, Y., PAN, Y. & DUAN, T. 2014b. Lithocholic acid-induced placental tumor necrosis factor-α upregulation and syncytiotrophoblast cell apoptosis in intrahepatic cholestasis of pregnancy. *Hepatol Res,* 44**,** 532-41.

DUQUETTE, R. A., SHMYGOL, A., VAILLANT, C., MOBASHERI, A., POPE, M., BURDYGA, T. & WRAY, S. 2005. Vimentin-positive, c-kit-negative interstitial cells in human and rat uterus: a role in pacemaking? *Biol Reprod,* 72**,** 276-83.

EARNEST, D. L., HOLUBEC, H., WALI, R. K., JOLLEY, C. S., BISSONETTE, M., BHATTACHARYYA, A. K., ROY, H., KHARE, S. & BRASITUS, T. A. 1994. Chemoprevention of azoxymethane-induced colonic carcinogenesis by supplemental dietary ursodeoxycholic acid. *Cancer Res,* 54**,** 5071-4.

EGGINS, B. R. 2002. Chemical sensors and biosensors. *Analytical techniques in the sciences.* Chichester ; Hoboken, N.J.: J. Wiley,.

ELORANTA, M. L., HEINONEN, S., MONONEN, T. & SAARIKOSKI, S. 2001. Risk of obstetric cholestasis in sisters of index patients. *Clin Genet,* 60**,** 42-5.

ERLINGER, S. 1990. Role of intracellular organelles in the hepatic transport of bile acids. *Biomed Pharmacother,* 44**,** 409-16.

ERLINGER, S. 2016. Intrahepatic cholestasis of pregnancy: A risk factor for cancer, autoimmune and cardiovascular diseases? *Clin Res Hepatol Gastroenterol,* 40**,** 139-40.

ESPLIN, M. S., FAUSETT, M. B., FAUX, D. S. & GRAVES, S. W. 2003. Changes in the isoforms of the sodium pump in the placenta and myometrium of women in labor. *Am J Obstet Gynecol,* 188**,** 759-64.

ESTIÚ, M. C., FRAILUNA, M. A., OTERO, C., DERICCO, M., WILLIAMSON, C., MARIN, J. J. G. & MACIAS, R. I. R. 2017. Relationship between early onset severe intrahepatic cholestasis of pregnancy and higher risk of meconium-stained fluid. *PLoS One,* 12**,** e0176504.

ESTIÚ, M. C., MONTE, M. J., RIVAS, L., MOIRÓN, M., GOMEZ-RODRIGUEZ, L., RODRIGUEZ-BRAVO, T., MARIN, J. J. & MACIAS, R. I. 2015. Effect of ursodeoxycholic acid treatment on the altered progesterone and bile acid homeostasis in the mother-placenta-foetus trio during cholestasis of pregnancy. *Br J Clin Pharmacol,* 79**,** 316-29.

FAN, X., ZHOU, Q., ZENG, S., ZHOU, J., PENG, Q., ZHANG, M. & DING, Y. 2014. Impaired fetal myocardial deformation in intrahepatic cholestasis of pregnancy. *J Ultrasound Med,* 33**,** 1171-7.

FANG, X., WONG, S. & MITCHELL, B. F. 1996. Relationships among sex steroids, oxytocin, and their receptors in the rat uterus during late gestation and at parturition. *Endocrinology,* 137**,** 3213-9.

FANJUL-BOLADO, P., QUEIPO, P., LAMAS-ARDISANA, P. J. & COSTA-GARCÍA, A. 2007. Manufacture and evaluation of carbon nanotube modified screen-printed electrodes as electrochemical tools. *Talanta,* 74**,** 427-33.

FENG, C., LI, W. J., HE, R. H., SUN, X. W., WANG, G. & WANG, L. Q. 2018. Impacts of different methods of conception on the perinatal outcome of intrahepatic cholestasis of pregnancy in twin pregnancies. *Sci Rep,* 8**,** 3985.

FERGUSON, J. E., GORMAN, J. V., BRUNS, D. E., WEIR, E. C., BURTIS, W. J., MARTIN, T. J. & BRUNS, M. E. 1992. Abundant expression of parathyroid hormone-related protein in human amnion and its association with labor. *Proc Natl Acad Sci U S A,* 89**,** 8384-8.

FERRARIS, R., COLOMBATTI, G., FIORENTINI, M. T., CAROSSO, R., AROSSA, W. & DE LA PIERRE, M. 1983. Diagnostic value of serum bile acids and routine liver function tests in hepatobiliary diseases. Sensitivity, specificity, and predictive value. *Dig Dis Sci,* 28**,** 129-36.

FERREIRA, J. J., BUTLER, A., STEWART, R., GONZALEZ-COTA, A. L., LYBAERT, P., AMAZU, C., REINL, E. L., WAKLE-PRABAGARAN, M., SALKOFF, L., ENGLAND, S. K. & SANTI, C. M. 2019. Oxytocin can regulate myometrial smooth muscle excitability by inhibiting the Na. *J Physiol,* 597**,** 137-149.

FERREIRA, M., COXITO, P. M., SARDÃO, V. A., PALMEIRA, C. M. & OLIVEIRA, P. J. 2005. Bile acids are toxic for isolated cardiac mitochondria: a possible cause for hepatic-derived cardiomyopathies? *Cardiovasc Toxicol,* 5**,** 63-73.

FERRI, T., CAMPANELLA, L. & DE ANGELIS, G. 1984. Differential-pulse polarographic determination of cholic acids. *Analyst,* 109**,** 923-5.

FISK, N. M., BYE, W. B. & STOREY, G. N. 1988. Maternal features of obstetric cholestasis: 20 years experience at King George V Hospital. *Aust N Z J Obstet Gynaecol,* 28**,** 172-6.

FISK, N. M. & STOREY, G. N. 1988. Fetal outcome in obstetric cholestasis. *Br J Obstet Gynaecol,* 95**,** 1137-43.

FLOREANI, A., PATERNOSTER, D., MELIS, A. & GRELLA, P. V. 1996. S-adenosylmethionine versus ursodeoxycholic acid in the treatment of intrahepatic cholestasis of pregnancy: preliminary results of a controlled trial. *Eur J Obstet Gynecol Reprod Biol,* 67**,** 109-13.

FORTUNATI, S., ROZZI, A., CURTI, F., GIANNETTO, M., CORRADINI, R. & CARERI, M. 2019. Single-Walled Carbon Nanotubes as Enhancing Substrates for PNA-Based Amperometric Genosensors. *Sensors (Basel),* 19.

FRIEDLAENDER, P. & OSLER, M. 1967. Icterus and pregnancy. *Am J Obstet Gynecol,* 97**,** 894-900.

FRIEDMAN, D. M., KIM, M. Y., COPEL, J. A., DAVIS, C., PHOON, C. K., GLICKSTEIN, J. S., BUYON, J. P. & INVESTIGATORS, P. 2008. Utility of cardiac monitoring in fetuses at risk for congenital heart block: the PR Interval and Dexamethasone Evaluation (PRIDE) prospective study. *Circulation,* 117**,** 485-93.

FUCHS, A. R., FUCHS, F., HUSSLEIN, P. & SOLOFF, M. S. 1984. Oxytocin receptors in the human uterus during pregnancy and parturition. *Am J Obstet Gynecol,* 150**,** 734-41.

GAO, H., CHEN, L. J., LUO, Q. Q., LIU, X. X., HU, Y., YU, L. L. & ZOU, L. 2014. Effect of cholic acid on fetal cardiac myocytes in intrahepatic choliestasis of pregnancy. *J Huazhong Univ Sci Technolog Med Sci,* 34**,** 736-739.

GAO, L., LU, C., XU, C., TAO, Y., CONG, B. & NI, X. 2008. Differential regulation of prostaglandin production mediated by corticotropin-releasing hormone receptor type 1 and type 2 in cultured human placental trophoblasts. *Endocrinology,* 149**,** 2866-76.

GARFIELD, R. E., HAYASHI, R. H. & HARPER, M. J. 1987. In vitro studies on the control of human myometrial gap junctions. *Int J Gynaecol Obstet,* 25**,** 241-8.

GARFIELD, R. E., SIMS, S. & DANIEL, E. E. 1977. Gap junctions: their presence and necessity in myometrium during parturition. *Science,* 198**,** 958-60.

GEENES, V., CHAMBERS, J., KHURANA, R., SHEMER, E. W., SIA, W., MANDAIR, D., ELIAS, E., MARSCHALL, H. U., HAGUE, W. & WILLIAMSON, C. 2015. Rifampicin in the treatment of severe intrahepatic cholestasis of pregnancy. *Eur J Obstet Gynecol Reprod Biol,* 189**,** 59-63.

GEENES, V., CHAPPELL, L. C., SEED, P. T., STEER, P. J., KNIGHT, M. & WILLIAMSON, C. 2014a. Association of severe intrahepatic cholestasis of pregnancy with adverse pregnancy outcomes: a prospective population-based case-control study. *Hepatology,* 59**,** 1482-91.

GEENES, V., LÖVGREN-SANDBLOM, A., BENTHIN, L., LAWRANCE, D., CHAMBERS, J., GURUNG, V., THORNTON, J., CHAPPELL, L., KHAN, E., DIXON, P., MARSCHALL, H. U. & WILLIAMSON, C. 2014b. The reversed feto-maternal bile acid gradient in intrahepatic cholestasis of pregnancy is corrected by ursodeoxycholic acid. *PLoS One,* 9**,** e83828.

GEENES, V. & WILLIAMSON, C. 2009. Intrahepatic cholestasis of pregnancy. *World J Gastroenterol,* 15**,** 2049-66.

GEENES, V. L., LIM, Y. H., BOWMAN, N., TAILOR, H., DIXON, P. H., CHAMBERS, J., BROWN, L., WYATT-ASHMEAD, J., BHAKOO, K. & WILLIAMSON, C. 2011. A placental phenotype for intrahepatic cholestasis of pregnancy. *Placenta,* 32**,** 1026-32.

GENÇOSMANOĞLU TÜRKMEN, G., VURAL YILMAZ, Z., DAĞLAR, K., KARA, Ö., SANHAL, C. Y., YÜCEL, A. & UYGUR, D. 2018. Low serum vitamin D level is associated with intrahepatic cholestasis of pregnancy. *J Obstet Gynaecol Res,* 44**,** 1712-1718.

GEORGAKILAS, V., PERMAN, J. A., TUCEK, J. & ZBORIL, R. 2015. Broad family of carbon nanoallotropes: classification, chemistry, and applications of fullerenes, carbon dots, nanotubes, graphene, nanodiamonds, and combined superstructures. *Chem Rev,* 115**,** 4744-822.

GEORGIOU, E. X., LEI, K., LAI, P. F., YULIA, A., HERBERT, B. R., CASTELLANOS, M., MAY, S. T., SOORANNA, S. R. & JOHNSON, M. R. 2016. The study of progesterone action in human myometrial explants. *Mol Hum Reprod,* 22**,** 877-89.

GERASIMENKO, J. V., FLOWERDEW, S. E., VORONINA, S. G., SUKHOMLIN, T. K., TEPIKIN, A. V., PETERSEN, O. H. & GERASIMENKO, O. V. 2006. Bile acids induce Ca2+ release from both the endoplasmic reticulum and acidic intracellular calcium stores through activation of inositol trisphosphate receptors and ryanodine receptors. *J Biol Chem,* 281**,** 40154-63.

GERMAIN, A. M., KATO, S., CARVAJAL, J. A., VALENZUELA, G. J., VALDES, G. L. & GLASINOVIC, J. C. 2003. Bile acids increase response and expression of human myometrial oxytocin receptor. *Am J Obstet Gynecol,* 189**,** 577-82.

GHOSH, R. E., BERILD, J. D., STERRANTINO, A. F., TOLEDANO, M. B. & HANSELL, A. L. 2018. Birth weight trends in England and Wales (1986-2012): babies are getting heavier. *Arch Dis Child Fetal Neonatal Ed,* 103**,** F264-F270.

GIMPL, G. & FAHRENHOLZ, F. 2000. Human oxytocin receptors in cholesterol-rich vs. cholesterol-poor microdomains of the plasma membrane. *Eur J Biochem,* 267**,** 2483-97.

GLANTZ, A., MARSCHALL, H. U., LAMMERT, F. & MATTSSON, L. A. 2005. Intrahepatic cholestasis of pregnancy: a randomized controlled trial comparing dexamethasone and ursodeoxycholic acid. *Hepatology,* 42**,** 1399-405.

GLANTZ, A., MARSCHALL, H. U. & MATTSSON, L. A. 2004. Intrahepatic cholestasis of pregnancy: Relationships between bile acid levels and fetal complication rates. *Hepatology,* 40**,** 467-74.

GOLDENBERG, R. L., CULHANE, J. F., IAMS, J. D. & ROMERO, R. 2008. Epidemiology and causes of preterm birth. *Lancet,* 371**,** 75-84.

GOLDSMITH, L. T., WEISS, G., PALEJWALA, S., PLANT, T. M., WOJTCZUK, A., LAMBERT, W. C., AMMUR, N., HELLER, D., SKURNICK, J. H., EDWARDS, D. & COLE, D. M. 2004. Relaxin regulation of endometrial structure and function in the rhesus monkey. *Proc Natl Acad Sci U S A,* 101**,** 4685-9.

GONZALEZ, M. C., REYES, H., ARRESE, M., FIGUEROA, D., LORCA, B., ANDRESEN, M., SEGOVIA, N., MOLINA, C. & ARCE, S. 1989. Intrahepatic cholestasis of pregnancy in twin pregnancies. *J Hepatol,* 9**,** 84-90.

GORELIK, J., HARDING, S. E., SHEVCHUK, A. I., KORALAGE, D., LAB, M., DE SWIET, M., KORCHEV, Y. & WILLIAMSON, C. 2002. Taurocholate induces changes in rat cardiomyocyte contraction and calcium dynamics. *Clin Sci (Lond),* 103**,** 191-200.

GORELIK, J., SHEVCHUK, A. I., DIAKONOV, I., DE SWIET, M., LAB, M., KORCHEV, Y. & WILLIAMSON, C. 2003. Dexamethasone and ursodeoxycholic acid protect against the arrhythmogenic effect of taurocholate in an in vitro study of rat cardiomyocytes. *BJOG,* 110**,** 467-74.

GRAATSMA, E. M., JACOD, B. C., VAN EGMOND, L. A., MULDER, E. J. & VISSER, G. H. 2009. Fetal electrocardiography: feasibility of long-term fetal heart rate recordings. *BJOG,* 116**,** 334-7; discussion 337-8.

GRAF, G. A., YU, L., LI, W. P., GERARD, R., TUMA, P. L., COHEN, J. C. & HOBBS, H. H. 2003. ABCG5 and ABCG8 are obligate heterodimers for protein trafficking and biliary cholesterol excretion. *J Biol Chem,* 278**,** 48275-82.

GREGORY, R. B., HUGHES, R. & BARRITT, G. J. 2004. Induction of cholestasis in the perfused rat liver by 2-aminoethyl diphenylborate, an inhibitor of the hepatocyte plasma membrane Ca2+ channels. *J Gastroenterol Hepatol,* 19**,** 1128-34.

GRIESHABER, D., MACKENZIE, R., VÖRÖS, J. & REIMHULT, E. 2008. Electrochemical Biosensors - Sensor Principles and Architectures. *Sensors (Basel),* 8**,** 1400-1458.

GRUSZCZYNSKA-LOSY, M., WENDER-OZEGOWSKA, E., WIRSTLEIN, P. & SZCZEPANSKA, M. 2019. Assessment of selected parameters of placental microstructure in patients with intrahepatic cholestasis of pregnancy. *Ginekol Pol,* 90**,** 452-457.

GUARINO, M. P., CONG, P., CICALA, M., ALLONI, R., CAROTTI, S. & BEHAR, J. 2007. Ursodeoxycholic acid improves muscle contractility and inflammation in symptomatic gallbladders with cholesterol gallstones. *Gut,* 56**,** 815-20.

GURUNG, V., MIDDLETON, P., MILAN, S. J., HAGUE, W. & THORNTON, J. G. 2013. Interventions for treating cholestasis in pregnancy. *Cochrane Database Syst Rev***,** CD000493.

GÄLMAN, C., ANGELIN, B. & RUDLING, M. 2005. Bile acid synthesis in humans has a rapid diurnal variation that is asynchronous with cholesterol synthesis. *Gastroenterology,* 129**,** 1445-53.

GÜNAYDIN, B., BAYRAM, M., ALTUĞ, M., CEVHER, S. & BOZKURT, N. 2017. Retrospective analysis of maternal, fetal, and neonatal outcomesof intrahepatic cholestasis of pregnancy at Gazi University. *Turk J Med Sci,* 47**,** 583-586.

HAAS, D. M., IMPERIALE, T. F., KIRKPATRICK, P. R., KLEIN, R. W., ZOLLINGER, T. W. & GOLICHOWSKI, A. M. 2009. Tocolytic therapy: a meta-analysis and decision analysis. *Obstet Gynecol,* 113**,** 585-94.

HAGEN, B. M., BOYMAN, L., KAO, J. P. & LEDERER, W. J. 2012. A comparative assessment of fluo Ca2+ indicators in rat ventricular myocytes. *Cell Calcium,* 52**,** 170-81.

HANAFI, N. I., MOHAMED, A. S., MD NOOR, J., ABDU, N., HASANI, H., SIRAN, R., OSMAN, N. J., AB RAHIM, S. & SHEIKH ABDUL KADIR, S. H. 2016. Ursodeoxycholic acid upregulates ERK and Akt in the protection of cardiomyocytes against CoCl2. *Genet Mol Res,* 15.

HARDY, D. B., JANOWSKI, B. A., COREY, D. R. & MENDELSON, C. R. 2006. Progesterone receptor plays a major antiinflammatory role in human myometrial cells by

antagonism of nuclear factor-kappaB activation of cyclooxygenase 2 expression. *Mol Endocrinol,* 20**,** 2724-33.

HE, P., WANG, F., JIANG, Y., ZHONG, Y., LAN, Y. & CHEN, S. 2014. Placental proteome alterations in women with intrahepatic cholestasis of pregnancy. *Int J Gynaecol Obstet,* 126**,** 256-9.

HEIDARI KANI, M., CHAN, E. C., YOUNG, R. C., BUTLER, T., SMITH, R. & PAUL, J. W. 2017. 3D Cell Culturing and Possibilities for Myometrial Tissue Engineering. *Ann Biomed Eng,* 45**,** 1746-1757.

HEINONEN, S. & KIRKINEN, P. 1999. Pregnancy outcome with intrahepatic cholestasis. *Obstet Gynecol,* 94**,** 189-93.

HENRY, A. & WELSH, A. W. 2015. Monitoring intrahepatic cholestasis of pregnancy using the fetal myocardial performance index: a cohort study. *Ultrasound Obstet Gynecol,* 46**,** 571-8.

HERRERA, C. A., MANUCK, T. A., STODDARD, G. J., VARNER, M. W., ESPLIN, S., CLARK, E. A. S., SILVER, R. M. & ELLER, A. G. 2018. Perinatal outcomes associated with intrahepatic cholestasis of pregnancy. *J Matern Fetal Neonatal Med,* 31**,** 1913-1920.

HEUMAN, D. M. 1989. Quantitative estimation of the hydrophilic-hydrophobic balance of mixed bile salt solutions. *J Lipid Res,* 30**,** 719-30.

HIKASA, Y., TANIDA, N., SAWADA, K., FURUKAWA, K., KANO, M. & SHIMOYAMA, T. 1989. Effects of 5 beta-chol-3-en-24-oic acid, and lithocholic acid and its sulfates on prostaglandin E2 output in perfusion of the rat colon. *Gastroenterol Jpn,* 24**,** 16-21.

HOFMANN, A. F. 1999. The continuing importance of bile acids in liver and intestinal disease. *Arch Intern Med,* 159**,** 2647-58.

HU, J., LIU, L., GONG, Y., ZHANG, L., GAN, X., LUO, X., YU, T., ZHONG, X., DENG, X., HU, L., ZHANG, Z. & DONG, X. 2018. Linc02527 promoted autophagy in Intrahepatic cholestasis of pregnancy. *Cell Death Dis,* 9**,** 979.

HU, L. D., YU, B. P. & YANG, B. 2012. Deoxycholic acid inhibits smooth muscle contraction via protein kinase C-dependent modulation of L-type Ca2+ channels in rat proximal colon. *Mol Med Rep,* 6**,** 833-7.

HU, Y. Y., LIU, J. C. & XING, A. Y. 2015. Oxidative stress markers in intrahepatic cholestasis of pregnancy: a prospective controlled study. *Eur Rev Med Pharmacol Sci,* 19**,** 3181-6.

HUANG, J. L., WEN, Z. C., LEE, W. L., CHANG, M. S. & CHEN, S. A. 1998. Changes of autonomic tone before the onset of paroxysmal atrial fibrillation. *Int J Cardiol,* 66**,** 275-83.

HUANG, R., HUANG, Y., ZENG, G., LI, M. & JIN, Y. 2020. Ursodeoxycholic acid inhibits intimal hyperplasia, vascular smooth muscle cell excessive proliferation, migration via blocking miR-21/PTEN/AKT/mTOR signaling pathway. *Cell Cycle,* 19**,** 918-932.

HUIKURI, H. V., MÄKIKALLIO, T. H. & PERKIÖMÄKI, J. 2003. Measurement of heart rate variability by methods based on nonlinear dynamics. *J Electrocardiol,* 36 Suppl**,** 95-9.

HUSAIN, S. Z., ORABI, A. I., MUILI, K. A., LUO, Y., SARWAR, S., MAHMOOD, S. M., WANG, D., CHOO-WING, R., SINGH, V. P., PARNESS, J., ANANTHANARAVANAN, M., BHANDARI, V. & PERIDES, G. 2012. Ryanodine receptors contribute to bile acid-induced pathological calcium signaling and pancreatitis in mice. *Am J Physiol Gastrointest Liver Physiol,* 302**,** G1423-33.

HÄMÄLÄINEN, S. T., TURUNEN, K., MATTILA, K. J., KOSUNEN, E. & SUMANEN, M. 2019. Intrahepatic cholestasis of pregnancy and comorbidity: A 44-year follow-up study. *Acta Obstet Gynecol Scand,* 98**,** 1534-1539.

IBRAHIM, E., DIAKONOV, I., ARUNTHAVARAJAH, D., SWIFT, T., GOODWIN, M., MCILVRIDE, S., NIKOLOVA, V., WILLIAMSON, C. & GORELIK, J. 2018. Bile acids and their respective conjugates elicit different responses in neonatal cardiomyocytes: role of Gi protein, muscarinic receptors and TGR5. *Sci Rep,* 8**,** 7110.

IKEGAMI, T., MATSUZAKI, Y., SHODA, J., KANO, M., HIRABAYASHI, N. & TANAKA, N. 1998. The chemopreventive role of ursodeoxycholic acid in azoxymethane-treated rats: suppressive effects on enhanced group II phospholipase A2 expression in colonic tissue. *Cancer Lett,* 134**,** 129-39.

ILICIC, M., BUTLER, T., ZAKAR, T. & PAUL, J. W. 2017. The expression of genes involved in myometrial contractility changes during ex situ culture of pregnant human uterine smooth muscle tissue. *J Smooth Muscle Res,* 53**,** 73-89.

INAGAKI, N., GONOI, T., CLEMENT, J. P., WANG, C. Z., AGUILAR-BRYAN, L., BRYAN, J. & SEINO, S. 1996. A family of sulfonylurea receptors determines the pharmacological properties of ATP-sensitive K+ channels. *Neuron,* 16**,** 1011-7.

ISRAEL, E. J., GUZMAN, M. L. & CAMPOS, G. A. 1986. Maximal response to oxytocin of the isolated myometrium from pregnant patients with intrahepatic cholestasis. *Acta Obstet Gynecol Scand,* 65**,** 581-2.

IWAHASHI, M., MURAGAKI, Y., OOSHIMA, A. & UMESAKI, N. 2003. Decreased type I collagen expression in human uterine cervix during pregnancy. *J Clin Endocrinol Metab,* 88**,** 2231-5.

JAIN, R., SURI, V., CHOPRA, S., CHAWLA, Y. K. & KOHLI, K. K. 2013. Obstetric cholestasis: outcome with active management. *J Obstet Gynaecol Res,* 39**,** 953-9.

JAIN, U., LAI, C. W., XIONG, S., GOODWIN, V. M., LU, Q., MUEGGE, B. D., CHRISTOPHI, G. P., VANDUSSEN, K. L., CUMMINGS, B. P., YOUNG, E., HAMBOR, J. & STAPPENBECK, T. S. 2018. Temporal Regulation of the Bacterial Metabolite Deoxycholate during Colonic Repair Is Critical for Crypt Regeneration. *Cell Host Microbe,* 24**,** 353-363.e5.

JANEGITZ, B. C., CANCINO, J. & ZUCOLOTTO, V. 2014. Disposable biosensors for clinical diagnosis. *J Nanosci Nanotechnol,* 14**,** 378-89.

JENKIN, G. 1992. Oxytocin and prostaglandin interactions in pregnancy and at parturition. *J Reprod Fertil Suppl,* 45**,** 97-111.

JIA, W., BANDODKAR, A. J., VALDÉS-RAMÍREZ, G., WINDMILLER, J. R., YANG, Z., RAMÍREZ, J., CHAN, G. & WANG, J. 2013. Electrochemical tattoo biosensors for real-time noninvasive lactate monitoring in human perspiration. *Anal Chem,* 85**,** 6553-60.

JIN, J., PAN, S. L., HUANG, L. P., YU, Y. H., ZHONG, M. & ZHANG, G. W. 2015. Risk factors for adverse fetal outcomes among women with early- versus late-onset intrahepatic cholestasis of pregnancy. *Int J Gynaecol Obstet,* 128**,** 236-40.

JMARI, K., MIRONNEAU, C. & MIRONNEAU, J. 1986. Inactivation of calcium channel current in rat uterine smooth muscle: evidence for calcium- and voltage-mediated mechanisms. *J Physiol,* 380**,** 111-26.

JOHNSTON, W. G. & BASKETT, T. F. 1979. Obstetric cholestasis. A 14 year review. *Am J Obstet Gynecol,* 133**,** 299-301.

JONES, K., SHMYGOL, A., KUPITTAYANANT, S. & WRAY, S. 2004. Electrophysiological characterization and functional importance of calcium-activated chloride channel in rat uterine myocytes. *Pflugers Arch,* 448**,** 36-43.

JOUBERT, P. 1978. Cholic acid and the heart: in vitro studies of the effect on heart rate and myocardial contractility in the rat. *Clin Exp Pharmacol Physiol,* 5**,** 9-16.

JOUTSINIEMI, T., EKBLAD, U., ROSÉN, K. G. & TIMONEN, S. 2019. Waveform analysis of the fetal ECG in labor in patients with intrahepatic cholestasis of pregnancy. *J Obstet Gynaecol Res,* 45**,** 306-312.

JOUTSINIEMI, T., TIMONEN, S., LINDEN, M., SUVITIE, P. & EKBLAD, U. 2015. Intrahepatic cholestasis of pregnancy: observational study of the treatment with low-dose ursodeoxycholic acid. *BMC Gastroenterol,* 15**,** 92.

JURATE, K., RIMANTAS, Z., JOLANTA, S., VLADAS, G. & LIMAS, K. 2017. Sensitivity and Specificity of Biochemical Tests for Diagnosis of Intrahepatic Cholestasis of Pregnancy. *Ann Hepatol,* 16**,** 569-573.

KADRIYE, Y., DOĞA, Ö., MERVE, Ö., FILIZ HALICI, Ö., YÜKSEL, O. & ŞEVKI, Ç. 2019. Assessment of Mechanical Fetal PR Interval in Intrahepatic Cholestasis of Pregnancy and Its Relationship with the Severity of the Disease. *Am J Perinatol*.

KANO, M., SHODA, J., IRIMURA, T., UEDA, T., IWASAKI, R., URASAKI, T., KAWAUCHI, Y., ASANO, T., MATSUZAKI, Y. & TANAKA, N. 1998. Effects of long-term ursodeoxycholate administration on expression levels of secretory low-molecular-weight phospholipases A2 and mucin genes in gallbladders and biliary composition in patients with multiple cholesterol stones. *Hepatology,* 28**,** 302-13.

KAPLOWITZ, N., KOK, E. & JAVITT, N. B. 1973. Postprandial serum bile acid for the detection of hepatobiliary disease. *JAMA,* 225**,** 292-3.

KAUPPILA, A., KIVELÄ, A., KONTULA, K. & TUIMALA, R. 1980. Serum progesterone, estradiol, and estriol before and during induced labor. *Am J Obstet Gynecol,* 137**,** 462-6.

KAUR, B. S. & TRIADAFILOPOULOS, G. 2002. Acid- and bile-induced PGE(2) release and hyperproliferation in Barrett's esophagus are COX-2 and PKC-epsilon dependent. *Am J Physiol Gastrointest Liver Physiol,* 283**,** G327-34.

KAWABE, A., SHIMADA, Y., SOMA, T., MAEDA, M., ITAMI, A., KAGANOI, J., KIYONO, T. & IMAMURA, M. 2004. Production of prostaglandinE2 via bile acid is enhanced by trypsin and acid in normal human esophageal epithelial cells. *Life Sci,* 75**,** 21-34.

KAWAKITA, T., PARIKH, L. I., RAMSEY, P. S., HUANG, C. C., ZEYMO, A., FERNANDEZ, M., SMITH, S. & IQBAL, S. N. 2015. Predictors of adverse neonatal outcomes in intrahepatic cholestasis of pregnancy. *Am J Obstet Gynecol,* 213**,** 570.e1-8.

KEBAPCILAR, A. G., KEBAPCILAR, L., TANER, C. E., BOZKAYA, G., SAHIN, G. & GOKULU, S. G. 2010a. Is increased maternal endothelin-1 concentration associated with neonatal asphyxia and preterm delivery in intrahepatic cholestasis of pregnancy? *Arch Gynecol Obstet,* 282**,** 617-21.

KEBAPCILAR, A. G., TANER, C. E., KEBAPCILAR, L. & BOZKAYA, G. 2010b. High mean platelet volume, low-grade systemic coagulation, and fibrinolytic activation are associated with pre-term delivery and low APGAR score in intrahepatic cholestasis of pregnancy. *J Matern Fetal Neonatal Med,* 23**,** 1205-10.

KEELAN, J. A. 2018. Intrauterine inflammatory activation, functional progesterone withdrawal, and the timing of term and preterm birth. *J Reprod Immunol,* 125**,** 89-99.

KELLY, R. W. 2002. Inflammatory mediators and cervical ripening. *J Reprod Immunol,* 57**,** 217-24.

KEMPLER, P., VÁRADI, A., KÁDAR, E. & SZALAY, F. 1994. Autonomic and peripheral neuropathy in primary biliary cirrhosis: evidence of small sensory fibre damage and prolongation of the QT interval. *J Hepatol,* 21**,** 1150-1.

KHAN, R. N., SMITH, S. K., MORRISON, J. J. & ASHFORD, M. L. 1997. Ca2+ dependence and pharmacology of large-conductance K+ channels in nonlabor and labor human uterine myocytes. *Am J Physiol,* 273**,** C1721-31.

KILARSKI, W. M., DUPONT, E., COPPEN, S., YEH, H. I., VOZZI, C., GOURDIE, R. G., REZAPOUR, M., ULMSTEN, U., ROOMANS, G. M. & SEVERS, N. J. 1998. Identification of two further gap-junctional proteins, connexin40 and connexin45, in human myometrial smooth muscle cells at term. *Eur J Cell Biol,* 75**,** 1-8.

KIM, D. M., KIM, M. Y., REDDY, S. S., CHO, J., CHO, C. H., JUNG, S. & SHIM, Y. B. 2013. Electron-transfer mediator for a NAD-glucose dehydrogenase-based glucose sensor. *Anal Chem,* 85**,** 11643-9.

KIM, J. Y., KIM, K. H., LEE, J. A., NAMKUNG, W., SUN, A. Q., ANANTHANARAYANAN, M., SUCHY, F. J., SHIN, D. M., MUALLEM, S. & LEE, M. G. 2002. Transporter-mediated bile acid uptake causes Ca2+-dependent cell death in rat pancreatic acinar cells. *Gastroenterology,* 122**,** 1941-53.

KIM, N. H., PARK, J. H., PARK, J. S. & JOUNG, Y. H. 2017. The Effect of Deoxycholic Acid on Secretion and Motility in the Rat and Guinea Pig Large Intestine. *J Neurogastroenterol Motil,* 23**,** 606-615.

KIMURA, T., TANIZAWA, O., MORI, K., BROWNSTEIN, M. J. & OKAYAMA, H. 1992. Structure and expression of a human oxytocin receptor. *Nature,* 356**,** 526-9.

KIRBAS, A., BIBEROGLU, E., DAGLAR, K., İSKENDER, C., ERKAYA, S., DEDE, H., UYGUR, D. & DANISMAN, N. 2014. Neutrophil-to-lymphocyte ratio as a diagnostic marker of intrahepatic cholestasis of pregnancy. *Eur J Obstet Gynecol Reprod Biol,* 180**,** 12-5.

KIRBAS, A., BIBEROGLU, E., ERSOY, A. O., DIKMEN, A. U., KOCA, C., ERDINC, S., UYGUR, D., CAGLAR, T. & BIBEROGLU, K. 2016. The role of interleukin-17 in intrahepatic cholestasis of pregnancy. *J Matern Fetal Neonatal Med,* 29**,** 977-81.

KIRBAS, O., BIBEROGLU, E. H., KIRBAS, A., DAGLAR, K., KURMUS, O., DANISMAN, N. & BIBEROGLU, K. 2015. Evaluation of ventricular repolarization in pregnant women with intrahepatic cholestasis. *Int J Cardiol,* 189**,** 25-9.

KISHORE, A. H., LIANG, H., KANCHWALA, M., XING, C., GANESH, T., AKGUL, Y., POSNER, B., READY, J. M., MARKOWITZ, S. D. & WORD, R. A. 2017. Prostaglandin dehydrogenase is a target for successful induction of cervical ripening. *Proc Natl Acad Sci U S A,* 114**,** E6427-E6436.

KISSINGER, P. T. 2005. Biosensors-a perspective. *Biosens Bioelectron,* 20**,** 2512-6.

KITAZAWA, T., ETO, M., WOODSOME, T. P. & BRAUTIGAN, D. L. 2000. Agonists trigger G protein-mediated activation of the CPI-17 inhibitor phosphoprotein of myosin light chain phosphatase to enhance vascular smooth muscle contractility. *J Biol Chem,* 275**,** 9897-900.

KLOUDA, J., BAREK, J., KOCOVSKY, P., HERL, T., MATYSIK, F.-M., NESMERAK, K. & SCHWARZOVA-PECKOVA, K. 2018. B ile acids: Electrochemical oxidation on bare electrodes after acid-induced dehydration. *Electrochemistry Communications,* 86**,** 99-103.

KNOCK, G. A., TRIBE, R. M., HASSONI, A. A. & AARONSON, P. I. 2001. Modulation of potassium current characteristics in human myometrial smooth muscle by 17beta-estradiol and progesterone. *Biol Reprod,* 64**,** 1526-34.

KOIDE, S., ITO, N. & KARUBE, I. 2007. Development of a micro-planar amperometric bile acid biosensor for urinalysis. *Biosens Bioelectron,* 22**,** 2079-85.

KOIVUROVA, S., HARTIKAINEN, A. L., KARINEN, L., GISSLER, M., HEMMINKI, E., MARTIKAINEN, H., TUOMIVAARA, L. & JÄRVELIN, M. R. 2002. The course of pregnancy and delivery and the use of maternal healthcare services after standard IVF in Northern Finland 1990-1995. *Hum Reprod,* 17**,** 2897-903.

KOMURA, T., NIU, G., YAMAGUCHI, T., ASANO, M. & MATSUDA, A. 2004. Coupled Electron-Proton Transport in Electropolymerized Methylene Blue and the Influences of Its Protonation Level on the Rate of Electron Exchange with β-Nicotinamide Adenine Dinucleotide. *Electroanalysis: An International Journal Devoted to Fundamental and Practical Aspects of Electroanalysis,* 16**,** 1791-1800.

KONDRACKIENE, J., BEUERS, U. & KUPCINSKAS, L. 2005. Efficacy and safety of ursodeoxycholic acid versus cholestyramine in intrahepatic cholestasis of pregnancy. *Gastroenterology,* 129**,** 894-901.

KONG, X., KONG, Y., ZHANG, F., WANG, T. & ZHU, X. 2018. Expression and significance of dendritic cells and Th17/Treg in serum and placental tissues of patients with intrahepatic cholestasis of pregnancy. *J Matern Fetal Neonatal Med,* 31**,** 901-906.

KREEK, M. J., WESER, E., SLEISENGER, M. H. & JEFFRIES, G. H. 1967. Idiopathic cholestasis of pregnancy. The response to challenge with the synthetic estrogen, ethinyl estradiol. *N Engl J Med,* 277**,** 1391-5.

KULLAK-UBLICK, G. A., STIEGER, B., HAGENBUCH, B. & MEIER, P. J. 2000. Hepatic transport of bile salts. *Semin Liver Dis,* 20**,** 273-92.

KUMAGAI, M., KIMURA, A., TAKEI, H., KUROSAWA, T., AOKI, K., INOKUCHI, T. & MATSUISHI, T. 2007. Perinatal bile acid metabolism: bile acid analysis of meconium of preterm and full-term infants. *J Gastroenterol,* 42**,** 904-10.

KUMAR, D. P., RAJAGOPAL, S., MAHAVADI, S., MIRSHAHI, F., GRIDER, J. R., MURTHY, K. S. & SANYAL, A. J. 2012. Activation of transmembrane bile acid receptor TGR5 stimulates insulin secretion in pancreatic β cells. *Biochem Biophys Res Commun,* 427**,** 600-5.

KUMAR, S., AHLAWAT, W., KUMAR, R. & DILBAGHI, N. 2015. Graphene, carbon nanotubes, zinc oxide and gold as elite nanomaterials for fabrication of biosensors for healthcare. *Biosens Bioelectron,* 70**,** 498-503.

KUMAR, S. A. & CHEN, S. M. 2008. Electroanalysis of NADH Using Conducting and Redox Active Polymer/Carbon Nanotubes Modified Electrodes-A Review. *Sensors (Basel),* 8**,** 739-766.

LAATIKAINEN, T. 1978. Postprandial serum bile acids in cholestasis of pregnancy. *Ann Clin Res,* 10**,** 307-12.

LAATIKAINEN, T. & IKONEN, E. 1977. Serum bile acids in cholestasis of pregnancy. *Obstet Gynecol,* 50**,** 313-8.

LAATIKAINEN, T. & TULENHEIMO, A. 1984. Maternal serum bile acid levels and fetal distress in cholestasis of pregnancy. *Int J Gynaecol Obstet,* 22**,** 91-4.

LAATIKAINEN, T. J. 1975. Fetal bile acid levels in pregnancies complicated by maternal intrahepatic cholestasis. *Am J Obstet Gynecol,* 122**,** 852-6.

LAUDANSKI, P., CHARKIEWICZ, K., KISIELEWSKI, R., KUC, P., KOC-ZORAWSKA, E., RABA, G., KRACZKOWSKI, J., DYMICKA-PIEKARSKA, V., CHABOWSKI, A., KACEROVSKY, M., JACOBSSON, B., ZABIELSKI, P. & BLACHNIO-ZABIELSKA, A. 2016. Plasma C16-Cer levels are increased in patients with preterm labor. *Prostaglandins Other Lipid Mediat,* 123**,** 40-5.

LAURENCE, B. H. & SIMMONDS, W. J. 1963. The Effect Of Bile Salts On Contraction Of Visceral Smooth Muscle. *Aust J Exp Biol Med Sci,* 41**,** 343-8.

LAWRANCE, D., WILLIAMSON, C., BOUTELLE, M. & CASS, A. 2015. Development of a disposable bile acid biosensor for use in the management of cholestasis. *Journal of Analytical Methods***,** 3714-3719.

LEBLANC, N., LEDOUX, J., SALEH, S., SANGUINETTI, A., ANGERMANN, J., O'DRISCOLL, K., BRITTON, F., PERRINO, B. A. & GREENWOOD, I. A. 2005. Regulation of calcium-activated chloride channels in smooth muscle cells: a complex picture is emerging. *Can J Physiol Pharmacol,* 83**,** 541-56.

LEE, H. B., MEESEEPONG, M., TRUNG, T. Q., KIM, B. Y. & LEE, N. E. 2020. A wearable lab-on-a-patch platform with stretchable nanostructured biosensor for non-invasive immunodetection of biomarker in sweat. *Biosens Bioelectron,* 156**,** 112133.

LEE, R. H., INCERPI, M. H., MILLER, D. A., PATHAK, B. & GOODWIN, T. M. 2009. Sudden fetal death in intrahepatic cholestasis of pregnancy. *Obstet Gynecol,* 113**,** 528-31.

LEE, R. H., KWOK, K. M., INGLES, S., WILSON, M. L., MULLIN, P., INCERPI, M., PATHAK, B. & GOODWIN, T. M. 2008. Pregnancy outcomes during an era of aggressive management for intrahepatic cholestasis of pregnancy. *Am J Perinatol,* 25**,** 341-5.

LEE, W. S., NGO-ANH, T. J., BRUENING-WRIGHT, A., MAYLIE, J. & ADELMAN, J. P. 2003. Small conductance Ca2+-activated K+ channels and calmodulin: cell surface expression and gating. *J Biol Chem,* 278**,** 25940-6.

LEE, W. Y., HAN, S. H., CHO, T. S., YOO, Y. H. & LEE, S. M. 1999. Effect of ursodeoxycholic acid on ischemia/reperfusion injury in isolated rat heart. *Arch Pharm Res,* 22**,** 479-84.

LI, L., CHEN, W., MA, L., LIU, Z. B., LU, X., GAO, X. X., LIU, Y., WANG, H., ZHAO, M., LI, X. L., CONG, L., XU, X. & CHEN, Y. H. 2020. Continuous association of total bile acid levels with the risk of small for gestational age infants. *Sci Rep,* 10**,** 9257.

LI, X., HAN, K. Q., SHI, Y. N., MEN, S. Z., LI, S., SUN, M. H., DONG, H., LU, J. J., MA, L. J., ZHAO, M., LI, D. & LIU, W. 2017. [Effects and mechanisms of ursodeoxycholic acid on isoprenaline-Induced myocardial fibrosis in mice]. *Zhonghua Yi Xue Za Zhi,* 97**,** 387-391.

LI, Y., HE, J., CHEN, J., NIU, Y., ZHAO, Y., ZHANG, Y. & YU, C. 2018. A dual-type responsive electrochemical immunosensor for quantitative detection of PCSK9 based on n-C. *Biosens Bioelectron,* 101**,** 7-13.

LIN, J., GU, W. & HOU, Y. 2019. Diagnosis and prognosis of early-onset intrahepatic cholestasis of pregnancy: a prospective study. *J Matern Fetal Neonatal Med,* 32**,** 997-1003.

LING, B., YAO, F., ZHOU, Y., CHEN, Z., SHEN, G. & ZHU, Y. 2007. Cell-mediated immunity imbalance in patients with intrahepatic cholestasis of pregnancy. *Cell Mol Immunol,* 4**,** 71-5.

LIONG, S. & LAPPAS, M. 2014. Endoplasmic reticulum stress is increased after spontaneous labor in human fetal membranes and myometrium where it regulates the expression of prolabor mediators. *Biol Reprod,* 91**,** 70.

LIU, C. C. 2012. Electrochemical based biosensors. *Biosensors (Basel),* 2**,** 269-72.

LIU, J., MURRAY, A. M., MANKUS, E. B., IRELAND, K. E., ACOSTA, O. M. & RAMSEY, P. S. 2018. Adjuvant Use of Rifampin for Refractory Intrahepatic Cholestasis of Pregnancy. *Obstet Gynecol,* 132**,** 678-681.

LIU, K. K., WU, R. G., CHUANG, Y. J., KHOO, H. S., HUANG, S. H. & TSENG, F. G. 2010. Microfluidic systems for biosensing. *Sensors (Basel),* 10**,** 6623-61.

LO, J. O., SHAFFER, B. L., ALLEN, A. J., LITTLE, S. E., CHENG, Y. W. & CAUGHEY, A. B. 2015. Intrahepatic cholestasis of pregnancy and timing of delivery. *J Matern Fetal Neonatal Med,* 28**,** 2254-8.

LOFTHOUSE, E. M., TORRENS, C., MANOUSOPOULOU, A., NAHAR, M., CLEAL, J. K., O'KELLY, I. M., SENGERS, B. G., GARBIS, S. D. & LEWIS, R. M. 2019. Ursodeoxycholic acid inhibits uptake and vasoconstrictor effects of taurocholate in human placenta. *FASEB J,* 33**,** 8211-8220.

LOMBARDI, F., TARRICONE, D., TUNDO, F., COLOMBO, F., BELLETTI, S. & FIORENTINI, C. 2004. Autonomic nervous system and paroxysmal atrial fibrillation: a study based on the analysis of RR interval changes before, during and after paroxysmal atrial fibrillation. *Eur Heart J,* 25**,** 1242-8.

LONGO, M., JAIN, V., VEDERNIKOV, Y. P., HANKINS, G. D., GARFIELD, R. E. & SAADE, G. R. 2003. Effects of L-type Ca(2+)-channel blockade, K(+)(ATP)-channel opening and nitric oxide on human uterine contractility in relation to gestational age and labour. *Mol Hum Reprod,* 9**,** 159-64.

LOUDON, J. A., ELLIOTT, C. L., HILLS, F. & BENNETT, P. R. 2003. Progesterone represses interleukin-8 and cyclo-oxygenase-2 in human lower segment fibroblast cells and amnion epithelial cells. *Biol Reprod,* 69**,** 331-7.

LUCCHINI, M., WAPNER, R. J., CHIA-LING, N. C., TORRES, C., YANG, J., WILLIAMS, I. A. & FIFER, W. P. 2020. Effects of maternal sleep position on fetal and maternal heart rate patterns using overnight home fetal ECG recordings. *Int J Gynaecol Obstet*.

LUCKAS, M. J., TAGGART, M. J. & WRAY, S. 1999. Intracellular calcium stores and agonist-induced contractions in isolated human myometrium. *Am J Obstet Gynecol,* 181**,** 468-76.

LUCKAS, M. J. & WRAY, S. 2000. A comparison of the contractile properties of human myometrium obtained from the upper and lower uterine segments. *BJOG,* 107**,** 1309-11.

LUDVIGSSON, J. F., BERGQUIST, A., MONTGOMERY, S. M. & BAHMANYAR, S. 2014. Risk of diabetes and cardiovascular disease in patients with primary sclerosing cholangitis. *J Hepatol,* 60**,** 802-8.

LUKA, G., AHMADI, A., NAJJARAN, H., ALOCILJA, E., DEROSA, M., WOLTHERS, K., MALKI, A., AZIZ, H., ALTHANI, A. & HOORFAR, M. 2015. Microfluidics Integrated Biosensors: A Leading Technology towards Lab-on-a-Chip and Sensing Applications. *Sensors (Basel),* 15**,** 30011-31.

LUKIVSKAYA, O. Y., MASKEVICH, A. A. & BUKO, V. U. 2001. Effect of ursodeoxycholic acid on prostaglandin metabolism and microsomal membranes in alcoholic fatty liver. *Alcohol,* 25**,** 99-105.

LUNZER, M., BARNES, P., BYTH, K. & O'HALLORAN, M. 1986. Serum bile acid concentrations during pregnancy and their relationship to obstetric cholestasis. *Gastroenterology,* 91**,** 825-9.

LUO, L., AUBRECHT, J., LI, D., WARNER, R. L., JOHNSON, K. J., KENNY, J. & COLANGELO, J. L. 2018. Assessment of serum bile acid profiles as biomarkers of liver injury and liver disease in humans. *PLoS One,* 13**,** e0193824.

LYE, S., OU, C., TEOH, T., ERB, G., STEVENS, Y., CASPER, R. & CHALLIS, J. 1998. The molecular basis of labour and tocolysis. *Fetal and Maternal Medicine Review,* 10 (3)**,** 121-136.

LYE, S. J. & CHALLIS, J. R. 1982. Inhibition by PGI-2 of myometrial activity in vivo in non-pregnant ovariectomized sheep. *J Reprod Fertil,* 66**,** 311-5.

LYE, S. J., MITCHELL, J., NASHMAN, N., OLDENHOF, A., OU, R., SHYNLOVA, O. & LANGILLE, L. 2001. Role of mechanical signals in the onset of term and preterm labor. *Front Horm Res,* 27**,** 165-78.

LÓPEZ BERNAL, A., RIVERA, J., EUROPE-FINNER, G. N., PHANEUF, S. & ASBÓTH, G. 1995. Parturition: activation of stimulatory pathways or loss of uterine quiescence? *Adv Exp Med Biol,* 395**,** 435-51.

MACIAS, R. I., MARIN, J. J. & SERRANO, M. A. 2009. Excretion of biliary compounds during intrauterine life. *World J Gastroenterol,* 15**,** 817-28.

MACKENZIE, L. W., WORD, R. A., CASEY, M. L. & STULL, J. T. 1990. Myosin light chain phosphorylation in human myometrial smooth muscle cells. *Am J Physiol,* 258**,** C92-8.

MACLENNAN, A. H. & GRANT, P. 1991. Human relaxin. In vitro response of human and pig myometrium. *J Reprod Med,* 36**,** 630-4.

MACLENNAN, A. H., GRANT, P. & BORTHWICK, A. C. 1991. Relaxin and relaxin c-peptide levels in human reproductive tissues. *Reprod Fertil Dev,* 3**,** 577-83.

MADAZLI, R., YUKSEL, M. A., ONCUL, M., TUTEN, A., GURALP, O. & AYDIN, B. 2015. Pregnancy outcomes and prognostic factors in patients with intrahepatic cholestasis of pregnancy. *J Obstet Gynaecol,* 35**,** 358-61.

MAEDA, K., KIMURA, A., YAMATO, Y. & MATSUISHI, T. 2003. Perinatal bile acid metabolism: analysis of urinary unsaturated ketonic bile acids in preterm and full-term infants. *Acta Paediatr,* 92**,** 216-20.

MAIGAARD, S., FORMAN, A., BROGAARD-HANSEN, K. P. & ANDERSSON, K. E. 1986. Inhibitory effects of nitrendipine on myometrial and vascular smooth muscle in human pregnant uterus and placenta. *Acta Pharmacol Toxicol (Copenh),* 59**,** 1-10.

MAKIEVA, S., HUTCHINSON, L. J., RAJAGOPAL, S. P., RINALDI, S. F., BROWN, P., SAUNDERS, P. T. & NORMAN, J. E. 2016. Androgen-Induced Relaxation of Uterine Myocytes Is Mediated by Blockade of Both Ca(2+) Flux and MLC Phosphorylation. *J Clin Endocrinol Metab,* 101**,** 1055-65.

MALHOTRA, B. D. & CHAUBEY, A. 2003. Biosensors for clinical diagnostics industry. *Sensors and Actuators B: Chemical,* 91**,** 117-127.

MALIK, M. & CATHERINO, W. H. 2012. Development and validation of a three-dimensional in vitro model for uterine leiomyoma and patient-matched myometrium. *Fertil Steril,* 97**,** 1287-93.

MANNA, L. B., OVADIA, C., LÖVGREN-SANDBLOM, A., CHAMBERS, J., BEGUM, S., SEED, P., WALKER, I., CHAPPELL, L. C., MARSCHALL, H. U. & WILLIAMSON, C. 2019. Enzymatic quantification of total serum bile acids as a monitoring strategy for women with intrahepatic cholestasis of pregnancy receiving ursodeoxycholic acid treatment: a cohort study. *BJOG,* 126**,** 1633-1640.

MANZOTTI, C., CASAZZA, G., STIMAC, T., NIKOLOVA, D. & GLUUD, C. 2019. Total serum bile acids or serum bile acid profile, or both, for the diagnosis of intrahepatic cholestasis of pregnancy. *Cochrane Database Syst Rev,* 7**,** CD012546.

MARIN, J. J., MACIAS, R. I., BRIZ, O., PEREZ, M. J., BLAZQUEZ, A. G., ARRESE, M. & SERRANO, M. A. 2008. Molecular bases of the fetal liver-placenta-maternal liver excretory pathway for cholephilic compounds. *Liver Int,* 28**,** 435-54.

MARK, D., HAEBERLE, S., ROTH, G., VON STETTEN, F. & ZENGERLE, R. 2010. Microfluidic lab-on-a-chip platforms: requirements, characteristics and applications. *Chem Soc Rev,* 39**,** 1153-82.

MARSCHALL, H. U., WIKSTRÖM SHEMER, E., LUDVIGSSON, J. F. & STEPHANSSON, O. 2013. Intrahepatic cholestasis of pregnancy and associated hepatobiliary disease: a population-based cohort study. *Hepatology,* 58**,** 1385-91.

MARTIN, P. 1977. The influence of the parasympathetic nervous system on atrioventricular conduction. *Circ Res,* 41**,** 593-9.

MARTINEAU, M., PAPACLEOVOULOU, G., ABU-HAYYEH, S., DIXON, P. H., JI, H., POWRIE, R., LARSON, L., CHIEN, E. K. & WILLIAMSON, C. 2014a. Cholestatic pregnancy is associated with reduced placental 11βHSD2 expression. *Placenta,* 35**,** 37-43.

MARTINEAU, M., RAKER, C., POWRIE, R. & WILLIAMSON, C. 2014b. Intrahepatic cholestasis of pregnancy is associated with an increased risk of gestational diabetes. *Eur J Obstet Gynecol Reprod Biol,* 176**,** 80-5.

MATO, J. M. & LU, S. C. 2007. Role of S-adenosyl-L-methionine in liver health and injury. *Hepatology,* 45**,** 1306-12.

MAWSON, A. R. 2016. A Role for the Liver in Parturition and Preterm Birth. *J Transl Sci,* 2**,** 154-159.

MAZZELLA, G., RIZZO, N., AZZAROLI, F., SIMONI, P., BOVICELLI, L., MIRACOLO, A., SIMONAZZI, G., COLECCHIA, A., NIGRO, G., MWANGEMI, C., FESTI, D., RODA, E., NICOLA, R., FRANCESCO, A., PATRIZIA, S., LUCIANO, B., ANNA, M., GIULIANA, S., ANTONIO, C., GIOVANNI, N., CONSTANCE, M., DAVIDE, F. & ENRICO, R. 2001. Ursodeoxycholic acid administration in patients with cholestasis of pregnancy: effects on primary bile acids in babies and mothers. *Hepatology,* 33**,** 504-8.

MCCALLUM, L. A., PIERCE, S. L., ENGLAND, S. K., GREENWOOD, I. A. & TRIBE, R. M. 2011. The contribution of Kv7 channels to pregnant mouse and human myometrial contractility. *J Cell Mol Med,* 15**,** 577-86.

MCLEAN, M., BISITS, A., DAVIES, J., WOODS, R., LOWRY, P. & SMITH, R. 1995. A placental clock controlling the length of human pregnancy. *Nat Med,* 1**,** 460-3.
MEDICI, A., PEDRINI, P., DE BATTISTI , A., FANTIN, G., FOGAGNOLO, M. & GUERRINI, A. 2001. Anodic electrochemical oxidation of cholic acid. *Steroids,* 66**,** 63-9.
MEHRVAR, M. & ABDI, M. 2004. Recent developments, characteristics, and potential applications of electrochemical biosensors. *Anal Sci,* 20**,** 1113-26.
MEI, Y., GAO, L., LIN, Y., LUO, D., ZHOU, X. & HE, L. 2019. Predictors of adverse perinatal outcomes in intrahepatic cholestasis of pregnancy with dichorionic diamniotic twin pregnancies. *J Matern Fetal Neonatal Med,* 32**,** 472-476.
MEI, Y., LIN, Y., LUO, D., GAO, L. & HE, L. 2018. Perinatal outcomes in intrahepatic cholestasis of pregnancy with monochorionic diamniotic twin pregnancy. *BMC Pregnancy Childbirth,* 18**,** 291.
MEIER, P. J. & STIEGER, B. 2002. Bile salt transporters. *Annu Rev Physiol,* 64**,** 635-61.
MELLA, M. T., KOHARI, K., JONES, R., PEÑA, J., FERRARA, L., STONE, J. & LAMBERTINI, L. 2016. Mitochondrial gene expression profiles are associated with intrahepatic cholestasis of pregnancy. *Placenta,* 45**,** 16-23.
MENON, R., JONES, J., GUNST, P. R., KACEROVSKY, M., FORTUNATO, S. J., SAADE, G. R. & BASRAON, S. 2014. Amniotic fluid metabolomic analysis in spontaneous preterm birth. *Reprod Sci,* 21**,** 791-803.
MIKI, T., MIURA, T., HOTTA, H., TANNO, M., YANO, T., SATO, T., TERASHIMA, Y., TAKADA, A., ISHIKAWA, S. & SHIMAMOTO, K. 2009. Endoplasmic reticulum stress in diabetic hearts abolishes erythropoietin-induced myocardial protection by impairment of phospho-glycogen synthase kinase-3beta-mediated suppression of mitochondrial permeability transition. *Diabetes,* 58**,** 2863-72.
MIKUCKA-NICZYPORUK, A., PIERZYNSKI, P., LEMANCEWICZ, A., KOSINSKI, P., CHARKIEWICZ, K., KNAS, M., KACEROVSKY, M., BLACHNIO-ZABIELSKA, A. & LAUDANSKI, P. 2020. Role of sphingolipids in the pathogenesis of intrahepatic cholestasis. *Prostaglandins Other Lipid Mediat,* 147**,** 106399.
MIRAGOLI, M., KADIR, S. H., SHEPPARD, M. N., SALVARANI, N., VIRTA, M., WELLS, S., LAB, M. J., NIKOLAEV, V. O., MOSHKOV, A., HAGUE, W. M., ROHR, S., WILLIAMSON, C. & GORELIK, J. 2011. A protective antiarrhythmic role of ursodeoxycholic acid in an in vitro rat model of the cholestatic fetal heart. *Hepatology,* 54**,** 1282-92.
MITCHELL, B. F. & SCHMID, B. 2001. Oxytocin and its receptor in the process of parturition. *J Soc Gynecol Investig,* 8**,** 122-33.
MITCHELL, B. F. & TAGGART, M. J. 2009. Are animal models relevant to key aspects of human parturition? *Am J Physiol Regul Integr Comp Physiol,* 297**,** R525-45.
MIYOSHI, T., UMEKAWA, T., HOSODA, H., ASADA, T., FUJIWARA, A., KUROSAKI, K. I., SHIRAISHI, I., NAKAI, M., NISHIMURA, K., MIYAZATO, M., KANGAWA, K., IKEDA, T., YOSHIMATSU, J. & MINAMINO, N. 2018. Plasma natriuretic peptide levels in fetuses with congenital heart defect and/or arrhythmia. *Ultrasound Obstet Gynecol,* 52**,** 609-616.
MOEHLENBROCK, M. J. & MINTEER, S. D. 2011. Introduction to the field of enzyme immobilization and stabilization. *Methods Mol Biol,* 679**,** 1-7.
MOHAMED, A. S., HANAFI, N. I., SHEIKH ABDUL KADIR, S. H., MD NOOR, J., ABDUL HAMID HASANI, N., AB RAHIM, S. & SIRAN, R. 2017. Ursodeoxycholic acid protects cardiomyocytes against cobalt chloride induced hypoxia by regulating transcriptional mediator of cells stress hypoxia inducible factor 1α and p53 protein. *Cell Biochem Funct,* 35**,** 453-463.
MOMEN, M. A., MONDEN, Y., HOUCHI, H. & UMEMOTO, A. 2002. Effect of ursodeoxycholic acid on azoxymethane-induced aberrant crypt foci formation in rat colon: in vitro potential role of intracellular Ca2+. *J Med Invest,* 49**,** 67-73.

MONGA, M., KU, C. Y., DODGE, K. & SANBORN, B. M. 1996. Oxytocin-stimulated responses in a pregnant human immortalized myometrial cell line. *Biol Reprod,* 55**,** 427-32.

MONTE, M. J., MARIN, J. J., ANTELO, A. & VAZQUEZ-TATO, J. 2009. Bile acids: chemistry, physiology, and pathophysiology. *World J Gastroenterol,* 15**,** 804-16.

MONTE, M. J., RODRIGUEZ-BRAVO, T., MACIAS, R. I., BRAVO, P., EL-MIR, M. Y., SERRANO, M. A., LOPEZ-SALVA, A. & MARIN, J. J. 1995. Relationship between bile acid transplacental gradients and transport across the fetal-facing plasma membrane of the human trophoblast. *Pediatr Res,* 38**,** 156-63.

MOORE, F., DA SILVA, C., WILDE, J. I., SMARASON, A., WATSON, S. P. & LÓPEZ BERNAL, A. 2000. Up-regulation of p21- and RhoA-activated protein kinases in human pregnant myometrium. *Biochem Biophys Res Commun,* 269**,** 322-6.

MORAN, C. J., FRIEL, A. M., SMITH, T. J., CAIRNS, M. & MORRISON, J. J. 2002. Expression and modulation of Rho kinase in human pregnant myometrium. *Mol Hum Reprod,* 8**,** 196-200.

MORGAN, T. K. 2016. Role of the Placenta in Preterm Birth: A Review. *Am J Perinatol,* 33**,** 258-66.

MORRISON, J. J., DEARN, S. R., SMITH, S. K. & AHMED, A. 1996. Activation of protein kinase C is required for oxytocin-induced contractility in human pregnant myometrium. *Hum Reprod,* 11**,** 2285-90.

MOSHER, A. A., RAINEY, K. J., BOLSTAD, S. S., LYE, S. J., MITCHELL, B. F., OLSON, D. M., WOOD, S. L. & SLATER, D. M. 2013. Development and validation of primary human myometrial cell culture models to study pregnancy and labour. *BMC Pregnancy Childbirth,* 13 Suppl 1**,** S7.

MOSS, A. J., SCHWARTZ, P. J., CRAMPTON, R. S., LOCATI, E. & CARLEEN, E. 1985. The long QT syndrome: a prospective international study. *Circulation,* 71**,** 17-21.

MOYO, M., OKONKWO, J. O. & AGYEI, N. M. 2012. Recent advances in polymeric materials used as electron mediators and immobilizing matrices in developing enzyme electrodes. *Sensors (Basel),* 12**,** 923-53.

MURRAY, C. J., VOS, T., LOZANO, R., NAGHAVI, M., FLAXMAN, A. D., MICHAUD, C., EZZATI, M., SHIBUYA, K., SALOMON, J. A., ABDALLA, S., ABOYANS, V., ABRAHAM, J., ACKERMAN, I., AGGARWAL, R., AHN, S. Y., ALI, M. K., ALVARADO, M., ANDERSON, H. R., ANDERSON, L. M., ANDREWS, K. G., ATKINSON, C., BADDOUR, L. M., BAHALIM, A. N., BARKER-COLLO, S., BARRERO, L. H., BARTELS, D. H., BASÁÑEZ, M. G., BAXTER, A., BELL, M. L., BENJAMIN, E. J., BENNETT, D., BERNABÉ, E., BHALLA, K., BHANDARI, B., BIKBOV, B., BIN ABDULHAK, A., BIRBECK, G., BLACK, J. A., BLENCOWE, H., BLORE, J. D., BLYTH, F., BOLLIGER, I., BONAVENTURE, A., BOUFOUS, S., BOURNE, R., BOUSSINESQ, M., BRAITHWAITE, T., BRAYNE, C., BRIDGETT, L., BROOKER, S., BROOKS, P., BRUGHA, T. S., BRYAN-HANCOCK, C., BUCELLO, C., BUCHBINDER, R., BUCKLE, G., BUDKE, C. M., BURCH, M., BURNEY, P., BURSTEIN, R., CALABRIA, B., CAMPBELL, B., CANTER, C. E., CARABIN, H., CARAPETIS, J., CARMONA, L., CELLA, C., CHARLSON, F., CHEN, H., CHENG, A. T., CHOU, D., CHUGH, S. S., COFFENG, L. E., COLAN, S. D., COLQUHOUN, S., COLSON, K. E., CONDON, J., CONNOR, M. D., COOPER, L. T., CORRIERE, M., CORTINOVIS, M., DE VACCARO, K. C., COUSER, W., COWIE, B. C., CRIQUI, M. H., CROSS, M., DABHADKAR, K. C., DAHIYA, M., DAHODWALA, N., DAMSERE-DERRY, J., DANAEI, G., DAVIS, A., DE LEO, D., DEGENHARDT, L., DELLAVALLE, R., DELOSSANTOS, A., DENENBERG, J., DERRETT, S., DES JARLAIS, D. C., DHARMARATNE, S. D., et al. 2012. Disability-adjusted life years (DALYs) for 291 diseases and injuries in 21 regions, 1990-2010: a systematic analysis for the Global Burden of Disease Study 2010. *Lancet,* 380**,** 2197-223.

MURTAZINA, D. A., CHUNG, D., ULLOA, A., BRYAN, E., GALAN, H. L. & SANBORN, B. M. 2011. TRPC1, STIM1, and ORAI influence signal-regulated intracellular and endoplasmic reticulum calcium dynamics in human myometrial cells. *Biol Reprod,* 85**,** 315-26.
MWANIKI, M. K., ATIENO, M., LAWN, J. E. & NEWTON, C. R. 2012. Long-term neurodevelopmental outcomes after intrauterine and neonatal insults: a systematic review. *Lancet,* 379**,** 445-52.
MYERBURG, R. J., INTERIAN, A., MITRANI, R. M., KESSLER, K. M. & CASTELLANOS, A. 1997. Frequency of sudden cardiac death and profiles of risk. *Am J Cardiol,* 80**,** 10F-19F.
MYERS, S. I., RIVA, A., KALLEY-TAYLOR, B. & BARTULA, L. 1995. Taurodeoxycholic acid stimulates rabbit gallbladder eicosanoid release. *Prostaglandins Leukot Essent Fatty Acids,* 52**,** 35-9.
NADEEM, L., SHYNLOVA, O., MATYSIAK-ZABLOCKI, E., MESIANO, S., DONG, X. & LYE, S. 2016. Molecular evidence of functional progesterone withdrawal in human myometrium. *Nat Commun,* 7**,** 11565.
NADEEM, L., SHYNLOVA, O., MESIANO, S. & LYE, S. 2017. Progesterone Via its Type-A Receptor Promotes Myometrial Gap Junction Coupling. *Sci Rep,* 7**,** 13357.
NAGASE, H. & WOESSNER, J. F. 1999. Matrix metalloproteinases. *J Biol Chem,* 274**,** 21491-4.
NAKAMURA, K., TOKIWA, K. & NISHINO, H. 1994. The effects on cellular functions of bile acid and trypsin in stagnant bile juice in anomalous arrangement of the pancreaticobiliary duct. *Cancer Lett,* 86**,** 53-8.
NAKAMURA, S., KAWANO, Y., KAMIHIGASHI, S., SUGANO, T., NARAHARA, H. & MIYAKAWA, I. 2001. Effect of ceramide analogs on interleukin-1alpha-induced production of prostaglandin E2 by amnion-derived (WISH) cells. *Acta Obstet Gynecol Scand,* 80**,** 12-7.
NAKAO, K., INOUE, Y., OKABE, K., KAWARABAYASHI, T. & KITAMURA, K. 1997. Oxytocin enhances action potentials in pregnant human myometrium--a study with microelectrodes. *Am J Obstet Gynecol,* 177**,** 222-8.
NARISAWA, T., TAKAHASHI, M., NIWA, M., FUKAURA, Y. & WAKIZAKA, A. 1987. Involvement of prostaglandin E2 in bile acid-caused promotion of colon carcinogenesis and anti-promotion by the cyclooxygenase inhibitor indomethacin. *Jpn J Cancer Res,* 78**,** 791-8.
NICASTRI, P. L., DIAFERIA, A., TARTAGNI, M., LOIZZI, P. & FANELLI, M. 1998. A randomised placebo-controlled trial of ursodeoxycholic acid and S-adenosylmethionine in the treatment of intrahepatic cholestasis of pregnancy. *Br J Obstet Gynaecol,* 105**,** 1205-7.
NICE 2017. Intrapartum care for healthy women and babies (clinical guideline No. 190). Retrieved from https://www.nice.org.uk/Guidance/CG190.
NIJHUIS, J. G., PRECHTL, H. F., MARTIN, C. B. & BOTS, R. S. 1982. Are there behavioural states in the human fetus? *Early Hum Dev,* 6**,** 177-95.
NISHIGAKI, Y., OHNISHI, H., MORIWAKI, H. & MUTO, Y. 1996. Ursodeoxycholic acid corrects defective natural killer activity by inhibiting prostaglandin E2 production in primary biliary cirrhosis. *Dig Dis Sci,* 41**,** 1487-93.
NISHIURA, H., KIMURA, A., YAMATO, Y., AOKI, K., INOKUCHI, T., KUROSAWA, T. & MATSUISHI, T. 2010. Developmental pattern of urinary bile acid profile in preterm infants. *Pediatr Int,* 52**,** 44-50.
NOLAN, D. G., MARTIN, L. S., NATARAJAN, S. & HUME, R. F. 1994. Fetal compromise associated with extreme fetal bile acidemia and maternal primary sclerosing cholangitis. *Obstet Gynecol,* 84**,** 695-6.
OHYA, Y. & SPERELAKIS, N. 1989. Modulation of single slow (L-type) calcium channels by intracellular ATP in vascular smooth muscle cells. *Pflugers Arch,* 414**,** 257-64.

OLAUSSON, M., MJÖRNSTEDT, L., WRAMNER, L., PERSSON, H., KARLBERG, I. & FRIMAN, S. 1992. Adjuvant treatment with ursodeoxycholic acid prevents acute rejection in rats receiving heart allografts. *Transpl Int,* 5 Suppl 1**,** S539-41.

OUDE ELFERINK, R. P. & PAULUSMA, C. C. 2007. Function and pathophysiological importance of ABCB4 (MDR3 P-glycoprotein). *Pflugers Arch,* 453**,** 601-10.

OVADIA, C., SEED, P. T., SKLAVOUNOS, A., GEENES, V., DI ILLIO, C., CHAMBERS, J., KOHARI, K., BACQ, Y., BOZKURT, N., BRUN-FURRER, R., BULL, L., ESTIÚ, M. C., GRYMOWICZ, M., GUNAYDIN, B., HAGUE, W. M., HASLINGER, C., HU, Y., KAWAKITA, T., KEBAPCILAR, A. G., KEBAPCILAR, L., KONDRACKIENĖ, J., KOSTER, M. P. H., KOWALSKA-KAŃKA, A., KUPČINSKAS, L., LEE, R. H., LOCATELLI, A., MACIAS, R. I. R., MARSCHALL, H. U., OUDIJK, M. A., RAZ, Y., RIMON, E., SHAN, D., SHAO, Y., TRIBE, R., TRIPODI, V., YAYLA ABIDE, C., YENIDEDE, I., THORNTON, J. G., CHAPPELL, L. C. & WILLIAMSON, C. 2019. Association of adverse perinatal outcomes of intrahepatic cholestasis of pregnancy with biochemical markers: results of aggregate and individual patient data meta-analyses. *Lancet,* 393**,** 899-909.

OVADIA, C. & WILLIAMSON, C. 2016. Intrahepatic cholestasis of pregnancy: Recent advances. *Clin Dermatol,* 34**,** 327-34.

OZEL, A., ALICI DAVUTOGLU, E., ERIC OZDEMIR, M., OZTUNC, F. & MADAZLI, R. 2018. Assessment of fetal left ventricular modified myocardial performance index and its prognostic significance for adverse perinatal outcome in intrahepatic cholestasis of pregnancy. *J Matern Fetal Neonatal Med***,** 1-11.

OZLER, A., UCMAK, D., EVSEN, M. S., KAPLAN, I., ELBEY, B., ARICA, M. & KAYA, M. 2014. Immune mechanisms and the role of oxidative stress in intrahepatic cholestasis of pregnancy. *Cent Eur J Immunol,* 39**,** 198-202.

OZTAS, E., ERKENEKLI, K., OZLER, S., ERSOY, A. O., KURT, M., UYGUR, D. & DANISMAN, N. 2015. Can routine laboratory parameters predict adverse pregnancy outcomes in intrahepatic cholestasis of pregnancy? *J Perinat Med,* 43**,** 667-74.

OZTAS, E., OZLER, S., ERSOY, A. O., ERKENEKLI, K., SUCAK, A., ERGIN, M., UYGUR, D. & DANISMAN, N. 2016. Placental ADAMTS-12 Levels in the Pathogenesis of Preeclampsia and Intrahepatic Cholestasis of Pregnancy. *Reprod Sci,* 23**,** 475-81.

OZTEKIN, D., AYDAL, I., OZTEKIN, O., OKCU, S., BOREKCI, R. & TINAR, S. 2009. Predicting fetal asphyxia in intrahepatic cholestasis of pregnancy. *Arch Gynecol Obstet,* 280**,** 975-9.

PAK, J. M., ADEAGBO, A. S., TRIGGLE, C. R., SHAFFER, E. A. & LEE, S. S. 1994. Mechanism of bile salt vasoactivity: dependence on calcium channels in vascular smooth muscle. *Br J Pharmacol,* 112**,** 1209-15.

PALEJWALA, S., STEIN, D. E., WEISS, G., MONIA, B. P., TORTORIELLO, D. & GOLDSMITH, L. T. 2001. Relaxin positively regulates matrix metalloproteinase expression in human lower uterine segment fibroblasts using a tyrosine kinase signaling pathway. *Endocrinology,* 142**,** 3405-13.

PALMA, J., REYES, H., RIBALTA, J., HERNÁNDEZ, I., SANDOVAL, L., ALMUNA, R., LIEPINS, J., LIRA, F., SEDANO, M., SILVA, O., TOHÁ, D. & SILVA, J. J. 1997. Ursodeoxycholic acid in the treatment of cholestasis of pregnancy: a randomized, double-blind study controlled with placebo. *J Hepatol,* 27**,** 1022-8.

PALMA, J., REYES, H., RIBALTA, J., IGLESIAS, J., GONZALEZ, M. C., HERNANDEZ, I., ALVAREZ, C., MOLINA, C. & DANITZ, A. M. 1992. Effects of ursodeoxycholic acid in patients with intrahepatic cholestasis of pregnancy. *Hepatology,* 15**,** 1043-7.

PAPACLEOVOULOU, G., ABU-HAYYEH, S., NIKOLOPOULOU, E., BRIZ, O., OWEN, B. M., NIKOLOVA, V., OVADIA, C., HUANG, X., VAARASMAKI, M., BAUMANN, M., JANSEN, E., ALBRECHT, C., JARVELIN, M. R., MARIN, J. J., KNISELY, A. S. & WILLIAMSON, C.

2013. Maternal cholestasis during pregnancy programs metabolic disease in offspring. *J Clin Invest,* 123**,** 3172-81.
PAREDES, R. M., ETZLER, J. C., WATTS, L. T., ZHENG, W. & LECHLEITER, J. D. 2008. Chemical calcium indicators. *Methods,* 46**,** 143-51.
PARKINGTON, H. C., STEVENSON, J., TONTA, M. A., PAUL, J., BUTLER, T., MAITI, K., CHAN, E. C., SHEEHAN, P. M., BRENNECKE, S. P., COLEMAN, H. A. & SMITH, R. 2014. Diminished hERG K+ channel activity facilitates strong human labour contractions but is dysregulated in obese women. *Nat Commun,* 5**,** 4108.
PARKINGTON, H. C., TONTA, M. A., BRENNECKE, S. P. & COLEMAN, H. A. 1999a. Contractile activity, membrane potential, and cytoplasmic calcium in human uterine smooth muscle in the third trimester of pregnancy and during labor. *Am J Obstet Gynecol,* 181**,** 1445-51.
PARKINGTON, H. C., TONTA, M. A., DAVIES, N. K., BRENNECKE, S. P. & COLEMAN, H. A. 1999b. Hyperpolarization and slowing of the rate of contraction in human uterus in pregnancy by prostaglandins E2 and f2alpha: involvement of the Na+ pump. *J Physiol,* 514 (Pt 1)**,** 229-43.
PARÍZEK, A., SIMJÁK, P., CERNÝ, A., SESTINOVÁ, A., ZDENKOVÁ, A., HILL, M., DUSKOVÁ, M., VLK, R., KOKRDOVÁ, Z., KOUCKÝ, M. & VÍTEK, L. 2016. Efficacy and safety of ursodeoxycholic acid in patients with intrahepatic cholestasis of pregnancy. *Ann Hepatol,* 15**,** 757-61.
PASINSZKI, T., KREBSZ, M., TUNG, T. T. & LOSIC, D. 2017. Carbon Nanomaterial Based Biosensors for Non-Invasive Detection of Cancer and Disease Biomarkers for Clinical Diagnosis. *Sensors (Basel),* 17.
PATEL, S., PINHEIRO, M., FELIX, J. C., OPPER, N., OUZOUNIAN, J. G. & LEE, R. H. 2014. A case-control review of placentas from patients with intrahepatic cholestasis of pregnancy. *Fetal Pediatr Pathol,* 33**,** 210-5.
PATERNOSTER, D. M., FABRIS, F., PALÙ, G., SANTAROSSA, C., BRACCIANTE, R., SNIJDERS, D. & FLOREANI, A. 2002. Intra-hepatic cholestasis of pregnancy in hepatitis C virus infection. *Acta Obstet Gynecol Scand,* 81**,** 99-103.
PATOLSKY, F., ZHENG, G. & LIEBER, C. M. 2006. Nanowire-based biosensors. *Anal Chem,* 78**,** 4260-9.
PEREZ, M. J., MACIAS, R. I. & MARIN, J. J. 2006. Maternal cholestasis induces placental oxidative stress and apoptosis. Protective effect of ursodeoxycholic acid. *Placenta,* 27**,** 34-41.
PERKIÖMÄKI, J., UKKOLA, O., KIVINIEMI, A., TULPPO, M., YLITALO, A., KESÄNIEMI, Y. A. & HUIKURI, H. 2014. Heart rate variability findings as a predictor of atrial fibrillation in middle-aged population. *J Cardiovasc Electrophysiol,* 25**,** 719-24.
PETERSEN, L. K., SKAJAA, K. & ULDBJERG, N. 1992. Serum relaxin as a potential marker for preterm labour. *Br J Obstet Gynaecol,* 99**,** 292-5.
PETERSEN, L. K., SVANE, D., ULDBJERG, N. & FORMAN, A. 1991. Effects of human relaxin on isolated rat and human myometrium and uteroplacental arteries. *Obstet Gynecol,* 78**,** 757-62.
PHILLIPPE, M. 1994. Protein kinase C, an inhibitor of oxytocin-stimulated phasic myometrial contractions. *Biol Reprod,* 50**,** 855-9.
PIEBER, D., ALLPORT, V. C., HILLS, F., JOHNSON, M. & BENNETT, P. R. 2001. Interactions between progesterone receptor isoforms in myometrial cells in human labour. *Mol Hum Reprod,* 7**,** 875-9.
PILLAI, M. & JAMES, D. 1990. Behavioural states in normal mature human fetuses. *Arch Dis Child,* 65**,** 39-43.

PIÉRI, J. F., CROWE, J. A., HAYES-GILL, B. R., SPENCER, C. J., BHOGAL, K. & JAMES, D. K. 2001. Compact long-term recorder for the transabdominal foetal and maternal electrocardiogram. *Med Biol Eng Comput,* 39**,** 118-25.

PRAKASH, S., PINTI, M. & BHUSHAN, B. 2012. Theory, fabrication and applications of microfluidic and nanofluidic biosensors. *Philos Trans A Math Phys Eng Sci,* 370**,** 2269-303.

PRIETO-SIMÓN, B. & FÀBREGAS, E. 2004. Comparative study of electron mediators used in the electrochemical oxidation of NADH. *Biosens Bioelectron,* 19**,** 1131-8.

PULJIC, A., KIM, E., PAGE, J., ESAKOFF, T., SHAFFER, B., LACOURSIERE, D. Y. & CAUGHEY, A. B. 2015. The risk of infant and fetal death by each additional week of expectant management in intrahepatic cholestasis of pregnancy by gestational age. *Am J Obstet Gynecol,* 212**,** 667.e1-5.

QIN, P., TANG, X., ELLOSO, M. M. & HARNISH, D. C. 2006. Bile acids induce adhesion molecule expression in endothelial cells through activation of reactive oxygen species, NF-kappaB, and p38. *Am J Physiol Heart Circ Physiol,* 291**,** H741-7.

QIN, X., NI, X., MAO, X., YING, H. & DU, Q. 2017a. Cholestatic pregnancy is associated with reduced VCAM1 expression in vascular endothelial cell of placenta. *Reprod Toxicol,* 74**,** 23-31.

QIN, Y., WANG, Y., LIU, O., JIA, L., FANG, W., DU, J. & WEI, Y. 2017b. Tauroursodeoxycholic Acid Attenuates Angiotensin II Induced Abdominal Aortic Aneurysm Formation in Apolipoprotein E-deficient Mice by Inhibiting Endoplasmic Reticulum Stress. *Eur J Vasc Endovasc Surg,* 53**,** 337-345.

RAINER, P. P., PRIMESSNIG, U., HARENKAMP, S., DOLESCHAL, B., WALLNER, M., FAULER, G., STOJAKOVIC, T., WACHTER, R., YATES, A., GROSCHNER, K., TRAUNER, M., PIESKE, B. M. & VON LEWINSKI, D. 2013. Bile acids induce arrhythmias in human atrial myocardium--implications for altered serum bile acid composition in patients with atrial fibrillation. *Heart,* 99**,** 1685-92.

RAJESH, K. G., SUZUKI, R., MAEDA, H., YAMAMOTO, M., YUTONG, X. & SASAGURI, S. 2005. Hydrophilic bile salt ursodeoxycholic acid protects myocardium against reperfusion injury in a PI3K/Akt dependent pathway. *J Mol Cell Cardiol,* 39**,** 766-76.

RANI, S., SREENIVASAIAH, P. K., KIM, J. O., LEE, M. Y., KANG, W. S., KIM, Y. S., AHN, Y., PARK, W. J., CHO, C. & KIM, D. H. 2017. Tauroursodeoxycholic acid (TUDCA) attenuates pressure overload-induced cardiac remodeling by reducing endoplasmic reticulum stress. *PLoS One,* 12**,** e0176071.

RAVI, M., PARAMESH, V., KAVIYA, S. R., ANURADHA, E. & SOLOMON, F. D. 2015. 3D cell culture systems: advantages and applications. *J Cell Physiol,* 230**,** 16-26.

RECHNITZ, G. A. & NAKAMURA, R. M. 1988. Future of biosensors in the clinical laboratory. *Journal of Clinical Laboratory Analysis,* 2**,** 131-133.

REINL, E. L., CABEZA, R., GREGORY, I. A., CAHILL, A. G. & ENGLAND, S. K. 2015. Sodium leak channel, non-selective contributes to the leak current in human myometrial smooth muscle cells from pregnant women. *Mol Hum Reprod,* 21**,** 816-24.

RENTHAL, N. E., CHEN, C. C., WILLIAMS, K. C., GERARD, R. D., PRANGE-KIEL, J. & MENDELSON, C. R. 2010. miR-200 family and targets, ZEB1 and ZEB2, modulate uterine quiescence and contractility during pregnancy and labor. *Proc Natl Acad Sci U S A,* 107**,** 20828-33.

REYES, H. 2008. Sex hormones and bile acids in intrahepatic cholestasis of pregnancy. *Hepatology,* 47**,** 376-9.

REYES, H., GONZALEZ, M. C., RIBALTA, J., ABURTO, H., MATUS, C., SCHRAMM, G., KATZ, R. & MEDINA, E. 1978. Prevalence of intrahepatic cholestasis of pregnancy in Chile. *Ann Intern Med,* 88**,** 487-93.

REZAI, S., LORA, I. & HENDERSON, C. E. 2015. Severe intrahepatic cholestasis of pregnancy is a risk factor for preeclampsia in singleton and twin pregnancies. *Am J Obstet Gynecol,* 213**,** 877.

RIOSECO, A. J., IVANKOVIC, M. B., MANZUR, A., HAMED, F., KATO, S. R., PARER, J. T. & GERMAIN, A. M. 1994. Intrahepatic cholestasis of pregnancy: a retrospective case-control study of perinatal outcome. *Am J Obstet Gynecol,* 170**,** 890-5.

RIVARD, A. L., STEER, C. J., KREN, B. T., RODRIGUES, C. M., CASTRO, R. E., BIANCO, R. W. & LOW, W. C. 2007. Administration of tauroursodeoxycholic acid (TUDCA) reduces apoptosis following myocardial infarction in rat. *Am J Chin Med,* 35**,** 279-95.

RIVAS, G. A., RUBIANES, M. D., RODRÍGUEZ, M. C., FERREYRA, N. F., LUQUE, G. L., PEDANO, M. L., MISCORIA, S. A. & PARRADO, C. 2007. Carbon nanotubes for electrochemical biosensing. *Talanta,* 74**,** 291-307.

RO, J. Y., CHO, T. S. & HONG, S. S. 1986. The effects of cholates on smooth muscle strips and cardiac muscle. *Kor. J. Pharmacol,* 16**,** 41-50.

RODRÍGUEZ, M., MORENO, J., MÁRQUEZ, R., ELTIT, R., MARTINEZ, F., SEPÚLVEDA-MARTÍNEZ, A. & PARRA-CORDERO, M. 2016. Increased PR Interval in Fetuses of Patients with Intrahepatic Cholestasis of Pregnancy. *Fetal Diagn Ther,* 40**,** 298-302.

ROMANO, M., BIFULCO, P., CESARELLI, M., SANSONE, M. & BRACALE, M. 2006. Foetal heart rate power spectrum response to uterine contraction. *Med Biol Eng Comput,* 44**,** 188-201.

ROMERO, F., FREDIANI-NETO, E., PAIVA, T. B. & PAIVA, A. C. 1993. Role of Na+/Ca++ exchange in the relaxant effect of sodium taurocholate on the guinea-pig ileum smooth muscle. *Naunyn Schmiedebergs Arch Pharmacol,* 348**,** 325-31.

ROMERO, R., GOMEZ, R., GHEZZI, F., YOON, B. H., MAZOR, M., EDWIN, S. S. & BERRY, S. M. 1998. A fetal systemic inflammatory response is followed by the spontaneous onset of preterm parturition. *Am J Obstet Gynecol,* 179**,** 186-93.

ROMERO, R., MUNOZ, H., GOMEZ, R., PARRA, M., POLANCO, M., VALVERDE, V., HASBUN, J., GARRIDO, J., GHEZZI, F., MAZOR, M., TOLOSA, J. E. & MITCHELL, M. D. 1996. Increase in prostaglandin bioavailability precedes the onset of human parturition. *Prostaglandins Leukot Essent Fatty Acids,* 54**,** 187-91.

RONCAGLIA, N., LOCATELLI, A., ARREGHINI, A., ASSI, F., CAMERONI, I., PEZZULLO, J. C. & GHIDINI, A. 2004. A randomised controlled trial of ursodeoxycholic acid and S-adenosyl-l-methionine in the treatment of gestational cholestasis. *BJOG,* 111**,** 17-21.

SABATÉ DEL RÍO, J., HENRY, O. Y. F., JOLLY, P. & INGBER, D. E. 2019. An antifouling coating that enables affinity-based electrochemical biosensing in complex biological fluids. *Nat Nanotechnol,* 14**,** 1143-1149.

SANBORN, B. M. 2000. Relationship of ion channel activity to control of myometrial calcium. *J Soc Gynecol Investig,* 7**,** 4-11.

SANBORN, B. M. 2007. Hormonal signaling and signal pathway crosstalk in the control of myometrial calcium dynamics. *Semin Cell Dev Biol,* 18**,** 305-14.

SANBORN, B. M., KU, C. Y., SHLYKOV, S. & BABICH, L. 2005. Molecular signaling through G-protein-coupled receptors and the control of intracellular calcium in myometrium. *J Soc Gynecol Investig,* 12**,** 479-87.

SANHAL, C. Y., DAGLAR, K., KARA, O., YILMAZ, Z. V., TURKMEN, G. G., EREL, O., UYGUR, D. & YUCEL, A. 2018. An alternative method for measuring oxidative stress in intrahepatic cholestasis of pregnancy: thiol/disulphide homeostasis. *J Matern Fetal Neonatal Med,* 31**,** 1477-1482.

SANHAL, C. Y., KARA, O. & YUCEL, A. 2017. Can fetal left ventricular modified myocardial performance index predict adverse perinatal outcomes in intrahepatic cholestasis of pregnancy? *J Matern Fetal Neonatal Med,* 30**,** 911-916.

SARGIN ORUÇ, A., SEÇKIN, B., ÖZCAN, N., ÖZYER, S., UZUNLAR, Ö. & DANIŞMAN, N. 2014. Role of postprandial bile acids in prediction of perinatal outcome in intrahepatic cholestasis of pregnancy. *J Obstet Gynaecol Res,* 40**,** 1883-9.

SASSOLAS, A., BLUM, L. J. & LECA-BOUVIER, B. D. 2012. Immobilization strategies to develop enzymatic biosensors. *Biotechnol Adv,* 30**,** 489-511.

SCALIA, S., TIRENDI, S., PAZZI, P. & BOUSQUET, E. 1995. Assay of free bile acids in pharmaceutical preparations by HPLC with electrochemical detection. 115**,** 249-253.

SCHIEDERMAIER, P., HANSEN, S., ASDONK, D., BRENSING, K. & SAUERBRUCH, T. 2000. Effects of ursodeoxycholic acid on splanchnic and systemic hemodynamics. A double-blind, cross-over, placebo-controlled study in healthy volunteers. *Digestion,* 61**,** 107-12.

SCHNEIDER, U., SCHLEUSSNER, E., FIEDLER, A., JAEKEL, S., LIEHR, M., HAUEISEN, J. & HOYER, D. 2009. Fetal heart rate variability reveals differential dynamics in the intrauterine development of the sympathetic and parasympathetic branches of the autonomic nervous system. *Physiol Meas,* 30**,** 215-26.

SCHULTZ, F., HASAN, A., ALVAREZ-LAVIADA, A., MIRAGOLI, M., BHOGAL, N., WELLS, S., POULET, C., CHAMBERS, J., WILLIAMSON, C. & GORELIK, J. 2016. The protective effect of ursodeoxycholic acid in an in vitro model of the human fetal heart occurs via targeting cardiac fibroblasts. *Prog Biophys Mol Biol,* 120**,** 149-63.

SCHWACHTGEN, L., HERRMANN, M., GEORG, T., SCHWARZ, P., MARX, N. & LINDINGER, A. 2005. Reference values of NT-proBNP serum concentrations in the umbilical cord blood and in healthy neonates and children. *Z Kardiol,* 94**,** 399-404.

SENIOR, J., MARSHALL, K., SANGHA, R. & CLAYTON, J. K. 1993. In vitro characterization of prostanoid receptors on human myometrium at term pregnancy. *Br J Pharmacol,* 108**,** 501-6.

SENTILHES, L., VERSPYCK, E., PIA, P. & MARPEAU, L. 2006. Fetal death in a patient with intrahepatic cholestasis of pregnancy. *Obstet Gynecol,* 107**,** 458-60.

SEPÚLVEDA, W. H., GONZÁLEZ, C., CRUZ, M. A. & RUDOLPH, M. I. 1991. Vasoconstrictive effect of bile acids on isolated human placental chorionic veins. *Eur J Obstet Gynecol Reprod Biol,* 42**,** 211-5.

SETCHELL, K. D., DUMASWALA, R., COLOMBO, C. & RONCHI, M. 1988. Hepatic bile acid metabolism during early development revealed from the analysis of human fetal gallbladder bile. *J Biol Chem,* 263**,** 16637-44.

SETCHELL, K. D., GALZIGNA, L., O'CONNELL, N., BRUNETTI, G. & TAUSCHEL, H. D. 2005. Bioequivalence of a new liquid formulation of ursodeoxycholic acid (Ursofalk suspension) and Ursofalk capsules measured by plasma pharmacokinetics and biliary enrichment. *Aliment Pharmacol Ther,* 21**,** 709-21.

SHAN, D., HU, Y., QIU, P., MATHEW, B. S., CHEN, Y., LI, S., LIN, L., WANG, Z. & LI, L. 2016. Intrahepatic Cholestasis of Pregnancy in Women With Twin Pregnancy. *Twin Res Hum Genet,* 19**,** 697-707.

SHAND, A. W., DICKINSON, J. E. & D'ORSOGNA, L. 2008. Refractory fetal supraventricular tachycardia and obstetric cholestasis. *Fetal Diagn Ther,* 24**,** 277-81.

SHAO, Y., YAO, Z., LU, J., LI, H., WU, W. & DING, M. 2007. [Change of heart rate power spectrum and its association with sudden death in the fetuses of rats with intrahepatic cholestasis of pregnancy]. *Sheng Wu Yi Xue Gong Cheng Xue Za Zhi,* 24**,** 1215-9.

SHARMA, N., PANDA, S. & SINGH, A. S. 2016. Obstetric Outcome During an Era of Active Management for Obstetrics Cholestasis. *J Obstet Gynaecol India,* 66**,** 38-41.

SHAY, J. W. & WRIGHT, W. E. 2005. Use of telomerase to create bioengineered tissues. *Ann N Y Acad Sci,* 1057**,** 479-91.

SHEIKH ABDUL KADIR, S. H., MIRAGOLI, M., ABU-HAYYEH, S., MOSHKOV, A. V., XIE, Q., KEITEL, V., NIKOLAEV, V. O., WILLIAMSON, C. & GORELIK, J. 2010. Bile acid-induced arrhythmia is mediated by muscarinic M2 receptors in neonatal rat cardiomyocytes. *PLoS One,* 5**,** e9689.

SHYNLOVA, O., TSUI, P., DOROGIN, A. & LYE, S. J. 2008. Monocyte chemoattractant protein-1 (CCL-2) integrates mechanical and endocrine signals that mediate term and preterm labor. *J Immunol,* 181**,** 1470-9.

SIGNORELLI, P., AVAGLIANO, L., REFORGIATO, M. R., TOPPI, N., CASAS, J., FABRIÀS, G., MARCONI, A. M., GHIDONI, R. & CARETTI, A. 2016. De novo ceramide synthesis is involved in acute inflammation during labor. *Biol Chem,* 397**,** 147-55.

SILBER, A., HAMPP, N. & SCHUHMANN, W. 1996. Poly(methylene blue)-modified thick-film gold electrodes for the electrocatalytic oxidation of NADH and their application in glucose biosensors. *Biosens Bioelectron,* 11**,** 215-23.

SIMPSON, J. M. 2006. Fetal arrhythmias. *Ultrasound Obstet Gynecol,* 27**,** 599-606.

SINISALO, J., VANHANEN, H., PAJUNEN, P., VAPAATALO, H. & NIEMINEN, M. S. 1999. Ursodeoxycholic acid and endothelial-dependent, nitric oxide-independent vasodilatation of forearm resistance arteries in patients with coronary heart disease. *Br J Clin Pharmacol,* 47**,** 661-5.

SIRICILLA, S., KNAPP, K. M., ROGERS, J. H., BERGER, C., SHELTON, E. L., MI, D., VINSON, P., CONDON, J., PARIA, B. C., REESE, J., SHENG, Q. & HERINGTON, J. L. 2019. Comparative analysis of myometrial and vascular smooth muscle cells to determine optimal cells for use in drug discovery. *Pharmacol Res,* 146**,** 104268.

SMITH, V., ARUNTHAVANATHAN, S., NAIR, A., ANSERMET, D., DA SILVA COSTA, F. & WALLACE, E. M. 2018. A systematic review of cardiac time intervals utilising non-invasive fetal electrocardiogram in normal fetuses. *BMC Pregnancy Childbirth,* 18**,** 370.

SOORANNA, S. R., LEE, Y., KIM, L. U., MOHAN, A. R., BENNETT, P. R. & JOHNSON, M. R. 2004. Mechanical stretch activates type 2 cyclooxygenase via activator protein-1 transcription factor in human myometrial cells. *Mol Hum Reprod,* 10**,** 109-13.

SOUZA, G. R., TSENG, H., GAGE, J. A., MANI, A., DESAI, P., LEONARD, F., LIAO, A., LONGO, M., REFUERZO, J. S. & GODIN, B. 2017. Magnetically Bioprinted Human Myometrial 3D Cell Rings as A Model for Uterine Contractility. *Int J Mol Sci,* 18.

SPARROW, M. P. & SIMMONDS, W. J. 1965. The effect of bile salts on contractility and calcium depletion of polarized and depolarized smooth muscle. *J Pharmacol Exp Ther,* 150**,** 208-15.

STERRENBURG, K., VISSER, W., SMIT, L. S. & CORNETTE, J. 2014. Acidosis: A potential explanation for adverse fetal outcome in intrahepatic cholestasis of pregnancy. A case report. *Obstet Med,* 7**,** 177-9.

STIEGER, B. & MEIER, P. J. 2011. Pharmacogenetics of drug transporters in the enterohepatic circulation. *Pharmacogenomics,* 12**,** 611-31.

STOCK, S. J. & ISMAIL, K. M. 2016. Which intervention reduces the risk of preterm birth in women with risk factors? *BMJ,* 355**,** i5206.

STONE, P. R., BURGESS, W., MCINTYRE, J. P., GUNN, A. J., LEAR, C. A., BENNET, L., MITCHELL, E. A., THOMPSON, J. M. & MATERNAL SLEEP IN PREGNANCY RESEARCH GROUP, T. E. U. O. A. 2017. Effect of maternal position on fetal behavioural state and heart rate variability in healthy late gestation pregnancy. *J Physiol,* 595**,** 1213-1221.

STRAND, S. A., STRASBURGER, J. F. & WAKAI, R. T. 2019. Fetal magnetocardiogram waveform characteristics. *Physiol Meas,* 40**,** 035002.

STRASBURGER, J. F., CHEULKAR, B. & WICHMAN, H. J. 2007. Perinatal arrhythmias: diagnosis and management. *Clin Perinatol,* 34**,** 627-52, vii-viii.

STREHLOW, S. L., PATHAK, B., GOODWIN, T. M., PEREZ, B. M., EBRAHIMI, M. & LEE, R. H. 2010. The mechanical PR interval in fetuses of women with intrahepatic cholestasis of pregnancy. *Am J Obstet Gynecol,* 203**,** 455.e1-5.

SUBBARAMAIAH, K., CHUNG, W. J. & DANNENBERG, A. J. 1998. Ceramide regulates the transcription of cyclooxygenase-2. Evidence for involvement of extracellular signal-regulated kinase/c-Jun N-terminal kinase and p38 mitogen-activated protein kinase pathways. *J Biol Chem,* 273**,** 32943-9.

SUNAGANE, N., KOBORI, T., URONO, T. & KUBOTA, K. 1990. Possible mechanisms of spasmolytic action of bile salts on the isolated guinea-pig gallbladder. *Nihon Heikatsukin Gakkai Zasshi,* 26**,** 143-50.

TAKANO, S., ITO, Y., YOKOSUKA, O., OHTO, M., UCHIUMI, K., HIROTA, K. & OMATA, M. 1994. A multicenter randomized controlled dose study of ursodeoxycholic acid for chronic hepatitis C. *Hepatology,* 20**,** 558-64.

TASAKA, K., MASUMOTO, N., MIYAKE, A. & TANIZAWA, O. 1991. Direct measurement of intracellular free calcium in cultured human puerperal myometrial cells stimulated by oxytocin: effects of extracellular calcium and calcium channel blockers. *Obstet Gynecol,* 77**,** 101-6.

TAYLOR, M. J., SMITH, M. J., THOMAS, M., GREEN, A. R., CHENG, F., OSEKU-AFFUL, S., WEE, L. Y., FISK, N. M. & GARDINER, H. M. 2003. Non-invasive fetal electrocardiography in singleton and multiple pregnancies. *BJOG,* 110**,** 668-78.

TAYYAR, A. T., KOZALI, S., YETKIN YILDIRIM, G., KARAKUS, R., YUKSEL, I. T., EREL, O., NESELIOGLU, S. & EROGLU, M. 2019. Role of ischemia-modified albumin in the evaluation of oxidative stress in intrahepatic cholestasis of pregnancy. *J Matern Fetal Neonatal Med,* 32**,** 3836-3840.

TEMEL YÜKSEL, İ., ASLAN ÇETIN, B., KÖROĞLU, N., AYDOĞAN MATHYK, B. & ERDEM, B. 2019. Inflammatory marker YKL-40 levels in intrahepatic cholestasis of pregnancy. *Gynecol Endocrinol,* 35**,** 635-637.

TEODORCZYK, M. & PURDYT, W. C. 1990. An amperometric enzyme electrode for the determination of 3alpha-hydroxysteroids. *Talanta,* 37**,** 795-800.

TERENTYEV, D., VIATCHENKO-KARPINSKI, S., VALDIVIA, H. H., ESCOBAR, A. L. & GYÖRKE, S. 2002. Luminal Ca2+ controls termination and refractory behavior of Ca2+-induced Ca2+ release in cardiac myocytes. *Circ Res,* 91**,** 414-20.

THIBAULT, N. & BALLET, F. 1993. Effect of bile acids on intracellular calcium in isolated rat hepatocyte couplets. *Biochem Pharmacol,* 45**,** 289-93.

THORLING, L. 1955. Jaundice in pregnancy; a clinical study. *Acta Med Scand Suppl,* 302**,** 1-123.

THORNTON, S., GILLESPIE, J. I., GREENWELL, J. R. & DUNLOP, W. 1992. Mobilization of calcium by the brief application of oxytocin and prostaglandin E2 in single cultured human myometrial cells. *Exp Physiol,* 77**,** 293-305.

TIAN, G., DING, M., XU, B., HE, Y., LYU, W., JIN, M. & ZHANG, X. 2018. A novel electrochemical biosensor for ultrasensitive detection of serum total bile acids based on enzymatic reaction combined with the double oxidation circular amplification strategy. *Biosens Bioelectron,* 118**,** 31-35.

TOI, P. T., TRUNG, T. Q., DANG, T. M. L., BAE, C. W. & LEE, N. E. 2019. Highly Electrocatalytic, Durable, and Stretchable Nanohybrid Fiber for On-Body Sweat Glucose Detection. *ACS Appl Mater Interfaces,* 11**,** 10707-10717.

TOWBIN, H., STAEHELIN, T. & GORDON, J. 1979. Electrophoretic transfer of proteins from polyacrylamide gels to nitrocellulose sheets: procedure and some applications. *Proc Natl Acad Sci U S A,* 76**,** 4350-4.

TRIBE, R. M., DANN, A. T., KENYON, A. P., SEED, P., SHENNAN, A. H. & MALLET, A. 2010. Longitudinal profiles of 15 serum bile acids in patients with intrahepatic cholestasis of pregnancy. *Am J Gastroenterol,* 105**,** 585-95.

TUCKER, O. N., DANNENBERG, A. J., YANG, E. K. & FAHEY, T. J. 2004. Bile acids induce cyclooxygenase-2 expression in human pancreatic cancer cell lines. *Carcinogenesis,* 25**,** 419-23.

TURDI, S., HU, N. & REN, J. 2013. Tauroursodeoxycholic acid mitigates high fat diet-induced cardiomyocyte contractile and intracellular Ca2+ anomalies. *PLoS One,* 8**,** e63615.

TURNER, A. P. F., KARUBE, I. & WILSON, G. S. 1987. *Biosensors : fundamentals and applications,* Oxford, Oxford University Press.

TURTON, P., ARROWSMITH, S., PRESCOTT, J., BALLARD, C., BRICKER, L., NEILSON, J. & WRAY, S. 2013. A comparison of the contractile properties of myometrium from singleton and twin pregnancies. *PLoS One,* 8**,** e63800.

ULDBJERG, N., EKMAN, G., MALMSTRÖM, A., OLSSON, K. & ULMSTEN, U. 1983. Ripening of the human uterine cervix related to changes in collagen, glycosaminoglycans, and collagenolytic activity. *Am J Obstet Gynecol,* 147**,** 662-6.

ULLOA, A., GONZALES, A. L., ZHONG, M., KIM, Y. S., CANTLON, J., CLAY, C., KU, C. Y., EARLEY, S. & SANBORN, B. M. 2009. Reduction in TRPC4 expression specifically attenuates G-protein coupled receptor-stimulated increases in intracellular calcium in human myometrial cells. *Cell Calcium,* 46**,** 73-84.

VAN DEN BERG, M. P., HAAKSMA, J., BROUWER, J., TIELEMAN, R. G., MULDER, G. & CRIJNS, H. J. 1997. Heart rate variability in patients with atrial fibrillation is related to vagal tone. *Circulation,* 96**,** 1209-16.

VAN LEEUWEN, P., CYSARZ, D., EDELHÄUSER, F. & GRÖNEMEYER, D. 2013. Heart rate variability in the individual fetus. *Auton Neurosci,* 178**,** 24-8.

VAN LEEUWEN, P., LANGE, S., GEUE, D. & GRÖNEMEYER, D. 2007. Heart rate variability in the fetus: a comparison of measures. *Biomed Tech (Berl),* 52**,** 61-5.

VAN VLIET, E. O., BOORMANS, E. M., DE LANGE, T. S., MOL, B. W. & OUDIJK, M. A. 2014. Preterm labor: current pharmacotherapy options for tocolysis. *Expert Opin Pharmacother,* 15**,** 787-97.

VANNUCCINI, S., BOCCHI, C., SEVERI, F. M., CHALLIS, J. R. & PETRAGLIA, F. 2016. Endocrinology of human parturition. *Ann Endocrinol (Paris),* 77**,** 105-13.

VASAVAN, T., FERRARO, E., IBRAHIM, E., DIXON, P., GORELIK, J. & WILLIAMSON, C. 2018. Heart and bile acids - Clinical consequences of altered bile acid metabolism. *Biochim Biophys Acta Mol Basis Dis,* 1864**,** 1345-1355.

VEENSTRA, R. D., WANG, H. Z., BEYER, E. C. & BRINK, P. R. 1994. Selective dye and ionic permeability of gap junction channels formed by connexin45. *Circ Res,* 75**,** 483-90.

VIDIMAR, V., CHAKRAVARTI, D., BULUN, S. E., YIN, P., NOWAK, R., WEI, J. J. & KIM, J. J. 2018. The AKT/BCL-2 Axis Mediates Survival of Uterine Leiomyoma in a Novel 3D Spheroid Model. *Endocrinology,* 159**,** 1453-1462.

VINK, J. & FELTOVICH, H. 2016. Cervical etiology of spontaneous preterm birth. *Semin Fetal Neonatal Med,* 21**,** 106-12.

VOGEL, C. & MARCOTTE, E. M. 2012. Insights into the regulation of protein abundance from proteomic and transcriptomic analyses. *Nat Rev Genet,* 13**,** 227-32.

VON HAEHLING, S., SCHEFOLD, J. C., JANKOWSKA, E. A., SPRINGER, J., VAZIR, A., KALRA, P. R., SANDEK, A., FAULER, G., STOJAKOVIC, T., TRAUNER, M., PONIKOWSKI, P., VOLK, H. D., DOEHNER, W., COATS, A. J., POOLE-WILSON, P. A. & ANKER, S. D. 2012. Ursodeoxycholic acid in patients with chronic heart failure: a double-blind, randomized, placebo-controlled, crossover trial. *J Am Coll Cardiol,* 59**,** 585-92.

WACKER-GUSSMANN, A., PLANKL, C., SEWALD, M., SCHNEIDER, K. M., OBERHOFFER, R. & LOBMAIER, S. M. 2018. Fetal cardiac time intervals in healthy pregnancies - an

observational study by fetal ECG (Monica Healthcare System). *J Perinat Med,* 46**,** 587-592.
WALSH, M. P. 1991. The Ayerst Award Lecture 1990. Calcium-dependent mechanisms of regulation of smooth muscle contraction. *Biochem Cell Biol,* 69**,** 771-800.
WANG, C., CHEN, X., ZHOU, S. F. & LI, X. 2011. Impaired fetal adrenal function in intrahepatic cholestasis of pregnancy. *Med Sci Monit,* 17**,** CR265-71.
WANG, L., LU, Z., ZHOU, X., DING, Y. & GUAN, L. 2019a. Effects of intrahepatic cholestasis of pregnancy on hepatic function, changes of inflammatory cytokines and fetal outcomes. *Exp Ther Med,* 17**,** 2979-2984.
WANG, S. Y., YOSHINO, M., SUI, J. L., WAKUI, M., KAO, P. N. & KAO, C. Y. 1998. Potassium currents in freshly dissociated uterine myocytes from nonpregnant and late-pregnant rats. *J Gen Physiol,* 112**,** 737-56.
WANG, Z., DONG, M., CHU, H. & HE, J. 2004. Increased serum levels of neopterin and soluble interleukin-2 receptor in intrahepatic cholestasis of pregnancy. *Acta Obstet Gynecol Scand,* 83**,** 1067-70.
WANG, Z., YU, R., ZENG, H., WANG, X., LUO, S., LI, W., LUO, X. & YANG, T. 2019b. Nucleic acid-based ratiometric electrochemiluminescent, electrochemical and photoelectrochemical biosensors: a review. *Mikrochim Acta,* 186**,** 405.
WARMERDAM, G. J. J., VULLINGS, R., VAN LAAR, J. O. E. H., VAN DER HOUT-VAN DER JAGT, M. B., BERGMANS, J. W. M., SCHMITT, L. & OEI, S. G. 2018. Detection rate of fetal distress using contraction-dependent fetal heart rate variability analysis. *Physiol Meas,* 39**,** 025008.
WEI, W. & HU, Y. Y. 2014. Expression of hypoxia-regulated genes and glycometabolic genes in placenta from patients with intrahepatic cholestasis of pregnancy. *Placenta,* 35**,** 732-6.
WEISS, G., GOLDSMITH, L. T., SACHDEV, R., VON HAGEN, S. & LEDERER, K. 1993. Elevated first-trimester serum relaxin concentrations in pregnant women following ovarian stimulation predict prematurity risk and preterm delivery. *Obstet Gynecol,* 82**,** 821-8.
WEISS, G., O'BYRNE, E. M. & STEINETZ, B. G. 1976. Relaxin: a product of the human corpus luteum of pregnancy. *Science,* 194**,** 948-9.
WELSH, T., JOHNSON, M., YI, L., TAN, H., RAHMAN, R., MERLINO, A., ZAKAR, T. & MESIANO, S. 2012. Estrogen receptor (ER) expression and function in the pregnant human myometrium: estradiol via ERα activates ERK1/2 signaling in term myometrium. *J Endocrinol,* 212**,** 227-38.
WIKSTRÖM SHEMER, E., MARSCHALL, H. U., LUDVIGSSON, J. F. & STEPHANSSON, O. 2013. Intrahepatic cholestasis of pregnancy and associated adverse pregnancy and fetal outcomes: a 12-year population-based cohort study. *BJOG,* 120**,** 717-23.
WIKSTRÖM SHEMER, E., THORSELL, M., ÖSTLUND, E., BLOMGREN, B. & MARSCHALL, H. U. 2012. Stereological assessment of placental morphology in intrahepatic cholestasis of pregnancy. *Placenta,* 33**,** 914-8.
WIKSTRÖM SHEMER, E. A., STEPHANSSON, O., THURESSON, M., THORSELL, M., LUDVIGSSON, J. F. & MARSCHALL, H. U. 2015. Intrahepatic cholestasis of pregnancy and cancer, immune-mediated and cardiovascular diseases: A population-based cohort study. *J Hepatol,* 63**,** 456-61.
WILLIAMSON, C. & GEENES, V. 2014. Intrahepatic cholestasis of pregnancy. *Obstet Gynecol,* 124**,** 120-33.
WILLIAMSON, C., GORELIK, J., EATON, B. M., LAB, M., DE SWIET, M. & KORCHEV, Y. 2001. The bile acid taurocholate impairs rat cardiomyocyte function: a proposed mechanism for intra-uterine fetal death in obstetric cholestasis. *Clin Sci (Lond),* 100**,** 363-9.

WONG, L. F., SHALLOW, H. & O'CONNELL, M. P. 2008. Comparative study on the outcome of obstetric cholestasis. *J Matern Fetal Neonatal Med,* 21**,** 327-30.
WORD, R. A., CASEY, M. L., KAMM, K. E. & STULL, J. T. 1991. Effects of cGMP on [Ca2+]i, myosin light chain phosphorylation, and contraction in human myometrium. *Am J Physiol,* 260**,** C861-7.
WORD, R. A., TANG, D. C. & KAMM, K. E. 1994. Activation properties of myosin light chain kinase during contraction/relaxation cycles of tonic and phasic smooth muscles. *J Biol Chem,* 269**,** 21596-602.
WU, W. B., MENON, R., XU, Y. Y., ZHAO, J. R., WANG, Y. L., LIU, Y. & ZHANG, H. J. 2016. Downregulation of peroxiredoxin-3 by hydrophobic bile acid induces mitochondrial dysfunction and cellular senescence in human trophoblasts. *Sci Rep,* 6**,** 38946.
WU, W. B., XU, Y. Y., CHENG, W. W., WANG, Y. X., LIU, Y., HUANG, D. & ZHANG, H. J. 2015. Agonist of farnesoid X receptor protects against bile acid induced damage and oxidative stress in mouse placenta--a study on maternal cholestasis model. *Placenta,* 36**,** 545-51.
WU, W. X., UNNO, N., MA, X. H. & NATHANIELSZ, P. W. 1998. Inhibition of prostaglandin production by nimesulide is accompanied by changes in expression of the cassette of uterine labor-related genes in pregnant sheep. *Endocrinology,* 139**,** 3096-103.
WU, Y. C., CHIU, C. F. & HSUEH, C. T. 2018. The role of bile acids in cellular invasiveness of gastric cancer. *Cancer Cell Int,* 18**,** 75.
XIA, X. M., FAKLER, B., RIVARD, A., WAYMAN, G., JOHNSON-PAIS, T., KEEN, J. E., ISHII, T., HIRSCHBERG, B., BOND, C. T., LUTSENKO, S., MAYLIE, J. & ADELMAN, J. P. 1998. Mechanism of calcium gating in small-conductance calcium-activated potassium channels. *Nature,* 395**,** 503-7.
XIAO, Q., WANG, G., LUO, Z. & XU, Q. 2010. The mechanism of stem cell differentiation into smooth muscle cells. *Thromb Haemost,* 104**,** 440-8.
XIAO, Z. L., BIANCANI, P., CAREY, M. C. & BEHAR, J. 2003. Hydrophilic but not hydrophobic bile acids prevent gallbladder muscle dysfunction in acute cholecystitis. *Hepatology,* 37**,** 1442-50.
XU, T., ZHOU, Z., LIU, N., DENG, C., HUANG, G., ZHOU, F., LIU, X. & WANG, X. 2019. Disrupted compensatory response mediated by Wolfram syndrome 1 protein and corticotrophin-releasing hormone family peptides in early-onset intrahepatic cholestasis pregnancy. *Placenta,* 83**,** 63-71.
YAMADA, T., ISHIDA, Y., NAKAMURA, Y. & SHIMADA, S. 2011. Bile-acid-induced calcium signaling in mouse esophageal epithelial cells. *Biochem Biophys Res Commun,* 414**,** 789-94.
YAMATO, Y., KIMURA, A., INOUE, T., KUROSAWA, T. & KATO, H. 2001. Fetal bile acid metabolism: analysis of urinary 3beta-monohydroxy-delta(5) bile acid in preterm infants. *Biol Neonate,* 80**,** 19-25.
YANG, J., CHEN, C., LIU, M. & ZHANG, S. 2019. Women successfully treated for severe intrahepatic cholestasis of pregnancy do not have increased risks for adverse perinatal outcomes. *Medicine (Baltimore),* 98**,** e16214.
YAO, Y., XU, F., CHEN, M., XU, Z. & ZHU, Z. 2010. Adsorption behavior of methylene blue on carbon nanotubes. *Bioresour Technol,* 101**,** 3040-6.
YAYLA ABIDE, Ç., VURAL, F., KILIÇÇI, Ç., BOSTANCI ERGEN, E., YENIDEDE, İ., ESER, A. & PEKIN, O. 2017. Can we predict severity of intrahepatic cholestasis of pregnancy using inflammatory markers? *Turk J Obstet Gynecol,* 14**,** 160-165.
YE, D., HAN, D. Y. & WANG, J. R. 1991. [Effects of ursodeoxycholic acid on mechanical and electric activities in isolated guinea pig heart muscles]. *Zhong Xi Yi Jie He Za Zhi,* 11**,** 289-90, 262.

YILMAZ, U. T., UZUN, D. & YILMAZ, H. 2015. A new method for rapid and sensitive determination of cholic acid in gallbladder bile using voltammetric techniques. *Microchemical Journal,* 122**,** 159-163.
YOCHUM, M., LAFORÊT, J. & MARQUE, C. 2018. Multi-scale and multi-physics model of the uterine smooth muscle with mechanotransduction. *Comput Biol Med,* 93**,** 17-30.
YOON, B. H., ROMERO, R., JUN, J. K., MAYMON, E., GOMEZ, R., MAZOR, M. & PARK, J. S. 1998. An increase in fetal plasma cortisol but not dehydroepiandrosterone sulfate is followed by the onset of preterm labor in patients with preterm premature rupture of the membranes. *Am J Obstet Gynecol,* 179**,** 1107-14.
YOU, S., CUI, A. M., HASHMI, S. F., ZHANG, X., NADOLNY, C., CHEN, Y., CHEN, Q., BUSH, X., HURD, Z., ALI, W., QIN, G. & DENG, R. 2020. Dysregulation of bile acids increases the risk for preterm birth in pregnant women. *Nat Commun,* 11**,** 2111.
YOUNG, R. C. 2007. Myocytes, myometrium, and uterine contractions. *Ann N Y Acad Sci,* 1101**,** 72-84.
YOUNG, R. C. 2016. Mechanotransduction mechanisms for coordinating uterine contractions in human labor. *Reproduction,* 152**,** R51-61.
YOUNG, R. C. & ZHANG, P. 2005. Inhibition of in vitro contractions of human myometrium by mibefradil, a T-type calcium channel blocker: support for a model using excitation-contraction coupling, and autocrine and paracrine signaling mechanisms. *J Soc Gynecol Investig,* 12**,** e7-12.
YOUNGER, J. D., REITMAN, E. & GALLOS, G. 2017. Tocolysis: Present and future treatment options. *Semin Perinatol,* 41**,** 493-504.
YU, B., ZHANG, Y. Q. & HONG, W. B. 1990. Miniaturization of a liquid membrane sensor for the determination of bile acids. *Biosens Bioelectron,* 5**,** 215-22.
YU, J. T. & LÓPEZ BERNAL, A. 1998. The cytoskeleton of human myometrial cells. *J Reprod Fertil,* 112**,** 185-98.
YUAN, M., JUMMER, M. J., MILTON, R. D., QUAH, T. & MINTEER, S. D. 2019. Efficient NADH Regeneration by a Redox Polymer-Immobilized

Enzymatic System. *ACS Catalysis,* 9**,** 5486-5495.
YUE, Y., XU, D., WANG, Y., WANG, X. & XIA, F. 2018. Effect of inducible nitric oxide synthase and neuropeptide Y in plasma and placentas from intrahepatic cholestasis of pregnancy. *J Obstet Gynaecol Res,* 44**,** 1377-1383.
ZAPATA, R., SANDOVAL, L., PALMA, J., HERNÁNDEZ, I., RIBALTA, J., REYES, H., SEDANO, M., TOHÁ, D. & SILVA, J. J. 2005. Ursodeoxycholic acid in the treatment of intrahepatic cholestasis of pregnancy. A 12-year experience. *Liver Int,* 25**,** 548-54.
ZARDI, E. M., ABBATE, A., ZARDI, D. M., DOBRINA, A., MARGIOTTA, D., VAN TASSELL, B. W., VAN TASSEL, B. W., AFELTRA, A. & SANYAL, A. J. 2010. Cirrhotic cardiomyopathy. *J Am Coll Cardiol,* 56**,** 539-49.
ZAVECZ, J. H. & BATTARBEE, H. D. 2010. The role of lipophilic bile acids in the development of cirrhotic cardiomyopathy. *Cardiovasc Toxicol,* 10**,** 117-29.
ZECCA, E., DE LUCA, D., MARRAS, M., CARUSO, A., BERNARDINI, T. & ROMAGNOLI, C. 2006. Intrahepatic cholestasis of pregnancy and neonatal respiratory distress syndrome. *Pediatrics,* 117**,** 1669-72.
ZHANG, F., SUBBARAMAIAH, K., ALTORKI, N. & DANNENBERG, A. J. 1998. Dihydroxy bile acids activate the transcription of cyclooxygenase-2. *J Biol Chem,* 273**,** 2424-8.
ZHANG, G. H., CONG, A. R., XU, G. B., LI, C. B., YANG, R. F. & XIA, T. A. 2005. An enzymatic cycling method for the determination of serum total bile acids with recombinant 3alpha-hydroxysteroid dehydrogenase. *Biochem Biophys Res Commun,* 326**,** 87-92.
ZHANG, L. J., XIANG, H. & DING, Y. L. 2009a. [Influence of total bile acid in maternal serum and cord blood on neonatal cardiac function from intrahepatic cholestasis of pregnancy]. *Zhonghua Fu Chan Ke Za Zhi,* 44**,** 188-90.

ZHANG, Q., NAKAKI, T., IWAMI, D., NIIMI, M. & SHIRASUGI, N. 2009b. Induction of regulatory T cells and indefinite survival of fully allogeneic cardiac grafts by ursodeoxycholic acid in mice. *Transplantation,* 88**,** 1360-70.

ZHANG, R., PAN, X. H. & XIAO, L. 2015. Expression of vascular endothelial growth factor (VEGF) under hypoxia in placenta with intrahepatic cholestasis of pregnancy and its clinically pathological significance. *Int J Clin Exp Pathol,* 8**,** 11475-9.

ZHANG, X., ZHU, M., XU, B., CUI, Y., TIAN, G., SHI, Z. & DING, M. 2016a. Indirect electrochemical detection for total bile acids in human serum. *Biosens Bioelectron,* 85**,** 563-7.

ZHANG, Y., HUANG, X., ZHOU, J., YIN, Y., ZHANG, T. & CHEN, D. 2018. PPARγ provides anti-inflammatory and protective effects in intrahepatic cholestasis of pregnancy through NF-κB pathway. *Biochem Biophys Res Commun,* 504**,** 834-842.

ZHANG, Y., PAN, Y., LIN, C., ZHENG, Y., SUN, H., ZHANG, H., WANG, J., YUAN, M., DUAN, T., DU, Q. & CHEN, J. 2016b. Bile acids evoke placental inflammation by activating Gpbar1/NF-κB pathway in intrahepatic cholestasis of pregnancy. *J Mol Cell Biol,* 8**,** 530-541.

ZHOU, H., ZHANG, Z., YU, P., SU, L., OHSAKA, T. & MAO, L. 2010. Noncovalent attachment of NAD+ cofactor onto carbon nanotubes for preparation of integrated dehydrogenase-based electrochemical biosensors. *Langmuir,* 26**,** 6028-32.

ZHU, J., DONG, X., LIU, Q., WU, C., WANG, Q., LONG, Z. & LI, L. 2016. Hydrophobic bile acids relax rat detrusor contraction via inhibiting the opening of the Na^{+}/Ca^{2+} exchanger. *Sci Rep,* 6**,** 21358.

ZHU, L., ZHAI, J., YANG, R., TIAN, C. & GUO, L. 2007. Electrocatalytic oxidation of NADH with Meldola's blue functionalized carbon nanotubes electrodes. *Biosens Bioelectron,* 22**,** 2768-73.

ZHUANG, X., CUI, A. M., WANG, Q., CHENG, X. Y., SHEN, Y., CAI, W. H., LI, H. B., ZHANG, S. & QIN, G. 2017. Liver Dysfunction during Pregnancy and Its Association of With Preterm Birth in China: A Prospective Cohort Study. *EBioMedicine,* 26**,** 152-156.

ZIMMERMANN, M. & KALUSCHE, D. 2001. Fluctuation in autonomic tone is a major determinant of sustained atrial arrhythmias in patients with focal ectopy originating from the pulmonary veins. *J Cardiovasc Electrophysiol,* 12**,** 285-91.

ZÖHRER, E., RESCH, B., SCHARNAGL, H., SCHLAGENHAUF, A., FAULER, G., STOJAKOVIC, T., HOFER, N., LANG, U. & JAHNEL, J. 2016. Serum bile acids in term and preterm neonates: A case-control study determining reference values and the influence of early-onset sepsis. *Medicine (Baltimore),* 95**,** e5219.